THÈSE

En vue de l'obtention du

DOCTORAT DE L'UNIVERSITÉ DE TOULOUSE

Délivré par : *l'Université Toulouse 3 Paul Sabatier (UT3 Paul Sabatier)*

Présentée et soutenue le *25/09/2015* par :
Cécile ICHARD

Random media and processes estimation using non-linear filtering techniques : application to ensemble weather forecast and aircraft trajectories

JURY

Dominique BAKRY	Examinateur	UPS
Henk BLOM	Examinateur	TU Delft
Stéphane puechmorel	Examinateur	ENAC
Arnaud DOUCET	Rapporteur	Oxford University
Fredrik GUSTAFSSON	Rapporteur	Linköping University
Christophe BAEHR	Directeur de thèse	Météo-France
Jaap HEIJSTEK	Invité	NLR

École doctorale et spécialité :
 MITT : Domaine Mathématiques : Mathématiques appliquées
Unité de Recherche :
 CNRM-GAME (UMR 3589)
Directeur(s) de Thèse :
 Pierre DEL MORAL et *Christophe BAEHR*
Rapporteurs :
 Arnaud DOUCET et *Fredrik GUSTAFSSON*

Acknowledgements

One day before handing in my thesis to the University library, I become aware that writing acknowledgement is not the easiest part of the thesis job. I thought so far, that acknowledgement was just a mandatory work to be politically correct and that I could write them in one hour. I was wrong, I needed two. Joking aside, I know at this time that this work would not have been possible without the existence of many people.

As I am sure that I am going to forget someone, I would like first to apologize for those I forgot. Sorry guys, you did not help me enough to remember you during a stressing moment.

All joking aside, I would like to thank my Phd supervisor, Christophe Baehr, who gave birth to this wonderful research subject, and who gave me precious hint to progress during my work. As I like to say, he is my "scientific" father, and as in a father-daughter relationship, our relation was far from being linear. So I would like to thank him for being supportive and comprehensive during these three years. I also would like to thank my others Phd supervisor, Pierre Del Moral and Marcel Mongeau for having a complete confidence in my work.

Then I would like to express my thanks to the rapporteurs, Arnaud Doucet and Fredrik Gustafsson, for accepting to examine my Phd thesis and making a really detailed report who helps me a lot to enhance my work.

I should like to express my thanks for the unfailing support and the help all along the way to my adventure colleagues: Lucie, Antoine, Thomas. It was hard. Stepping back, I think that I would have abandoned without you, your happiness, your support and your Kleenex. They know what they did for me and I do not need to precise it here.

Some other people make this adventure possible. The team GMEI and more specifically TRAMM, as well as CTI, represented respectively by Alain, Bruno (say "le chef") and Serge. Your support and your confidence were important and your help for making a good Phd was precious. Thank you.

Many other persons help me to achieve my goals. At ONERA, Christelle Vergé with who I could work on theoretical aspects and share my Phd experience. It was a pleasure to work with you and have some beers around Toulouse. At Météo-France, I express my thanks to Carole Labadie for introducing me with PEARPEGE, to Fran cois Bouttier for giving me the opportunity to work with PEAROME data, to Alan Hally for giving me hints to use netcdf data and to Emmanuel Riggi-Carrolo for giving me another point of view on my situation. At ENAC, when I needed them, they were present. So I would like

Contents

"Foresee is to projecting into the future what has been perceived in the past"

<div align="right">Henri Bergson</div>

1

Introduction

From air carrier point of view, air transportation generates a turnover really important, but produces thin net margins. Thus the profitability is approaching zero which leads to a highly competitive market where each Euro saved represents a little gain. Air-traffic growth combined with high security standards is stressing out the current system of Air Traffic Management (ATM). For these reasons, they launched together two vast research programs. One in Europe, named Single European Sky ATM Research (SESAR) and one in the United-States called Next Generation Air Transportation System (NextGen). Both programs aim to use the most recent techniques to optimize and automate the air-traffic management. This thesis work is led in that general framework.

The use of aircraft trajectories models to weight ensemble weather forecasts according to observations delivered by air-traffic control radars and estimation techniques is an issue at the interplay between three scientific domains. It is based on solid mechanics to study and model aircraft systems, on atmospheric sciences to use and understand ensemble weather forecasts and on applied mathematics to rigorously pose the estimation problem and propose consistent algorithm to solve it. In this thesis, we focus on demonstrating the contribution of estimation techniques to solve current issues on aircraft trajectory prediction. Particularly, we put our interest on reducing the trajectory prediction uncertainty induced by weather forecast errors.

1.1 Key challenges

1.1.1 Air Traffic Control Context

Air transportation is a core component of the modern world and actively participates to the globalization process. Most of locations on the Earth can be reached by less than one day of journey. People and goods can travel long distances in a really short period of time which creates and multiplies opportunities in commerce, science and leisure. All these new possibilities impact the global economy. In 2001, aviation accounted for €220 billion of added value, and 4 million jobs in Europe, as it has been highlighted in Argüelles et al. (2001). These figures include the output of air carriers, airports, aerospace manufacturers and air navigation service providers.

ATM aims to organize the air-traffic flow throughout the world to insure security and efficiency. Its first goal being security, ATM wants to ensure that accidents remain at low levels in spite of the increasing of air-traffic. In practical terms, this implies for aircraft to avoid congested areas, hazardous weather conditions and other aircraft. Its second purpose is to increase the airspace capacity without compromising safety. These objectives have to be fulfilled in the most cost-effective way to minimize the cost per flight, in terms of fuel consumption, delays and administration costs. Finally ATM needs to operate under certain degree of predictability and flexibility, so that changes and interventions can be made.

To meet the security demands while facing the air-traffic growth, ATM built air transportation rules around a rigid structure made of way-points and airways. To give an idea of the routing structure we give an illustration on Figure 1.1 of airways above Flight Level (FL) 195 which are represented by blue lines. Nevertheless, most of these rules were established decades ago, when aircraft had to follow strict paths over radar beacon in order to enhance radar monitoring and assure air-traffic separation.

In order to facilitate the air-traffic control, this system is not centralized and administrated by different operators. This has led to the airspace fragmentation. The largest regular division of airspace is the Flight Information Region (FIR). Any portion of the atmosphere belongs to some specific FIR, even those above oceans. On Figure 1.2, the European air-space fragmentation is illustrated. Then, depending on the altitude, if the aircraft is landing or taking off, different Air-Traffic Control Centers (ATCC) are responsible of the security. These units are the places where air-traffic controllers operate. They have different tasks in charge: coordinating aircraft movements, ensuring separation between them, directing them between take-off, landing, and also in case of severe weather conditions, and finally guaranteeing smooth air-traffic flow with minimal delays.

According to Eurocontrol, around 10 million flights take place inside the European airspace every year. Developing economies in Asia, Africa and South America have already a significant impact in the air-traffic growth. However, the increase in air-traffic is far from being linear in time and uniform in space as it is related to the fuel prices and the location of ground transportation infrastructures.

Figure 1.1: Airways (represented by blue lines) and way-points (intersecting points) over France for the upper flight information region (above FL195). Credits: SIA
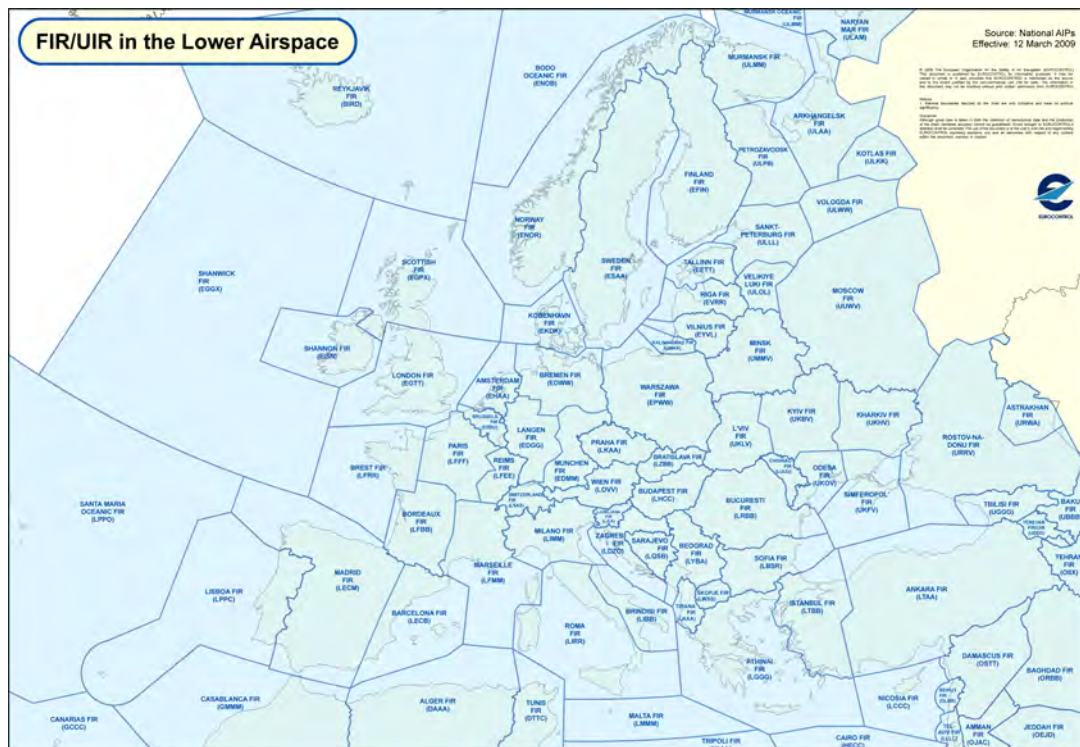
Figure 1.2: FIR over Europe depicted by blue lines. Credits: "Eurocontrol FIR and UIR in the lower airspace - 12 March 2009" by Eurocontrol

The Air Traffic Control (ATC) system has operated reliably in its present form for many years. However, the increasing demand for air travel is stressing it to its limits, Schaufele (2013); Eurocontrol (2013); ICAO (2013). The increase could lead to both safety and performance degradation in the near future, and place an additional burden on the already overloaded human operators. One of the most promising propositions to solve this problem is increasing the level of automation. It is believed that by doing this, the efficiency of ATC can be improved and the tasks of human operators simplified, Ballin et al. (2002); Hu et al. (2002); Weber et al. (2007); Wollkind et al. (2004); Yang and Kuchar (1997). A number of different approaches to increase the level of automation in the ATC process have been proposed and one of them consists in the automation of separation insurance. That is rely on Conflict Detection and Resolution (CDR) strategies. They consist in predicting the trajectories of aircraft, analysing them to decide whether there is a possible loss of separation and if there is issue advisories on how to resolve the problem.

Many more functionalities of the Decision Support Tool (DST) directly rely on an accurate Trajectory Prediction (TP): controller posting, workload estimation, arrival sequencing, to name the most important ones. Therefore accurate TP is the core component of automated systems in ATC.

However, TP is also the weakness of the current automation ATC systems and a major issue in the ATC research community, even more since the shift toward 4D trajectories (SESAR EU (2007) and NextGen project FAA (2007)) has been made.

Indeed, large TP uncertainty forces ATC to use larger separations between aircraft, thus reducing the total number of aircraft a given sector can handle. Moreover fear of loss separation can decrease the fuel efficiency or affect the time of arrival of the aircraft involved as manoeuvres used are based on either changes in direction, velocity or altitude.

The challenge is to reduce the uncertainty of the aircraft states prediction on a temporal horizon of at least 20 minutes, which is the normal temporal horizon for predicting trajectories and detecting conflicts. By doing this, TP accuracy will be enhanced. This improvement will help ATC to handle the increasing air-traffic demand. To achieve this, the information of the current state of the aircraft and its environment shall be reliable.

As a matter of fact, the Flight Management System (FMS), core component of modern aircraft, has access to the measurements from the aircraft's sensor and creates its own TP, which is updated frequently. Therefore we should expect that is the most accurate one. Thanks to Data Link, it should be possible for the ground control to receive data from this on-board TP. Unfortunately, this promising technology is not implemented in every aircraft. Moreover, a DST should efficiently generate scenarios and, today, it is unrealistic to receive many trajectories from on-board systems and merge all the trajectories from all aircraft in real time. Therefore the ground TP is still an essential component of the future ATC system and we decide to adopt in this work the ground point of view to predict aircraft trajectories.

1.1.2 Trajectory prediction and uncertainties

To compute aircraft trajectories in advance, a TP tool needs different information. Some concern the flight intent, others are directly related to the aircraft and finally some are environmental parameters. A trajectory can roughly be separated in three phases: climb, cruise, and descent. Each phase has its own particularities. In this thesis, we focus our attention on trajectory prediction during cruise phase as it is the phase where the most of fuel is burned and the most of time is spent.

Most influencing environmental parameters during cruise phase are wind and temperature. For example, before departure, weather forecasts allow air-carriers and pilot to choose the optimal route in terms of fuel consumption and flight time, to estimate the time of arrival and the needed fuel quantity to make the journey. During the flight, the knowledge of these quantities allow the pilot to follow the scheduled route and adjust the air-speed. In order to understand the wind influence, one has to keep in mind that wind is defined as the air-masses movement. As the aircraft is flying inside a moving air-mass, from the ground point of view, its speed depends on its proper speed and the wind speed. That explains why going from London to New-York takes more time than doing the way back. Indeed the North Atlantic Jet-Stream flows in direction of Europe with favourable high winds for aircraft travelling that direction. Furthermore, aircraft cruise speed is given in Mach number which corresponds to the ratio between the airspeed of the aircraft and the sound celerity in the air mass. However the sound celerity depends on the temperature as it influences the density of the air mass. Thus, temperature is also a crucial environmental parameter for trajectory prediction.

An important source of uncertainty in aircraft trajectory prediction concerns the meteorological parameters and more particularly the wind forecast error. In this work, we will concentrate on the trajectory prediction error induced by wind forecast error. Indeed as it was proved in Green and Vivona (1996); Jackson et al. (1999); Mondoloni et al. (2002); Mondoloni (2006a,b); Chaloulos and Lygeros (2007), a part of the along track error made to predict the aircraft trajectories is due to the wind forecast error. This can be explained by two facts: the current FMS design and the way weather forecasts are provided to ATC, air-carriers and pilot. FMS is a core-component of modern aircraft. They are made to give control sequences to the auto-pilot in a way that every aircraft follow its flight plan (in space) in an optimal way, but does not propose controls to compensate along track deviations. Then, it participates to propagate errors from weather forecast to trajectory prediction errors. In addition, weather forecasts used in aeronautics have been normalized by the International Civil Aviation Organization (ICAO), Annex 3: Meteorological Services for International Air Navigation. This text provides standards and recommended practices covering the following key areas: Meteorological Observing, Meteorological Forecasts, Meteorological Warnings to aircraft, Aircraft Meteorological reports, Communication and dissemination of Meteorological information. It follows from this ICAO regulation, that weather forecasts are provided around the globe by two meteorological centres. The weather forecast grids, established decades ago, are currently old-

fashioned compared to the actual and current meteorological services capabilities. They do not reflect neither the numerical weather forecast state of the art. Pull it together, this turns out to deteriorate the trajectory prediction accuracy.

To reduce trajectory prediction uncertainties due to wind forecast errors, several solutions were proposed. In Delahaye et al. (2003), wind field estimation is performed using Extended Kalman Filter (EKF) and a linearised aircraft dynamic model. Delahaye demonstrates for constant wind and a number of turns (with known turn rate) the accuracy of his method. Another solution, proposed and studied in Lymperopoulos et al. (2006); Lymperopoulos and Lygeros (2008a,b, 2009, 2010), consists in using statistical errors on weather forecast to get statistical errors on trajectory predictions. They formulate this problem as a high dimensional state estimation problem and use particle filtering method to reduce TP inaccuracies related to wind forecast errors. Their work was innovative as the particle filter which was developed allow them to handle the non-linear aircraft dynamics, and the results obtained demonstrate the capacity of such methods to solve the TP inaccuracy issue. The use of particle filters in air-traffic applications traces back to the tracking issue of flying objects, Blom and Bloem (2003); Gustafsson et al. (2002); Karlsson (2002); Lin et al. (2002); Nordlund (2002); Blom and Bloem (2005); Schön et al. (2005); Vermaak et al. (2005). Indeed these methods provide a convenient, effective and powerful mean to estimate signals whose dynamics are non-linear with non-Gaussian noises. However, in Lymperopoulos and Lygeros (2008a), the wind forecast error is modelled as an isotropic random field. Then the wind field error depends on the distance between two points but does not depend on the actual location neither on the meteorological phenomenon being forecast. Nevertheless, as it has been highlighted in Baehr and Huet (2011), weather forecasting error depends on the location and more particularly on the meteorological phenomenon being forecast.

In this work, we aim to reduce the hypothesis formulated about the random field using ensemble weather forecasts. Indeed ensemble weather forecasts give several atmospheric evolution scenarios which reflect the lack of knowledge about the initial state of the atmosphere. These scenarios enable to explore the uncertainties about the state of the atmosphere, Epstein (1969). Then using these atmospheric scenarios as input parameters for the trajectory predictors, we can evaluate the performance of each weather forecast member regarding the performance of the trajectory predictor with respect to the radar observations. Finally, we can give a score to each member of the ensemble weather forecast reflecting its performance. The basic idea lying behind these considerations is that aircraft experience the real wind field and that radar measurements encapsulate information about the wind aircraft experienced: aircraft are used as local moving sensor of the wind field.

From the ground point of view, the lack of knowledge about aircraft parameters is another uncertainty source. By aircraft parameters, one should understand aerodynamic parameters coming into play in the flight dynamic equations developed in Chapter 3. Their unavailability can have a negative effect on the trajectory prediction accuracy. Then, we propose to consider all the unavailable coefficients to air traffic controllers as random coefficients.

All these considerations, detailed in Chapter 3, turn the aircraft evolution processes out to be a random process influenced by a random environment with possibly unknown fixed parameters. Thus, to improve the accuracy of the trajectory prediction using radar measurements of several aircraft, we propose to formulate the high dimensional state estimation problem in distribution space. From there, we propose three novel particle filtering algorithms, named *Labeled island particle filter*, *Labeled Island particle MCMC* and *patchwork labeled island particle filter*, to solve it. The first one can handle independent aircraft from which local wind field estimations can be obtain or can fuse all aircraft measurements to give an overall estimation of homogeneous wind field. The second one tackles the triple estimation problem concerning random processes evolving in a random media with unknown fixed parameters. The third algorithm is able to estimate random wind field decomposed in homogeneous domains using aircraft trajectory processes evolving inside them. The key innovation of the methods developed here is that no specific hypothesis is needed on the wind field error underlying structure.

The performance of each algorithm is illustrated through simulation based studies. They treat the case of multiple aircraft in cruise phase, with known airspeed and aerodynamics parameters. Even if this case is utopia for ATC, as they do not have access to these parameters on the ground, these numerical experiments aim to determine whether information contained inside aircraft trajectories is sufficient to weight the ensemble weather forecast and reduce TP inaccuracies. Results obtained using ground radar information only, are promising. Proposed algorithms, each for its proper use, are able to retrieve the wind member closer to the real wind conditions. Considering the weather conditions which took place on the 22nd of May, the wind field can be decomposed in two homogeneous sub-domains. On Figure 1.3 we represent the time evolution of the wind members weight obtained using the *patchwork labeled island particle filter* for one subdomain. These weights represent the likelihood of the member of the ensemble weather forecast with respect to the air-traffic observations on the sub-domain considered. As one may observe at the beginning of the experiment all members have the same weight. As times goes some members of the ensemble weather forecast have a weight less and less important and others have a higher and higher weight. That means that regarding the air-traffic prediction performance made using the ensemble weather forecast, some members are less efficient than others comparing with the air-traffic observations, particularly member 31,26 and 19.

1.2 State estimation for random processes evolving in a random media

State estimation for random processes using their related observation process can be formulated as the estimation of the conditional expectation of the process given its observations. It follows that, for linear systems with Gaussian noises, the conditional expectation can be optimally estimated using Kalman filters, Kalman (1960); Kalman and
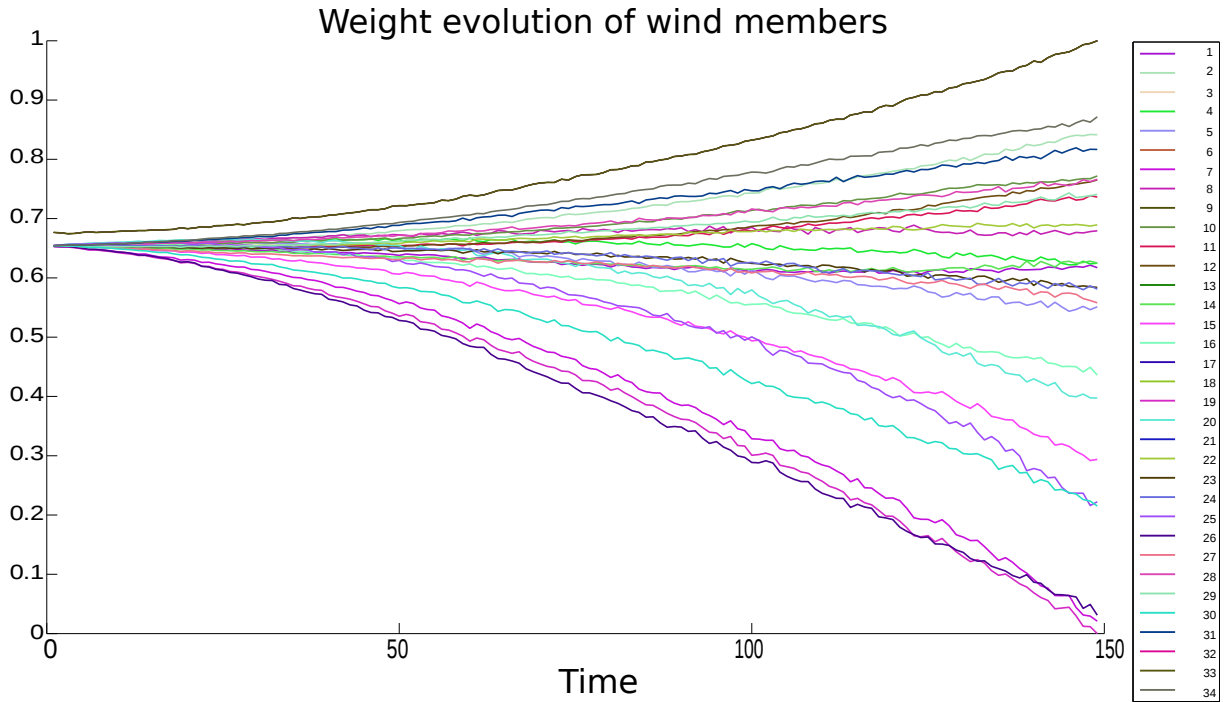
Figure 1.3: Time evolution of the ensemble weather forecasts weights thanks to the patch-work labeled island particle filter for the sub-domain 2. Time is represented on the x-coordinate. On the y-coordinate, the weight value is represented. At the beginning of the experiment, all the members of the ensemble weather forecasts are equidistributed, then some scenarios have a higher weight as time goes

Bucy (1961), in the maximum likelihood sense. Except this specific case, the optimal estimate can be approximated using particle simulation methods. These methods also known as Sequential Monte-Carlo (SMC) methods have been first applied to state space models in the series of work: Handschin and Mayne (1969); Handschin (1970); Akashi and Kumamoto (1977). From there, several algorithms to enhance the estimation obtained by particle filters were proposed, for example in Doucet (1998). Doucet proposes in his work a solution to state estimation using sequential importance sampling with resampling. Such filters also named interacting particle filters where studied for the first time in Del Moral (1996a) and applied in various domains, see Doucet and Johansen (2009) for a complete survey. Interacting particle filters are briefly presented in Chapter 2.

However, as we said previously, aircraft trajectories can be seen as a stochastic process influenced by a random field. Thus, the estimation question turns out to be a double estimation issue where the evolution kernel of the estimated random process depends on a random quantity needed to be estimated. Then classical particle filters, such as interacting particle filters are not sufficient. To solve the combined estimation problem, when the random process model shows special substructure such as in a linear stochastic state space model, the idea used consists in taking advantages of the underlying linearity structure using *Rao-Blackwellization* techniques, as in Hendeby et al. (2010); Saha and Gustafsson (2012). Such filters were introduced as mixture Kalman-filters in Chen and Liu (2000), Rao-Blackwellized particle filters in Doucet et al. (2000) and as Interacting Kalman Filters (IKF) in Del Moral (2004).

For the application case we are concerned with, aircraft dynamics are highly non-linear. Then these algorithms cannot be used without using linearisation techniques. In Özkan et al. (2013); Lundquist et al. (2014), this difficulty is overcome using Marginalized particle filter, for dynamical noises in the exponential family. Another solution proposed in Del Moral (2004) is based on interacting particle systems, taking into account both randomness sources. This idealized algorithm would be a SMC on the couple defined by the environment and the conditional law of the process evolving in this environment given the history of the environment. Nonetheless the computation of the previous conditional law is not tractable. We propose to use in this work interacting systems of interacting particles as they have been introduced in Johansen et al. (2012). There are two-level interacting particle systems. The top level is made of an environment proposition and an empirical measure approximating the law of the process evolving in the proposed environment. The second level of interacting particle gives the empirical measure. The derived algorithm is named by us as *Labeled islands particle filters* in reference to the work of Vergé in Vergé et al. (2013). To qualify the ensuing estimator, we study the $\mathbb{L}^p$ bounds error and give a first convergence result.

As we said, some aircraft parameters can be considered as fixed parameters. Then fixed parameter estimation is added to the double state estimation problem. This issue can be cast into the more general framework of joint parameter and state estimation. To overcome this question, different methods were recently developed, see for example Poyiadjis et al. (2005); Andrieu et al. (2010); Chopin et al. (2013); Crisan and Miguez (2013). In Andrieu et al. (2010), the idea used to estimate both state and parameter was to use the empirical measure obtained through particle filters inside a Markov Chain Monte-Carlo (MCMC) method. Then we propose to adapt the method proposed by Andrieu to the case of random process evolving in a random media. This gives rise to the *labeled islands particle MCMC* method.

Another issue which is at stake when one wants to estimate a random field using random process observations, is the punctuality of the random process from which we want to retrieve information on the higher dimension random field. The estimation of the random field is done along the random path of the random process, then the random process has to be followed. This question was addressed in Baehr (2009, 2010) using acquisition processes to estimate turbulence from 3D local wind measurements. Nevertheless, it is believed that by fusing several observations from different aircraft the wind field error estimation is enhanced. To fuse several observations made at different locations, the wind field error has to be homogeneous. However as we have already mention, the wind forecast error depends on the phenomenon being forecast and so is not homogeneous. Thus we extend the work made in Baehr to random field decomposed in homogeneous domains and propose an algorithm which can deal with several random processes evolving in a random environment decomposed in homogeneous sub-domains. This algorithm is named by us as *Patchwork Labeled Island Particle filters.*

1.3   Document organization

To detail what we have briefly presented in the introduction, the thesis dissertation is divided into three chapters. In Chapter 2, we develop the stochastic algorithms able to solve the estimation problem we are concerned with: estimation of random punctual processes evolving in a random medium decomposed in homogeneous sub-domains. To this end, we briefly present in Section 2.1 interacting particle system for the sake of state estimation. Then we introduce in Section 2.2, the Labeled island particle model convenient to deal with random process evolving in a random environment. Theoretical results to qualify the ensuing estimator are also detailed. In Section 2.4 we intend to build a basic model which can deal with punctual random processes evolving in a random field decomposed in homogeneous sub-domains. The subsequent algorithm is also detailed. The trajectory prediction tool we develop and use for numerical experiments is presented in Chapter 3. This chapter starts with the theoretical foundation of the aircraft dynamic equations in Section 3.1 and ends with the stochastic version of the state equations in Section 3.2. The deterministic model is transformed into a stochastic one in order to take into account uncertainties about atmosphere, aircraft parameters and initial conditions. Chapter 4 concerns the numerical part of the thesis work and gives illustrations for the different algorithms we have developed. It ends with the first estimation results obtained on a realistic simulated air-traffic and real weather ensemble forecasts. The conclusion of this thesis dissertation, Chapter 5, gives the perspectives of this pioneering work for ATM.

*"Define me first what you mean by God and I will tell you
if I believe"*

Albert Einstein

2

Particle filters for random processes evolving in a random environment

As we mention in the introduction, we want to reduce trajectory prediction inaccuracies taking into account all the uncertainties sources. To this end, we intend to estimate both aircraft parameters, e.g mass, but also the atmospheric parameters which influence the aircraft dynamics based on observations of the aircraft process. This question can be formulated as a filtering problem where the signal is evolving in a random media, the signal being the aircraft trajectory and the random media the atmosphere. Estimating a process whose evolution is influenced by a random media is an issue which is at stake in different areas. For example, in the fields of economy, when one wants to estimate the option price with an unknown volatility (see the model developed in Cont (2006)). Several area of applied probabilities tries to deal with random motions in random media. One of them is dedicated to the study of Random Walk in Random Environment, see Zeitouni (2004); Révész (2005); Bogachev (2007) for a broad survey in the domain, and try to establish under which conditions on the environment the process shows specific behaviour such as transience and recurrence. However, in this area, the random processes considered take always their value in discrete state space, e.g $\mathbb{Z}$. In our case the state space is continuous as aircraft does not evolve on a grid. Another domain where random environment are considered is when one want to study wave propagation in an unknown material. In this topic of applied mathematics, the main goal is to infer the medium properties from the propagation of waves, see Fouque et al. (2007) and reference therein for an introduction in the domain. As the aim of our study is to estimate the environment where aircraft are evolving, the question cannot be formulated as a wave equation in a random media. We choose to use Hidden Markov Model (HMM) or state space model to model our double

estimation question. Indeed, they offer a convenient mean to study stochastic dynamical systems and appear to be the most adapted framework for estimation questions.

In this chapter, we begin with the general non linear filtering theory and the particle approximation of the filtering equations. Then we detail filtering techniques well adapted for stochastic processes evolving in a random environment. Various filtering techniques are presented but only in their discrete time form. The interested reader to continuous filtering problems can refer to Mitter (1982).

2.1   Non-linear filtering techniques

Filtering problems consist in computing conditional distributions of a state signal given a sequence of observations. Kalman filter, also known as linear quadratic estimator (LQE), is an algorithm that uses a series of measurements observed over time, containing noise (random variations) and other inaccuracies, and produces estimates of unknown variables that tend to be more precise than those based on a single measurement alone. More formally, the Kalman filter operates recursively on streams of noisy input data to produce a statistically optimal estimate of the underlying system state. The filter is named after Rudolf (Rudy) E. Kálmán, one of the first developers of this theory. When the dynamics of the signal is linear and the observational noise Gaussian, the optimal solution to state estimation is given by the previous filter, Kalman (1960); Kalman and Bucy (1961). When the process takes discrete values, the estimation can be done using HMM filters, Baum and Petrie (1966); Baum et al. (1970). However when the dynamics are non-linear, as it is for aircraft dynamics (see Chapter 3), and the state space continuous another method should be used. Over the last two decades particle simulation has been widely used to solve many state estimation problems. These methods, also known as SMC methods have been first applied to state space models by Handschin and Mayne (1969); Handschin (1970) and Akashi and Kumamoto (1977). During the 1990s, several particle filters algorithm which are belonging to SMC methods were proposed. Gordon et al. proposed in Gordon et al. (1993) a new algorithm given by bootstrap filters. Independently, Kitagawa proposed in Kitagawa (1996) another solution named Monte Carlo filters. In the meantime Doucet et al. in Doucet (1998) gave a solution through sequential importance sampling with resampling (SISR). Such filters also known as interacting particle filters have been first studied by Del Moral in Del Moral (1996a) and applied in various domains, see Doucet et al. (2001); Cappe et al. (2007); Doucet and Johansen (2009) for a complete survey. Del Moral presents in Del Moral (2004) a more general framework in which filtering problems can be cast but also convergence results of the particle approximation. In this section we recall the Feynman-Kac formulation of the estimation problem, as well as its particle approximation.

2.1.1 Notations

First, let us define some notations used in the rest of the document. For $(m, n) \in \mathbb{Z}^2$ such that $m \leq n$ we denote $[\![m, n]\!] \triangleq \{m, m+1, \ldots, n\} \subset \mathbb{Z}$. We will use the vector notation $a_{m:n} \triangleq (a_m, \ldots, a_n)$. Moreover, $\mathbb{R}_+$ and $\mathbb{R}_+^*$ denote the sets of non-negative and positive real numbers respectively, and $\mathbb{N}^*$ the set of positive integers.

$\mathsf{N}(\mu, \Sigma)$ denotes a multivariate Gaussian distribution with mean μ and covariance matrix Σ.

In the sequel we assume that all random variables are defined on a common probability space $(\Omega, \mathcal{F}, \mathbb{P})$. For some given measurable space $(\mathsf{E}, \mathcal{E})$ we denote by $\mathsf{M}(\mathsf{E})$ and $\mathcal{P}(\mathsf{E}) \subset \mathsf{M}(\mathsf{E})$ the set of measures and probability measures on $(\mathsf{E}, \mathcal{E})$, respectively. In addition, we denote by $\mathsf{F}(\mathsf{E})$ the set of real-valued measurable functions on $(\mathsf{E}, \mathcal{E})$ and by $\mathcal{B}_b(\mathsf{E}) \subset \mathsf{F}(\mathsf{E})$ the set of bounded such functions for the uniform norm. For any $\nu \in \mathsf{M}(\mathsf{E})$ and $f \in \mathsf{F}(\mathsf{E})$ we denote by $\nu f \triangleq \int f(x) \, \nu(\mathrm{d}x)$ the Lebesgue integral of f under ν whenever this is well-defined. Now, given also some other $(\mathsf{Y}, \mathcal{Y})$ measurable space, an *unnormalized transition kernel* K from $(\mathsf{E}, \mathcal{E})$ to $(\mathsf{Y}, \mathcal{Y})$ is a mapping from $\mathsf{E} \times \mathcal{Y}$ to $\mathbb{R}$ such that for all $\mathsf{A} \in \mathcal{Y}$, $x \mapsto K(x, \mathsf{A})$ is a non-negative measurable function on E and for all $x \in \mathsf{E}$, $\mathsf{A} \mapsto K(x, \mathsf{A})$ is a measure on $(\mathsf{Y}, \mathcal{Y})$. If $K(x, \mathsf{Y}) = 1$ for all $x \in \mathsf{E}$, then K is called a *transition kernel* (or simply a *kernel*). The kernel K induces two integral operators, one acting on functions and the other on measures. More specifically, let $f \in \mathsf{F}(\mathsf{E})$ and $\nu \in \mathsf{M}(\mathsf{E})$ and define the measurable function

$$Kf : \mathsf{E} \ni x \mapsto \int f(y) \, K(x, \mathrm{d}y)$$

and the measure

$$\nu K : \mathcal{Y} \ni \mathsf{A} \mapsto \int K(x, \mathsf{A}) \, \nu(\mathrm{d}x)$$

whenever these quantities are well-defined. Finally, let K be as above and let L be another unnormalized transition kernels from $(\mathsf{Y}, \mathcal{Y})$ to some third measurable space $(\mathsf{Z}, \mathcal{Z})$; then we define the *product* of K and L as the unnormalized transition kernel

$$KL : \mathsf{E} \times \mathcal{Z} \ni (x, \mathsf{A}) \mapsto \int K(x, \mathrm{d}y) \, L(y, \mathsf{A})$$

from $(\mathsf{E}, \mathcal{E})$ to $(\mathsf{Z}, \mathcal{Z})$ whenever this is well-defined.

2.1.2 Non-linear filtering problems

Suppose that at every time step, the state of the Markov chain $X_n \in \mathsf{E}_n$ is partially observed by the process $Y_n \in \mathsf{F}_n$, where X_n is a Markov process with transition kernel M_n and initial distribution η_0 in a measurable space $(\mathsf{E}, \mathcal{E})$. The observation process Y_n is defined on $(\mathsf{F}_n, \mathcal{F}_n)$ and we suppose that it is related to the process by the observation function h_n such that $Y_n = h_n(X_n, V_n)$ where V_n is a Markovian observation noise distributed according to the probability measure q_n. The filtering problem consists in computing the conditional distributions of $(X_0, \ldots, X_n)$ given the observations $(Y_0, \ldots, Y_n)$.

Suppose that for every time step n, the laws $h_n(X_n, V_n)$ and V_n are absolutely continuous and $g_n(x_n, .)$ is the corresponding density, then we get the following formula for the likelihood function:

$$\mathbb{P}(Y_n \in \mathrm{d}y_n | X_n = x_n) = g_n(x_n, y_n)q_n(\mathrm{d}y_n)$$

From which, we deduce the updating filter:

$$\mathbb{P}((X_0, \ldots, X_n) \in \mathrm{d}(x_0, \ldots, x_n) | Y_0 = y_0, \ldots, Y_n = y_n) =$$
$$\frac{1}{\hat{\mathscr{Z}}_n} \left\{ \prod_{p=0}^{n} g_p(x_n, y_n) \right\} \mathbb{P}((X_0, \ldots, X_n) \in \mathrm{d}(x_0, \ldots, x_n)) \quad (2.1)$$

where the normalizing constant $\hat{\mathscr{Z}}_n$ is given by:

$$\hat{\mathscr{Z}}_n \triangleq \int \left\{ \prod_{p=0}^{n} g_p(x_n, y_n) \right\} \mathbb{P}((X_0, \ldots, X_n) \in \mathrm{d}(x_0, \ldots, x_n)).$$

Using the fact that X_n is a Markov chain of transition kernel M_n and initial distribution η_0, we have that:

$$\mathbb{P}((X_0, \ldots, X_n) \in \mathrm{d}(x_0, \ldots, x_n)) = \eta_0(\mathrm{d}x_0)M_1(x_0, \mathrm{d}x_1) \ldots M_n(x_{n-1}, \mathrm{d}x_n)$$

Then (2.1) can be rewritten as follows:

$$\mathbb{P}((X_0, \ldots, X_n) \in \mathrm{d}(x_0, \ldots, x_n) | Y_0 = y_0, \ldots, Y_n = y_n) =$$
$$\frac{1}{\hat{\mathscr{Z}}_n} \left\{ \prod_{p=0}^{n} g_p(x_n, y_n) \right\} \eta_0(\mathrm{d}x_0)M_1(x_0, \mathrm{d}x_1) \ldots M_n(x_{n-1}, \mathrm{d}x_n) \quad (2.2)$$

We can also define the prediction filter which allows the prediction of the future state using the previous observations:

$$\mathbb{P}((X_0, \ldots, X_{n+1}) \in \mathrm{d}(x_0, \ldots, x_{n+1}) | Y_0 = y_0, \ldots, Y_n = y_n) =$$
$$\frac{1}{\mathscr{Z}_{n+1}} \left\{ \prod_{p=0}^{n} g_p(x_n, y_n) \right\} \eta_0(\mathrm{d}x_0)M_1(x_0, \mathrm{d}x_1) \ldots M_{n+1}(x_n, \mathrm{d}x_{n+1}) \quad (2.3)$$

where $\mathscr{Z}_{n+1} \triangleq \int \left\{ \prod_{p=0}^{n} g_p(x_n, y_n) \right\} \mathbb{P}((X_0, \ldots, X_{n+1}) \in \mathrm{d}(x_0, \ldots, x_{n+1}))$

The measure defined by (2.2) and (2.3), corresponds to Feynman-Kac path measures denoted respectively by $\hat{\mathbb{Q}}_n$ and $\mathbb{Q}_{n+1}$ (Del Moral (2004)).

Let fix the observation sequence $Y_0 = y_0, \ldots, Y_n = y_n$ and set $G_n(x_n) \triangleq g_n(x_n, y_n)$. Define the nth-time marginals η_n and $\hat{\eta}_n$ of the measures $\mathbb{Q}_n$ and $\hat{\mathbb{Q}}_n$ for any bounded

14

measurable functions $f_n \in \mathcal{B}_b(\mathsf{E}_n)$ by:

$$\eta_n(f_n) = \gamma_n(f_n)/\gamma_n(1) \tag{2.4}$$

with $\gamma_n(f_n) \triangleq \mathbb{E}_{\eta_0}\left[f_n(X_n)\prod_{p=0}^{n-1}G_p(X_p)\right]$ and

$$\hat{\eta}_n(f_n) = \hat{\gamma}_n(f_n)/\hat{\gamma}_n(1) \tag{2.5}$$

where $\hat{\gamma}_n(f_n) \triangleq \mathbb{E}_{\eta_0}\left[f_n(X_n)\prod_{p=0}^{n}G_p(X_p)\right]$.

For every time step $n \geq 0$ and $f_n \in \mathcal{B}_b(\mathsf{E}_n)$, (2.4) and (2.5) are related by the following relation:

$$\hat{\eta}_n(f_n) = \eta_n(G_n f_n)/\eta_n(G_n) \tag{2.6}$$

and

$$\eta_{n+1} = \hat{\eta}_n M_{n+1} \tag{2.7}$$

Equation (2.6) can be written as a Boltzmann-Gibbs transformation, Ψ_n, associated to the potential function G_n, where the Boltzmann Gibbs measure, $\Psi_n(\eta)$ is defined for any $\eta \in \mathcal{P}(\mathsf{E}_n)$ by:

$$\Psi_n(\eta)(\mathrm{d}x_n) = \frac{1}{\eta(G_n)}G_n(x_n)\eta(\mathrm{d}x_n) \tag{2.8}$$

Using (2.8), we define the mapping Φ_n from $\mathcal{P}(\mathsf{E}_{n-1})$ to $\mathcal{P}(\mathsf{E}_n)$ for any $\eta \in \mathcal{P}(\mathsf{E}_{n-1})$ by:

$$\Phi_n(\eta) \triangleq \Psi_{n-1}(\eta)M_n \tag{2.9}$$

Then we resume the updating-prediction filtering recursions by the following diagram:

$$\eta_n \xrightarrow{\text{updating}} \hat{\eta}_n = \Psi_n(\eta_n) \xrightarrow{\text{prediction}} \eta_{n+1} = \hat{\eta}_n M_{n+1} \tag{2.10}$$

These processes cannot be computed except when the processes involved are linear with Gaussian dynamic and observation noises, for which an explicit solution was given by Kalman and Bucy, Kalman (1960); Kalman and Bucy (1961). Besides, Del Moral gives in Del Moral (1996b) a solution to approximate theses quantities based upon interacting particles for more general cases.

2.1.3 Particle filters

Particle filters are particle approximations of the conditional distributions η_n and $\hat{\eta}_n$ defined by (2.4) and (2.5) respectively. In order to present the particle approximation based on Feynman-Kac flow measures, we introduce McKean models which are special cases of Feynman-Kac dynamic well adapted to deal with filtering problem. As we have seen, Feynman-Kac measures evolve sequentially in two steps, this recursion can be written in the following form:

$$\eta_{n+1} = \Phi_n(\eta_n) \tag{2.11}$$

This last equation (2.11) can be rewritten:

$$\eta_{n+1} = \eta_n K_{n+1,\eta_n} \tag{2.12}$$

where K_{n+1,η_n} is a non unique collection of Markov kernels from E_n to E_{n+1} which satisfy the compatibility condition, $\eta K_{n+1,\eta} = \Phi_n(\eta)$, with Φ_n defined by (2.9). The kernel $K_{n+1,\eta}$ is called the McKean interpretation of the flow η, it is defined by:

$$K_{n+1,\eta} = S_{n,\eta} M_{n+1}$$

The McKean interpretation, $K_{n+1,\eta}$, is far from being unique and the kernel $S_{n,\eta}$ can be defined in several ways. For example, the compatibility condition is satisfied by both following kernels:

- $S_{n,\eta}(x_n, .) = \Psi_n(\eta)(.)$

- $S_{n,\eta}(x_n, .) = G_n(x_n)\delta_{x_n}(.) + (1 - G_n(x_n))\Psi_n(\eta)(.)$

Once one has chosen the selection kernel $S_{n,\eta}$,(2.10) can be rewritten in the following form:

$$\eta_n \xrightarrow{\text{updating}} \hat{\eta}_n = \eta_n S_{n,\eta_n} \xrightarrow{\text{prediction}} \eta_{n+1} = \hat{\eta}_n M_{n+1} \tag{2.13}$$

Del Moral et al. show in Del Moral et al. (2001) that the error variance is reduced and that the algorithm is more stable using the second kernel. Other kernels exist giving more precise estimation, however the computation cost being higher we choose to use the second kernel for the rest of the study.

When the likelihood function G_n is strictly positive and bounded by one, the second selection kernel can be interpreted as a random walk where the walker, the particle, remains in the same site with probability G_n, otherwise it jumps to a new location according to the Boltzmann Gibbs distribution $\Psi_n(\eta)$. Then the selection kernel $S_{n,\eta}$ favours regions with hight potential. For filtering problems, recalling that G_n corresponds to the likelihood function, that means that particles close to the current observation are more likely to be kept.

Let N be some positive integer. A N-interacting particle system associated with the sequence $(G_n, M_n)_{n\in\mathbb{N}}$ and the initial distribution η_0, is a sequence of non-homogeneous Markov chain, denoted by ξ_n, taking value in the product space E_n^N,

$$\xi_n \triangleq (\xi_n^i)_{i=1}^N = (\xi_n^1, \ldots, \xi_n^N) \in \mathsf{E}_n^N \triangleq \underbrace{\mathsf{E}_n \times \ldots \times \mathsf{E}_n}_{N \text{ times}}.$$

The initial state of the Markov chain ξ_0 consists in N independent random variables with common distribution η_0. The interacting particle system $(\xi_n^i)_{i=1}^N$ explores the state space E_n and with the dynamic given to it, empirically samples the law η_n. Each particle i of the system consists in a random variable $\xi_n^i \in \mathsf{E}_n$. The ensuing empirical process denoted

by η_n^N is defined by:

$$\eta_n^N \triangleq \frac{1}{N} \sum_{i=1}^{N} \delta_{\xi_n^i}. \tag{2.14}$$

The elementary transition of the Markov chain ξ_n from E_n^N to E_{n+1}^N is given for any $x_n \triangleq (x_n^1, \ldots, x_n^N) \in \mathsf{E}_n^N$ by:

$$\mathbb{P}_{\eta_0}^N (\xi_{n+1} \in \mathrm{d}x_{n+1} \,|\, \xi_n) \triangleq \prod_{i=1}^{N} \overline{\Phi}_{n+1}(\eta_n^N)(\mathrm{d}x_{n+1}^i)$$

$$= \prod_{i=1}^{N} S_{n,\eta_n^N} M_{n+1}(\xi_n^i, \mathrm{d}x_{n+1}^i)$$

where S_{n,η_n^N} is given by:

$$S_{n,\eta_n^N}(\xi_n^i, .) = G_n(\xi_n^i)\delta_{\xi_n^i}(.) + (1 - G_n(\xi_n^i))\Psi_n(\eta_n^N)(.)$$

with

$$\Psi_n(\eta_n^N)(\mathrm{d}x) \triangleq \sum_{j=1}^{N} \frac{G_n(\xi_n^j)}{\sum\limits_{k=1}^{N} G_n(\xi_n^k)} \delta_{\xi_n^j}(\mathrm{d}x)$$

In other words, the evolution of the particle swarm consists in two steps : a selection and a mutation. In the selection step, the particles $(\xi_n^i)_{i=1}^N$ are selected/rejected with probability proportional to their potentials $(G_n(\xi_n^i))_{i=1}^N$, rejected particles are then resample multinomially among the particle swarm. Then the mutation step is performed independently using the kernel M_{n+1}. The evolution scheme of the particles is illustrated on and detailed in .

Algorithm 1 Interacting Particle Filter - IPF

Require: η_0, $(M_p)_{p=0}^n$ et $(S_p)_{p=0}^n$
Ensure: Particle approximation of η_n
  $\boxed{\text{Begin}}$
  1. INITIALIZATION $p = 0$
  Sample $(\xi_0^i)_{i=1}^N \overset{i.i.d}{\sim} \eta_0$,
  for $p = 0, \ldots, n$ **do**
    3. SELECTION OF PARTICLES
    Particles are accepted/rejected with probability proportional to $\left(G_p(\xi_p^i)\right)_{i=1}^N$:
    For accepted particles: $\hat{\xi}_p^i = \xi_p^i$
    If rejected, particles are replaced by other particles chosen among all particles in the following way:
    Sample $I_p = (I_p^i)_{i=1}^N$ according to a multinomial distribution with probability $\propto \left(G_p(\xi_p^i)\right)_{i=1}^N$, then:
    $\hat{\xi}_p^i = \xi_p^{I_p^i}$
    4. MUTATION OF ISLAND
    Sample independently ξ_{p+1}^i according to $M_p(\hat{\xi}_p^i, .)$
  end for
  $\boxed{\text{End}}$
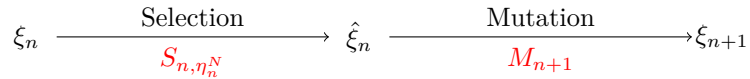
Figure 2.1: Evolution scheme of the interacting particle system.

Using this algorithm one can empirically sample the measure η_n at each time step n using the empirical measure η_n^N. The $\mathbb{L}^p$ error estimates, the almost sure convergence and the asymptotic behaviour of the estimation error are available to qualify the subsequent estimator η_n^N, see Del Moral (2004). We recall here one basic result which is going to be extended in Section 2.2 for random processes in random environment.

Theorem 2.1.1 (Del Moral (2004), Theorem 7.4.4 page 246)**.** *For every $n \geq 0$ and $p \geq 1$, there exist finite constants C_n^p such that:*

$$\forall f_n \in \mathcal{B}_b(\mathsf{E}_n), \quad \mathbb{E}_{\eta_0}\left[|\eta_n^N(f_n) - \eta_n(f_n)|^p\right]^{1/p} \leq \frac{C_n^p}{\sqrt{N}}\|f_n\| \tag{2.15}$$

Moreover we have that for any $f_n \in \mathcal{B}_b(\mathsf{E}_n)$ and $n \geq 0$,

$$\eta_n^N(f_n) \xrightarrow{a.s} \eta_n(f_n) \text{ as } N \longrightarrow \infty$$

This result was presented in Del Moral and Guionnet (2001), as well as the time uniform $\mathbb{L}^p$ bound. From there, many other results to qualify the particle approximations of Feynman-Kac measure are available in the literature, see Chapters 2-3 in Doucet et al. (2001), Crisan and Doucet (2002) and for a full treatise Del Moral (2004). Recent works on consistency and asymptotic normality for more general classes of algorithms can be found in Chopin (2004); Künsch (2005); Douc and Moulines (2007) and Del Moral et al. (2012).

2.2 Non-linear filtering for stochastic processes evolving in a random environment

The precedent section recalls general definitions about Feynman-Kac formalism and how to use it in order to estimate signals using observations. The signal to estimate was supposed to be a Markov chain with kernel transition M_n. Recalling the introduction, our problem consists in a double estimation. One concerns the environment and the other one the random process itself. Then, particle filters as presented in the precedent section cannot be used.

To solve the combined problem of state and fixed parameter estimation, a wide variety of methods have been studied. For linear dynamic systems, basic estimation techniques are available, see Ljung (1998). For more general state space models, the classical method used is based on extended Kalman filter. However it has been shown that this approach may give biased and divergent estimations, Ljung (1979). Kitagawa in Kitagawa (1998)

has first proposed the use of a particle filter to estimate simultaneously the states and the parameters in a general non-linear non-Gaussian state space model. The idea was to augment the state vector with unknown parameters and then perform particle filter estimation on the augmented state space model. However, the main drawback of considering the parameter as an auxiliary variable is that the number of particles needed to have a rather acceptable estimation explodes with the dimension, see Liu and West (2001). Therefore augmenting the state space dimension can be inefficient. Nevertheless Ching et al. (2006) show in their paper comparative results between particle filters and extended Kalman filters on several examples. It indicates that particle filters give better results especially when non linearity cannot be neglected. Another recent solution was given by Andrieu et al. (2010) and consists in using sequential Monte Carlo methods inside Markov chain Monte Carlo methods. However this method is not recursive and cannot be performed on-line. For recursive estimation, when models show special substructure such as in linear stochastic state space model with unknown parameters, the idea is to take advantage of the underlying linearity structure using *Rao-Blackwellization* techniques as in Hendeby et al. (2010); Saha and Gustafsson (2012). Such filters have been introduced as mixture Kalman filters in Chen and Liu (2000), Rao-Blackwellized particle filters in Doucet et al. (2000); Li et al. (2004); Schön et al. (2005) and as interacting Kalman filters (IKF) in Del Moral (2004); Zghal et al. (2014).

However when the dynamics are non-linear, as for aircraft dynamics, an analytic resolution is not possible without making further model simplifications. A method based on interacting particle systems, which takes into account the randomness due to the environment and also the randomness coming from the process itself, was proposed by Del Moral in Del Moral (2004). This idealized algorithm would be a sequential Monte Carlo (SMC) algorithm on the couple defined by the random environment and the conditional law of the process evolving in this random environment given the history of the environment. Nonetheless, the calculation of the previous conditional law is not tractable in practice when the dynamics are non-linear. Therefore another approximation level is necessary in order to estimate this conditional law. In this section, we recall the Feynman-Kac formulation of the filtering problem for random process in random media taken from Del Moral (2004). Then we propose to use interacting systems of interacting particles as it has been suggested by Johansen et al. (2012). These interacting systems can be seen as a two-level interacting particle system. The top level particles are composed of an environment proposition and an empirical measure which gives an approximation of the process law evolving in the proposed environment. The empirical measure is obtained by the second level of interacting particles. This nested structure was used in Montemerlo et al. (2002) to estimate the pose of a mobile robot and positions of people surrounding it, in Baehr (2010) for mean field processes and in Ichard et al. (2013) for air-traffic process in random atmospheric environment.

2.2.1 Filtering problem for a random process in a random environment

Using the same notations as in Section 2.1.1, suppose that at every time step $n \geq 0$, the evolution kernel M_n of the Markov chain X_n depends on the realization of another random process Θ_n. This section is devoted to the Feynman-Kac formulation of the filtering problem for random processes in random media. In order to avoid any confusion, all the quantities which refer to the random process Θ_n (respectively X_n) may be identified by the exponent Θ (respectively X).

Let (Θ_n, X_n) be an $\mathsf{E}_n \triangleq (\mathsf{E}_n^\Theta, \mathsf{E}_n^X)$-valued Markov chain which is partially observed by the process $Y_n \in \mathsf{F}_n$. Suppose that the process Θ_n is a Markov process of transition kernel M_n^Θ and initial distribution η_0^Θ which influences the evolution of the process X_n through its evolution kernel. Then suppose that X_n is also a Markov process with transition kernel $M_{\theta_n,n}^X$ and initial distribution $\eta_{\theta_0}^X$.

The observation process Y_n is defined on $(\mathsf{F}_n, \mathcal{F}_n)$ and we suppose that it is related to the process by the observation function h_n such that $Y_n = h_n(X_n, \Theta_n, V_n)$ where V_n is a Markovian observation noise distributed according to the probability measure q_n. The filtering problem consists in computing the conditional distributions of $((\Theta_0, X_0), \ldots, (\Theta_n, X_n))$ given the observations $(Y_0, \ldots, Y_n)$.

Suppose that for every time step n, the laws $h_n(\Theta_n, X_n, V_n)$ and V_n are absolutely continuous and $g_n(\theta_n, x_n, .)$ is the corresponding density, then we have the following formula:

$$\mathbb{P}(Y_n \in \mathrm{d}y_n | X_n = x_n, \Theta_n = \theta_n) = g_n(\theta_n, x_n, y_n) q_n(\mathrm{d}y_n)$$

The modelling of the filtering problem corresponds to a classical Feynman-Kac formulation in a random environment. In this section we recall some important definitions and results. A complete overview can be found in Del Moral (2004).

Traditional Feynman-Kac path measure

In this section we consider both the evolution of the environment and the stochastic process inside this environment, the traditional Feynman Kac path measure allow us to model the filtering problem.

The stochastic process $\{\Theta_n, X_n, Y_n\}_{n \geq 0}$ is a Markov chain taking value in E_n with $\mathsf{E}_n \triangleq \mathsf{E}_n^\Theta \times \mathsf{E}_n^X \times \mathsf{F}_n$ under $\mathbb{P}_n$ with respect to its natural filtration. Its transition kernel T_n from E_{n-1} to E_n is defined by:

$$T_n((\theta_{n-1}, x_{n-1}, y_{n-1}), \mathrm{d}(\theta_n, x_n, y_n)) = g_n(\theta_n, x_n, y_n) M_n^\Theta(\theta_{n-1}, \mathrm{d}\theta_n) M_{\theta_n,n}^X(x_{n-1}, \mathrm{d}x_n) q_n(\mathrm{d}y_n)$$
$$(2.16)$$

The initial distribution of this chain is denoted by η_0 and given by:

$$\eta_0(\mathrm{d}(\theta_0, x_0, y_0)) = \eta_0^\Theta(\mathrm{d}\theta_0) \eta_{\theta_0}^X(\mathrm{d}x_0) g_0(\theta_0, x_0, y_0) q_0(dy_0) \qquad (2.17)$$

where $\eta_0^\Theta \in \mathcal{P}(\mathsf{E}_0^\Theta)$ and $\eta_{\theta_0}^X \in \mathcal{P}(\mathsf{E}_0^X)$.

Now, we fix the sequence of observations $Y = y$ and we define the functions G_n, for $n \geq 0$ by:

$$G_n(\theta_n, x_n) \triangleq g_n(\theta_n, x_n, y_n)$$

One can gets that the conditional probability of the sequence $(\Theta_{0:n}, X_{0:n})$ given the sequence of observations $Y_{0:n-1} = y_{0:n-1}$, is given by:

$$\mathbb{P}_{\eta_0,n}\left((\Theta_{0:n}, X_{0:n}) \in d(\theta_{0:n}, x_{0:n}) \big| Y_{0:n-1} = y_{0:n-1}\right) = \frac{1}{\mathcal{Z}_n}\left\{\prod_{p=0}^{n-1} G_p(\theta_p, x_p)\right\} \eta_0\left(d(\theta_0, x_0)\right)$$
$$M_1^\Theta(\theta_0, d\theta_1)M_{\theta_1,1}^X(x_0, dx_1) \ldots M_n^\Theta(\theta_{n-1}, d\theta_n)M_{\theta_n,n}^X(x_{n-1}, dx_n) \quad (2.18)$$

with normalizing constant:

$$\mathcal{Z}_n = \mathbb{E}_{\eta_0}\left[\prod_{p=0}^{n-1} G_p(\Theta_p, X_p)\right] > 0,$$

We denote by $\mathbb{Q}_{\eta_0,n}$ the quantity defined by (2.18) which corresponds to the traditional Feynman-Kac path measure. We denote by $\hat{\mathbb{Q}}_{\eta_0,n}$ the updated version of $\mathbb{Q}_{\eta_0,n}$ which is given by:

$$\hat{\mathbb{Q}}_{\eta_0,n}(d((\theta_0, x_0), \ldots, (\theta_n, x_n))) = \mathbb{P}_{\eta_0,n}\left((\Theta_{0:n}, X_{0:n}) \in d(\theta_{0:n}, x_{0:n}) \big| Y_{0:n} = y_{0:n}\right)$$
$$= \frac{1}{\hat{\mathcal{Z}}_n}\left\{\prod_{p=0}^{n} G_p(\theta_p, x_p)\right\} \eta_0\left(d(\theta_0, x_0)\right)$$
$$M_1^\Theta(\theta_0, d\theta_1)M_{\theta_1,1}^X(x_0, dx_1) \ldots M_n^\Theta(\theta_{n-1}, d\theta_n)M_{\theta_n,n}^X(x_{n-1}, dx_n)$$
$$(2.19)$$

where $\hat{\mathcal{Z}}_n \triangleq \mathbb{E}_{\eta_0}\left[\prod_{p=0}^{n} G_p(\Theta_p, X_p)\right] = \mathcal{Z}_{n+1}$. As in the classical filtering problem we could define a particle approximation of the marginal Feynman-Kac measure $\mathbb{Q}_n$ and $\hat{\mathbb{Q}}_n$. However as we mention in the introduction of this section, increase the dimension of the state space makes the number of particles needed to obtain a rather good estimation explodes, see Liu and West (2001). In addition, in the context of aircraft trajectory prediction, the environment state space is quite large : approximately 10^5. Therefore we develop another model which allows one to consider the law of the stochastic process X_n as a stochastic process itself. To this end we introduce the quenched Feynman-Kac flow of measure $\eta_{\hat{\theta}_{0:n},n}^X$.

Quenched process

Fix the environment sequence $\Theta_{0:n} = \theta_{0:n} \in \prod\limits_{p=0}^{n} \mathsf{E}_p^\Theta$, one gets:

$$\mathbb{P}_{\theta_{0:n},n}\left(X_{0:n} \in d(x_0, \ldots, x_n) | Y_{0:n-1} = (y_0, \ldots, y_{n-1})\right)$$
$$= \frac{1}{\mathcal{Z}_{\theta_{0:n},n}} \left\{ \prod_{p=0}^{n-1} G_{p,\theta_p}(x_p) \right\} \eta_{\theta_0}^X(\mathrm{d}x_0) M_{\theta_1,1}^X(x_0, \mathrm{d}x_1) \ldots M_{\theta_n,n}^X(x_{n-1}, \mathrm{d}x_n) \quad (2.20)$$

with normalizing constant:

$$\mathcal{Z}_{\theta_{0:n},n} = \mathbb{E}_{\eta_{\theta_0}^X}\left[\prod_{p=0}^{n-1} G_{p,\theta_p}(X_p) \right] > 0,$$

and random potential functions:

$$G_{p,\theta_p} : x_p \in \mathsf{E}_p^X \mapsto G_{p,\theta_p}(x_p) = G_p(\theta_p, x_p) \quad (2.21)$$

The quantity defined by (2.20) is also denoted by $\mathbb{Q}_{\theta_{0:n},n}$ and called the quenched Feynman-Kac path measure. We denote the updated version as before by $\hat{\mathbb{Q}}_{\theta_{0:n},n}$ given by:

$$\hat{\mathbb{Q}}_{\theta_{0:n},n}(\mathrm{d}(x_0, \ldots, x_n)) = \mathbb{P}_{\theta_{0:n},n}\left(X_{0:n} \in \mathrm{d}(x_0, \ldots, x_n) \big| Y_{0:n} = (y_0, \ldots, y_n)\right)$$
$$= \frac{1}{\hat{\mathcal{Z}}_{\theta_{0:n},n}} \left\{ \prod_{p=0}^{n} G_{p,\theta_p}(x_p) \right\} \eta_{\theta_0}^X(\mathrm{d}x_0) \quad (2.22)$$
$$M_{\theta_1,1}^X(x_0, \mathrm{d}x_1) \ldots M_{\theta_n,n}^X(x_{n-1}, \mathrm{d}x_n)$$

where $\hat{\mathcal{Z}}_{\theta_{0:n},n} \triangleq \mathbb{E}_{\eta_{\theta_0}^X}\left[\prod\limits_{p=0}^{n} G_{p,\theta_p}(X_p) \right]$.

We can associate to it the quenched distribution flow denoted by $\eta_{\theta_{0:n},n}^X$ which is defined for all $f_n \in \mathcal{B}_b(\mathsf{E}_n^X)$ as follow:

$$\eta_{\theta_{0:n},n}^X = \gamma_{\theta_{0:n},n}^X(f_n)/\gamma_{\theta_{0:n},n}^X(1) \quad (2.23)$$

where the unnormalized Feynman-Kac measure $\gamma_{\theta_{0:n},n}^X$ is given for all $f_n \in \mathcal{B}_b(\mathsf{E}_n^X)$ by:

$$\gamma_{\theta_{0:n},n}^X \triangleq \mathbb{E}_{\eta_{\theta_0}^X}\left[f_n(X_n) \prod_{p=0}^{n-1} G_{\theta_p,p}(X_p) \right]. \quad (2.24)$$

We can notice that the normalized Feynman Kac measure as in the precedent section corresponds to the prediction step in a Bayesian framework:

$$\eta_{\theta_{0:n},n}^X = \mathrm{Law}(X_n | Y_{0:n-1} = (y_0, \ldots, y_{n-1}), \Theta_{0:n} = (\theta_0, \ldots, \theta_n))$$

The updated version of this distribution denoted by $\hat{\eta}_{\theta_{0:n},n}^X$ which corresponds to the

updating filter is given for all $f_n \in \mathcal{B}_b(\mathsf{E}_n^X)$ by:

$$\hat{\eta}_{\theta_{0:n},n}^X = \hat{\gamma}_{\theta_{0:n},n}^X(f_n)/\hat{\gamma}_{\theta_{0:n},n}^X(1) \tag{2.25}$$

where the unnormalized Feynman-Kac measure $\hat{\gamma}_{\theta_{0:n},n}^X$ is given for all $f_n \in \mathcal{B}_b(\mathsf{E}_n^X)$ by:

$$\hat{\gamma}_{\theta_{0:n},n}^X \triangleq \mathbb{E}_{\eta_{\theta_0}^X}\left[f_n(X_n)\prod_{p=0}^n G_{\theta_p,p}(X_p)\right].$$

As it is the case for classical filtering problem, quantities defined by (2.23) and (2.25) are related by the following operations :

$$\hat{\eta}_{\theta_{0:n},n}^X(f_n) = \eta_{\theta_{0:n},n}^X(G_{\theta_n,n}f_n)/\eta_{\theta_{0:n},n}^X(G_{\theta_n,n}) \tag{2.26}$$

and

$$\eta_{\theta_{0:n+1},n+1}^X = \hat{\eta}_{\theta_{0:n},n}^X M_{\theta_{n+1},n+1}^X \tag{2.27}$$

Equation (2.26) can be written as a Boltzmann-Gibbs transformation, $\Psi_{\theta_n,n}^X$, associated to the potential function $G_{\theta_n,n}$, where the Boltzmann Gibbs measure, $\Psi_{\theta_n,n}^X(\eta_{\theta_{0:n},n}^X)$ is defined for any $\eta_{\theta_{0:n},n}^X \in \mathcal{P}(\mathsf{E}_n^X)$ by:

$$\Psi_{\theta_n,n}^X(\eta_{\theta_{0:n},n}^X)(\mathrm{d}x_n) = \frac{1}{\eta_{\theta_{0:n},n}^X(G_{\theta_n,n})}G_{\theta_n,n}(x_n)\eta_{\theta_{0:n},n}^X(\mathrm{d}x_n) \tag{2.28}$$

Using (2.28), we define the mapping Φ_n^X from $\mathcal{P}(\mathsf{E}_{n-1}^X)$ to $\mathcal{P}(\mathsf{E}_n^X)$ for any $\eta_{\theta_{0:n-1},n-1}^X \in \mathcal{P}(\mathsf{E}_{n-1}^X)$ by:

$$\begin{aligned}
\Phi_n^X : \left(\mathsf{E}_{n-1}^\Theta \times \mathsf{E}_n^\Theta\right) \times \mathcal{P}(\mathsf{E}_{n-1}^X) &\rightarrow \mathcal{P}(\mathsf{E}_n^X) \\
\left((\theta_{n-1},\theta_n),\eta_{\theta_{0:n-1},n-1}^X\right) &\mapsto \Psi_{\theta_{n-1},n-1}^X(\eta_{\theta_{0:n-1},n-1}^X)M_{\theta_n,n}^X
\end{aligned} \tag{2.29}$$

Then we resume the updating-prediction filtering recursions by the following diagram:

$$\eta_{\theta_{0:n-1},n-1}^X \xrightarrow{\text{updating}} \hat{\eta}_{\theta_{0:n-1},n-1}^X = \Psi_{\theta_n,n}^X(\eta_{\theta_{0:n-1},n-1}^X) \xrightarrow{\text{prediction}} \eta_{\theta_{0:n},n}^X = \hat{\eta}_{\theta_{0:n-1},n-1}^X M_{\theta_n,n}^X \tag{2.30}$$

As it was done for the classical filtering problem, we write the McKean interpretation of the quenched Feynman-Kac measure $\eta_{\theta_{0:n},n}^X$. The non linear recursion (2.29) can be rewritten in the following recursive form:

$$\eta_{\theta_{0:n},n}^X = \eta_{\theta_{0:n-1},n-1}^X K_{n,\eta_{\theta_{0:n-1},n-1}^X}^X \tag{2.31}$$

where $K_{n,\eta_{\theta_{0:n-1},n-1}^X}^X$ is a transition kernel defined by:

$$K_{n,\eta_{\theta_{0:n-1},n-1}^X}^X = S_{n-1,\eta_{\theta_{0:n-1},n-1}^X} M_{\theta_n,n}^X \tag{2.32}$$

with $S_{n-1,\eta_{\theta_{0:n-1},n-1}^X}$ a selection kernel. The McKean interpretation being not unique,

the selection kernel $S_{n-1,\eta^X_{\theta_{0:n-1},n-1}}$ can be written in several ways. As for the classical algorithm we choose the following kernel:

$$S_{n-1,\eta^X_{\theta_{0:n-1},n-1}}(x_{n-1},.) = G_{n-1,\theta_{n-1}}(x_{n-1})\delta_{x_{n-1}}(.) + (1 - G_{n-1,\theta_{n-1}}(x_{n-1}))\Psi^X_{\theta_{n-1},n-1}(\eta^X_{\theta_{0:n-1},n-1})(.)$$

These processes cannot be computed except when the processes involved are linear with Gaussian dynamic and observation noises, for which an explicit solution was given by Kalman and Bucy Kalman (1960); Kalman and Bucy (1961). Besides, in Section 2.1.3 we introduce particle filters which is a solution to approximate these quantities based upon interacting particles. The remaining problem here, is that we do not know the environment realization. Then, the quenched Feynman-Kac flow cannot be used to model our problem. Therefore, we have to consider the environment as a random process also.

Random distribution process

As we do not know the random environment where the stochastic process evolves, the quenched Feynman-Kac measure cannot be used in order to model the law of the filtering problem. So we have to use another quantity which is a third Feynman-Kac measure but this time in distribution space, to this end we introduce the sequence $\overline{X}_n = (\Theta_n, \eta^X_{\Theta_{0:n},n}) \in \overline{\mathsf{E}}_n \triangleq \mathsf{E}^\Theta_n \times \mathcal{P}(\mathsf{E}^X_n)$.

As it has been shown by Del Moral in Del Moral (2004), p. 85 , the pair process is a Markov chain.

Proposition 2.2.1. *The stochastic process $\overline{X}_n$ is a Markov chain under $\mathbb{P}_{\eta_0}$ with transition kernel $\overline{M}_n$ defined for all $\overline{f}_n \in \mathcal{B}_b(\overline{\mathsf{E}}_n)$ and $(\theta_n, \eta^X_{\theta_{0:n},n}) \in \overline{\mathsf{E}}_n$ by:*

$$\overline{M}_n((\theta_{n-1}, \eta^X_{\theta_{0:n-1},n-1}), \mathrm{d}(\theta_n, \eta^X_{\theta_{0:n},n}))(\overline{f}_n)$$
$$\triangleq \int_{\mathsf{E}^\Theta_n} M^\Theta_n(\theta_{n-1}, \mathrm{d}\theta_n)\overline{f}_n(\theta_n, \Phi^X_n(\theta_{n-1}, \theta_n, \eta^X_{\theta_{0:n-1},n-1})) \quad (2.33)$$

and initial distribution, denoted by $\overline{\eta}_0 \in \mathcal{P}(\overline{\mathsf{E}}_0)$ given by:

$$\overline{\eta}_0(\mathrm{d}(u,\nu)) = \eta^\Theta_0(\mathrm{d}u)\delta_{\eta^X_{\theta_0}}(\mathrm{d}\nu)$$

Proof. $\forall \overline{f}_n \in \mathcal{B}_b(\overline{\mathsf{E}}_n)$:

$$\mathbb{E}_{\overline{\eta}_0}[\overline{f}_n(\overline{X}_n) \mid \sigma(\overline{X}_0, \ldots, \overline{X}_{n-1})] = \mathbb{E}_{\overline{\eta}_0}[\overline{f}_n(\Theta_n, \eta^X_{\Theta_{0:n},n}) \mid \sigma(\overline{X}_0, \ldots, \overline{X}_{n-1})]$$
$$= \mathbb{E}_{\overline{\eta}_0}[\overline{f}_n(\Theta_n, \Phi^X_n\left((\Theta_{n-1}, \Theta_n), \eta^X_{\Theta_{0:n-1},n-1}\right) \mid \sigma(\overline{X}_0, \ldots, \overline{X}_{n-1})].$$

As $\overline{X}_{n-1} = (\Theta_{n-1}, \eta^X_{\Theta_{0:n-1},n-1})$, we have :

$$\mathbb{E}_{\overline{\eta}_0}[\overline{f}_n(\overline{X}_n) \mid \sigma(\overline{X}_0, \ldots, \overline{X}_{n-1})] = \mathbb{E}_{\overline{\eta}_0}[\overline{f}_n(\Theta_n, \Phi^X_n\left((\Theta_{n-1}, \Theta_n), \eta^X_{\Theta_{0:n-1},n-1}\right) \mid \sigma(\overline{X}_0, \ldots, \overline{X}_{n-1})]$$
$$= \int_{\mathsf{E}^\Theta_n} \overline{f}_n(\theta_n, \Phi^X_n((\Theta_{n-1}, \theta_n), \eta^X_{\Theta_{0:n-1},n-1}))M^\Theta_n(\Theta_{n-1}, \mathrm{d}\theta_n)$$

$\square$

Then we can define another Feynman Kac flow $\overline{\eta}_n$ and $\overline{\gamma}_n$, denoting respectively the normalized and unnormalized Feynman Kac distribution in distribution space. They are defined for all $\overline{f}_n \in \mathcal{B}_b(\overline{\mathsf{E}}_n)$ by the following relations:

$$\overline{\eta}_n(\overline{f}_n) \triangleq \overline{\gamma}_n(\overline{f}_n)/\overline{\gamma}_n(1) \tag{2.34}$$

and

$$\overline{\gamma}_n(\overline{f}_n) \triangleq \mathbb{E}_{\eta_0}\left[\overline{f}_n(\overline{X}_n) \prod_{p=0}^{n-1} \overline{G}_p(\overline{X}_p)\right]$$

where

$$\overline{G}_p : (u, \mu) \in \overline{\mathsf{E}}_p \mapsto \overline{G}_p(u, \mu) = \int_{\mathsf{E}_p^X} \mu(\mathrm{d}y)G_p(u, y) = \mu(G_p(u, .)) \tag{2.35}$$

From Del Moral (2004) (p. 86), we have that $\overline{\eta}_n$ satisfies a non linear recursive equation :

Proposition 2.2.2. *For every $n \geq 1$, $\overline{\eta}_n$ satisfies the following non linear recursive equation :*

$$\overline{\eta}_n = \overline{\Psi}_{n-1}(\overline{\eta}_{n-1})\overline{M}_n = \overline{\Phi}_n(\overline{\eta}_{n-1}),$$

where the application $\overline{\Psi}_n : \mathcal{P}(\overline{\mathsf{E}}_n) \to \mathcal{P}(\overline{\mathsf{E}}_n)$, is defined for every $\overline{f}_n \in \mathcal{B}_b(\overline{\mathsf{E}}_n)$ by :

$$\overline{\Psi}_n(\eta)(\overline{f}_n) = \eta(\overline{G}_n\overline{f}_n)/\eta(\overline{G}_n),$$

and the operator $\overline{\Phi}_n$ is defined by :

$$\begin{array}{rcl} \overline{\Phi}_n : \mathcal{P}(\overline{\mathsf{E}}_{n-1}) & \to & \mathcal{P}(\overline{\mathsf{E}}_n) \\ \eta & \mapsto & \overline{\Psi}_{n-1}(\eta)\overline{M}_n. \end{array} \tag{2.36}$$

In other words, defining $\hat{\overline{\eta}}_n \triangleq \hat{\overline{\gamma}}_n(f_n)/\hat{\overline{\gamma}}_n(1)$ with $\hat{\overline{\gamma}}_n \triangleq \mathbb{E}_{\overline{\eta}_0}\left[\overline{f}_n(\overline{X}_n) \prod_{p=0}^{n} \overline{G}_p(\overline{X}_p)\right]$, these two quantities are related by the following relations:

$$\hat{\overline{\eta}}_n(f_n) = \overline{\eta}_n(\overline{G}_n f_n)/\overline{\eta}_n(\overline{G}_n) \tag{2.37}$$

and

$$\overline{\eta}_{n+1} = \hat{\overline{\eta}}_n\overline{M}_{n+1} \tag{2.38}$$

By direct inspection, we have that $\overline{\eta}_n$ corresponds to the predicting filter and $\hat{\overline{\eta}}_n$ to the updating filter. And we can resume these relations by the diagram:

$$\overline{\eta}_n \xrightarrow{\text{updating}} \hat{\overline{\eta}}_n = \overline{\Psi}_n(\overline{\eta}_n) \xrightarrow{\text{prediction}} \overline{\eta}_{n+1} = \hat{\overline{\eta}}_n\overline{M}_{n+1} \tag{2.39}$$

In the non linear case, equation (2.36) cannot be solved analytically. Therefore, in the next section, we introduce an interacting particle system to approximate this sequence of Feynman-Kac measures $(\overline{\eta}_n)_{n \in \mathbb{N}}$.

2.2.2 Particle filters for random process evolving in a random environment

As we have seen, Feynman-Kac measures in distribution space also evolve sequentially in two steps as mentioned in Proposition 2.2.2. This recursion can be written in the following form:

$$\overline{\eta}_{n+1} = \overline{\eta}_n \overline{K}_{n+1,\overline{\eta}_n}$$

where $\overline{K}_{n+1,\overline{\eta}_n}$ is a kernel defined by:

$$\overline{K}_{n+1,\overline{\eta}_n} = \overline{S}_{n,\overline{\eta}_n} \overline{M}_{n+1}$$

with $\overline{S}_{n+1,\overline{\eta}_n}$ a selection kernel. The McKean interpretation far from being unique as we mention already in this document still involves a selection kernel. As we mention previously, we choose the kernel with a sampling/resampling scheme:

$$\overline{S}_{n,\overline{\eta}_n}(\overline{x}_n, .) = \overline{G}_n(\overline{x}_n)\delta_{\overline{x}_n}(.) + (1 - \overline{G}_n(\overline{x}_n))\overline{\Psi}_n(\overline{\eta}_n)(.)$$

This section is about the interacting particle model associated to the Feynman-Kac distribution flow we are interested in : $\overline{\eta}_n$ associated to the Feynman-Kac measure defined by (2.34). One considers the process $\overline{X}_n$ associated with the pair $(\overline{G}_n, \overline{M}_n)$, where the transition kernel $\overline{M}_n$ is defined by (2.33) and the potential function $\overline{G}_n$ is defined in (2.35).

Idealized interacting particle model

Let N_1 be some positive integer. A N_1-interacting particle system associated with the sequence $((\overline{G}_n, \overline{M}_n))_{n \in \mathbb{N}}$ and the initial distribution $\overline{\eta}_0$, is a sequence of non-homogeneous Markov chain, denoted by $\overline{X}_n^{[N_1]}$, taking value in the product space $\overline{\mathsf{E}}_n^{N_1}$,

$$\overline{X}_n^{[N_1]} \triangleq (\overline{X}_n^i)_{i=1}^{N_1} = (\overline{X}_n^1, \ldots, \overline{X}_n^{N_1}) \in \overline{\mathsf{E}}_n^{N_1} \triangleq \underbrace{\overline{\mathsf{E}}_n \times \ldots \times \overline{\mathsf{E}}_n}_{N_1 \text{ times}}.$$

The initial state of the Markov chain $\overline{X}_0^{[N_1]}$ consists in N_1 independent random variables with common distribution $\overline{\eta}_0$. The interacting particle system $(\overline{X}_n^i)_{i=1}^{N_1}$ explores the state space $\overline{\mathsf{E}}_n$ and with the dynamic given to it, empirically samples the law $\overline{\eta}_n$. Each particle i of the system consists in a random variable $\overline{X}_n^i = (\theta_n^i, \eta_{\theta_{0:n}^i,n}^X) \in \overline{\mathsf{E}}_n$. Therefore, the empirical process $\overline{\eta}_n^{N_1}$ is defined by:

$$\overline{\eta}_n^{N_1} \triangleq \frac{1}{N_1} \sum_{i=1}^{N_1} \delta_{\overline{X}_n^i}. \tag{2.40}$$

The elementary transition of the Markov chain $\overline{X}_n^{[N_1]}$ from $\overline{\mathsf{E}}_n^{N_1}$ to $\overline{\mathsf{E}}_{n+1}^{N_1}$ is given for any $\overline{x}_n^{[N_1]} \triangleq (\overline{x}_n^1, \ldots, \overline{x}_n^{N_1}) \in \overline{\mathsf{E}}_n^{N_1}$ by:

$$\mathbb{P}_{\overline{\eta}_0}^{N_1}\left(\overline{X}_{n+1}^{[N_1]} \in \mathrm{d}\overline{x}_{n+1}^{[N_1]} \,|\, \overline{X}_n^{[N_1]}\right) \triangleq \prod_{i=1}^{N_1} \overline{\Phi}_{n+1}(\overline{\eta}_n^{N_1})(\mathrm{d}\overline{x}_{n+1}^i)$$

Thanks to (2.36), we have:

$$\mathbb{P}_{\overline{\eta}_0}^{N_1}\left(\overline{X}_{n+1}^{[N_1]} \in \mathrm{d}\overline{x}_{n+1}^{[N_1]} \,|\, \overline{X}_n^{[N_1]}\right) = \prod_{i=1}^{N_1} \sum_{j=1}^{N_1} \frac{\overline{G}_n(\overline{X}_n^j)}{\sum_{k=1}^{N_1} \overline{G}_n(\overline{X}_n^k)} \overline{M}_{n+1}(\overline{X}_n^j, \mathrm{d}\overline{x}_{n+1}^i).$$

Thus, the evolution of the particle swarm consists in two steps : a selection and a mutation. In the selection step, the particles $(\overline{X}_n^i)_{i=1}^{N_1}$ are selected multinomially with probability proportional to their potentials $(\overline{G}_n(\overline{X}_n^i))_{i=1}^{N_1}$. Selected particles are identified with a hat on Figure 2.2. Then the mutation step is performed independently using the kernel $\overline{M}_{n+1}$. The evolution scheme of the particles is illustrated on Figure 2.2. Using

$$\overline{X}_n^{[N_1]} = \left((\theta_n^i, \eta_{\theta_{0:n}^i, n}^X)\right)_{i=1}^{N_1} \xrightarrow[\overline{\Psi}_n(\overline{\eta}_n^{N_1})]{\text{Selection}} \left((\hat{\theta}_n^i, \eta_{\hat{\theta}_{0:n}^i, n}^X)\right)_{i=1}^{N_1} \xrightarrow[\overline{M}_{n+1}]{\text{Mutation}} \left((\theta_{n+1}^i, \eta_{\theta_{0:n+1}^i, n+1}^X)\right)_{i=1}^{N_1}$$

$$M_{n+1}^{\Theta} \searrow \qquad \nearrow \Phi_{n+1}^X((\hat{\theta}_n^i, \theta_{n+1}^i), \eta_{\hat{\theta}_{0:n}^i, n}^X)$$

$$\left((\theta_{n+1}^i, \eta_{\hat{\theta}_{0:n}^i, n}^X)\right)_{i=1}^{N_1}$$

Figure 2.2: Evolution scheme of the interacting particle system for exact measures.

this algorithm one can empirically sample the measure $\overline{\eta}_n$ at each time step n. Several results are available to qualify the subsequent estimator. However, as one may have noticed, for each θ_n^i the measure $\eta_{\theta_{0:n}^i, n}^X$ corresponds to the quenched distributions defined in (2.23). That means that one should have the exact quenched measure associated with the parameter realization $\theta_{0:n}^i$ to use that standard particle algorithm. This can happen in two special cases.

Firstly, one special case is when the transition kernel $M_{\theta_n, n}^X$ is Gaussian and the initial distribution $\eta_{\theta_0}^X$ is Gaussian. Indeed, it turns out that this particle algorithm corresponds to mixture Gaussian filters developed in Chen and Liu (2000), to Rao-Blackwellized particle filters developed in Doucet et al. (2000) and to the interacting Kalman filters (IKF) (see Del Moral (2004), Zghal et al. (2014)). That is a N_1-interacting particle model which is composed of N_1 particles where the measure value part are Gaussian distributions. In other words, for each particle θ_n^i, one iterative step of the Kalman filter is run to update the measure, *i.e.* one prediction step and one correction step. Those filters are then competing through the selection step using the transformation $\overline{\Psi}_n$ defined in (2.35). For example let us consider the case where Θ_n is a E_n^{Θ}-process with initial distribution η_0^{Θ} and elementary transition kernel M_n^{Θ}. For a realization $\theta_{0:n}$ of $\Theta_{0:n}$, consider that (X_n, Y_n) is a $\mathbb{R}^{p+q}$-Markov chain, for positive integers (p, q), defined through the linear Gaussian

system :

$$\begin{cases} X_n &=& A_{\theta_n,n} X_{n-1} + a_{\theta_n,n} + B_{\theta_n,n} \varepsilon_n^X, & n \geq 1 \\ Y_n &=& C_{\theta_n,n} X_n + c_{\theta_n,n} + D_{\theta_n,n} \varepsilon_n^Y, & n \geq 0. \end{cases}$$

$(A_{\theta_n,n}, B_{\theta_n,n}, C_{\theta_n,n}, D_{\theta_n,n})$ and $(a_{\theta_n,n}, c_{\theta_n,n})$ are respectively matrices and deterministic vectors of appropriate dimension which may depend on a parameter θ_n. The sequences ε_n^X and ε_n^Y are two independent white noises, independent from the initial condition X_0. There are Gaussian random variables whose mean and variance are given by

$$X_0 \sim \mathsf{N}(m_{\theta_0,0}, \Sigma_{\theta_0,0}), \quad \varepsilon_n^X \sim \mathsf{N}(0, \Sigma_n^X), \quad \text{and } \varepsilon_n^Y \sim \mathsf{N}(0, \Sigma_n^Y).$$

In this framework, $\eta_{\theta_{0:n},n}^X$ corresponds to the conditional law of X_n given the observations $Y_{0:n-1} = y_{0:n-1}$ and the history of the parameter $\theta_{0:n}$, also called optimal predictor. One wants to estimate recursively the law of the couple $(\Theta_n, \eta_{\theta_{0:n},n}^X)$ using observations $Y_{0:n-1} = y_{0:n-1}$. For that purpose, one needs to introduce the optimal filtering which is the conditional law of X_n given the observations $Y_{0:n} = y_{0:n}$ and the history of the parameter $\theta_{0:n}$. It turns out that these previous distributions are Gaussian respectively denoted by $\eta_{\theta_{0:n},n}^X = \mathsf{N}(m_{\theta_n,n}, \Sigma_{\theta_n,n})$ and $\mathsf{N}(\hat{m}_{\theta_n,n}, \hat{\Sigma}_{\theta_n,n})$. Thus,

$$\begin{aligned} \hat{m}_{\theta_n,n} &= \mathbb{E}_{\theta_{0:n}}[X_n \mid Y_{0:n}] \\ \hat{\Sigma}_{\theta_n,n} &= \mathbb{E}_{\theta_{0:n}}\left[(X_n - \hat{m}_{\theta_n,n})(X_n - \hat{m}_{\theta_n,n})^T\right] \\ m_{\theta_{n+1},n+1} &= \mathbb{E}_{\theta_{0:n+1}}[X_{n+1} \mid Y_{0:n}] \\ \Sigma_{\theta_{n+1},n+1} &= \mathbb{E}_{\theta_{0:n+1}}\left[(X_{n+1} - m_{\theta_{n+1},n+1})(X_{n+1} - m_{\theta_{n+1},n+1})^T\right]. \end{aligned}$$

Moreover, the mapping Φ_{n+1}^X defined in (2.29) which is used to update the measure valued part $\eta_{\theta_{0:n},n}^X$ corresponds to a complete step of the Kalman filter evolution between predictors. This means that $\Phi_{n+1}^X((\theta_n, \theta_{n+1}), \mathsf{N}(m_{\theta_n,n}, \Sigma_{\theta_n,n}))$ is also a Gaussian distribution whose mean and covariance matrix are obtained recursively through two steps:

$$\mathsf{N}(m_{\theta_n,n}, \Sigma_{\theta_n,n}) \xrightarrow{\text{Correction}} \mathsf{N}(\hat{m}_{\theta_n,n}, \hat{\Sigma}_{\theta_n,n}) \xrightarrow{\text{Prediction}} \mathsf{N}(m_{\theta_{n+1},n+1}, \Sigma_{\theta_n,n}).$$

The first one is a correction step which is given by

$$\begin{cases} \hat{m}_{\theta_n,n} &=& m_{\theta_n,n} + K_{\theta_n,n}(Y_n - (C_{\theta_n,n} m_{\theta_n,n} + c_{\theta_n,n})) \\ \hat{\Sigma}_{\theta_n,n} &=& (I - K_{\theta_n,n} C_{\theta_n,n}) \Sigma_{\theta_n,n} \end{cases}$$

where I is the identity matrix and $K_{\theta_n,n}$ is the classical gain matrix

$$K_{\theta_n,n} \triangleq \Sigma_{\theta_n,n} (C_{\theta_n,n})^T \left(C_{\theta_n,n} \Sigma_{\theta_n,n} (C_{\theta_n,n})^T + D_{\theta_n,n} \Sigma_n^Y (D_{\theta_n,n})^T\right)^{-1}.$$

The second step is the predicting step:

$$\begin{cases} m_{\theta_{n+1},n+1} & = & A_{\theta_{n+1},n+1}\hat{m}_{\theta_n,n} + a_{\theta_{n+1},n+1} \\ \Sigma_{\theta_{n+1},n+1} & = & A_{\theta_{n+1},n+1}\hat{\Sigma}_{\theta_n,n}(A_{\theta_{n+1},n+1})^T + B_{\theta_{n+1},n+1}\Sigma^X_{n+1}(B_{\theta_{n+1},n+1})^T. \end{cases}$$

Then all the Kalman filters attached to each realization θ^i_{n+1} for $i \in [\![1, N_1]\!]$ interact through their potential $\bar{G}_{n+1}(\theta^i_{n+1}, \eta^X_{\theta^i_{0:n+1},n+1})$ defined in (2.35) by

$$\bar{G}_{n+1}(\theta^i_{n+1}, \eta^X_{\theta^i_{0:n+1},n+1}) = \eta^X_{\theta^i_{0:n+1},n+1}(G_{\theta^i_{n+1},n+1}) = \mathsf{N}(m_{\theta^i_{n+1},n+1}, \Sigma_{\theta^i_{n+1},n+1})(G_{\theta^i_{n+1},n+1})$$

where $G_{\theta^i_{n+1},n+1}$ is the likelihood function defined for every $x_{n+1} \in \mathsf{E}^X_{n+1}$ by

$$G_{\theta^i_{n+1},n+1}(x_{n+1}) = \frac{\mathrm{dN}(C_{\theta^i_{n+1},n+1}x_{n+1}, \Sigma^Y_{n+1})}{\mathrm{dN}(0, \Sigma^Y_{n+1})}.$$

One finally ends up with the following expression:

$$\begin{aligned} \bar{G}_{n+1}&(\theta^i_{n+1}, \eta^X_{\theta^i_{0:n+1},n+1}) \\ &= \frac{\mathrm{dN}(C_{\theta^i_{n+1},n+1}m_{\theta^i_{n+1},n+1}, C_{\theta^i_{n+1},n+1}\Sigma_{\theta^i_{n+1},n+1}(C_{\theta^i_{n+1},n+1})^T + \Sigma^Y_{n+1})}{\mathrm{dN}(0, \Sigma^Y_{n+1})}. \end{aligned} \quad (2.41)$$

See Del Moral (2004) for further details. The interacting Kalman filter for this general example is given by Algorithm 2.

Algorithm 2 Interacting Kalman Filter - IKF

Require: $\overline{\eta}_0$, $(\overline{M}_p)_{p=0}^n$, $(\overline{\Psi}_p)_{p=0}^n$, $m_{\theta_0^i,0}$ and $\Sigma_{\theta_0^i,0}$

Ensure: Interacting Kalman approximation of $\overline{\eta}_n$

$\boxed{\text{Begin}}$

1. INITIALIZATION $p = 0$

for $i \in [\![1, N_1]\!]$ **do**

   Sample $\tilde{X}_0^i = (\theta_0^i, \eta_{\theta_0^i,0}^X) \sim \tilde{\eta}_0$, *i.e.* $\theta_0^i \overset{i.i.d}{\sim} \eta_0^\Theta$ and $\eta_{\theta_0^i,0}^X = \mathsf{N}(m_{\theta_0^i,0}, \Sigma_{\theta_0^i,0})$.

end for

2. SELECTION OF KALMAN FILTERS

Sample $I_p = (I_p^i)_{i=1}^{N_1}$ according to a multinomial distribution with probability proportional to $\left(\bar{G}_p(\theta_p^k, \eta_{\theta_{0:p}^k,p}^X) \right)_{k=1}^{N_1}$ given by (2.41).

for $i \in [\![1, N_1]\!]$ **do**

   3. UPDATING STEP FOR EACH KALMAN FILTER
   $$
   \begin{cases}
   \hat{m}_{\theta_p^{I_p^i},p} &= m_{\theta_p^{I_p^i},p} + K_{\theta_p^{I_p^i},p}(Y_n - C_{\theta_p^{I_p^i},p} m_{\theta_p^{I_p^i},p}) \\
   \hat{\Sigma}_{\theta_p^{I_p^i},p} &= \left(I - K_{\theta_p^{I_p^i},p} C_{\theta_p^{I_p^i},p} \right) \Sigma_{\theta_p^{I_p^i},p}
   \end{cases}
   $$
   4. MUTATION OF EACH ISLAND
   Sample independently θ_{p+1}^i according to $M_{p+1}^\Theta(\theta_p^{I_p^i}, .)$
   5. PREDICTION STEP FOR EACH KALMAN FILTER
   $$
   \begin{cases}
   m_{\theta_{p+1}^i,p+1} &= A_{\theta_{p+1}^i,p+1}\hat{m}_{\theta_p^{I_p^i},p} + a_{\theta_{p+1}^i,p+1} \\
   \Sigma_{\theta_{p+1}^i,p+1} &= A_{\theta_{p+1}^i,p+1}\hat{\Sigma}_{\theta_p^{I_p^i},p}(A_{\theta_{p+1}^i,p+1})^T + B_{\theta_{p+1}^i,p+1}\Sigma_{p+1}^X(B_{\theta_{p+1}^i,p+1})^T
   \end{cases}
   $$

end for

$p \longleftarrow p + 1$ go to step 2.

$\boxed{\text{End}}$

Secondly, when the non linear equation (2.29) can be solved analytically *i.e.* when one has access to the exact measure $\eta_{\theta_{0:n}^i,n}^X$, one can apply a simple interacting particle model as described in Figure 2.2, where each particle corresponds to the pair: parameter and exact measure. For example, in Özkan et al. (2013); Lundquist et al. (2014) they use the idealized interacting particle model as the dynamical noises are in the exponential family. However, in most cases, this equation cannot be solved analytically, so that an additional approximation is needed in order to estimate the measure $\eta_{\theta_{0:n}^i,n}^X$ for each $i \in [\![1, N_1]\!]$. The next subsection is dedicated to the derivation of an algorithm to deal with this constraint.

Labeled island particle model

To tackle the case where $\eta_{\theta_{0:n}^i,n}^X$, $i \in [\![1, N_1]\!]$ is not analytically known, the idea consists in using a particle estimation of $\eta_{\theta_{0:n}^i,n}^X$ inside the previous interacting particle model. The ensuing algorithm will be called *labeled island particle model* in reference to the island particle model developed in Vergé et al. (2013), even if in the present case, each island i have a label θ_n^i whose evolution is given by the Markov kernel M_n^Θ. The labeled island particle model consists in associating to each term of the sequence $(\theta_n^i)_{i=1}^{N_1}$ a sub N_2-

interacting particle system. We call sub N_2-interacting particle system associated with the sequence $((G_{\theta_n^i,n}, M_{\theta_n^i,n}^X))_{n\in\mathbb{N}}$ and the initial distribution $\eta_{\theta_0^i,0}^X$, the sequence of non-homogeneous Markov chain $(\xi_n^{i,j})_{j=1}^{N_2}$ taking value in the product space E_n^{X,N_2}, that is :

$$\xi_n^{i,[N_2]} \triangleq (\xi_n^{i,j})_{j=1}^{N_2} \triangleq (\xi_n^{i,1}, \ldots, \xi_n^{i,N_2}) \in \mathsf{E}_n^{X,N_2} \triangleq \underbrace{\mathsf{E}_n^X \times \ldots \times \mathsf{E}_n^X}_{N_2 \text{ times}}.$$

The initial state of the Markov chain $(\xi_0^{i,j})_{j=1}^{N_2}$ consists in sampling N_2 independent random variables with common distribution $\eta_{\theta_0^i,0}^X$.

The interacting particle system, denoted by $(\xi_n^{i,j})_{j=1}^{N_2}$, explore the state space E_n^X and with the dynamic given to it, empirically sample the law $\eta_{\theta_{0:n}^i,n}^X$.

Denoting the empirical measure by:

$$\eta_{\theta_{0:n}^i,n}^{X,N_2} \triangleq \frac{1}{N_2} \sum_{j=1}^{N_2} \delta_{\xi_n^{i,j}}, \qquad (2.42)$$

the elementary transition of the process $\xi_n^{i,[N_2]}$ from E_n^{X,N_2} to E_{n+1}^{X,N_2} is given for any $x_n^{[N_2]} = (x_n^1, \ldots, x_n^{N_2}) \in \mathsf{E}_n^{X,N_2}$ by:

$$\begin{aligned}
\mathbb{P}_{\eta_{\theta_0}^X}^{N_2} \left(\xi_{n+1}^{i,[N_2]} \in dx_{n+1}^{[N_2]} \mid \xi_n^{i,[N_2]} \right) &\triangleq \prod_{j=1}^{N_2} \Phi_{n+1}^X \left((\theta_n^i, \theta_{n+1}^i), \eta_{\theta_{0:n}^i,n}^{X,N_2} \right) (dx_{n+1}^j) \\
&= \prod_{j=1}^{N_2} \Psi_{\theta_n^i,n}^X (\eta_{\theta_{0:n}^i,n}^{X,N_2}) M_{\theta_{n+1}^i,n+1}^X (\xi_n^{i,j}, dx_{n+1}^j) \quad \text{using (2.29)} \\
&= \prod_{j=1}^{N_2} \sum_{k=1}^{N_2} \frac{G_{\theta_n^i,n}(\xi_n^{i,k})}{\sum_{\ell=1}^{N_2} G_{\theta_n^i,n}(\xi_n^{i,\ell})} M_{\theta_{n+1}^i,n+1}^X (\xi_n^{i,k}, dx_{n+1}^j) \quad \text{by (2.28)}.
\end{aligned}$$

Define the mapping $\tilde{\Phi}_n^X$ by:

$$\begin{aligned}
\tilde{\Phi}_n^X : \mathsf{E}_{n-1}^\Theta \times \mathsf{E}_n^\Theta \times \mathcal{P}(\mathsf{E}_{n-1}^X) &\rightarrow \mathcal{P}(\mathsf{E}_n^X) \\
((u,v), \nu) &\mapsto \prod_{j=1}^{N_2} \Phi_n^X((u,v), \nu)(dx_n^j),
\end{aligned}$$

then

$$\eta_{\theta_{0:n+1}^i,n+1}^{X,N_2} = \tilde{\Phi}_{n+1}^X \left((\theta_n^i, \theta_{n+1}^i), \eta_{\theta_{0:n}^i,n}^{X,N_2} \right). \qquad (2.43)$$

So, the evolution of the particle swarm $\xi_n^{i,[N_2]}$ consists in two steps: a selection and a mutation. In the selection step, the particles are selected multinomially with probability proportional to their potentials $\left(G_{\theta_n^i,n}(\xi_n^{i,j}) \right)_{j=1}^{N_2}$. Then the mutation step is performed independently using the kernel $M_{\theta_{n+1}^i,n+1}^X$. Hence, at each iteration $n \in \mathbb{N}$, the empirical measure $\eta_{\theta_{0:n}^i,n}^{X,N_2}$ approximates $\eta_{\theta_{0:n}^i,n}^X$ when N_2 tends to ∞. Replacing $\eta_{\theta_{0:n}^i,n}^X$ by $\eta_{\theta_{0:n}^i,n}^{X,N_2}$ inside the first algorithm presented, one gets a nested particle model named *labeled island particle model*.

In order to derive precisely this algorithm, first introduce the following sequence $\tilde{X}_n$ on $\overline{\mathsf{E}}_n = \mathsf{E}_n^\Theta \times \mathcal{P}(\mathsf{E}_n^X)$, defined by $\tilde{X}_n \triangleq (\Theta_n, \eta_{\Theta_{0:n},n}^{X,N_2})$, *i.e.* the couple environment and empir-

ical measure of the process X_n conditionally on $\Theta_{0:n}$, where $\eta_{\Theta_{0:n},n}^{X,N_2} \triangleq \sum_{j=1}^{N_2} \delta_{\xi_n^j}/N_2$.

Proposition 2.2.3. $\tilde{X}_n$ *is a* $\overline{\mathsf{E}}_n$*-Markov chain with transition kernel* $\tilde{M}_n$ *defined for every function* $\overline{f}_n \in \mathcal{B}_b(\overline{\mathsf{E}}_n)$ *and* $(u, \nu) \in \overline{\mathsf{E}}_n$ *by*

$$\tilde{M}_n(\overline{f}_n)(u, \nu) = \int_{\mathsf{E}_n^{\Theta}} M_n^{\Theta}(u, \mathrm{d}v)\overline{f}_n(v, \tilde{\Phi}_n^X((u, v), \nu)), \tag{2.44}$$

where $\tilde{\Phi}_n^X$ *is defined in* (2.43), *and with initial distribution* $\tilde{\eta}_0 \in \mathcal{P}(\overline{\mathsf{E}}_0)$ *given by:*

$$\tilde{\eta}_0(\mathrm{d}(u, \nu)) \triangleq \eta_0^{\Theta}(\mathrm{d}u)\delta_{\eta_{\theta_0,0}^{X,N_2}}(\mathrm{d}\nu).$$

Proof. Let $\sigma(\tilde{X}_0, \ldots, \tilde{X}_n)$ stands for the σ-algebra generated by the random variables $\tilde{X}_p$, $0 \leq p \leq n$. For all $\overline{f}_n \in \mathcal{B}_b(\overline{\mathsf{E}}_n)$:

$$\mathbb{E}_{\tilde{\eta}_0}[\overline{f}_n(\tilde{X}_n) \mid \sigma(\tilde{X}_0, \ldots, \tilde{X}_{n-1})] = \mathbb{E}_{\tilde{\eta}_0}[\overline{f}_n(\Theta_n, \eta_{\Theta_{0:n},n}^{X,N_2}) \mid \sigma(\tilde{X}_0, \ldots, \tilde{X}_{n-1})]$$

using (2.43)

$$= \mathbb{E}_{\tilde{\eta}_0}[\overline{f}_n(\Theta_n, \tilde{\Phi}_n^X((\Theta_{n-1}, \Theta_n), \eta_{\Theta_{0:n-1},n-1}^{X,N_2}) \mid \sigma(\tilde{X}_0, \ldots, \tilde{X}_{n-1})].$$

Recalling that $\tilde{X}_{n-1} = (\Theta_{n-1}, \eta_{\Theta_{0:n-1},n-1}^{X,N_2})$, one can conclude that

$$\mathbb{E}_{\tilde{\eta}_0}[\overline{f}_n(\tilde{X}_n) \mid \sigma(\tilde{X}_0, \ldots, \tilde{X}_{n-1})] = \mathbb{E}_{\tilde{\eta}_0}[\overline{f}_n(\tilde{X}_n) \mid \tilde{X}_{n-1}]$$

$$= \int_{\mathsf{E}_n^{\Theta}} \overline{f}_n(\theta_n, \tilde{\Phi}_n^X((\Theta_{n-1}, \theta_n), \eta_{\Theta_{0:n-1},n-1}^{X,N_2})M_n^{\Theta}(\Theta_{n-1}, \mathrm{d}\theta_n).$$

$\square$

To the Markov chain $\tilde{X}_n$, one may associate the Feynman-Kac distribution defined for every $\overline{f}_n \in \mathcal{B}_b(\overline{\mathsf{E}}_n)$ by

$$\tilde{\eta}_n(\overline{f}_n) \triangleq \tilde{\gamma}_n(\overline{f}_n)/\tilde{\gamma}_n(\mathbb{1}), \tag{2.45}$$

where $\tilde{\gamma}_n$ is defined such that

$$\tilde{\gamma}_n(\overline{f}_n) \triangleq \mathbb{E}_{\tilde{\eta}_0}\left[\overline{f}_n(\tilde{X}_n) \prod_{p=0}^{n-1} \overline{G}_p(\tilde{X}_p)\right],$$

with $\overline{G}_p$ defined in (2.35).

In a similar way to $\overline{\eta}_n$, the measure $\tilde{\eta}_n$ satisfies a recursive equation $\tilde{\eta}_n = \overline{\Psi}_{n-1}(\tilde{\eta}_{n-1})\tilde{M}_n$, with $\overline{\Psi}_{n-1}$ the application defined in (2.36). This non linear equation can be rewritten as

$$\tilde{\eta}_n = \tilde{\Phi}_n(\tilde{\eta}_{n-1}), \tag{2.46}$$

$$\tilde{X}_n^{[N_1]} = \left((\theta_n^i, \eta_{\theta_{0:n}^i,n}^{X,N_2}) \right)_{i=1}^{N_1} \xrightarrow[\overline{\Psi}_n(\tilde{\eta}_n^{N_1})]{\text{Selection}} \left((\hat{\theta}_n^i, \eta_{\hat{\theta}_{0:n}^i,n}^{X,N_2}) \right)_{i=1}^{N_1} \xrightarrow[\tilde{M}_{n+1}]{\text{Mutation}} \left((\theta_{n+1}^i, \eta_{\theta_{0:n+1}^i,n+1}^{X,N_2}) \right)_{i=1}^{N_1}$$

$$M_{n+1}^\Theta \searrow \qquad \nearrow \tilde{\phi}_{n+1}^X((\hat{\theta}_n^i,\theta_{n+1}^i),\eta_{\hat{\theta}_{0:n}^i,n}^{X,N_2})$$

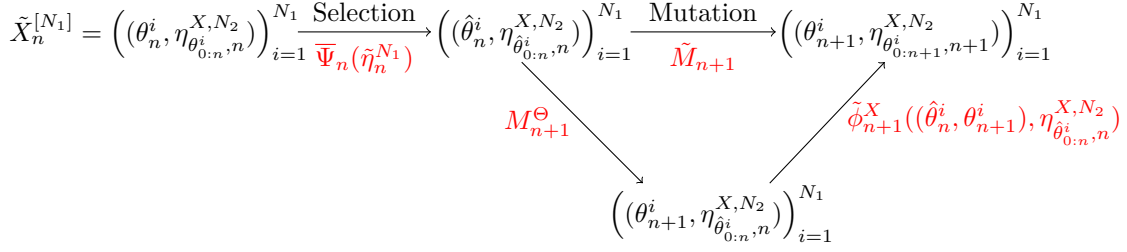$$\left((\theta_{n+1}^i, \eta_{\hat{\theta}_{0:n}^i,n}^{X,N_2}) \right)_{i=1}^{N_1}$$

Figure 2.3: Evolution scheme of the labeled island particle model.

where the mapping $\tilde{\Phi}_n$ is defined as follows:

$$\begin{aligned} \tilde{\Phi}_n : \mathcal{P}(\overline{\mathsf{E}}_{n-1}) &\rightarrow \mathcal{P}(\overline{\mathsf{E}}_n) \\ \eta &\mapsto \overline{\Psi}_{n-1}(\eta)\tilde{M}_n. \end{aligned} \tag{2.47}$$

As in Section 2.2.2, when this equation cannot be solved analytically one may use a particle model to approximate the probability measure $\tilde{\eta}_n$. In this case, the particles $\{\tilde{X}_n^i \triangleq (\theta_n^i, \eta_{\theta_{0:n}^i,n}^{X,N_2}), \ i \in [\![1, N_1]\!]\}$, would be testing points on the state space $\overline{\mathsf{E}}_n$, for $(N_1, N_2) \in (\mathbb{N}^*)^2$. These particles explore the state space $\overline{\mathsf{E}}_n$ and their dynamics empirically sample the law $\tilde{\eta}_n$ when N_1 gets large. An interacting particle system associated with the couple $(\overline{G}_n, \tilde{M}_n)$ and the initial distribution $\tilde{\eta}_0$, is a sequence of non-homogeneous Markov chain, $\tilde{X}_n^{[N_1]}$, taking value in the product space $\overline{\mathsf{E}}_n^{N_1}$, defined by

$$\tilde{X}_n^{[N_1]} \triangleq (\tilde{X}_n^i)_{i=1}^{N_1} = (\tilde{X}_n^1, \dots, \tilde{X}_n^{N_1}) \in \overline{\mathsf{E}}_n^{N_1}.$$

The initial state of the Markov chain $\tilde{X}_0^{[N_1]}$ consists in N_1 independent random variables with common distribution $\tilde{\eta}_0$. Denote by $\tilde{\eta}_n^{N_1}$ the empirical measure at time n, which is defined by

$$\tilde{\eta}_n^{N_1} \triangleq \frac{1}{N_1} \sum_{i=1}^{N_1} \delta_{\tilde{X}_n^i}. \tag{2.48}$$

The elementary probability transition, is given for any $\overline{x}_{n+1}^{[N_1]} \in \overline{\mathsf{E}}_{n+1}^{N_1}$ by

$$\mathbb{P}_{\tilde{\eta}_0}^{N_1}(\tilde{X}_{n+1}^{[N_1]} \in \mathrm{d}\overline{x}_{n+1}^{[N_1]} \,|\, \tilde{X}_n^{[N_1]}) = \prod_{i=1}^{N_1} \overline{\Psi}_n(\tilde{\eta}_n^{N_1})\tilde{M}_{n+1}(\tilde{X}_n^i, \mathrm{d}\overline{x}_{n+1}^i).$$

The particle evolution is summarized in Figure 2.3 where by definitions (2.35) and (2.42),

$$\overline{G}_n(\tilde{X}_n^i) = \frac{1}{N_2} \sum_{j=1}^{N_2} G_n(\theta_n^i, \xi_n^{i,j}) = \frac{1}{N_2} \sum_{j=1}^{N_2} G_{\theta_n^i,n}(\xi_n^{i,j}).$$

The ensuing algorithm is described in Algorithm 3. This algorithm is the same as the one presented in Montemerlo et al. (2002) to estimate the pose of the mobile robot meanwhile tracking the position of surrounding people, and Johansen et al. (2012).

For every $n \geq 0$, $\tilde{\eta}_n^{N_1}$ is an estimator of $\tilde{\eta}_n$, obtained through the labeled island particle

---

Algorithm 3 Labeled island particle algorithm

Require: $\tilde{\eta}_0$, $(\tilde{M}_p)_{p=0}^n$ and $(\overline{\Psi}_p)_{p=0}^n$
Ensure: Particle approximation of $\tilde{\eta}_n$

$\boxed{\text{Begin}}$

1. $\underline{\text{INITIALIZATION}}$ $p = 0$

for $i = 1, \ldots, N_1$ **do**

  Sample $\tilde{X}_0^i = (\theta_0^i, \eta_{\theta_0^i,0}^{X,N_2}) \sim \tilde{\eta}_0$, that is

$$\theta_0^i \overset{i.i.d}{\sim} \eta_0^\Theta, \; \xi_0^{i,j} \overset{i.i.d}{\sim} \eta_{\theta_0^i,0}^X \text{ and } \eta_{\theta_0^i,0}^{X,N_2} = \frac{1}{N_2} \sum_{j=1}^{N_2} \delta_{\xi_0^{i,j}}.$$

end for

for $p = 0, \ldots, n$ **do**

  2. $\underline{\text{SELECTION OF ISLANDS}}$

  Sample $I_p = (I_p^i)_{i=1}^{N_1}$ according to a multinomial distribution with probability propor-

  tional to $\left(\frac{1}{N_2} \sum_{j=1}^{N_2} G_p(\theta_p^i, \xi_p^{i,j}) \right)_{i=1}^{N_1}$

  for $i = 1, \ldots, N_1$ **do**

    3. $\underline{\text{SELECTION OF PARTICLES INSIDE EACH ISLAND}}$

    Sample $J_p^i = (J_p^{i,j})_{j=1}^{N_2}$ according to a multinomial distribution with probability

    proportional to $\left(G_p(\theta_p^{I_p^i}, \xi_p^{I_p^i,j}) \right)_{j=1}^{N_2}$

    4. $\underline{\text{MUTATION OF EACH ISLAND}}$

    Sample independently θ_{p+1}^i according to $M_{p+1}^\Theta(\theta_p^{I_p^i}, .)$

    for $j = 1, \ldots, N_2$ **do**

      5. $\underline{\text{MUTATION OF PARTICLES}}$

      Sample $\xi_{p+1}^{i,j}$ according to $M_{\theta_{p+1}^i,p+1}^X(\xi_p^{I_p^i,J_p^{i,j}}, .)$

    end for

  end for

end for

$\boxed{\text{End}}$

---

model, i.e. for every $\overline{f}_n \in \mathcal{B}_b(\overline{\mathsf{E}}_n)$,

$$\tilde{\eta}_n^{N_1}(\overline{f}_n) = \frac{1}{N_1} \sum_{i=1}^{N_1} \overline{f}_n(\theta_n^i, \eta_{\theta_{0:n}^i, n}^{X, N_2})$$

converges to $\tilde{\eta}_n(\overline{f}_n)$ when $N_1 \to +\infty$.

In a conjoint work with Vergé, we show in Ichard and Vergé (2015) some convergence results for the presented algorithm. In particular we focus our attention on the $\mathbb{L}^p$ error bound between the empirical measure $\tilde{\eta}_n^{N_1}$ and $\overline{\eta}_n$. Then we get a time uniform bound. Finally we prove the almost sure convergence of the empirical measure towards towards the target measure. We transcript here these theoretical results. The full version of the submitted paper is attached in Section A.1.

2.2.3 Estimation error and $\mathbb{L}^p$ bounds

We are interested in this section in the $\mathbb{L}^p$ bounds of the difference between the estimator $\tilde{\eta}_n^{N_1}$ and the measure $\overline{\eta}_n$. To get these bounds we will use several notations. We define them before going further.

Notations

Let $(\mathsf{E}, \mathcal{E})$ be a measurable space. For a real-valued measurable function $h \in \mathcal{B}_b(\mathsf{E})$, we denote the oscillator norm $\mathrm{osc}(h) \triangleq \sup_{(x,x')\in\mathsf{E}^2} |h(x) - h(x')|$, and $\mathrm{Osc}_1(\mathsf{E})$ the convex set of $\mathcal{E}$-measurable functions with oscillations less than one. The sup norm of h is noted $\|h\|_\infty \triangleq \sup_{x\in\mathsf{E}} |h(x)|$ and the $\mathbb{L}^p$-norm $\|.\|_p$. $\mathcal{B}_1(\mathsf{E}) \subset \mathcal{B}_b(\mathsf{E})$ refers to the set of functions whose sup norm is less than one. For two probability measures $(\mu, \eta) \in \mathcal{P}(\mathsf{E})^2$, the Zolotarev semi-norm $\|.\|_{\mathfrak{F}}$ attached to $\mathfrak{F}$ a countable collection of bounded measurable functions in $\mathcal{B}_1(\mathsf{E})$ is defined by

$$\|\mu - \eta\|_{\mathfrak{F}} \triangleq \sup_{f\in\mathfrak{F}} |\mu(f) - \eta(f)|.$$

To measure the size of a given class $\mathfrak{F}$, one considers the covering numbers $\mathcal{N}(\varepsilon, \mathfrak{F}, \mathbb{L}^p(\mu))$ defined as the minimal number of $\mathbb{L}^p(\mu)$-balls of radius $\varepsilon > 0$ needed to cover $\mathfrak{F}$. Let $\mathcal{N}(\varepsilon, \mathfrak{F})$ and $I(\mathfrak{F})$ denote respectively the uniform covering numbers and entropy integral given by

$$\mathcal{N}(\varepsilon, \mathfrak{F}) \triangleq \sup_{\mu\in\mathcal{P}(\mathsf{E})} \mathcal{N}(\varepsilon, \mathfrak{F}, \mathbb{L}^2(\mu)) \tag{2.49}$$

$$I(\mathfrak{F}) \triangleq \int_0^1 \sqrt{\log(1 + \mathcal{N}(\varepsilon, \mathfrak{F}))} \mathrm{d}\varepsilon. \tag{2.50}$$

Let $\wedge$ denote the minimum operator and $\vee$ denote the maximum operator. For a kernel M defined on E, the Dobrushin coefficient of M is

$$\beta(M) \triangleq \sup_{f\in\mathrm{Osc}_1(\mathsf{E})} \mathrm{osc}(M(f)).$$

Let $(d(n))_{n\geq 0}$ be a sequence defined for every $m \geq 0$ by

$$
\begin{cases}
d(2m)^{2m} \triangleq (2m)_m 2^{-m} \\
d(2m+1)^{2m+1} \triangleq \dfrac{(2m+1)_{m+1}}{\sqrt{m+1/2}} 2^{-m+1/2},
\end{cases}
$$

where for any positive integers $(p,q) \in (\mathbb{N}^*)^2$, $(q+p)_p \triangleq (q+p)!/q!$.

For $n \in \mathbb{N}$, introduce the Feynman-Kac semi-groups $\overline{Q}_n$ (resp. $Q^X_{\theta_{n-1:n},n}$) such that for all $(\overline{x}_n, \overline{x}_{n+1}) \in \overline{\mathsf{E}}_n \times \overline{\mathsf{E}}_{n+1}$ (resp. $(x_n, x_{n+1}) \in \mathsf{E}^X_n \times \mathsf{E}^X_{n+1}$),

$$
\overline{Q}_{n+1}(\overline{x}_n, \mathrm{d}\overline{x}_{n+1}) \triangleq \overline{G}_n(\overline{x}_n)\overline{M}_{n+1}(\overline{x}_n, \mathrm{d}\overline{x}_{n+1}),
$$

$$
\left(\text{resp. } Q^X_{\theta_{n:n+1},n+1}(x_n, \mathrm{d}x_{n+1}) \triangleq G_{\theta_n,n}(x_n)M^X_{\theta_{n+1},n+1}(x_n, \mathrm{d}x_{n+1})\right).
$$

For every $(p,n) \in (\mathbb{N})^2$ such that $p < n$, set

$$
\overline{Q}_{p,n} \triangleq \overline{Q}_{p+1}\ldots\overline{Q}_n, \quad \text{and} \quad \overline{P}_{p,n} \triangleq \overline{Q}_{p,n}/\overline{Q}_{p,n}(\mathbb{1}),
$$

$$
\left(\text{resp. } Q^X_{\theta_{p:n},p,n} \triangleq Q^X_{\theta_{p:p+1},p+1}\ldots Q^X_{\theta_{n-1:n},n} \text{ and } P^X_{\theta_{p:n},p,n}(f_n) \triangleq Q^X_{\theta_{p:n},p,n}(f_n)/Q^X_{\theta_{p:n},p,n}(\mathbb{1})\right),
$$

and set the normalizing constant

$$
\overline{G}_{p,n} \triangleq \overline{Q}_{p,n}(\mathbb{1}), \quad \left(\text{resp.} G_{\theta_{p:n},p,n} \triangleq Q^X_{\theta_{p:n},p,n}(\mathbb{1})\right).
$$

Finally, set

$$
\overline{g}_{p,n} \triangleq \sup_{(\overline{x}_p, \overline{y}_p) \in (\overline{\mathsf{E}}_p)^2} \frac{\overline{G}_{p,n}(\overline{x}_p)}{\overline{G}_{p,n}(\overline{y}_p)}, \quad \left(\text{resp. } g_{\theta_{p:n},p,n} \triangleq \sup_{(x_p, y_p) \in (\mathsf{E}^X_p)^2} \frac{G_{\theta_{p:n},p,n}(x_p)}{G_{\theta_{p:n},p,n}(y_p)}\right).
$$

In order to study the difference between $\tilde{\eta}^{N_1}_n$ and $\overline{\eta}_n$, we use several results taken from Del Moral (2004). Then, we will always assume that for all $n \in \mathbb{N}$, the potential functions $G_{\theta_n,n}$ defined in (2.21) satisfy the following condition (G_θ):
there exists a sequence of strictly positive number $\epsilon_n(G_\theta) \in (0,1]$ such that for any $(x_n, y_n) \in (\mathsf{E}^X_n)^2$:

$$
G_{\theta_n,n}(x_n) \geq \epsilon_n(G_\theta)G_{\theta_n,n}(y_n) > 0 \tag{G_θ}
$$

Therefore, for all $n \in \mathbb{N}$, the potential functions $\overline{G}_n$ satisfy the following condition $(\overline{G})$:
there exists a sequence of strictly positive number $\epsilon_n(\overline{G}) \in (0,1]$ such that for any $(\overline{x}_n, \overline{y}_n) \in (\overline{\mathsf{E}}_n)^2$:

$$
\overline{G}_n(\overline{x}_n) \geq \epsilon_n(\overline{G})\overline{G}_n(\overline{y}_n) > 0 \tag{$\overline{G}$}
$$

Moreover we always assume that the collection of distributions $\left(\overline{M}_{n+1}(\overline{x}_n, .)\right)_{\overline{x}_n \in \overline{\mathsf{E}}_n}$ are absolutely continuous with one another. That is for every $n \geq 0$ and $(\overline{x}_n, \overline{y}_n) \in (\overline{\mathsf{E}}_n)^2$, one has

$$
\overline{M}_{n+1}(\overline{x}_n, .) \ll \overline{M}_{n+1}(\overline{y}_n, .).
$$

In addition, we assume that the collection of distributions $\left(M^X_{\theta_{n+1},n+1}(x_n, .)\right)_{x_n \in \mathsf{E}^X_n}$ are

absolutely continuous with one another. That is for every $n \geq 0$, $\theta_{n+1} \in \mathsf{E}_{n+1}^{\Theta}$ and $(x_n, y_n) \in (\mathsf{E}_n^X)^2$, one has :

$$M_{\theta_{n+1},n+1}^X(x_n, .) \ll M_{\theta_{n+1},n+1}^X(y_n, .).$$

Note that for time homogeneous models on finite spaces condition those conditions are met as soon as the Markov chain is aperiodic and irreducible. Some examples are illustrated by typical examples in Del Moral (2004).

$\mathbb{L}^p$ bound

Consider that for all $n \in \mathbb{N}$, the product space $\overline{\mathsf{E}}_n = \mathsf{E}_n^{\Theta} \times \mathcal{P}(\mathsf{E}_n^X)$ is equipped with the norm $\| \cdot \|_{\overline{\mathsf{E}}_n}$ such that for all $(u, v) \in (\mathsf{E}_n^{\Theta})^2$ and $(\nu, \eta) \in (\mathcal{P}(\mathsf{E}_n^X))^2$,

$$\|(u, \eta) - (v, \nu)\|_{\overline{\mathsf{E}}_n} = |u - v| + \|\eta - \nu\|_{\mathfrak{F}_n}.$$

where $\mathfrak{F}_n$ is a countable collection of functions in $\mathcal{B}_1(\mathsf{E}_n^X)$.

Theorem 2.2.1. *For any $p \in \mathbb{N}^*$, $n \in \mathbb{N}$, let $\overline{f}_n \in \mathrm{Osc}_1(\overline{\mathsf{E}}_n)$ be a k_n-Lipschitz function. Assume that for any $\theta_n \in \mathsf{E}_n^{\Theta}$, the kernel transition $M_{\theta_n,n}^X$ can be written as $M_{\theta_n,n}^X(x_{n-1}, \mathrm{d}x_n) = m_{\theta_n,n}^X(x_{n-1}, x_n)p_{\theta_n,n}(\mathrm{d}x_n)$ for some measurable function $m_{\theta_n,n}^X$ on $\mathsf{E}_{n-1}^X \times \mathsf{E}_n^X$ and some probability measure $p_{\theta_n,n} \in \mathcal{P}(\mathsf{E}_n^X)$. Furthermore, assume that there exists a collection of mappings $\alpha_{\theta_n,n}$ on E_n^X such that*

$$\sup_{x_{n-1} \in \mathsf{E}_{n-1}^X} |\log m_{\theta_n,n}^X(x_{n-1}, x_n)| \leq \alpha_{\theta_n,n}(x_n)$$

with $p_{\theta_n,n}(e^{3\alpha_{\theta_n,n}}) < \infty$.
Then, the $\mathbb{L}^p$ error is bounded by

$$\|\tilde{\eta}_n^{N_1}(\overline{f}_n) - \overline{\eta}_n(\overline{f}_n)\|_p \leq k_n \frac{a(p)}{\sqrt{N_2}}(I(\mathfrak{F}_n) + b(n)) + 2\frac{d(p)}{\sqrt{N_1}} \sum_{q=0}^{n} \overline{g}_{q,n}\beta(\overline{P}_{q,n}), \qquad (2.51)$$

where the sequence $d(n)$ is defined in (2.51), $I(\mathfrak{F}_n)$ is defined in (2.50), $(b(n))_{n \geq 0}$ is defined by

$$b(0) = 0 \text{ and } b(n+1) \leq g_{\theta_n,n}p_{\theta_{n+1},n+1}(e^{3\alpha_{\theta_{n+1},n+1}}) \sum_{q=0}^{n} g_{\theta_{q:n},q,n}\beta(P_{\theta_{q:n},q,n}),$$

and $a(n)$ is a sequence such that for all $n \in \mathbb{N}^*$, $a(n) \leq c\lceil n/2 \rceil!$ with c a universal constant.

Proof. Let $\overline{f}_n \in \mathrm{Osc}_1(\overline{\mathsf{E}}_n)$ be a k_n-Lipschitz function, and apply triangular inequality:

$$\|\tilde{\eta}_n^{N_1}(\overline{f}_n) - \overline{\eta}_n(\overline{f}_n)\|_p \leq \|\tilde{\eta}_n^{N_1}(\overline{f}_n) - \overline{\eta}_n^{N_1}(\overline{f}_n)\|_p + \|\overline{\eta}_n^{N_1}(\overline{f}_n) - \overline{\eta}_n(\overline{f}_n)\|_p,$$

where $\overline{\eta}_n$ is defined in (2.34). Then using Theorem 7.4.4 from Del Moral (2004), one can bound the second term

$$\|\overline{\eta}_n^{N_1}(\overline{f}_n) - \overline{\eta}_n(\overline{f}_n)\|_p \leq 2\frac{d(p)}{\sqrt{N_1}} \sum_{q=0}^{n} \overline{g}_{q,n}\beta(\overline{P}_{q,n}).$$

Therefore, in order to bound the first term, use the definitions of $\tilde{\eta}_n^{N_1}$ and $\overline{\eta}_n^{N_1}$ in (2.48) and (2.40) respectively :

$$
\begin{aligned}
\|\tilde{\eta}_n^{N_1}(\overline{f}_n) - \overline{\eta}_n^{N_1}(\overline{f}_n)\|_p &= \mathbb{E}_{\overline{\eta}_0}\left[|\tilde{\eta}_n^{N_1}(\overline{f}_n) - \overline{\eta}_n^{N_1}(\overline{f}_n)|^p\right]^{1/p} \\
&= \mathbb{E}_{\overline{\eta}_0}\left[\left|\frac{1}{N_1}\sum_{i=1}^{N_1}\left\{\overline{f}_n(\theta_n^i, \eta_{\theta_{0:n}^i,n}^{X,N_2}) - \overline{f}_n(\theta_n^i, \eta_{\theta_{0:n}^i,n}^{X})\right\}\right|^p\right]^{1/p} \\
&\leq \mathbb{E}_{\overline{\eta}_0}\left[\left(\frac{1}{N_1}\sum_{i=1}^{N_1}|\overline{f}_n(\theta_n^i, \eta_{\theta_{0:n}^i,n}^{X,N_2}) - \overline{f}_n(\theta_n^i, \eta_{\theta_{0:n}^i,n}^{X})|\right)^p\right]^{1/p}
\end{aligned}
$$

As $\overline{f}_n$ is k_n-Lipschitz, it follows

$$
\begin{aligned}
\left|\overline{f}_n(\theta_n^i, \eta_{\theta_{0:n}^i,n}^{X,N_2}) - \overline{f}_n(\theta_n^i, \eta_{\theta_{0:n}^i,n}^{X})\right| &\leq k_n \left\|(\theta_n^i, \eta_{\theta_{0:n}^i,n}^{X,N_2}) - (\theta_n^i, \eta_{\theta_{0:n}^i,n}^{X})\right\|_{\overline{\mathsf{E}}_n} \\
&\leq k_n \left\|\eta_{\theta_{0:n}^i,n}^{X,N_2} - \eta_{\theta_{0:n}^i,n}^{X}\right\|_{\mathfrak{F}_n}.
\end{aligned}
$$

where $\mathfrak{F}_n$ is a countable collection of functions in $\mathcal{B}_1(\mathsf{E}_n^X)$ Therefore one gets

$$
\|\tilde{\eta}_n^{N_1}(\overline{f}_n) - \overline{\eta}_n^{N_1}(\overline{f}_n)\|_p \leq \mathbb{E}_{\overline{\eta}_0}\left[\left(\frac{1}{N_1}\sum_{i=1}^{N_1}k_n\left\|\eta_{\theta_{0:n}^i,n}^{X,N_2} - \eta_{\theta_{0:n}^i,n}^{X}\right\|_{\mathfrak{F}_n}\right)^p\right]^{1/p}.
$$

Denoting by θ^* the value at which the maximum of the Zolotarev semi-norms for $i \in [\![1, N_1]\!]$ is reached, yields to

$$
\|\tilde{\eta}_n^{N_1}(\overline{f}_n) - \overline{\eta}_n^{N_1}(\overline{f}_n)\|_p \leq k_n \mathbb{E}_{\overline{\eta}_0}\left[\|\eta_{\theta_{0:n}^*,n}^{X,N_2} - \eta_{\theta_{0:n}^*,n}^{X}\|_{\mathfrak{F}_n}^p\right]^{1/p}.
$$

But, according to [Del Moral (2004), Corollary 7.4.4] (p. 247),

$$
\mathbb{E}_{\overline{\eta}_0}\left[\|\eta_{\theta_{0:n}^*,n}^{X,N_2} - \eta_{\theta_{0:n}^*,n}^{X}\|_{\mathfrak{F}_n}^p\right]^{1/p} \leq \frac{a(p)}{\sqrt{N_2}}(I(\mathfrak{F}_n) + b(n)),
$$

where $I(\mathfrak{F}_n)$ is the entropy of $\mathfrak{F}_n$ defined in (2.50). Finally one ends up with

$$
\|\tilde{\eta}_n^{N_1}(\overline{f}_n) - \overline{\eta}_n^{N_1}(\overline{f}_n)\|_p \leq k_n\frac{a(p)}{\sqrt{N_2}}(I(\mathfrak{F}_n) + b(n)) + 2\frac{d(p)}{\sqrt{N_1}}\sum_{q=0}^{n}\overline{g}_{q,n}\beta(\overline{P}_{q,n}).
$$

$\square$

Time uniform bound

Before stating the uniform estimate we define the following two additional conditions. There exists some integer $\overline{m} \geq 1$ and some numbers $\varepsilon_n(\overline{M}) \in {]0, 1[}$ such that for $n \in \mathbb{N}$ and $(\overline{x}_n, \overline{y}_n) \in \overline{\mathsf{E}}_n^2$, one has :

$$
\overline{M}_{n,n+\overline{m}}(\overline{x}_n, .) \triangleq \overline{M}_{n+1}\ldots\overline{M}_{n+\overline{m}}(\overline{x}_n, .) \geq \varepsilon_n(\overline{M})\overline{M}_{n,n+\overline{m}}(\overline{y}_n, .) \qquad ((\overline{M})_{\overline{m}})
$$

For all $i \in [\![1, N_1]\!]$, there exists some integer $m_i \geq 1$ and some numbers $\varepsilon_n(M_{\theta^i}^X) \in]0, 1[$ such that for $n \in \mathbb{N}$, $(x_n, y_n) \in (\mathsf{E}_n^X)^2$, and $\theta_{n+1:n+m_i}^i \in \mathsf{E}_{n+1}^\Theta \times \ldots \times \mathsf{E}_{n+m}^\Theta$, one has :

$$M_{\theta_{n+1:n+m_i}^i, n, n+m_i}^X(x_n, .) \triangleq M_{\theta_{n+1}^i, n+1}^X \ldots M_{\theta_{n+m_i}^i, n+m_i}^X(x_n, .)$$
$$\geq \varepsilon_n(M_{\theta^i}^X) M_{\theta_{n+1:n+m_i}^i, n, n+m}^X(y_n, .) \quad ((M_{\theta^i}^X)_{m_i})$$

Theorem 2.2.2. *Suppose that conditions $(\overline{G})$, $((\overline{M})_{\overline{m}})$ are met for some integer $\overline{m} \geq 1$ and some pair parameters $(\epsilon_n(\overline{G}), \varepsilon_n(\overline{M}))$ and set $\epsilon(\overline{G}) \triangleq \wedge_{n \geq 0} \epsilon_n(\overline{G})$ and $\varepsilon(\overline{M}) \triangleq \wedge_{n \geq 0} \varepsilon_n(\overline{M})$.*
Moreover, assume that for all $i \in [\![1, N_1]\!]$ conditions (G_θ) and $((M_{\theta^i}^X)_{m_i})$ hold true for some sequence of integer m_i and some pair parameters $(\epsilon_n(G_{\theta^i}), \varepsilon_n(M_{\theta^i}^X))$ and set $\epsilon(G_{\theta^i}) \triangleq \wedge_{n \geq 0} \epsilon_n(G_{\theta^i})$ and $\varepsilon(M_{\theta^i}^X) \triangleq \wedge_{n \geq 0} \varepsilon_n(M_{\theta^i}^X)$. Set $m \triangleq \vee_i m_i$.
Further assume that for all $n \geq 0$ and $\theta_n^i \in \mathsf{E}_n^\Theta$ the kernel transition $M_{\theta_n^i, n}^X$ has the form $M_{\theta_n^i, n}^X(x_{n-1}, \mathrm{d}x_n) = m_{\theta_n^i, n}^X(x_{n-1}, x_n) p_{\theta_n^i, n}(\mathrm{d}x_n)$ for some measurable function $m_{\theta_n^i, n}^X$ on $\mathsf{E}_{n-1}^X \times \mathsf{E}_n^X$ and some probability measure $p_{\theta_n^i, n} \in \mathcal{P}(\mathsf{E}_n^X)$.
Also assume that $\sup_{x_{n-1} \in \mathsf{E}_{n-1}^X} |\log m_{\theta_n^i, n}^X(x_{n-1}, x_n)| \leq \alpha_{\theta_n^i, n}(x_n)$ with $p_{\theta_n^i, n}(e^{3\alpha_{\theta_n^i, n}}) < \infty$ for some collection of mappings $\alpha_{\theta_n^i, n}$ on E_n^X, and set :

$$p_{\theta^i}(e^{3\alpha_{\theta^i}}) \triangleq \sup_{n \geq 0} p_{\theta_n^i, n}(e^{3\alpha_{\theta_n^i, n}}) < \infty \quad and \quad p_\theta(e^{3\alpha_\theta}) \triangleq \vee_i p_{\theta^i}(e^{3\alpha_{\theta^i}}).$$

Then for any $p \in \mathbb{N}^*$, any k_n-Lipschitz functions $\overline{f}_n \in \mathrm{Osc}_1(\overline{\mathsf{E}}_n)$ one has :

$$\sup_{n \geq 0} \sup_{\overline{f}_n \in \mathrm{Osc}_1(\overline{\mathsf{E}}_n)} \|\tilde{\eta}_n^{N_1}(\overline{f}_n) - \overline{\eta}_n(\overline{f}_n)\|_p \leq \frac{2d(p)\overline{m}}{\sqrt{N_1} \varepsilon(\overline{M})^3 \epsilon(\overline{G})^{2\overline{m}-1}} + \frac{k\,a(p)}{\sqrt{N_2}} \left(I + \frac{m p_\theta(e^{3\alpha_\theta})}{\varepsilon(M_\theta^X)^3 \epsilon(G_\theta)^{2m}} \right)$$

with

$$k = \sup_n k_n, \quad \varepsilon(M_\theta^X) = \wedge_i \varepsilon(M_{\theta^i}^X) > 0, \quad \epsilon(G_\theta) = \wedge_i \epsilon(G_{\theta^i}) > 0, \quad I \triangleq \sup_{n \geq 0} I(\mathfrak{F}_n) < \infty.$$

Proof.

$$\sup_{n \geq 0} \sup_{\overline{f}_n \in \mathrm{Osc}_1(\overline{\mathsf{E}}_n)} \|\tilde{\eta}_n^{N_1}(\overline{f}_n) - \overline{\eta}_n(\overline{f}_n)\|_p$$
$$\leq \sup_{n \geq 0} \sup_{\overline{f}_n \in \mathrm{Osc}_1(\overline{\mathsf{E}}_n)} \left(\|\tilde{\eta}_n^{N_1}(\overline{f}_n) - \overline{\eta}_n^{N_1}(\overline{f}_n)\|_p + \|\overline{\eta}_n^{N_1}(\overline{f}_n) - \overline{\eta}_n(\overline{f}_n)\|_p \right)$$
$$\leq \sup_{n \geq 0} \sup_{\overline{f}_n \in \mathrm{Osc}_1(\overline{\mathsf{E}}_n)} \|\tilde{\eta}_n^{N_1}(\overline{f}_n) - \overline{\eta}_n^{N_1}(\overline{f}_n)\|_p + \sup_{n \geq 0} \sup_{\overline{f}_n \in \mathrm{Osc}_1(\overline{\mathsf{E}}_n)} \|\overline{\eta}_n^{N_1}(\overline{f}_n) - \overline{\eta}_n(\overline{f}_n)\|_p$$

From [Del Moral (2004), Theorem 7.4.4] (p. 247), one has

$$\sup_{n \geq 0} \sup_{\overline{f}_n \in \mathrm{Osc}_1(\overline{\mathsf{E}}_n)} \|\overline{\eta}_n^{N_1}(\overline{f}_n) - \overline{\eta}_n(\overline{f}_n)\|_p \leq \frac{2d(p)\overline{m}}{\sqrt{N_1} \varepsilon(\overline{M})^3 \epsilon(\overline{G})^{2\overline{m}-1}},$$

since conditions $(\overline{G})$ and $((\overline{M})_{\overline{m}})$ hold true. Then it follows that the only term one has to work on is the following.

$$
\sup_{n \geq 0} \sup_{\overline{f}_n \in \mathrm{Osc}_1(\overline{\mathsf{E}}_n)} \left\| \tilde{\eta}_n^{N_1}(\overline{f}_n) - \overline{\eta}_n^{N_1}(\overline{f}_n) \right\|_p
$$

$$
= \sup_{n \geq 0} \sup_{\overline{f}_n \in \mathrm{Osc}_1(\overline{\mathsf{E}}_n)} \left\| \frac{1}{N_1} \sum_{i=1}^{N_1} \left\{ \overline{f}_n(\theta_n^i, \eta_{\theta_{0:n}^i,n}^{X,N_2}) - \overline{f}_n(\theta_n^i, \eta_{\theta_{0:n}^i,n}^{X}) \right\} \right\|_p
$$

$$
\leq \frac{1}{N_1} \sum_{i=1}^{N_1} \sup_{n \geq 0} \sup_{\overline{f}_n \in \mathrm{Osc}_1(\overline{\mathsf{E}}_n)} \left\| \overline{f}_n(\theta_n^i, \eta_{\theta_{0:n}^i,n}^{X,N_2}) - \overline{f}_n(\theta_n^i, \eta_{\theta_{0:n}^i,n}^{X}) \right\|_p
$$

As the function $\overline{f}_n$ is k_n-Lipschitz, for all $i \in [\![1, N_1]\!]$,

$$
\sup_{n \geq 0} \sup_{\overline{f}_n \in \mathrm{Osc}_1(\overline{\mathsf{E}}_n)} \left\| \overline{f}_n(\theta_n^i, \eta_{\theta_{0:n}^i,n}^{X,N_2}) - \overline{f}_n(\theta_n^i, \eta_{\theta_{0:n}^i,n}^{X}) \right\|_p
$$

$$
= \sup_{n \geq 0} \sup_{\overline{f}_n \in \mathrm{Osc}_1(\overline{\mathsf{E}}_n)} \mathbb{E}_{\overline{\eta}_0} \left[\left| \overline{f}_n(\theta_n^i, \eta_{\theta_{0:n}^i,n}^{X,N_2}) - \overline{f}_n(\theta_n^i, \eta_{\theta_{0:n}^i,n}^{X}) \right|^p \right]^{1/p}
$$

$$
\leq \sup_{n \geq 0} \mathbb{E}_{\overline{\eta}_0} \left[k_n^p \left\| \eta_{\theta_{0:n}^i,n}^{X,N_2} - \eta_{\theta_{0:n}^i,n}^{X} \right\|_{\mathfrak{F}_n}^p \right]^{1/p}
$$

$$
\leq \sup_{n \geq 0} k_n \mathbb{E}_{\overline{\eta}_0} \left[\left\| \eta_{\theta_{0:n}^i,n}^{X,N_2} - \eta_{\theta_{0:n}^i,n}^{X} \right\|_{\mathfrak{F}_n}^p \right]^{1/p}.
$$

Set $k \triangleq \sup_n k_n$, then

$$
\sup_{n \geq 0} \sup_{\overline{f}_n \in \mathrm{Osc}_1(\overline{\mathsf{E}}_n)} \left\| \overline{f}_n(\theta_n^i, \eta_{\theta_{0:n}^i,n}^{X,N_2}) - \overline{f}_n(\theta_n^i, \eta_{\theta_{0:n}^i,n}^{X}) \right\|_p \leq k \sup_{n \geq 0} \mathbb{E}_{\overline{\eta}_0} \left[\left\| \eta_{\theta_{0:n}^i,n}^{X,N_2} - \eta_{\theta_{0:n}^i,n}^{X} \right\|_{\mathfrak{F}_n}^p \right]^{1/p}
$$

From [Del Moral (2004), Corollary 7.4.5] (p. 249), as one assumes that there exists $m_i \geq 1$ for
$\theta_{n,n+m_i}^i \in \mathsf{E}_n^\Theta \times \ldots \times \mathsf{E}_{n+m_i}^\Theta$,

$$
\sup_{n \geq 0} \mathbb{E}_{\overline{\eta}_0} \left[\left\| \eta_{\theta_{0:n}^i,n}^{X,N_2} - \eta_{\theta_{0:n}^i,n}^{X} \right\|_{\mathfrak{F}_n}^p \right]^{1/p} \leq \frac{a(p)}{\sqrt{N_2}} \left(I + \frac{m_i p_{\theta^i}(e^{3\alpha_{\theta^i}})}{\varepsilon(M_{\theta^i}^X)^3 \epsilon(G_{\theta^i})^{2m_i}} \right),
$$

where $I \triangleq \sup_{n \geq 0} I(\mathfrak{F}_n) < \infty$. One concludes easily. $\qquad \square$

2.2.4 Asymptotic analysis of the labeled island particle algorithm

This section deals with the asymptotic behaviour of the labeled island particle algorithm. Especially, we focus on the almost sure convergence.

Using Theorem 2.2.1 obtained in Section 2.2.3, one can easily get the almost sure convergence of the double estimator $\tilde{\eta}_n^{N_1}$ toward $\overline{\eta}_n$ under the same assumptions as in Theorem 2.2.1.

Theorem 2.2.3. *Under the same assumptions as in Theorem 2.2.1, for all $n \geq 0$ and*

for every k_n- Lipschitz function $\overline{f}_n \in \mathrm{Osc}_1(\overline{\mathsf{E}}_n)$, one has

$$\tilde{\eta}_n^{N_1}(\overline{f}_n) \xrightarrow{a.s} \overline{\eta}_n(\overline{f}_n), \text{ as } N \to \infty,$$

with $N = N_1 N_2$ such that $N_1 = N^\alpha$ and $N_2 = N^{1-\alpha}$ for all $\alpha \in]0,1[$.

Proof. Let $\overline{f}_n \in \mathrm{Osc}_1(\mathsf{E}_n)$ be a k_n-Lipschitz function and $\varepsilon > 0$ a real constant. For all $p \in \mathbb{N}^*$, by Markov's inequality, one has

$$\mathbb{P}\left(|\tilde{\eta}_n^{N_1}(\overline{f}_n) - \overline{\eta}_n(\overline{f}_n)| > \varepsilon\right) \leq \frac{\mathbb{E}_{\overline{\eta}_0}\left[|\tilde{\eta}_n^{N_1}(\overline{f}_n) - \overline{\eta}_n(\overline{f}_n)|^p\right]}{\varepsilon^p}.$$

Then, applying Theorem 2.2.1, and noting

$$C(p,n) \triangleq k_n a(p)(I(\mathcal{F}_n) + b(n)) \quad \text{and} \quad \tilde{C}(p,n) \triangleq 2d(p) \sum_{q=0}^n \overline{g}_{q,n} \beta(\overline{P}_{q,n}),$$

one has

$$\|\tilde{\eta}_n^{N_1}(\overline{f}_n) - \overline{\eta}_n(\overline{f}_n)\|_p^p \leq \left(\frac{C(p,n)}{\sqrt{N^\alpha}} + \frac{\tilde{C}(p,n)}{\sqrt{N^{1-\alpha}}}\right)^p$$

$$= \sum_{k=0}^p \binom{p}{k} \frac{C(p,n)^k \tilde{C}(p,n)^{p-k}}{N^{(\alpha-\frac{1}{2})k + \frac{1-\alpha}{2}p}}.$$

The finite sequence $(s_{\alpha,p}(k))_{k=0}^p$ defined by $s_{\alpha,p}(k) = (\alpha - 1/2)k + (1-\alpha)p/2$ is bounded from below by

$$m_{\alpha,p} \triangleq \frac{\alpha p}{2} \mathbb{1}_{0<\alpha\leq 0.5} + \frac{(1-\alpha)p}{2} \mathbb{1}_{0.5<\alpha<1},$$

so that

$$\|\tilde{\eta}_n^{N_1}(\overline{f}_n) - \overline{\eta}_n(\overline{f}_n)\|_p^p \leq \frac{\left(C(p,n) + \tilde{C}(p,n)\right)^p}{N^{m_{\alpha,p}}}.$$

Choose p a positive integer such that $m_{\alpha,p} \geq 2$ i.e. satisfying

$$\begin{cases} p > \frac{4}{\alpha} & \text{if} \quad 0 < \alpha \leq 0.5 \\ p > \frac{4}{1-\alpha} & \text{if} \quad 0.5 < \alpha < 1. \end{cases} \tag{2.52}$$

Hence,

$$\|\tilde{\eta}_n^{N_1}(\overline{f}_n) - \overline{\eta}_n(\overline{f}_n)\|_p^p \leq \frac{\left(C(p,n) + \tilde{C}(p,n)\right)^p}{N^2}.$$

By comparison of series of non-negative general term with a convergent Riemann series, one concludes that the series

$$\sum_{N\geq 0} \mathbb{P}\left(|\tilde{\eta}_n^{N_1}(\overline{f}_n) - \overline{\eta}_n(\overline{f}_n)| > \varepsilon\right) \text{ is convergent,}$$

which implies by Borel-Cantelli's lemma, that

$$\tilde{\eta}_n^{N_1}(\overline{f}_n) \xrightarrow{a.s} \overline{\eta}_n(\overline{f}_n), \text{ as } N \to \infty.$$

$\square$

Taking such kind of N means that for a total budget N of particles, one can consider any decomposition (as a power of N) of the particles between islands and within each island.

2.3 Parameter and state space estimation in a random environment

Some aircraft parameters can be considered as fixed parameters, such as the lift or drag coefficients. In order to estimate them, we consider that the random process influenced by the environment depends on unknown fixed parameters. The parameters r are seen as the realization of a random variable R whose density is λ. In the sequel, we bring our attention on the triple estimation issue which consists in estimating the random process X_n which depends on the surrounding environment Θ_n but also on fixed parameters r.

This problem can be cast into the more general issue of joint parameter and state estimation which is at stake in different areas of applied mathematics, notably in financial mathematics. To overcome this question, different methods were recently developed, see for example Poyiadjis et al. (2005); Andrieu et al. (2010). In Andrieu et al. (2010), the idea used to estimate the state and the parameter of a random process was to use the empirical measure obtained through particle filters inside a Markov Chain Monte Carlo (MCMC) method. The ensuing algorithm is named Particle Markov chain Monte Carlo (PMCMC). This idea was developed and applied by Fernández-Villaverde and Rubio-Ramírez (2007); An and Schorfheide (2007) to approximate dynamic stochastic general equilibrium models. Andrieu et al. gave a formal proof of the algorithm convergence. Indeed particle filters provide unbiased estimation of the probability density of the random process which can be used inside MCMC methods to evaluate the likelihood ratio of the parameter proposition.

In this section, first we present MCMC methods. Then we recall the formalism of the PMCMC methods developed by Andrieu et al. and finally we give an adapted version of the PMCMC algorithm which can deal with the case where the random process evolves in a random environment.

2.3.1 Introduction to Markov Chain Monte Carlo methods

Stochastic algorithms are random searching procedures of a state space. Formally they can be modelled by an homogeneous $(\mathsf{E}, \mathcal{E})$-Markov chain $X = \{X_n, n \geq 0\}$ with kernel transition K from E to E. Generally, as time goes the random searching procedure becomes more and more sharp, in some sense. That is the distribution of the Markov chain denoted by η_n tends to, what is called, a stationary distribution denoted by π. The invariant or stationary distribution π of the Markov process X_n should verify:

$$\pi(A) = \int_{\mathsf{E}} \pi(\mathrm{d}x) K(x, A), \forall A \in \mathcal{E}$$

The asymptotic behaviour of the distributions η_n when n tends to infinity is a major problem in Markov chain theory. We do not intend here to give a full treatise on this question. In this paragraph we present the question of choosing in a clever way the kernel transition K and the Markov process in order to converge to the fixed stationary distribution π. MCMC samplers are irreducible and aperiodic Markov chains that have the target distribution as the invariant distribution. Several ways to construct such kernel transitions exist, such as the Metropolis-Hastings transition and the Gibbs sampler. The Metropolis-Hastings (MH) algorithm is the most popular MCMC method as it proposes a simple way to construct such homogeneous kernels. We attach here our attention on this algorithm.

A Metropolis Hasting transition of invariant distribution π consists in a two steps evolution: a proposition and an acceptance/rejection step. For any measure $\eta \in \mathsf{M}(\mathsf{E})$, symmetric Markovian transition kernel $Q(x, \mathrm{d}y)$ on E verify the following relation:

$$(\eta \times Q)(\mathrm{d}(x, y))_0 \triangleq \eta(\mathrm{d}x)Q(x, \mathrm{d}y) = \eta(\mathrm{d}y)Q(y, \mathrm{d}x) \triangleq (\eta \times Q)(\mathrm{d}(x, y))_1$$

The set of such transitions kernels are denoted by $\mathcal{Q}(\eta)$. For any $Q \in \mathcal{Q}(\eta)$, we define the acceptance ratio a for all $x, y \in \mathsf{E} \times \mathsf{E}$ such that:

$$a(x, y) = 1 \wedge \frac{\mathrm{d}(\eta \times Q)_1}{\mathrm{d}(\eta \times Q)_0}(x, y)$$

Then the two steps of the Metropolis-Hasting algorithm are given by two transitions kernels M and S which are respectively defined from E to $\mathsf{E} \times \mathsf{E}$ and from $\mathsf{E} \times \mathsf{E}$ to E by:

$$M(x, \mathrm{d}(y, y')) \triangleq \delta_x(\mathrm{d}y)Q(y, \mathrm{d}y') \tag{2.53}$$

$$S((y, y'), \mathrm{d}z) \triangleq a(y, y')\delta_{y'}(\mathrm{d}z) + (1 - a(y, y'))\delta_y(\mathrm{d}z) \tag{2.54}$$

where M corresponds to the proposition step and allow to explore the state space E and S is the acceptance/rejection step. Then the kernel K of the MCMC algorithm is given by:

$$
\begin{aligned}
K(x, \mathrm{d}z) &= \int_{\mathsf{E}} M(x, \mathrm{d}(y, y'))S((y, y'), \mathrm{d}z) \\
&= \int_{\mathsf{E} \times \mathsf{E}} \delta_x(\mathrm{d}y)Q(y, \mathrm{d}y')(a(y, y')\delta_{y'}(\mathrm{d}z) + (1 - a(y, y'))\delta_y(\mathrm{d}z)) \\
&= a(x, z)Q(x, \mathrm{d}z) + \left(1 - \int_{\mathsf{E}} a(x, y)Q(x, \mathrm{d}y)\right)\delta_x(\mathrm{d}z)
\end{aligned}
$$

The acceptance/rejection step allows to sometimes accept the moves and sometimes remain in place. Note that the acceptance ratio a indicates how probable the new proposed sample is with respect to the current sample, according to the distribution η. If we attempt to move to a point that is more probable than the existing point (i.e. a point in a higher-density region of η), we will always accept the move. However, if we attempt to move to a less probable point, we will sometimes reject the move, and the more the

relative drop in probability, the more likely we are to reject the new point. Thus, we will tend to stay in (and return large numbers of samples from) high-density regions of η, while only occasionally visiting low-density regions. Intuitively, this is why this algorithm works, and returns samples that follow the desired distribution π. This method can be used to sample a draw from any distribution, in the next paragraph we will see how it is used to sample from parameter posterior distributions in state space model.

2.3.2   Particle Markov Chain Monte Carlo methods for joint parameter state estimation

Let consider a filtering problem where the pair signal/observation has a fixed component r. Suppose now that the parameter r, is a realization of a random variable R taking value in the measurable space $(S, \mathcal{S})$ with distribution λ. For each realization of r, we define the following state space model. Suppose that at every time step, the state of a Markov chain $X_n \in \mathsf{E}_n$ is partially observed by the process $Y_n \in \mathsf{F}_n$, where X_n is a Markov process with transition kernel $M_{r,n}$ and initial distribution $\eta_{r,0}$ in a measurable space $(\mathsf{E}_n, \mathcal{E}_n)$. The observation process Y_n is defined on $(\mathsf{F}_n, \mathcal{F}_n)$ and we suppose that it is related to the process by the observation function h_n such that $Y_n = h_n(X_n, V_n)$ where V_n is a Markovian observation noise distributed according to the probability measure q_n. The filtering problem consists in computing the conditional distributions of $(X_0, \ldots, X_n)$ given the observations $(Y_0, \ldots, Y_n)$ but also the parameter posterior distribution $\mathbb{P}(R \in \mathrm{d}r | Y_{0:n} = y_{0:n})$. Suppose that for every time step n, the laws $h_n(r, X_n, V_n)$ and V_n are absolutely continuous and $g_{n,r}(x_n, .)$ is the corresponding density, then we get the following formula for the likelihood function:

$$\mathbb{P}(Y_n \in \mathrm{d}y_n | X_n = x_n, R = r) = g_{n,r}(x_n, y_n) q_n(\mathrm{d}y_n)$$

Fix the observation sequence such that $Y_{0:n} = y_{0:n}$ and define $G_{n,r}(x_n) \triangleq g_{n,r}(x_n, y_n)$. By the Bayes rule we have:

$$\mathbb{Q}_{r,n}(\mathrm{d}(x_0, \ldots, x_n)) \triangleq \mathbb{P}_{\eta_{r,0}}(X_{0:n} \in \mathrm{d}x_{0:n} | Y_{0:n-1} = y_{0:n-1}, R = r)$$

$$= \frac{1}{\mathscr{Z}_{r,n}} \left\{ \prod_{p=0}^{n-1} G_{n,r}(x_n) \right\} \eta_{r,0}(\mathrm{d}x_0) M_{r,1}(x_0, \mathrm{d}x_1) \ldots M_{r,n}(x_{n-1}, \mathrm{d}x_n)$$

where the normalizing constant $\mathscr{Z}_{r,n}$ is given by:

$$\mathscr{Z}_{r,n} \triangleq \mathbb{E}_{\eta_{r,0}} \left[\prod_{p=0}^{n-1} G_{n,r}(x_n) \right]$$

The updated probability measure $\hat{\mathbb{Q}}_{r,n}$ can also be defined:

$$\hat{\mathbb{Q}}_{r,n}(\mathrm{d}(x_0, \ldots, x_n)) = \frac{1}{\hat{\mathscr{Z}}_{r,n}} \left\{ \prod_{p=0}^{n-1} G_{n,r}(x_n) \right\} \eta_{r,0}(\mathrm{d}x_0) M_{r,1}(x_0, \mathrm{d}x_1) \ldots M_{r,n}(x_{n-1}, \mathrm{d}x_n)$$

where the normalizing constant $\hat{\mathcal{Z}}_{r,n}$ is given by:

$$\hat{\mathcal{Z}}_{r,n} \triangleq \mathbb{E}_{\eta_{r,0}}\left[\prod_{p=0}^{n} G_{n,r}(x_n)\right]$$

Therefore, when R is given equal to r, traditional particle filtering technique can be used to estimate the distribution of the signal. Let us introduce the marginal measure $\gamma_{r,n}$ of the path measure $\mathbb{Q}_{r,n}$ defined for all $f_n \in \mathcal{B}_b(\mathsf{E}_n)$ by:

$$\gamma_{r,n}(f_n) \triangleq \mathbb{E}_{\eta_{r,0}}\left[f_n(X_n)\prod_{p=0}^{n-1} G_{p,r}(X_p)\right] \tag{2.55}$$

We can also define the probability measure $\eta_{r,n}$ for all $f_n \in \mathcal{B}_b(\mathsf{E}_n)$ by:

$$\eta_{r,n}(f_n) \triangleq \frac{\gamma_{r,n}(f_n)}{\gamma_{r,n}(1)} \tag{2.56}$$

The last quantity (2.56) corresponds to the prediction step of the filter.

We also define the updated measure $\hat{\gamma}_{r,n}$ and the filtering probability measure $\hat{\eta}_{r,n}$ for all $f_n \in \mathcal{B}_b(\mathsf{E}_n)$ by:

$$\hat{\gamma}_{r,n}(f_n) = \gamma_{r,n}(G_{n,r}f_n) \tag{2.57}$$

$$\hat{\eta}_{r,n} = \frac{\hat{\gamma}_{r,n}(f_n)}{\hat{\gamma}_{r,n}(1)} \tag{2.58}$$

Here we can notice that the normalizing constant $\hat{\mathcal{Z}}_{r,n}$ which is the likelihood of the observations can be rewritten using the marginal measure:

$$\hat{\mathcal{Z}}_{r,n} = \hat{\gamma}_{r,n}(1) = \gamma_{r,n}(G_{n,r})$$
$$= \prod_{p=0}^{n} \eta_{r,p}(G_{n,r})$$

Taking the logarithm of this quantity, we obtain the log-likelihood, but a problem arises as the probability distributions $\eta_{r,p}$ are unknown. Therefore if one wants to use Expectation Maximization (EM) algorithm to retrieve the value of r, one has first to deal with the approximation of these quantities. These technique was developed in Poyiadjis et al. (2005) and use the particle approximation at each time step to evaluate the gradient of the log-likelihood. Here we present the algorithm proposed by Andrieu et al. (2010) which consists in using particle filters inside an MCMC method. To this end, going back to the original problem of the parameter posterior distribution estimation using the Bayes rule

we get:

$$\pi_n(\mathrm{d}r) \triangleq \mathbb{P}(R \in \mathrm{d}r | Y_{0:n} = y_{0:n}) = \frac{1}{\mathcal{Z}_{n+1}} \hat{\mathcal{Z}}_{r,n} \lambda(\mathrm{d}r)$$
$$= \frac{1}{\mathcal{Z}_{n+1}} \prod_{p=0}^{n} \underbrace{\eta_{r,p}(G_{p,r})}_{h_p(r)} \lambda(\mathrm{d}r)$$

where $\mathcal{Z}_{n+1} = \int_S \hat{\mathcal{Z}}_{r,n} \lambda(r) dr$.

One can observe that this quantity is written as a Feynman-Kac measure where the $h_p(r)$ are unknown. However, particle filters is a tool which allows their approximation. Then, consider the particle filter associated to the pair potential kernel $(G_{r,n}, M_{r,n})$ introduced in Section 2.1.3. We denote by $\eta_{r,n}^N$ the empirical measure which approximate the measure $\eta_{r,n}$.

As the empirical unnormalized measure associated is unbiased, Andrieu et al. (2010) use it to estimate the normalizing constant $\hat{\mathcal{Z}}_{r,n}$. The approximation of this quantity denoted by $\hat{\mathcal{Z}}_{r,n}^N$ is defined by:

$$\hat{\mathcal{Z}}_{r,n}^N \triangleq \gamma_{r,p}^N(G_{r,n})$$
$$= \prod_{p=0}^{n} \eta_{r,p}^N(G_{r,p})$$

Using the unbiased property of the particle filter, we have that $\mathbb{E}\left[\gamma_{r,n}^N(G_{r,n})\right] = \hat{\mathcal{Z}}_{r,n}$.

As the particle approximation of the $h_p(r)$ functions, denoted by $h_p^N(r)$, are going to be used, we introduce several quantities.

Let consider the complete genealogical tree of the particles evolving thanks to the pair potential/mutation $(G_{r,n}, M_{r,n})$. This tree is obtained when tracing back in time the ancestral lineage of each particle. Denoting $(\xi_{0,n}^i, \dots, \xi_{n,n}^i) \triangleq \xi_n^i$ the ancestral lineage of the ith-particle associated to the realization $R = r$, one can notice here that:

$$\frac{1}{N} \sum_{i=0}^{N} \delta_{(\xi_{0,n}^i, \dots, \xi_{n,n}^i)} \xrightarrow[N \to +\infty]{} \mathbb{Q}_{r,n}$$

Considering now the complete genealogical tree $\Xi_n \triangleq (\xi_p)_{p=0}^n$, defined such that:

$$\Xi_n = (\Xi_{0,n}, \dots, \Xi_{n,n}) = (\xi_0, \dots, \xi_n) \in \prod_{p=0}^{n} \mathsf{E}_p^N$$

where

$$\Xi_{p,n} = (\Xi_{p,n}^i)_{i=1}^N = (\xi_p^i)_{1 \le i \le N}$$

with $\xi_p^i = (\xi_{0,p}^i, \dots, \xi_{p,p}^i)$.

We define the approximation of the normalizing constant $\hat{\mathcal{Z}}_{r,n}$ by:

$$\hat{\mathcal{Z}}_{r,n}^N(\Xi_n) \triangleq \prod_{p=0}^{n} h_p(r, \xi_p)$$

where $h_p^N(r, \xi_p) \triangleq \eta_{r,p}^N(G_{p,r}) = \frac{1}{N} \sum_{i=0}^{N} G_{p,r}(\xi_p^i)$.

Let denote by $\bar{\mathcal{Z}}_{r,n}^N$ the following quantity:

$$\bar{\mathcal{Z}}_{r,n}^N(\Xi_n) \triangleq \frac{\hat{\mathcal{Z}}_{r,n}^N(\Xi_n)}{\hat{\mathcal{Z}}_{r,n}}$$

and $\mathbb{P}_{r,n}^N$ be the genealogical tree distribution associated to the realization r of R, we have that:

$$\pi_{r,n}^N(\Xi_n) = \bar{\mathcal{Z}}_{r,n}^N(\Xi_n)\mathbb{P}_{r,n}^N(\Xi_n)$$

Then

$$\begin{aligned}
\pi_n^N(r, \Xi_n) &= \pi_n^N(\Xi_n)\frac{1}{\hat{\mathcal{Z}}_n}\hat{\mathcal{Z}}_{r,n}\lambda(r) \\
&= \bar{\mathcal{Z}}_{r,n}^N(\Xi_n)\mathbb{P}_{r,n}^N(\Xi_n)\frac{1}{\hat{\mathcal{Z}}_n}\hat{\mathcal{Z}}_{r,n}\lambda(r) \\
&= \frac{\hat{\mathcal{Z}}_{r,n}^N(\Xi_n)}{\hat{\mathcal{Z}}_{r,n}}\mathbb{P}_{r,n}^N(\Xi_n)\frac{1}{\hat{\mathcal{Z}}_n}\hat{\mathcal{Z}}_{r,n}\lambda(r) \\
&= \frac{\hat{\mathcal{Z}}_{r,n}^N(\Xi_n)}{\hat{\mathcal{Z}}_n}\mathbb{P}_{r,n}^N(\Xi_n)\lambda(r) \\
&= \frac{1}{\hat{\mathcal{Z}}_n}\left\{\prod_{p=0}^{n} h_p^N(r, \xi_p)\right\}\mathbb{P}_{r,n}^N(\Xi_n)\lambda(r)
\end{aligned}$$

Marginalizing out with respect to the genealogical tree the distribution $\pi_n^N(r, \Xi_n)$ we obtain the empirical measure approximating $\pi_n(\mathrm{d}r)$ which is the parameter posterior distribution. Then, the idea consists in using MH algorithm to draw a sample from the target distribution $\pi_n^N(r, \Xi_n)$ with the proposition kernel given by:

$$K((r, \Xi_n), \mathrm{d}(r', \Xi_n')) = L(r, \mathrm{d}r')\mathbb{P}_{r',n}^N(\Xi_n')$$

where L is a reversible kernel with respect to λ and the acceptance/rejection ratio given by:

$$a((r, \Xi), \mathrm{d}(r', \Xi')) = 1 \wedge \frac{\hat{\mathcal{Z}}_{r',n}(\Xi')\lambda(r')L(r', \mathrm{d}r)}{\hat{\mathcal{Z}}_{r',n}(\Xi)\lambda(r)L(r, \mathrm{d}r')}$$

We present in Algorithm 4 the pseudo-code form of the particle MCMC algorithm.

2.3.3 Adaptation of the PMCMC algorithm for parameter and state estimation in a random environment

Going back to the problem we are concerned with, we have to consider also that the random process X_n is influenced by the random media Θ_n. Therefore the PMCMC algorithm developed by Andrieu et al. (2010) is not adapted. However, we present in this

---

Algorithm 4 Particle MCMC - PMCMC

Require: $\eta_{r,0}$, $(M_{r,n})_{n=0}^{T}$, $(G_{n,r})_{n=0}^{T}$ and r_0

Ensure: Particle approximation of $\mathbb{P}(R \in \mathrm{d}r | Y_{0:T} = y_{0:T})$ and $\mathbb{P}_{\eta_{r,0}}(X_{0:T} \in \mathrm{d}x_{0:T} | Y_{0:T} = y_{0:T}, R = r)$

$\boxed{\text{Begin}}$

1. Parameter initialization $p = 0$

$r_p = r_0$

for $p = 0, \dots, nsample$ **do**

  2. Particle filtering for r_p

  2.1 Initialization $n = 0$

  for $i = 1, \dots, N$ **do**

    Sample $\xi_0^i \sim \eta_{r,0}$,

  end for

  for $n = 0, \dots, T$ **do**

    2.2 Selection of particles

    Sample $I_n = (I_n^i)_{i=1}^{N}$ according to a multinomial distribution with probability $\propto$ $\left(G_{n,r_p}(\xi_{n,T}^i) \right)_{i=1}^{N}$

    Update the lineage vector $\hat{\xi}_n^i = (\xi_{0,n}^{I_n^i}, \dots, \xi_{n,n}^{I_n^i})$

    2.3. Mutation of particle

    Sample independently $\xi_{n+1,T}^i$ according to $M_{r,n}(\xi_{n,T}^{I_n^i}, .)$

    Update the lineage vector $\xi_{n+1}^i = (\xi_{0,n+1}^i, \dots, \xi_{n+1,n+1}^i)$

  end for

  3. Likelihood evaluation

  Evaluate $\hat{\mathcal{Z}}_{r_p,T}^N(\Xi_T)$

  4. Mutation of the parameter r_p

  Sample r^* using the kernel $L(r_p, .)$

  5. Particle filtering for r^*

  Repeat step 2 using r^* instead of r_p

  6. Likelihood evaluation

  Evaluate $\hat{\mathcal{Z}}_{r^*,T}^N(\Xi_T^*)$

  7. Acceptance rejection step

  $\begin{cases} r_{p+1} = r^* \\ \Xi_T^{p+1} = \Xi_T^* \end{cases}$ with probability $a((r_p, \Xi_T), (r^*, \Xi_T^*))$.

end for

$\boxed{\text{End}}$

---

paragraph an adaptation which uses the same idea as the PMCMC algorithm, that is using the particle approximation inside a Metropolis Hasting algorithm. First we recall all the notations taken from Section 2.2 and we adapt them to the additional problem of parameter posterior distributions estimation. Then we present the adapted algorithm which is named by us as labeled island particle MCMC method (liPMCMC).

Filtering and estimation problem

Using the same notations as in Section 2.2, we consider that the random process X_n depends now on the parameter R, which is a random variable on $(S, \mathcal{S})$ with distribution λ. As before Y_n stands for the partial observation process of (Θ_n, X_n). We want to estimate the conditional distribution of the process (Θ_n, X_n) using the observations Y_n but also the distribution of R given the sequence of observations. To model this filtering problem, one can use the model developed in Section 2.2. Nevertheless, all the quantities such as the quenched process and the process evolving in the distribution space depend on the parameter r. To make it clear in the notations, all the quantities which depends on r are identified by the subscript r. The random process in distribution space denoted by $\overline{X}_{r,n}$, is now given by:

$$\overline{X}_{r,n} = (\Theta_n, \eta^X_{\theta_{0:n}, r, n}) \in \overline{\mathsf{E}}_n \triangleq \mathsf{E}^\Theta_n \times \mathcal{P}(\mathsf{E}^X_n)$$

It is still a Markov chain, with initial distribution $\overline{\eta}_{r,0}$ and transition kernel $\overline{M}_{r,n}$. Therefore we can still use a Feynman-Kac path measure but this time in distribution space to denote the quantity we look for estimation. Let denote by $\overline{\mathbb{Q}}_{\overline{\eta}_{r,0}, r, n}$ this quantity which is defined by:

$$\overline{\mathbb{Q}}_{\overline{\eta}_{r,0}, r, n}(\mathrm{d}((\theta_0, \eta^X_{\theta_0, r}), \ldots, (\theta_n, \eta^X_{\theta_{0:n}, r, n}))) = \frac{1}{\overline{\mathcal{Z}}_{r,n}} \left\{ \prod_{p=0}^{n-1} \overline{G}_{p,r}(\overline{x}_p) \right\} \overline{\eta}_{r,0}(\mathrm{d}\overline{x}_0)$$
$$\overline{M}_{r,1}(\overline{x}_0, \mathrm{d}\overline{x}_1) \ldots \overline{M}_{r,n}(\overline{x}_{n-1}, \mathrm{d}\overline{x}_n) \quad (2.59)$$

with the normalizing constant $\overline{\mathcal{Z}}_{r,n}$ given by:

$$\overline{\mathcal{Z}}_{r,n} = \mathbb{E}_{\overline{\eta}_{r,0}} \left[\prod_{p=0}^{n-1} \overline{G}_{r,p}(\overline{X}_p) \right]$$

where the potential functions are defined for all $\overline{x}_p \in \overline{\mathsf{E}}_p$ such that:

$$\overline{G}_{p,r}(\overline{x}_p) = \int G_{p, \theta_p, r}(x_p) \eta^X_{\theta_{0:p}, r, p}(\mathrm{d}x_p)$$

The quantity defined by (2.59) corresponds to following conditional probability:

$$\mathbb{P}_{\overline{\eta}_{r,0}}(\overline{X}_{0:n} \in \mathrm{d}\overline{x}_{0:n} | Y_{0:n-1} = y_{0:n-1}, R = r)$$

Concerning the normalizing constant, we can observe that $\bar{\mathcal{Z}}_{r,n}$ corresponds to the likelihood $\mathbb{P}_{\bar{\eta}_{r,0}}(Y_{0:n-1} \in dy_{0:n-1}|R=r)$.

We denote by $\hat{\bar{\mathbb{Q}}}_{\bar{\eta}_{r,0},r,n}$ the updated version of the Feynman-Kac distribution $\bar{\mathbb{Q}}_{\bar{\eta}_{r,0},r,n}$, it corresponds to the conditional probability $\mathbb{P}_{\bar{\eta}_{r,0}}(\overline{X}_{0:n} \in d(\overline{x}_0,\ldots,\overline{x}_n)|Y_{0:n}=y_{0:n},R=r)$ and is given by:

$$\hat{\bar{\mathbb{Q}}}_{\bar{\eta}_{r,0},r,n}(d((\theta_0,\eta^X_{\theta_0,r}),\ldots,(\theta_n,\eta^X_{\theta_{0:n},r,n}))) = \frac{1}{\hat{\bar{\mathcal{Z}}}_{r,n}} \left\{ \prod_{p=0}^n \overline{G}_{r,p}(\overline{x}_p) \right\} \bar{\eta}_{r,0}(d\overline{x}_0)$$
$$\overline{M}_{r,1}(\overline{x}_0,d\overline{x}_1)\ldots\overline{M}_{r,n}(\overline{x}_{n-1},d\overline{x}_n) \quad (2.60)$$

with the normalizing constant $\hat{\bar{\mathcal{Z}}}_{r,n}$ given by:

$$\hat{\bar{\mathcal{Z}}}_{r,n} = \mathbb{E}_{\bar{\eta}_{r,0}}\left[\prod_{p=0}^n \bar{G}_{r,p}(\overline{X}_p) \right]$$

Therefore, when R is given equal to r, labeled island particle filtering technique can be used to estimate the distribution of the signal. Let us introduce the marginal measure $\overline{\gamma}_{r,n}$ of the path measure $\bar{\mathbb{Q}}_{r,n}$ defined for all $f_n \in \mathcal{B}_b(\mathsf{E}_n)$ by:

$$\overline{\gamma}_{r,n}(f_n) \triangleq \mathbb{E}_{\bar{\eta}_{r,0}}\left[f_n(\overline{X}_n) \prod_{p=0}^{n-1} \bar{G}_{p,r}(\overline{X}_p) \right] \quad (2.61)$$

We can also define the probability measure $\overline{\eta}_{r,n}$ for all $f_n \in \mathcal{B}_b(\overline{\mathsf{E}}_n)$ by:

$$\overline{\eta}_{r,n}(f_n) \triangleq \frac{\overline{\gamma}_{r,n}(f_n)}{\overline{\gamma}_{r,n}(1)} \quad (2.62)$$

The last quantity (2.62) corresponds to the prediction step of the filter.

We also define the updated measure $\hat{\overline{\gamma}}_{r,n}$ and the filtering probability measure $\hat{\overline{\eta}}_{r,n}$ for all $f_n \in \mathcal{B}_b(\overline{\mathsf{E}}_n)$ by:

$$\hat{\overline{\gamma}}_{r,n}(f_n) = \overline{\gamma}_{r,n}(\bar{G}_{n,r}f_n) \quad (2.63)$$

$$\hat{\overline{\eta}}_{r,n} = \frac{\hat{\overline{\gamma}}_{r,n}(f_n)}{\hat{\overline{\gamma}}_{r,n}(1)} \quad (2.64)$$

We can note here that the normalizing constant $\hat{\bar{\mathcal{Z}}}_{r,n}$ can be rewritten using the marginal Feynman-Kac measure such that:

$$\hat{\bar{\mathcal{Z}}}_{r,n} = \hat{\overline{\gamma}}_{r,n}(1) = \overline{\gamma}_{r,n}(\overline{G}_{r,n})$$
$$= \prod_{p=0}^n \underbrace{\overline{\eta}_{r,p}(\overline{G}_{r,p})}_{h_p(r)}$$

Now all the notations are defined we come back to the original problem: joint estima-

tion of state and parameter of the model. To do so, we use the Bayesian rule in order to obtain the following equation:

$$\pi_n(r) \triangleq \mathbb{P}(R \in dr | Y_{0:n} = y_{0:n}) = \frac{\mathbb{P}(Y_{0:n} \in dy_{0:n} | R = r)\mathbb{P}(R \in dr)}{\mathbb{P}(Y_{0:n} \in dy_{0:n})} \qquad (2.65)$$

where,

$$\mathbb{P}(Y_{0:n} \in dy_{0:n} | R = r) = \prod_{p=0}^{n} \underbrace{\mathbb{P}(Y_p \in dy_p | Y_{0:p-1} = dy_{0:p-1}, R = r)}_{h_p(r)}.$$

The quantity defined by (2.65) is the invariant measure we want to approximate. It can be rewritten as follow:

$$\pi_n(r) = \frac{1}{\hat{\bar{\mathcal{Z}}}_n} \prod_{p=0}^{n} h_p(r)\lambda(r)$$

where the quantity $\hat{\bar{\mathcal{Z}}}_n$ denotes $\int \hat{\bar{\mathcal{Z}}}_{r,n}\lambda(r)dr$.

The problem which arisen here is that we do not know the $h_p(r)$ functions as in the state space model. The idea developed in Andrieu et al. (2010) consists in using particle approximations of these functions as they are unbiased. However, in our case particle approximation cannot be used as the random process considered is lying in a random environment. To tackle this issue, we replace the particle filters by the labeled island particle estimations developed in Section 2.2.

Parameter estimation using labeled island particle MCMC methods

Now the question of the triple estimation is given, we propose in this paragraph a particle based solution to estimate the h_p functions as well as the normalizing constants. This solution is based on the Algorithm 3 develop in Section 2.2.2. Let us introduce $\tilde{X}_n^i$ the random vector in the product space $\overline{\mathsf{E}}_0 \times \ldots \times \overline{\mathsf{E}}_n$ defined by:

$$\tilde{X}_n^i \triangleq \left(\tilde{X}_{0,n}^i, \ldots, \tilde{X}_{n,n}^i \right)$$

where $\tilde{X}_{p,n}^i = \left(\theta_{p,n}^i, \eta_{\theta_{0:p,n}^i, r, p, n}^{X, N_2} \right)$ and $\theta_{p,n}^i$ corresponds to the ancestor at time p of the ith-island of time n and $\eta_{\theta_{0:p,n}^i, r, p, n}^{X, N_2}$ is the empirical measure associated.

$\tilde{X}_n^i$ represents the ancestral line associated with the ith current island and with the realization r of the parameter R.

A $\{N_1, N_2\}$-particle approximation of $\overline{\mathbb{Q}}_{r,n}$ is given by the occupation measure:

$$\frac{1}{N_1} \sum_{i=1}^{N_1} \delta_{\left(\tilde{X}_{0,n}^i, \ldots, \tilde{X}_{n,n}^i \right)}(\overline{x}_0, \ldots, \overline{x}_n)$$

Let denote by Ξ_n the complete genealogical tree which is defined as follows:

$$\Xi_n = (\Xi_{0,n}, \ldots, \Xi_{n,n}) \triangleq (\tilde{X}_0^{[N_1]}, \ldots, \tilde{X}_n^{[N_1]}) \in \prod_{p=0}^{n} \overline{\mathsf{E}}_p^{N_1}$$

with
$$\Xi_{p,n} = \left(\Xi_{p,n}^i\right)_{1 \le i \le N_1} = \left(\tilde{X}_p^i\right)_{1 \le i \le N_1}$$

and
$$\Xi_{p,n}^i = \tilde{X}_p^i \triangleq \left(\tilde{X}_{0,p}^i, \ldots, \tilde{X}_{p,p}^i\right)$$

We denote by $\hat{\bar{\mathcal{Z}}}_{r,n}^{N_1,N_2}$ the approximation of $\hat{\bar{\mathcal{Z}}}_{r,n}$ given by the complete genealogical tree Ξ_n which is defined as follow:

$$\hat{\bar{\mathcal{Z}}}_{r,n}^{N_1,N_2}(\Xi_n) \triangleq \prod_{p=0}^n h_p^{N_1,N_2}(r, \tilde{X}_p^{[N_1]})$$

where

$$
\begin{aligned}
h_p^{N_1,N_2}(r, \tilde{X}_p^{[N_1]}) &= \tilde{\eta}_{p,r}^{N_1}(\overline{G}_{r,p}) \\
&= \frac{1}{N_1} \sum_{i=1}^{N_1} \frac{1}{N_2} \sum_{j=1}^{N_2} G_{r,p}(\theta_{p,p}^i, \xi_{p,p}^{i,j}).
\end{aligned}
$$

Then we define $\bar{\mathcal{Z}}_{r,n}^{N_1,N_2}$ the approximation of $\bar{\mathcal{Z}}_{r,n}$ given by the labeled island particle algorithm

$$\bar{\mathcal{Z}}_{r,n}^{N_1,N_2}(\Xi_n) \triangleq \frac{\hat{\bar{\mathcal{Z}}}_{r,n}^{N_1,N_2}(\Xi_n)}{\hat{\mathcal{Z}}_{r,n}}.$$

Therefore, denoting by $\mathbb{P}_{r,n}^{N_1,N_2}$ the distribution of the genealogical tree Ξ_n associated with the realization $R = r$, we get:

$$\Pi_{r,n}^{N_1,N_2}(\Xi_n) = \bar{\mathcal{Z}}_{r,n}^{N_1,N_2}(\Xi_n) \mathbb{P}_{r,n}^{N_1,N_2}(\Xi_n).$$

Then

$$\Pi_n^{N_1,N_2}(r, \Xi_n) = \frac{1}{\hat{\bar{\mathcal{Z}}}_n} \left\{ \prod_{p=0}^n h_p^{N_1,N_2}(r, \tilde{X}_{p,p}) \right\} \mathbb{P}_{r,n}^{N_1,N_2}(\Xi_n) \lambda(r).$$

Marginalizing out with respect to Ξ_n the distribution $\Pi_n^{N_1,N_2}(r, \Xi_n)$, we obtain the empirical measure of measure $\pi_n(r)$ denoted by $\Pi_n^{N_1,N_2}(\Xi_n)$. So, using a MCMC algorithm, we can sample with respect to the invariant measure $\Pi_n^{N_1,N_2}(r, \Xi_n)$ with a coefficient of acceptance/rejection for two different proposition (r, Ξ_n) and (r', Ξ_n') given by:

$$a((r, \Xi_n), (r', \Xi_n')) = \min\left(1, \frac{\hat{\bar{\mathcal{Z}}}_{r,n}^{N_1,N_2}(\Xi_n')}{\hat{\bar{\mathcal{Z}}}_{r,n}^{N_1,N_2}(\Xi_n)}\right)$$

So in order to get the estimation of the parameter r, we can use the Algorithm 5 which is called labeled island particle MCMC algorithm. This is an MCMC algorithm which use a labeled island particle model to get the estimation of the likelihood quantities which enter in the acceptance/rejection ratio computation.

Since we made this adaptation, Chopin et al. in Chopin et al. (2013) introduced a kind of island particle models where each island is identified by a parameter proposition. They

---

Algorithm 5 Labeled island Particle MCMC - lipMCMC

Require: $\bar{\eta}_{r,0}$, $(\bar{M}_{r,n})_{n=0}^T$, $(\bar{G}_{n,r})_{n=0}^T$ and r_0

Ensure: Particle approximation of $\mathbb{P}(R \in \mathrm{d}r | Y_{0:T} = y_{0:T})$ and $\mathbb{P}(\overline{X}_{0:T} \in \mathrm{d}\overline{x}_{0:T} | Y_{0:T} = y_{0:T}, R = r)$

$\boxed{\text{Begin}}$

1. $\underline{\text{Parameter initialization}}$ $p = 0$

$r_p = r_0$

for $p = 0, \ldots, nsample$ **do**

  2. $\underline{\text{Island particle filtering for } r_p}$

  2.1 $\underline{\text{Initialization}}$ $n = 0$

  for $i = 1, \ldots, N_1$ **do**

    Sample $\tilde{X}_0^i = (\theta_0^i, \eta_{\theta_0^i, r_p, 0}^{X, N_2}) \sim \tilde{\eta}_{r_p, 0}$, $\theta_0^i \overset{i.i.d}{\sim} \eta_0^\Theta$, and $\eta_{\theta_0^i, r, 0}^{X, N_2} = \frac{1}{N_2} \sum_{j=1}^{N_2} \xi_0^{i,j}$ where $\xi_0^{i,j} \overset{i.i.d}{\sim}$

    $\eta_{\theta_0^i, r_p, 0}^X$

  end for

  for $n = 0, \ldots, T$ **do**

    2.2 $\underline{\text{Selection of islands}}$

    Sample $I_n = (I_n^i)_{i=1}^{N_1}$ according to a multinomial distribution with probability $\propto$

    $\left(\frac{1}{N_2} \sum_{j=1}^{N_2} G_{n,r_p}(\theta_n^i, \xi_n^{i,j}) \right)_{i=1}^{N_1}$

    for $i = 1, \ldots, N_1$ **do**

      2.3 $\underline{\text{Selection of particles inside each island}}$

      Sample $J_n^i = (J_n^{i,j})_{j=1}^{N_2}$ according to a multinomial distribution with probability

      $\propto \left(G_{n,r_p}(\theta^{I_n^i}, \xi_n^{I_n^i, j}) \right)_{j=1}^{N_2}$

    end for

    2.4. $\underline{\text{Mutation of Island}}$

    Sample independently θ_{n+1}^i according to $M_n^\Theta(\theta_n^{I_n^i}, .)$

    for $j = 1, \ldots, N_1$ **do**

      2.5 $\underline{\text{Mutation of particles}}$

      Sample $\xi_{n+1}^{i,j}$ according to $M_{\theta_{n,r_p}^i, n, r_p}^X(\xi^{I_n^i, J_n^{i,j}}, .)$

    end for

  end for

  3. $\underline{\text{Likelihood evaluation}}$

  Evaluate $\hat{\bar{\mathcal{Z}}}_{r_p, T}^{N_1, N_2}(\Xi_T)$

  4. $\underline{\text{Mutation of the parameter } r_p}$

  $r_p \rightsquigarrow r^*$

  5. $\underline{\text{Island particle filtering for } r^*}$

  Repeat step 2 using r^* instead of r_p

  6. $\underline{\text{Likelihood evaluation}}$

  Evaluate $\hat{\bar{\mathcal{Z}}}_{r^*, T}^{N_1, N_2}(\Xi_T^*)$

  7. $\underline{\text{Acceptance rejection step}}$

  $p \rightarrow p + 1$

  $\begin{cases} r_{p+1} = r^* \\ \Xi_T = \Xi_T^* \end{cases}$ with probability $a((r_p, \Xi_T), (r^*, \Xi_T^*))$.

end for

$\boxed{\text{End}}$

---

proposed an algorithm called SMC^2 which is a practical version of the idealized iterated batch importance sampling (IBIS) algorithm introduced by Chopin in Chopin (2002) for exploring a sequence of parameter posterior distributions. In the SMC^2 algorithm, islands of particles grow continuously with time as particles ancestral lines are required to estimate the likelihood increments, and by their product to estimate the total likelihood. The algorithm introduced by Crisan et al. in Crisan and Miguez (2013) is a different version of the SMC^2 which also allows the estimation of fixed parameters of a state-space dynamic system using sequential Monte Carlo methods. However, unlike the SMC^2 method, the proposed algorithm by Crisan et al. operates in a purely sequential and recursive manner. In particular, the scheme for the rejuvenation of the particles in the parameter space is simpler, given that it does not need the simulation of the auxiliary particle filter from initial time to evaluate the likelihood. Further developments to adapt Crisan work to our case constitutes a possible way to pursue the research about random process evolving in a random environment with unknown parameters.

2.4 Non-linear filtering for random point process in a decomposed random field

In this section, we are still interested in estimation techniques able to learn both a random process which evolves inside a random environment and the environment itself. However the nature of these processes was not detailed yet. Indeed when considering the application we are concerned with, aircraft evolving in a random atmospheric environment, we are in presence of a punctual random process which progresses in a higher dimension random field. The filtering problem, we put our interest on, consists in estimating the random atmospheric field along the random path of the aircraft. This question is also at hand in geophysics. For example in Baehr (2010), the problem treated concerns the turbulence estimation from 3D local wind measurements. In order to use these measurements, Baehr developed a model to take into a account the fact that the atmospheric flow is captured along a random path which can be modelled by a point process.

Hence we give in this section a brief presentation of the acquisition processes developed by Baehr (2010). As a matter of fact, they give one an adapted framework to deal with the estimation of the random atmospheric environment using aircraft processes. However, the aim of this work is to consider air-traffic process, that is several aircraft processes. So, we have to take into account several acquisition processes representing each aircraft evolving in the same atmospheric field. We propose a way to combine them in order to estimate the random atmospheric media on several domains instead of giving several point estimation of it. We develop an adaptation of the discrete acquisition process in an locally homogeneous random field proposed by Baehr to decomposed random field in homogeneous sub-domains.

2.4.1 Local estimation of random field using acquisition process

Estimating a random field using a quantity of lower dimension than the field makes appear difficulties. Indeed to give a good estimation of the random medium, one may lack of information. Before dealing with the filtering issue when using observations delivered by a random process leaving in a random field, we recall the stochastic modelling first introduced in Baehr (2009) in the context of atmospheric turbulent velocities estimation using LIDAR observations. To this end, let us remind that Θ_n was previously considered as a random environment. Now, take $\Theta_{n,x}$ as a multidimensional random field. That is a set of random variable taking value in E_n^Θ indexed by the time n and points x in the configuration space E whose dimension is greater than one. Then let us introduce a random process $Z_n \in \mathsf{E}$ whose evolution is independent from the evolution of $\Theta_{n,x}$. Instead of studying the random field on the whole configuration space E, we attach our attention on the value taken by the random field at Z_n. Then it appears clearly that estimating the random field on the whole space E using only the observations made along Z_n is not possible. However a local estimation is attainable. For that purpose, several quantities have to be defined such as the acquisition process, developed in Baehr (2010).

Definitions

First let us define what we mean by Acquisition system.

Definition 2.4.1 (Acquisition system, Baehr (2010))**.** *Let $\mathsf{E} \subset \mathbb{R}^d$, $d \in \mathbb{N}^*$ be a metric locally compact space of point called configuration space. E is endowed with the σ-algebra $\mathcal{E}$.*
Let $\mathsf{E}_n^\Theta \subset \mathbb{R}^{d'}$, $d' \in \mathbb{N}^*$ be a multidimensional space called phase space endowed with the σ-algebra $\mathcal{E}'$. Let $(\Omega, \mathcal{F}, (\mathcal{F}_n)_{n \geq 0}, \mathbb{P})$ be a complete filtered probability space. Let $N > 0$ be a positive integer and $x \in \mathsf{E}$ a point of the configuration space. Let Z_n be the $(\mathsf{E}, \mathcal{E})$-valued random variable family on $(\Omega, \mathcal{F}, \mathcal{F}_n)$ indexed by the time $n \in [\![0, N]\!]$ and $\Theta_{n,x}$ be the $(\mathsf{E}_n^\Theta, \mathcal{E}')$-valued random variable on $(\Omega, \mathcal{F}, \mathcal{F}_n)$ indexed by the time $n \in [\![0, N]\!]$ at the point $x \in \mathsf{E}$.
Then the pair of applications $\mathcal{F}_n$-measurable, $(Z_n, \Theta_{n,x})$ is called the acquisition System of the random vector field. The process Z_n is called the Acquisition Path and the family $\Theta_{n,x}$ is called the Acquisition Field.

Till now, this system does not relate the acquisition process Z_n to the Acquisition field $\Theta_{n,x}$. So, let us introduce the Acquisition process which is the Acquisition of the field along the acquisition path.

Definition 2.4.2 (Acquisition Process, Baehr (2010))**.** *Let $(Z_n, \Theta_{n,x})$ be a $(\mathsf{E}, \mathcal{E}) \times (\mathsf{E}_n^\Theta, \mathcal{E}')$-valued Acquisition system on the probability space $(\Omega, \mathcal{F}, \mathcal{F}_n, \mathbb{P})$. For any $n \in [\![0, N]\!]$, the Acquisition Process is defined by the $(\mathsf{E}_n^\Theta, \mathcal{E}')$-valued process on $(\Omega, \mathcal{F}, \mathcal{F}_n)$ A_n with*

$$A_n \triangleq \Theta_{n,Z_n}$$

As one can see here, the Acquisition process A_n, located at Z_n do not need the knowledge of the vector field everywhere. In addition, the nature of the acquisition process A_n is hardly linked to Z_n. We give now an example of acquisition process in continuous time which is fruitful for the air-traffic application.

Example 2.4.1 (Lagrangian acquisition process). *Let $\Theta_{n,x}$ be an $(\mathsf{E}_n^\Theta, \mathcal{E}')$-valued random bounded vector field $\mathcal{C}^\infty$. Let z_0 a point in E and for all $0 < t < T$, let W_t be a $\mathcal{F}_t$-Brownian motion on $(\Omega, \mathcal{F}, \mathcal{F}_t, \mathbb{P})$. We define the stochastic flow (see Arous (1989)):*

$$Z_t^{z_0} = z_0 + \int_0^t \Theta_{s, Z_s^{z_0}} \circ \mathrm{d}W_s$$

where $\circ$ signs the Stratonovich integral.

Then the Acquisition process is $A_t = \Theta_{t, Z_t^{z_0}}$. By analogy with physics, we call this process a Lagrangian acquisition.

We do not intend here to study the existence problem of the previous integral. The interested reader may refer to Mikulevicius and Rozovskii (2004) for the existence proof in the case of the $2D$ Stochastic Navier-Stockes equation. Now, recording the estimation problem of the random field along the random path, we introduce the acquisition process in locally homogeneous medium.

Definition 2.4.3 (Locally homogeneous Acquisition Process, Baehr (2010)). *For all $n \in \mathbb{N}$, let $(Z_n, \Theta_{n,x})$ be an $(\mathsf{E} \times \mathsf{E}_n^\Theta)$-valued Acquisition System and $A_n = \Theta_{n, Z_n}$ an Acquisition Process. The Acquisition System is said to be locally homogeneous if:*

- *E is a metrizable locally convex space with a convex set covering $\mathcal{A} = \bigcup\limits_{i \in I} \mathcal{A}_i$ where I is an index set.*

- *For all $n \in \mathbb{N}$ and any $x \in \mathsf{E}$, there exists $\epsilon_n > 0$ and $i \in I$ such that: $B(x, \epsilon_n) \subset \mathcal{A}_i$ with $B(x, \epsilon_n) \triangleq \{y \in \mathsf{E}, |x - y| \leq \epsilon_n\}$ and for all $y \in B(x, \epsilon_n) \triangleq B_n^\epsilon(x)$, $a \in \mathsf{E}_n^\Theta$, we have:*

$$\mathbb{P}(A_n \in \mathrm{d}a | Z_n = x) = \mathbb{P}(A_n \in \mathrm{d}a | Z_n = y)$$

We denote by $\mathbb{P}(A_n | Z_n \in B_n^\epsilon(x))$, the conditional probability law of the acquisition process A_n given that Z_n belongs to the ball $B_n^\epsilon(x)$

Now all the concepts are well defined, we remind here the model developed by Baehr (2010) to estimate the acquisition process given the acquisition path. In mathematical terms, this quantity corresponds to the conditional expectation:

$$\mathbb{E}\left[f(Z_n, A_n) | Z_{0:n} \in B_{0:n}\right]$$

with $B_{0:n}$ the hull of the balls given by $B_{0:n} = \bigcup\limits_{p \in [\![0, n]\!]} B_p^\epsilon$. Assume that the conditional probability $\mathbb{P}(A_n \in \mathrm{d}a | Z_n)$ is absolutely continuous with respect to the Lebesgue measure,

and that its density denoted by $p^{A_n|Z_n}(a|z)$ is given by the joint density:

$$p^{A_n|Z_n}(a|z) = \frac{p^{Z_n,A_n}(z,a)}{\int_{\mathsf{E}_n^\Theta} p^{Z_n,A_n}(z,a)\mathrm{d}a}.$$

Then the quantity $\mathbb{E}\left[f(Z_n, A_n)|Z_n \in B_n^\epsilon\right]$ can be rewritten as follow:

$$\begin{aligned}
\mathbb{E}\left[f(Z_n, A_n)|Z_n \in B_n^\epsilon\right] &= \int_{\mathsf{E}\times\mathsf{E}_n^\Theta} f(z,a) p^{A_n|Z_n\in B^\epsilon_n}(a|z)\mathrm{d}z\mathrm{d}a \\
&= \int_{\mathsf{E}\times\mathsf{E}_n^\Theta} f(z,a) \frac{p^{Z_n,A_n}(z,a)\mathbb{1}_{B_n^\epsilon(z)}}{\int_{\mathsf{E}} \mathbb{1}_{B_n^\epsilon(z)} p^{Z_n}(z)\mathrm{d}z}\mathrm{d}z\mathrm{d}a \quad = \frac{\mathbb{E}\left[f(Z_n, A_n)\mathbb{1}_{B_n^\epsilon}(Z_n)\right]}{\mathbb{E}\left[\mathbb{1}_{B_n^\epsilon}(Z_n)\right]}
\end{aligned}$$

Finally we have:

$$\mathbb{E}\left[f(Z_n, A_n)|Z_{0:n} \in B_{0:n}\right] = \frac{\mathbb{E}\left[f(Z_n, A_n)\prod_{p=0}^n \mathbb{1}_{B_p^\epsilon}(Z_p)\right]}{\mathbb{E}\left[\prod_{p=0}^n \mathbb{1}_{B_p^\epsilon}(Z_p)\right]}. \tag{2.66}$$

This quantity suggests an underlying Feynman-Kac structure. That is a two step evolution, as for the filtering equation, one for the mutation of the process, the second one being a selection defined thanks to the indicator function of the subset B_n^ϵ.

Acquisition process for one aircraft evolving in a random atmosphere

Let consider the acquisition process induced by the aircraft path, we define the acquisition system $(Z_n, \Theta_{n,x})$ composed of the aircraft position, denoted by Z_n, and the random atmospheric field taken at the position x, $\Theta_{n,x}$. Let A_n be the Lagrangian acquisition process Θ_{n,Z_n}. Here we suppose that we have access to the global field Θ_n, that is one can get the value of the random field at every point $x \in \mathsf{E}$ and the random field evolves thanks to a global model. This assumption is convenient here, because if the random atmospheric field had been described by a local model, then it would have been mandatory to introduce a Lagrangian acquisition process to model the local fluid evolution as in Baehr (2010). This remark being made, suppose that the acquisition system $(Z_n, \Theta_{n,x})$ is locally homogeneous.

The estimation problem we are concerned with can be written as the conditional expectation of the process (X_n, A_n) given the observations of X_n and $Z_n \in B_n^\epsilon$, illustrated by Figure 2.4. The random process X_n denotes the aircraft process which takes its value in E_n^X, where E_n^X encapsulate the dynamics parameters but also the position of the aircraft denoted by Z_n. In other terms, we want to estimate the following quantity:

$$\mathbb{E}\left[f(X_n, A_n)|Z_{0:n} \in B_{0:n}^\epsilon, Y_{0:n} = y_{0:n}\right].$$

As we have seen this conditional expectation can be written in the following form:
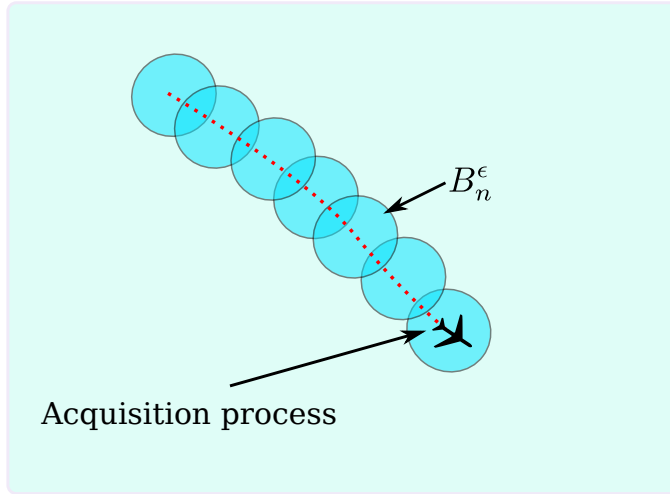
Figure 2.4: Acquisition process for one aircraft evolving in a random atmosphere

$$\mathbb{E}\left[f(X_n, A_n) | Z_{0:n} \in B^\epsilon_{0:n}, Y_{0:n} = y_{0:n}\right] = \frac{\mathbb{E}\left[f(X_n, A_n) \prod\limits_{p=0}^{n} \mathbb{1}_{B^\epsilon_p}(Z_p) | Y_{0:n} = y_{0:n}\right]}{\mathbb{E}\left[\prod\limits_{p=0}^{n} \mathbb{1}_{B^\epsilon_p}(Z_p)\right]}.$$

However, for every $p \in [\![0, n]\!]$ the ball B^ϵ_p is built from the process Z_n. Then the expectation $\mathbb{E}\left[\prod\limits_{p=0}^{n} \mathbb{1}_{B^\epsilon_p}(Z_p)\right]$ which corresponds to the probability for the path process $(Z_p)_{p=0}^{n}$ to be in the hull defined by the sequence of balls $(B^\epsilon_p)_{p=0}^{n}$, is equal to 1.

Finally we obtain:

$$\mathbb{E}\left[f(X_n, A_n) | Z_{0:n} \in B^\epsilon_{0:n}, Y_{0:n} = y_{0:n}\right] = \mathbb{E}\left[f(X_n, A_n) | Y_{0:n} = y_{0:n}\right].$$

To resume, the acquisition process we are interested in can be cast inside the class of filtering problems for random processes evolving in a random environment developed in Section 2.2.1. Indeed, if one considers that X_n corresponds to the Markovian stochastic process which is influenced by the random environment Θ_n which is also Markov, but now instead of considering Θ_n we consider the acquisition process Θ_{n,Z_n}, we can use the Interacting Kalman filter (Algorithm 2) or the labeled island particle filter (Algorithm 3), depending on the evolution model of X_n, to estimate both the law of X_n and Θ_{n,Z_n}. That is to estimate $(\Theta_{n,Z_n}, \eta^X_{\Theta_{0:n,Z_{0:n}},n})$.

2.4.2 Acquisition processes for fields decomposed in homogeneous sub-domains

As we have seen in the precedent section, acquisition processes are convenient to express the filtering problem we are interested in. Indeed we have seen that the estimation of the random field Θ_n along the path of one aircraft can be represented as an acquisition process. However, consider now that we have an air-traffic process, that is several aircraft evolving
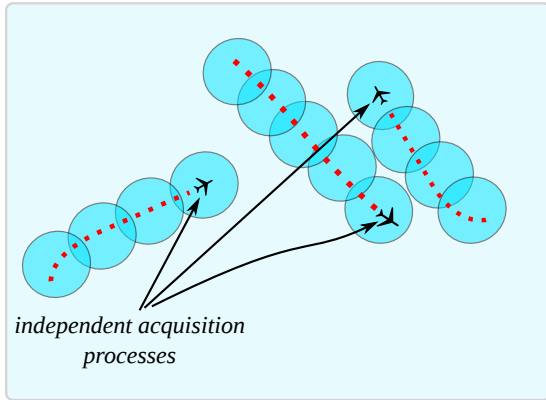
Figure 2.5: Aircrafts treated independently
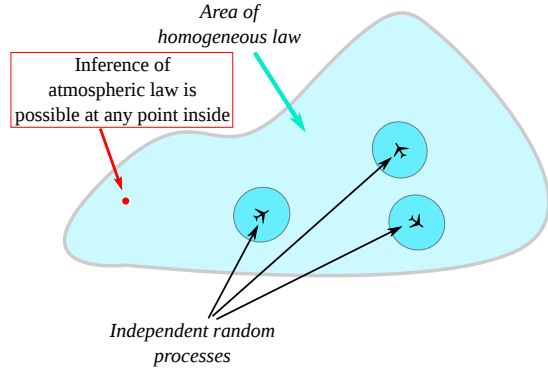
Figure 2.6: Integration of all aircrafts using homogeneous hypothesis

in the same random atmospheric field. Then we have different acquisition processes, one for each aircraft. If treated independently, we can estimate the random atmospheric field along each random path given by each aircraft, see Figure 2.5. Nevertheless the aim of this study is to use all the aircraft to give an overall estimation of the random field. Indeed, the benefits are expected to be much greater if one can fuse measurements from multiple aircraft at different time and location.

Then we have two choices. The first one consists in considering that the random field is globally homogeneous and uses every aircraft process to give an estimation of the random atmosphere, see Figure 2.6. Then we fall into the case of random processes evolving in a random atmosphere, and the labeled island particle filter developed in Section 2.2.2 is well adapted. The second choice is to consider that the random atmospheric field is composed of homogeneous sub-domains for which a local estimation is possible using all the aircraft evolving inside this homogeneous sub-domain, see Figure 2.7. As it is unrealistic to consider the atmosphere as an homogeneous random field, except for special cases, we choose the second option.

To this end we need to introduce the decomposition operation which allows one to obtain a partition of the random field Θ_n and the Lagrangian acquisition processes, as it is defined in Example 2.4.1, that gives one the opportunity to follow homogeneous sub-domains in time. Further we couple the Lagrangian acquisition processes with several aircraft acquisition processes to give extended local estimation of the random field. Finally we present a novel particle filter able to deal with random environment decomposed in homogeneous sub-domains.

Configuration space decomposition

This section is devoted to the configuration space decomposition, that is to the partition of E in sub-domains such that the random field Θ_n is homogeneous on every sub-domains. Consider that at initial time step, the deterministic operator Υ which acts on the power set $\mathcal{E} \times \mathcal{E}'$ of $\mathsf{E} \times \mathsf{E}_0^\Theta$ to $\mathcal{E}$ such that for any $\mathsf{D} \in \mathcal{E}$ and field $\Theta_0 \in \mathcal{E}'$ we have:

$$\Upsilon(\mathsf{D}, \Theta_0) \triangleq \{\mathsf{B}_{0,l}, l \in [\![1, k]\!]\} \cup \{\eth\} \tag{2.67}$$
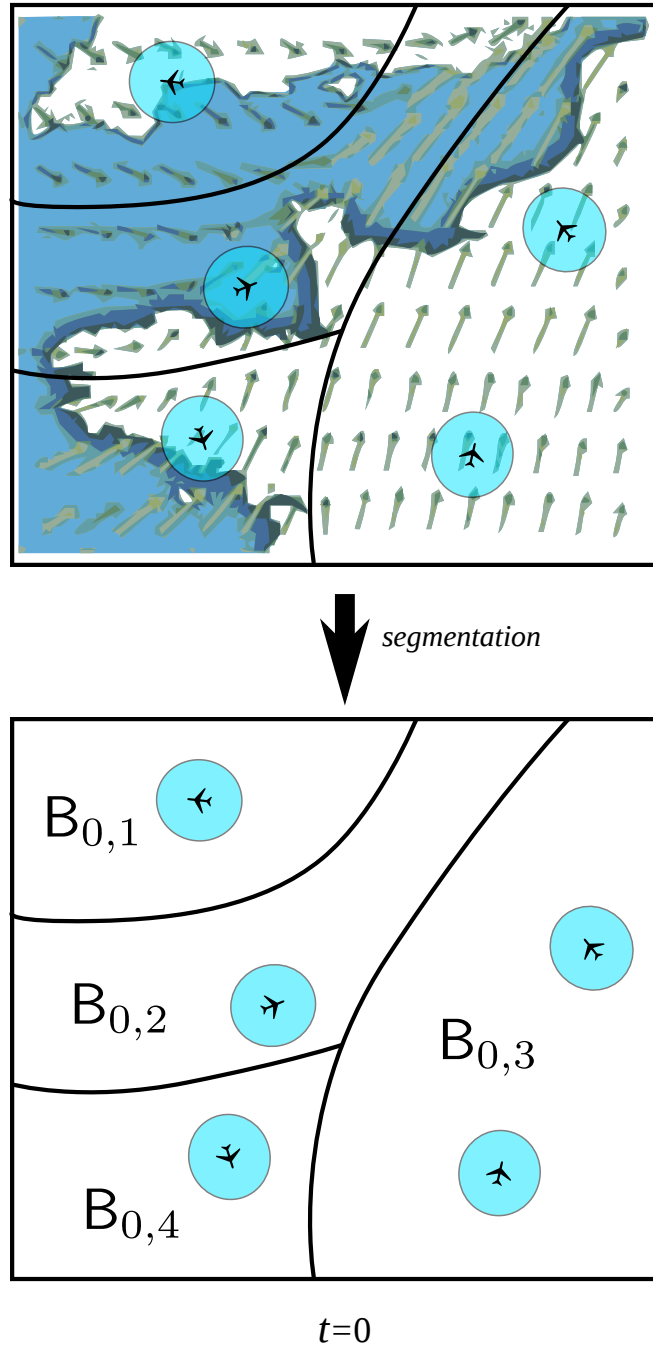
Figure 2.7: Aircrafts evolving in an homogeneous partition of the configuration space

where $\mho$ stands for an auxiliary cemetery point outside D. In other words, the operator Υ makes a partition of the set D. That means that the family of sets $(\mathsf{B}_{0,l})_{l=1}^{k}$ covers D, so $\bigcup_{l=1}^{k} \mathsf{B}_{0,l} = \mathsf{D}$. And the set-elements of the family are pairwise disjoint: for any $l \neq l'$, $\mathsf{B}_{0,l} \cap \mathsf{B}_{0,l'} = \emptyset$.

Moreover, we assume that the partition operator Υ makes an homogeneous decomposition of D, that is for any $l \in [\![1, k]\!]$, the random field Θ_0 is homogeneous on each $\mathsf{B}_{0,l}$. In other words, for any $x, y \in \mathsf{B}_{0,l}$, we have:

$$\mathbb{P}(\Theta_{0,Z} \in \mathrm{d}\theta_0 | Z = x) = \mathbb{P}(\Theta_{0,Z} \in \mathrm{d}\theta_0 | Z = y)$$

where $\Theta_{0,Z}$ is the random field Θ_0 located at Z. We illustrate the initial time decomposition in Figure 2.7.

We further assume that the characteristic time of the random process Z_n is less than the characteristic time of the environment. To understand what is meant by characteristic time, let us first introduce the characteristic time of the environment. Depending on the application one is concerned with, the environment evolution is described by different physical phenomenons. For example, the environment evolution can be described by a stochastic wave equation, see Millet and Sanz-Solé (1999); Peszat (2002), by stochastic transport equations as in Pope (1985); Flandoli et al. (2010) or/and by a stochastic diffusion equation. Another example is the Lagrangian description of the environment given by the stochastic flow, defined in Example 2.4.1, transported by the random medium. The characteristic time corresponding to the Lagrangian description of the environment, denoted by τ_L, is defined with respect to its natural filtration for every $x_0 \in \mathsf{E}$ and $\mathsf{B} \in \mathcal{E}$ by:

$$\tau_L^{x_0}(\mathsf{B}) \triangleq \inf\{t, x_0 + \int_0^t \Theta_{s,X_s^{x_0}} \circ \mathrm{d}W_s \in \mathsf{B}\}. \tag{2.68}$$

Then, it follows that the characteristic time of the environment depends on all the phenomenons influencing its evolution. We define the characteristic time of the environment, denoted by τ_Θ, to be the maximum over all characteristic times defined for every physical phenomenon which have an influence on the environment evolution. It is given for every $x_0 \in \mathsf{E}$ and $\mathsf{B} \subset \mathsf{E}$ by:

$$\tau_\Theta^{x_0}(\mathsf{B}) \triangleq \max_{i \in I} \tau_i^{x_0}(\mathsf{B}) \tag{2.69}$$

where the set $I \subset \mathbb{N}$ signs for all the physical phenomenons involved into the environment evolution. For the random process Z_n, the characteristic time denoted by $\tau_Z^{x_0}$ is defined with respect to its natural filtration such that for every $x_0 \in \mathsf{E}$ and $\mathsf{B} \in \mathcal{E}$ we have:

$$\tau_Z^{x_0}(\mathsf{B}) \triangleq \inf\{n, Z_n \in \mathsf{B} | Z_0 = x_0\}. \tag{2.70}$$

We suppose that both characteristic times are finite. Saying that the characteristic time of Z_n is less that the characteristic time of the environment means that the random process Z_n takes less time to join two points in space than the random medium. Then we
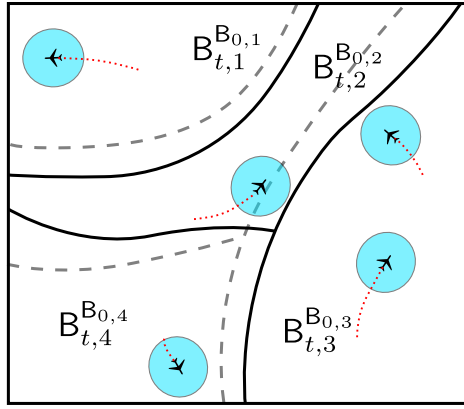
Figure 2.8: Configuration space decomposition after the evolution time lapse t originally given by Figure 2.7

suppose that for all $x_0 \in \mathsf{E}$ and $\mathsf{B} \in \mathcal{E}$ we have:

$$\tau_Z^{x_0}(\mathsf{B}) \ll \tau_\Theta^{x_0}(\mathsf{B}). \tag{τ}$$

Now, let us introduce the continuous Lagrangian acquisition process $\Theta_{t,\mathsf{B}_{t,l}^{\mathsf{B}_{0,l}}}$, where the stochastic flow $\mathsf{B}_{t,l}^{\mathsf{B}_{0,l}}$ is defined by:

$$\mathsf{B}_{t,l}^{\mathsf{B}_{0,l}} \triangleq \left\{ Z_t^{x_0} \in \mathsf{E}, Z_t^{x_0} = x_0 + \int_0^t \Theta_{s,Z_s^{x_0}} \circ \mathrm{d}W_s \text{ with } x_0 \in \mathsf{B}_{0,l} \right\} \tag{2.71}$$

where $\circ$ corresponds to the Stratonovich integral.

The stochastic flow $\mathsf{B}_{t,l}^{\mathsf{B}_{0,l}}$ corresponds to the domain $\mathsf{B}_{0,l}$ obtained after the evolution of the random field Θ_s during the time lapse t. Hence, this process allows one to capture the evolution of the homogeneous partition of D. The evolution is illustrated on Figure 2.8.

Going back to the discrete time acquisition process $\Theta_{n,\mathsf{B}_{n,l}^{\mathsf{B}_{0,l}}}$ we have that the pair process $(\mathsf{B}_{n,l}^{\mathsf{B}_{0,l}}, \Theta_{n,\mathsf{B}_{n,l}^{\mathsf{B}_{0,l}}})$ corresponds to the Lagrangian description of the random homogeneous field state originally in $\mathsf{B}_{0,l}$. Here we consider that the kernel transition of the random field Θ_n preserves the homogeneous condition for each sub-domains. That is $\mathsf{B}_{n,l}^{\mathsf{B}_{0,l}}$ is still an homogeneous sub-domain for the random field Θ_n, for every $x, y \in \mathsf{B}_{n,l}^{\mathsf{B}_{0,l}}$ we have:

$$\mathbb{P}(\Theta_{n,X}|X=x) = \mathbb{P}(\Theta_{n,X}|X=y). \tag{C_1}$$

Moreover we suppose that the kernel transition preserves the configuration space partition, that is:

$$\bigcup_{l=1}^k \mathsf{B}_{n,l}^{\mathsf{B}_{0,l}} = \mathsf{D}, \tag{C_2}$$

and for any $l \neq l'$, we have

$$\mathsf{B}_{n,l}^{\mathsf{B}_{0,l}} \cap \mathsf{B}_{n,l'}^{\mathsf{B}_{0,l'}} = \emptyset. \tag{C_3}$$

Then no homogeneous sub-domains can appear neither disappear with time.

Acquisition processes for decomposed homogeneous medium

As we have seen in the previous section, the decomposition of the configuration space in homogeneous sub-domains brings about an acquisition process. Thus we are in presence of two acquisition processes, one to take into account the acquisition of the random field Θ_n along the random path Z_n, the other one to follow homogeneous sub-domains $\mathsf{B}_{n,l}^{\mathsf{B}_{0,l}}$. The path given by $Z_0, \ldots, Z_n$ is assumed to be independent from the Lagrangian dynamic of the acquisition process $(\mathsf{B}_{n,l}^{\mathsf{B}_{0,l}}, \Theta_{n,\mathsf{B}_{n,l}^{\mathsf{B}_{0,l}}})$. Moreover, we suppose that the process Z_n evolves in the whole space E, that is it can be in any sub-domain $\mathsf{B}_{n,l}^{\mathsf{B}_{0,l}}$ but necessarily fall on into one of them as they made a partition of the configuration space E. Further we assume that the random field Θ_n evolves globally, then the evolution of Z_n which depends on the value of Θ_n at Z_n is accessible at any point of the configuration space.

Now we have made all these remarks, we mix two acquisition processes in order to estimate the random field on homogeneous sub-domains using the random path given by $Z_0, \ldots, Z_n$. The first one is the Lagrangian acquisition process $(\mathsf{B}_{n,l}^{\mathsf{B}_{0,l}}, \Theta_{n,\mathsf{B}_{n,l}^{\mathsf{B}_{0,l}}})$, and the other one is the acquisition process along the path which is independent from the sub-domains evolution denoted by (Z_n, Θ_{n,Z_n}). Using the homogeneity hypothesis of each sub-domains, we propose to estimate the conditional expectation of the pair process: random process Z_n, random media on $\mathsf{B}_{n,l}^{\mathsf{B}_{0,l}}$, given that the position process Z_n falls on the homogeneous sub-domain $\mathsf{B}_{n,l}^{\mathsf{B}_{0,l}}$, defined for any $f_n \in \mathcal{B}_b(\mathsf{E} \times \mathsf{E}_n^\Theta)$ by:

$$\mathbb{E}\left[f_n(Z_n, \Theta_{n,\mathsf{B}_{n,l}^{\mathsf{B}_{0,l}}})|Z_{0:n} \in \mathsf{B}_{0:n,l}^{\mathsf{B}_{0,l}}\right]. \tag{2.72}$$

The couple $(Z_n, \Theta_{n,\mathsf{B}_{n,l}^{\mathsf{B}_{0,l}}})$ is supposed to be a Markovian process whose evolution is given by the kernel transition T_n defined as follow:

$$T_n((z,\theta), \mathrm{d}(z',\theta')) = \mathbb{P}\left(Z_{n+1}, \Theta_{n+1,\mathsf{B}_{n+1,l}^{\mathsf{B}_{0,l}}} \in \mathrm{d}(z',\theta')|(Z_n, \Theta_{n,\mathsf{B}_{n,l}^{\mathsf{B}_{0,l}}}) = (z,\theta)\right).$$

Using the same reasoning as for (2.66), we have that (2.72) can be written as:

$$\frac{\mathbb{E}\left[f_n(Z_n, \Theta_{n,\mathsf{B}_{n,l}^{\mathsf{B}_{0,l}}}) \prod_{p=0}^{n} \mathbb{1}_{\mathsf{B}_{p,l}^{\mathsf{B}_{0,l}}}(Z_n)\right]}{\mathbb{E}\left[\prod_{p=0}^{n} \mathbb{1}_{\mathsf{B}_{p,l}^{\mathsf{B}_{0,l}}}(Z_p)\right]}.$$

Recording that Z_p is independent of the domain evolution $\mathsf{B}_{p,l}^{\mathsf{B}_{0,l}}$, the point process Z_p can fall on into $\mathsf{B}_{p,l}^{\mathsf{B}_{0,l}}$, but it can be every where else, that is in another sub-domain. Therefore the joint probability that Z_p is in $\mathsf{B}_{p,l}^{\mathsf{B}_{0,l}}$, for $p \in [\![1,n]\!]$ can nullify. In this case, the measure defined by (2.72) does not make sense and the estimation problem cannot be solved.

To overcome this issue, instead of considering only one random point process Z_n, we consider that we have several independent ones grouped under the notation $\mathbb{Z}_n = (Z_n^i)_{i=1}^M$. If there are enough random processes in E, then one can hope that at least one is present in each $\mathsf{B}_{p,l}^{\mathsf{B}_{0,l}}$ for $p \in [\![1,n]\!]$ and $l \in [\![1,k]\!]$. If none of them are in the sub-domain $\mathsf{B}_{n,l}^{\mathsf{B}_{0,l}}$,

there is no estimation problem for this area of E. That is the reason why, we consider only the estimation problem for the balls where at least one random point process Z_n^i falls on.

To sum up, we estimate the quantity defined by (2.72) for the acquisition process $\mathsf{B}_{n,l}^{\mathsf{B}_{0,\mathsf{l}}}$, where $l \in [\![1,k]\!]$ is such that at least one of the random point process Z_n^i is in $\mathsf{B}_{n,l}^{\mathsf{B}_{0,\mathsf{l}}}$. All the others acquisition processes cannot be evaluated. The estimation concerns the following quantities:

$$\hat{\chi}_n^l(f_n) \triangleq \frac{\mathbb{E}\left[f_n(\mathbb{Z}_n, \Theta_{n,\mathsf{B}_{n,l}^{\mathsf{B}_{0,l}}}) \prod_{p=0}^{n} G_p^{\mathsf{B}_{p,l}^{\mathsf{B}_{0,l}}}(\mathbb{Z}_p)\right]}{\mathbb{E}\left[\prod_{p=0}^{n} G_p^{\mathsf{B}_{p,l}^{\mathsf{B}_{0,l}}}(\mathbb{Z}_p)\right]} \tag{2.73}$$

and

$$\chi_n^l(f_n) \triangleq \frac{\mathbb{E}\left[f_n(\mathbb{Z}_n, \Theta_{n,\mathsf{B}_{n,l}^{\mathsf{B}_{0,l}}}) \prod_{p=0}^{n-1} G_p^{\mathsf{B}_{p,l}^{\mathsf{B}_{0,l}}}(\mathbb{Z}_p)\right]}{\mathbb{E}\left[\prod_{p=0}^{n-1} G_p^{\mathsf{B}_{p,l}^{\mathsf{B}_{0,l}}}(\mathbb{Z}_p)\right]} \tag{2.74}$$

where the potential function $G_p^{\mathsf{B}_{p,l}^{\mathsf{B}_{0,l}}}$ is defined as follow:

$$G_p^{\mathsf{B}_{p,l}^{\mathsf{B}_{0,l}}}(\mathbb{Z}_p) \triangleq (\mathbb{1}_{\mathsf{B}_{p,l}^{\mathsf{B}_{0,l}}}(Z_p^i))_{i=1}^{M}. \tag{2.75}$$

As one may observe, the potential function $G_p^{\mathsf{B}_{p,l}^{\mathsf{B}_{0,l}}}$ is equal to the sequence $\underbrace{(0,\ldots,0)}_{M\times}$, when no processes are present in the sub-domain $\mathsf{B}_{n,l}^{\mathsf{B}_{0,l}}$. However we made the assumption that there are enough random processes evolving inside E, that is $M \gg 1$, so that at least one falls inside $\mathsf{B}_{p,l}^{\mathsf{B}_{0,l}}$ for each $p \in [\![1,n]\!]$. It follows that $G_p^{\mathsf{B}_{p,l}^{\mathsf{B}_{0,l}}} \neq 0$.

Without changing the expression of (2.73), instead of considering the conditioning to the sub-domain $\mathsf{B}_{p,l}^{\mathsf{B}_{0,l}}$, we consider it on the cylinder $\mathsf{B}_{p,l}^{\mathsf{B}_{0,l}} \times \mathsf{E}_n^{\Theta}$ and we define the potential $\tilde{G}_p^{\mathsf{B}_{l,p}^{\mathsf{B}_{0,l}}}$ for the couple $(\mathbb{Z}_p, \Theta_{p,\mathsf{B}_{p,l}^{\mathsf{B}_{0,l}}})$ which is defined by:

$$\tilde{G}_p^{\mathsf{B}_{p,l}^{\mathsf{B}_{0,l}}}(\mathbb{Z}_p, \Theta_{p,\mathsf{B}_{p,l}^{\mathsf{B}_{0,l}}}) \triangleq G_p^{\mathsf{B}_{p,l}^{\mathsf{B}_{0,l}}}(\mathbb{Z}_p) \times \mathbb{1}_{\mathsf{E}_n^{\Theta}}(\Theta_{p,\mathsf{B}_{p,l}^{\mathsf{B}_{0,l}}}). \tag{2.76}$$

To this potential we associate the selection kernel $S_{p,\chi_n^l}^{\mathbb{Z}}$ defined for any $(z_p^M, \theta) \in \mathsf{E}_p^M \times \mathsf{E}_p^{\Theta}$ by:

$$S_{p,\chi_p^l}^{\mathbb{Z}}((z_p^M, \theta), .) = \tilde{G}_p^{\mathsf{B}_{p,l}^{\mathsf{B}_{0,l}}}(z_p^M, \theta)\delta_{(z_p^M,\theta)}(.) + (1 - \tilde{G}_p^{\mathsf{B}_{p,l}^{\mathsf{B}_{0,l}}}(z_p^M, \theta))\delta_{\{\mho\}}(.) \tag{2.77}$$

where $\mho$ corresponds to the auxiliary virtual cemetery point where the random point process ends if it outside $\mathsf{B}_{n,l}^{\mathsf{B}_{0,l}}$. Recording that for each $i \in [\![1,M]\!]$, we have supposed that:

$$T_n((z,\theta), \mathrm{d}(z',\theta')) = \mathbb{P}\left(Z_{n+1}^i, \Theta_{n+1,\mathsf{B}_{n+1,l}^{\mathsf{B}_{0,l}}} \in \mathrm{d}(z',\theta')|(Z_n^i, \Theta_{n,\mathsf{B}_{n,l}^{\mathsf{B}_{0,l}}}) = (z,\theta)\right).$$

$$\chi_n^l \xrightarrow[\substack{S_{n,\chi_n^l}^{\mathbb{Z}}}]{\text{Cutting}} \hat{\chi}_n^l = \chi_n^l S_{n,\chi_n^l}^{\mathbb{Z}} \xrightarrow[\mathbb{T}_{n+1}]{\text{Mutation}} \chi_{n+1}^l = \hat{\chi}_n^l \mathbb{T}_{n+1}$$

Figure 2.9: Evolution scheme of the coupled process.

We extend T_n, and set $T_n(\mho, .) = 0$. Then for the process $\mathbb{Z}$, we have:

$$\mathbb{P}(\mathbb{Z}_{n+1}, \Theta_{n+1, \mathsf{B}_{n+1,l}^{\mathsf{B}_{0,l}}} \in \mathrm{d}(z_{n+1}^M, \theta') | (\mathbb{Z}_n, \Theta_{n, \mathsf{B}_{n,l}^{\mathsf{B}_{0,l}}}) = (z_n^M, \theta))$$

$$= \prod_{i=1}^{M} \mathbb{P}(Z_{n+1}^i, \Theta_{n+1, \mathsf{B}_{n+1,l}^{\mathsf{B}_{0,l}}} \in \mathrm{d}(z_{n+1}^i, \theta') | (Z_n^i, \Theta_{n, \mathsf{B}_{n,l}^{\mathsf{B}_{0,l}}}) = (z_n^i, \theta))$$

as aircrafts evolves independently. Then it follows that:

$$\mathbb{P}\left(\mathbb{Z}_{n+1}, \Theta_{n+1, \mathsf{B}_{n+1,l}^{\mathsf{B}_{0,l}}} \in \mathrm{d}(z_{n+1}^M, \theta') | (\mathbb{Z}_n, \Theta_{n, \mathsf{B}_{n,l}^{\mathsf{B}_{0,l}}}) = (z_n^M, \theta)\right) = \prod_{i=1}^{M} T_n((z_{n+1}^i, \theta), \mathrm{d}(z_n^i, \theta'))$$

$$\triangleq \mathbb{T}_n((z_n^m, \theta), \mathrm{d}(z_{n+1}^M, \theta')). \tag{2.78}$$

Then from the initial distribution of the acquisition process:

$$\chi_0(\mathrm{d}(z_0^M, \theta_0)) = \mathbb{P}((\mathbb{Z}_0, \Theta_{0, \mathsf{B}_{0,l}}) \in \mathrm{d}(z_0^M, \theta_0)),$$

we have the time evolution scheme which is given by two step, a mutation given by $\mathbb{T}_n$ and a cutting step given by $S_{n,\chi_n^l}^{\mathbb{Z}}$. We resume this by the following equation:

$$\chi_n^l = \chi_{n-1}^l S_{n-1, \chi_{n-1}^l}^{\mathbb{Z}} \mathbb{T}_n. \tag{2.79}$$

Recording that $\hat{\chi}_{n-1}^l = \chi_{n-1}^l S_{n-1, \chi_{n-1}^l}^{\mathbb{Z}}$, we represent the two steps evolution scheme of the measure χ_n^l on Figure 2.9.

The coupling between the acquisition processes induced by the random point processes and the Lagrangian acquisition system to follow the homogeneous balls $\mathsf{B}_{n,l}^{\mathsf{B}_{0,l}}$ is a cutting of the random point processes after the Lagrangian mutation. Random processes which are outside the homogeneous sub-domain are ignored. The pair process is also a random process evolving in the random environment, then the work developed in Section 2.2.1 can also be used for this case. Except that now we have an additional step for the process $\mathbb{Z}_n$ given by the cutting step through the selection kernel $S_{n,\chi_n^l}^{\mathbb{Z}}$. That is for each sub-domain we have a 3 steps algorithm: the first allows one to make evolute the environment and the homogeneous sub-domains, the second consists in the dynamic evolution of the point processes using the global environment, the third enables one to keep only the random point processes which have fallen inside the homogeneous sub-domain after its evolution. That is, if one considers the random environment to be $\Theta_{n, \mathsf{B}_{n,l}^{\mathsf{B}_{0,l}}}$ and the random process

$\eta^{\mathbb{Z}}_{\Theta_{0:n},n}$ cut to $\mathsf{B}^{\mathsf{B}_{0,l}}_{n,l}$ then we fall again in the framework of random distribution processes, except that after the evolution of $\mathbb{Z}_n$, the random processes are selected using $S^{\mathbb{Z}}_{n-1,\chi^l_{n-1}}$ in order to consider only those which have fallen in $\mathsf{B}^{\mathsf{B}_{0,l}}_{n,l}$. Finally we try to estimate:

$$\overline{\eta}^l_n \triangleq \mathbb{E}\left[f(\Theta_{n,\mathsf{B}^{\mathsf{B}_{0,l}}_{n,l}}, \eta^{\mathbb{Z}}_{\Theta_{0:n},n}) | \mathbb{Z}_{0:n} \in \mathsf{B}^{\mathsf{B}_{0,l}}_{0:n,l}\right]. \tag{2.80}$$

In order to estimate (2.80), we develop a similar approximation procedure as for the measure $\overline{\eta}_n$ given by Proposition 2.2.1. To this end, let us define the quenched acquisition processes.

Quenched acquisition processes Fix the environment sequence $\Theta_{0:n} = \theta_{0:n} \in \prod_{p=0}^{n} \mathsf{E}^\Theta_p$, and for any $l \in [\![1,k]\!]$ set $\mathsf{B}^{\mathsf{B}_{0,l}}_{0:n,l} = \mathsf{b}^{\mathsf{b}_{0,l}}_{0:n,l}$, Suppose that the random process $\mathbb{Z}_n = (Z^i_n)^M_{i=1}$, composed of independent Markov processes with $M \gg 1$, is a Markov chain of transition kernel $M^{\mathbb{Z}}_{\theta_n,n}$ from E^M_{n-1} to E^M_n given by:

$$M^{\mathbb{Z}}_{\theta_n,n}(z^M_{n-1}, \mathrm{d}z^M_n) \triangleq \prod_{i=1}^{M} M^Z_{\theta_n,n}(z^i_{n-1}, \mathrm{d}z^i_n) \tag{2.81}$$

where the transition kernel $M^Z_{\theta_n,n}$ corresponds to the evolution of each random process extended to $\mathsf{D} \cup \{\mho\}$ by setting: $M^Z_{\theta_n,n}(\mho,.) = 0$. Its initial distribution is given by:

$$\eta^{\mathbb{Z}}_{\theta_0}(\mathrm{d}z^M_0) \triangleq \prod_{i=1}^{M} \eta^Z_{\theta_0}(\mathrm{d}z^i_0). \tag{2.82}$$

One finally gets:

$$\mathbb{P}_{\theta_{0:n},n}\left(\mathbb{Z}_{0:n} \in \mathrm{d}(z^M_0, \ldots, z^M_n) | \mathbb{Z}_{0,n} \in \mathsf{b}^{\mathsf{b}_{0,l}}_{0:n,l})\right) = \frac{1}{\mathcal{Z}^{\mathsf{b}_{0,l}}_{\theta_{0:n},n}}\left\{\prod_{p=0}^{n-1} G^{\mathsf{b}_{0,l}}_{\theta_p,p}(z^M_p)\right\}$$
$$\eta^Z_{\theta_0}(\mathrm{d}z^M_0)M^{\mathbb{Z}}_{\theta_1,1}(z^M_0, \mathrm{d}z^M_1)\ldots M^{\mathbb{Z}}_{\theta_n,n}(z^M_{n-1}, \mathrm{d}z^M_n) \tag{2.83}$$

with normalizing constant:

$$\mathcal{Z}^{\mathsf{b}_{0,l}}_{0:n,l} = \mathbb{E}_{\eta^X_{\theta_0}}\left[\prod_{p=0}^{n-1} G^{\mathsf{b}_{0,l}}_{\theta_p,p}(Z^M_p)\right]$$

which is strictly positive by construction (thanks to hypothesis $M \gg 1$ and condition (τ)). The random potential functions are defined using (2.76) such that:

$$G^{\mathsf{b}_{0,l}}_{\theta_p,p} : z^M_p \in \mathsf{E}^M_p \mapsto G^{\mathsf{b}_{0,l}}_{\theta_p,p}(z^M_p) = \tilde{G}^{\mathsf{b}_{0,l}}_p(\theta_p, z^M_p).$$

The quantity defined by (2.83) is also denoted by $\mathbb{Q}^{\mathsf{b}_{0,l}}_{\theta_{0:n},n}$ and called the quenched Feynman-Kac path measure cut to $\mathsf{b}^{\mathsf{b}_{0,l}}_{0:n,l}$. We denote the updated version as before by $\hat{\mathbb{Q}}^{\mathsf{b}_{0,l}}_{\theta_{0:n},n}$ given

by:

$$\hat{\mathbb{Q}}_{\theta_{0:n},n}^{\mathsf{b}_{0,l}}(\mathrm{d}(z_0^M,\ldots,z_n^M)) = \mathbb{P}_{\theta_{0:n},n}\left(\mathbb{Z}_{0:n} \in \mathrm{d}(z_0^M,\ldots,z_n^M)\middle|\mathbb{Z}_{0,n} \in \mathsf{b}_{0:n,l}^{\mathsf{b}_{0,l}}\right)$$

$$= \frac{1}{\hat{\mathcal{Z}}_{\theta_{0:n},n}^{\mathsf{b}_{0,l}}}\left\{\prod_{p=0}^{n} G_{\theta_p,p}^{\mathsf{b}_{p,l}}(z_p^M)\right\} \eta_{\theta_0}^{\mathbb{Z}}(\mathrm{d}x_0)M_{\theta_1,1}^{\mathbb{Z}}(z_0^M,\mathrm{d}z_1^M)\ldots M_{\theta_n,n}^{\mathbb{Z}}(z_{n-1}^M,\mathrm{d}z_n^M)$$

(2.84)

where $\hat{\mathcal{Z}}_{\theta_{0:n},n}^{\mathsf{b}_{0,l}} \triangleq \mathbb{E}_{\eta_{\theta_0}^{\mathbb{Z}}}\left[\prod_{p=0}^{n} G_{\theta_p,p}^{\mathsf{b}_{p,l}}(\mathbb{Z}_p)\right] > 0.$

We can associate to it the quenched distribution flow denoted by $\eta_{\theta_{0:n},n}^{\mathbb{Z},l}$ which is defined for all $f_n \in \mathcal{B}_b(\mathsf{E}_n^M)$ as follow:

$$\eta_{\theta_{0:n},n}^{\mathbb{Z},l}(f_n) = \gamma_{\theta_{0:n},n}^{\mathbb{Z},l}(f_n)/\gamma_{\theta_{0:n},n}^{\mathbb{Z},l}(1) \tag{2.85}$$

where the unnormalized Feynman-Kac measure $\gamma_{\theta_{0:n},n}^{\mathbb{Z},l}$ is given for all $f_n \in \mathcal{B}_b(\mathsf{E}_n^M)$ by:

$$\gamma_{\theta_{0:n},n}^{\mathbb{Z},l}(f_n) \triangleq \mathbb{E}\left[f_n(\mathbb{Z}_n)\prod_{p=0}^{n-1} G_{\theta_p,p}^{\mathsf{b}_{p,l}}(\mathbb{Z}_p)\right]. \tag{2.86}$$

The denominators are well defined by construction as $M \gg 1$ and under the condition (τ). We can notice that the normalized Feynman Kac measure as in the precedent section corresponds to the prediction step in a Bayesian framework:

$$\eta_{\theta_{0:n},n}^{\mathbb{Z},l} = \mathrm{Law}(\mathbb{Z}_n|\mathbb{Z}_{0:n-1} \in \mathsf{b}_{0:n-1}^{\mathsf{b}_{0,l}}, \Theta_{0,n} = (\theta_0,\ldots,\theta_n)).$$

The updated version of this distribution denoted by $\hat{\eta}_{\theta_{0:n},n}^{\mathbb{Z},l}$ which corresponds to the cutting step is given for all $f_n \in \mathcal{B}_b(\mathsf{E}_n^M)$ by:

$$\hat{\eta}_{\theta_{0:n},n}^{\mathbb{Z},l}(f_n) = \hat{\gamma}_{\theta_{0:n},n}^{\mathbb{Z},l}(f_n)/\hat{\gamma}_{\theta_{0:n},n}^{\mathbb{Z},l}(1) \tag{2.87}$$

where the unnormalized Feynman-Kac measure $\hat{\gamma}_{\theta_{0:n},n}^{\mathbb{Z},l}$ is given for all $f_n \in \mathcal{B}_b(\mathsf{E}_n^M)$ by:

$$\hat{\gamma}_{\theta_{0:n},n}^{\mathbb{Z},l}(f_n) \triangleq \mathbb{E}\left[f_n(\mathbb{Z}_n)\prod_{p=0}^{n} G_{\theta_p,p}^{\mathsf{b}_{p,l}}(\mathbb{Z}_p)\right].$$

As it is the case for classical filtering problem, quantities defined by (2.85) and (2.87) are related by the following operations:

$$\hat{\eta}_{\theta_{0:n},n}^{\mathbb{Z},l}(f_n) = \hat{\eta}_{\theta_{0:n},n}^{\mathbb{Z},l}(G_{\theta_n,n}^{\mathsf{b}_{n,l}}f_n)/\hat{\eta}_{\theta_{0:n},n}^{\mathbb{Z},l}(G_{\theta_n,n}^{\mathsf{b}_{n,l}}) \tag{2.88}$$

and

$$\eta_{\theta_{0:n+1},n+1}^{\mathbb{Z},l} = \hat{\eta}_{\theta_{0:n},n}^{\mathbb{Z},l}M_{\theta_{n+1},n+1}^{\mathbb{Z}}. \tag{2.89}$$

Equation (2.88) can be written as a Boltzmann-Gibbs transformation, $\Psi_{\theta_n,n}^{\mathbb{Z},l}$, associ-

ated to the potential function $G^{\mathbf{b}_{0,l}}_{\theta_{n,n}}$, where the Boltzmann Gibbs measure, $\Psi^{\mathbb{Z},l}_{\theta_n,n}(\eta^{\mathbb{Z},l}_{\theta_{0:n},n})$ is defined for any $\eta^{\mathbb{Z},l}_{\theta_{0:n},n} \in \mathcal{P}(\mathsf{E}^M_n)$ by:

$$\Psi^{\mathbb{Z},l}_{\theta_n,n}(\eta^{\mathbb{Z},l}_{\theta_{0:n},n})(\mathrm{d}z^M_n) = \frac{1}{\eta^{\mathbb{Z},l}_{\theta_{0:n},n}(G^{\mathbf{b}_{0,l}}_{\theta_n,n})} G^{\mathbf{b}_{0,l}}_{\theta_n,n}(z^M_n)\eta^{\mathbb{Z},l}_{\theta_{0:n},n}(\mathrm{d}z^M_n). \tag{2.90}$$

This update step allows one to take only random processes which fall into $\mathbf{b}^{\mathbf{b}_{0,l}}_{n,l}$. Thanks to the assumption on first hitting times (τ) we have formulated, the Boltzmann-Gibbs transformation is well-defined.

Using (2.90), we define the mapping $\Phi^{\mathbb{Z},l}_n$ from $\mathcal{P}(\mathsf{E}^M_{n-1})$ to $\mathcal{P}(\mathsf{E}^M_n)$ for any $\eta^{\mathbb{Z},l}_{\theta_{0:n-1},n-1} \in \mathcal{P}(\mathsf{E}^M_{n-1})$ by:

$$\begin{array}{rcl}
\Phi^{\mathbb{Z},l}_n : \left(\mathsf{E}^M_{n-1} \times \mathsf{E}^\Theta_n\right) \times \mathcal{P}(\mathsf{E}^M_{n-1}) & \to & \mathcal{P}(\mathsf{E}^M_n) \\
\left((\theta_{n-1},\theta_n),\eta^{\mathbb{Z},l}_{\theta_{0:n-1},n-1}\right) & \mapsto & \Psi^{\mathbb{Z},l}_{\theta_{n-1},n-1}(\eta^{\mathbb{Z},l}_{\theta_{0:n-1},n-1})M^{\mathbb{Z}}_{\theta_n,n}
\end{array} \tag{2.91}$$

Then we resume the cutting-prediction filtering recursions by the following diagram:

$$\eta^{\mathbb{Z},l}_{\theta_{0:n-1},n-1} \xrightarrow{\text{cutting}} \hat\eta^{\mathbb{Z},l}_{\theta_{0:n-1},n-1} = \Psi^{\mathbb{Z},l}_{\theta_n,n}(\eta^{\mathbb{Z},l}_{\theta_{0:n-1},n-1}) \xrightarrow{\text{prediction}} \eta^{\mathbb{Z},l}_{\theta_{0:n},n} = \hat\eta^{\mathbb{Z},l}_{\theta_{0:n-1},n-1}M^{\mathbb{Z}}_{\theta_n,n} \tag{2.92}$$

As it was done for the classical filtering problem, we write the McKean interpretation of the quenched Feynman-Kac measure $\eta^{\mathbb{Z},l}_{\theta_{0:n},n}$. The non linear recursion (2.91) can be rewritten in the following recursive form:

$$\eta^{\mathbb{Z},l}_{\theta_{0:n},n} = \eta^{\mathbb{Z},l}_{\theta_{0:n-1},n-1}K^{\mathbb{Z},l}_{n,\eta^{\mathbb{Z},l}_{\theta_{0:n-1},n-1}} \tag{2.93}$$

where $K^{\mathbb{Z},l}_{n,\eta^{\mathbb{Z},l}_{\theta_{0:n-1},n-1}}$ is a transition kernel defined by:

$$K^{\mathbb{Z},l}_{n,\eta^{\mathbb{Z},l}_{\theta_{0:n-1},n-1}} = S_{n-1,\eta^{\mathbb{Z},l}_{\theta_{0:n-1},n-1}}M^{\mathbb{Z}}_{\theta_n,n} \tag{2.94}$$

with $S_{n-1,\eta^{\mathbb{Z},l}_{\theta_{0:n-1},n-1}}$ the selection kernel associated to $G^{\mathbf{b}_{0,l}}_{\theta_{n-1},n-1}$

$$S^{\mathbb{Z}}_{n-1,\eta^{\mathbb{Z},l}_{\theta_{0:n-1},n-1}}((z^M_{n-1},\theta),.) = G^{\mathbf{b}_{0,l}}_{\theta_{n-1},n-1}(z^M_{n-1})\delta_{(z^M_{n-1})}(.) + (1-G^{\mathbf{b}_{0,l}}_{\theta_{n-1},n-1}(z^M_{n-1})\delta_{\{\mho\}}(.) \tag{2.95}$$

where $\mho$ has been introduced to be an auxiliary cemetery point not in D. The remaining problem here, is that we do not know the environment realization. Then, the quenched Feynman-Kac flow cannot be used to model our problem. Therefore, we have to consider the environment as a random process also.

Acquisition process in random distribution space   As we do not know the random environment where the stochastic process $\mathbb{Z}_n$ evolves, the quenched Feynman-Kac measure cannot be used in order to model the law of the filtering problem. So we have to use

another quantity which is a second Feynman-Kac measure but this time in distribution space, to this end we introduce the sequence $\overline{X}_n^l = (\Theta_{n,B_{n,l}^{B_{0,l}}}, \eta_{\theta_{0:n},n}^{\mathbb{Z},l}) \in \overline{E}_n \triangleq E_n^\Theta \times \mathcal{P}(E_n^M)$, for $l \in [\![1,k]\!]$. We recall here the condition (τ) formulated to ensure that homogeneous sub-domains are not emptied in one time step from all random processes present for the previous time step. As it was shown by Del Moral in Del Moral (2004), p. 85 , the pair process is a Markov chain.

Proposition 2.4.1. *The stochastic process $\overline{X}_n^l$ is a Markov chain under $\mathbb{P}_{\chi_0^l}$ with transition kernel $\overline{M}_n^l$ defined for all $\overline{f}_n \in \mathcal{B}_b(\overline{E}_n)$ and $(\theta_{n,b_{n,l}^{b_{0,l}}}, \eta_{\theta_{0:n},n}^{\mathbb{Z},l}) \in \overline{E}_n$ by:*

$$\overline{M}_n^l((\theta_{n-1,b_{n-1}^{b_{0,l}}}, \eta_{\theta_{0:n-1},n-1}^{\mathbb{Z},l}), \mathrm{d}(\theta_{n,b_n^{b_{0,l}}}, \eta_{\theta_{0:n},n}^{\mathbb{Z},l}))(\overline{f}_n)$$
$$\triangleq \int_{E_n^\Theta} M_n^\Theta(\theta_{n-1,b_{n-1}^{b_{0,l}}}, \mathrm{d}\theta_{n,b_n^{b_{0,l}}}) \overline{f}_n(\theta_{n,b_n^{b_{0,l}}}, \Phi_n^{\mathbb{Z},l}(\theta_{n-1}, \theta_n, \eta_{\theta_{0:n-1},n-1}^{\mathbb{Z},l})) \quad (2.96)$$

and initial distribution, denoted by $\overline{\eta}_0 \in \mathcal{P}(\overline{E}_0)$ given by:

$$\overline{\eta}_0^l(\mathrm{d}(u,\nu)) = \eta_{0,B_{0,l}}^\Theta(\mathrm{d}u)\delta_{\eta_{\theta_0,0}^{\mathbb{Z},l}}(\mathrm{d}\nu)$$

where $\eta_{0,B_{0,l}}^\Theta$ corresponds to the initial distribution of the random environment on $B_{0,l}$.

Proof. $\forall \overline{f}_n \in \mathcal{B}_b(\overline{E}_n)$:

$$\mathbb{E}_{\overline{\eta}_0}[\overline{f}_n(\overline{X}_n^l) \mid \sigma(\overline{X}_0^l, \ldots, \overline{X}_{n-1}^l)] = \mathbb{E}_{\overline{\eta}_0}[\overline{f}_n(\Theta_{n,B_{n,l}^{B_{0,l}}}, \eta_{\theta_{0:n},n}^{\mathbb{Z},l}) \mid \sigma(\overline{X}_0^l, \ldots, \overline{X}_{n-1}^l)]$$
$$= \mathbb{E}_{\overline{\eta}_0}[\overline{f}_n(\Theta_{n,B_{n,l}^{B_{0,l}}}, \Phi_n^{\mathbb{Z},l}((\Theta_{n-1},\Theta_n), \eta_{\theta_{0:n-1},n-1}^{\mathbb{Z},l}) \mid \sigma(\overline{X}_0^l, \ldots, \overline{X}_{n-1}^l)].$$

As $\overline{X}_{n-1}^l = (\Theta_{n-1,B_{n-1,l}^{B_{0,l}}}, \eta_{\theta_{0:n-1},n-1}^{\mathbb{Z},l})$, we have:

$$\mathbb{E}_{\overline{\eta}_0}[\overline{f}_n(\overline{X}_n^l) \mid \sigma(\overline{X}_0^l, \ldots, \overline{X}_{n-1}^l)] = \mathbb{E}_{\overline{\eta}_0}[\overline{f}_n(\Theta_{n,B_{n,l}^{B_{0,l}}}, \Phi_n^{\mathbb{Z},l}((\Theta_{n-1},\Theta_n), \eta_{\theta_{0:n-1},n-1}^{\mathbb{Z},l}) \mid \sigma(\overline{X}_0^l, \ldots, \overline{X}_{n-1}^l)]$$
$$= \int_{E_n^\Theta} \overline{f}_n(\theta_{n,b_{n,l}^{b_{0,l}}}, \Phi_n^{\mathbb{Z},l}((\Theta_{n-1},\theta_n), \eta_{\theta_{0:n-1},n-1}^{\mathbb{Z},l})) M_n^\Theta(\Theta_{n-1,B_{n-1}^{B_{0,l}}}, \mathrm{d}\theta_{n,b_{n,l}^{b_{0,l}}})$$

$\square$

As one may notice here, the assumption made on the fact that Θ_n evolves globally takes its importance here as $\mathbb{Z}_n$ needs a global knowledge of the random environment to evolve. The Markov property is not affected as $B_{n,l}^{B_{0,l}}$ depends only on the evolution of Θ_n from its definition.

Then we can define another Feynman Kac flow $\overline{\eta}_n^l$ and $\overline{\gamma}_n^l$, denoting respectively the normalized and unnormalized Feynman Kac distribution in distribution space. They are defined for all $\overline{f}_n \in \mathcal{B}_b(\overline{E}_n)$ by the following relations:

$$\overline{\eta}_n^l(\overline{f}_n) \triangleq \overline{\gamma}_n^l(\overline{f}_n)/\overline{\gamma}_n^l(1) \quad (2.97)$$

and

$$\overline{\gamma}_n^l(\overline{f}_n) \triangleq \mathbb{E}_{\chi_n^l}\left[\overline{f}_n(\overline{X}_n^l)\prod_{p=0}^{n-1}\overline{G}_p^l(\overline{X}_p^l)\right]$$

where

$$\overline{G}_p^l : (u,\mu) \in \overline{\mathsf{E}}_p \mapsto \overline{G}_p^l(u,\mu) = \int_{\mathsf{E}_p^M}\mu(\mathrm{d}y)\tilde{G}_p^{\mathsf{B}_{p,l}^{\mathsf{B}_{0,l}}}(u,y) = \mu(\tilde{G}_p^{\mathsf{B}_{p,l}^{\mathsf{B}_{0,l}}}(u,.)). \qquad (2.98)$$

From Del Moral (2004) (p. 86), we have that $\overline{\eta}_n^l$ satisfies a non linear recursive equation:

Proposition 2.4.2. *For every $n \geq 1$, $\overline{\eta}_n^l$ satisfies the following non linear recursive equation:*

$$\overline{\eta}_n^l = \overline{\Psi}_{n-1}^l(\overline{\eta}_{n-1}^l)\overline{M}_n^l = \overline{\Phi}_n^l(\overline{\eta}_{n-1}^l),$$

where the application $\overline{\Psi}_n^l : \mathcal{P}(\overline{\mathsf{E}}_n) \to \mathcal{P}(\overline{\mathsf{E}}_n)$, is defined for every $\overline{f}_n$ by:

$$\overline{\Psi}_n^l(\eta)(\overline{f}_n) = \eta(\overline{G}_n^l\overline{f}_n)/\eta(\overline{G}_n^l),$$

and the operator $\overline{\Phi}_n^l$ is defined by:

$$\begin{aligned}\overline{\Phi}_n^l : \mathcal{P}(\overline{\mathsf{E}}_{n-1}) &\to \mathcal{P}(\overline{\mathsf{E}}_n) \\ \eta &\mapsto \overline{\Psi}_{n-1}^l(\eta)\overline{M}_n^l.\end{aligned} \qquad (2.99)$$

In other words, defining $\hat{\overline{\eta}}_n^l \triangleq \hat{\overline{\gamma}}_n^l(\overline{f}_n)/\hat{\overline{\gamma}}_n^l(1)$ with $\hat{\overline{\gamma}}_n^l \triangleq \mathbb{E}_{\overline{\eta}_0^l}\left[\overline{f}_n(\overline{X}_n^l)\prod_{p=0}^{n}\overline{G}_p^l(\overline{X}_p^l)\right]$ those two quantities are related by the following relation:

$$\hat{\overline{\eta}}_n^l(f_n) = \overline{\eta}_n^l(\overline{G}_n^l\overline{f}_n)/\overline{\eta}_n^l(\overline{G}_n^l) \qquad (2.100)$$

and

$$\overline{\eta}_{n+1}^l = \hat{\overline{\eta}}_n^l\overline{M}_{n+1}^l. \qquad (2.101)$$

By direct inspection, we have that $\overline{\eta}_n^l$ corresponds to the predicting filter and $\hat{\overline{\eta}}_n^l$ to the updating filter. And we can resume these relations by the following diagram:

$$\overline{\eta}_n^l \xrightarrow{\text{updating}} \hat{\overline{\eta}}_n^l = \overline{\Psi}_n^l(\overline{\eta}_n^l) \xrightarrow{\text{prediction}} \overline{\eta}_{n+1}^l = \hat{\overline{\eta}}_n^l\overline{M}_{n+1}^l \qquad (2.102)$$

In the non linear case, equation (2.99) cannot be solved analytically. In the next paragraph, we introduce an interacting particle system to approximate this sequence of Feynman-Kac measures $((\overline{\eta}_n^l)_{l=1}^k)_{n\in\mathbb{N}}$.

Particle approximation and Patchwork Labeled Island Particle algorithm This section deals with the interacting "patchwork" labeled island model associated to the Feynman-Kac distribution flow: $\overline{\eta}_n^l$ for all $l \in [\![1,k]\!]$, we have defined in the previous paragraph.

As one may notice $\overline{\eta}_n^l$, defined by (2.97), has the same shape as $\overline{\eta}_n$, defined by (2.34).

Then using the same reasoning as in Section 2.2.2, we define a two level interacting particle systems. Nevertheless, here there is an additional step to make evolve the random process $\overline{X}_n^l$ given by the cutting step.

A (N_1, N_2)- interacting particle system associated to the pair $(\overline{G}_n^l, \overline{M}_n^l)$ defined by (2.98) and (2.96) and the initial distribution $\overline{\eta}_0^l$, is a sequence of non-homogeneous Markov chain, denoted by $\overline{X}_n^{l,[N_1,N_2]}$ taking value in the product space $\overline{\mathsf{E}}_n^{N_1}$,

$$\overline{X}_n^{l,[N_1,N_2]} \triangleq (\overline{X}_n^{l,i})_{i=1}^{N_1} = \underbrace{(\overline{X}_n^{l,1}, \ldots, \overline{X}_n^{l,N_1})}_{N_1 \text{times}} \triangleq (\theta_{n,\mathsf{b}_{n,l}^{i,\mathsf{b}_{0,l}}}^{i}, \eta_{\theta_{0:n}^i,n}^{\mathbb{Z},l,N_2})_{i=1}^{N_1}$$

where $\eta_{\theta_{0:n}^i,n}^{\mathbb{Z},l,N_2} = \frac{1}{N_2^{i,l,n}} \sum\limits_{j=1}^{N_2^{i,l,n}} \delta_{\xi_n^{i,j}}$ such that $N_2^{i,l,n}$ is given by the number of particles $\xi_n^{i,j}$ in $\mathsf{b}_{n,l}^{i,\mathsf{b}_{0,l}}$. This figure being different from zero for at least one l as the number of random process has been supposed to be large.

The initial state of the Markov chain $\overline{X}_0^{l,[N_1,N_2]}$ consists in N_1 independent random variables with common distribution $\overline{\eta}_0^l$. To obtain the initial state, we proceed as follow:

- First sample $\theta_0^i \sim \eta_0^\Theta$ for $i = 1, \ldots, N_1$.

- Using Υ, get for each θ_0^i, the decomposition of D:

$$\Upsilon(\theta_0^i, \mathsf{D}) = \{\mathsf{b}_{0,l}^i, l = 1, \ldots, k\}.$$

- For each $i = 1, \ldots, N_1$, sample $\xi_0^{i,j} \sim \eta_{\theta_0}^{\mathbb{Z}}$ for $j = 1, \ldots, N_2$.

- For each $i = 1, \ldots, N_1$, keep $\xi_0^{i,j} \in \mathsf{b}_{0,l}^i$.

Set $\overline{\eta}_n^{l,N_1}$ the empirical measure at time n, defined by:

$$\overline{\eta}_n^{l,N_1} \triangleq \frac{1}{N_1} \sum_{i=1}^{N_1} \delta_{\overline{X}_n^{l,i}}, \tag{2.103}$$

the elementary probability transition, is given for any $\overline{x}_{n+1}^{l,N_1} \in \overline{\mathsf{E}}_{n+1}^{[N_1]}$ by:

$$\mathbb{P}_{\overline{\eta}_0^l}^{N_1}(\overline{X}_{n+1}^{l,N_1} \in \mathrm{d}\overline{x}_{n+1}^{l,N_1} | \overline{X}_n^{l,N_1}) = \prod_{p=0}^{N_1} \overline{\Phi}_n^l(\overline{\eta}_n^{l,N_1})(\mathrm{d}\overline{x}_{n+1}^{l,i}). \tag{2.104}$$

Finally the simple genetic model associated to the Feynman-Kac distribution flow $\overline{\eta}_n^l$ consists in N_1 particles where the measure valued part is the particle approximation of the quenched quantities defined by $\eta_{\theta_{0:n}^i,n}^{\mathbb{Z},l,N_2}$ for $i \in [\![1, N_1]\!]$.

We give an illustration of the evolution scheme followed by the particle in Figure 2.10. The ensuing algorithm is described in Algorithm 6.
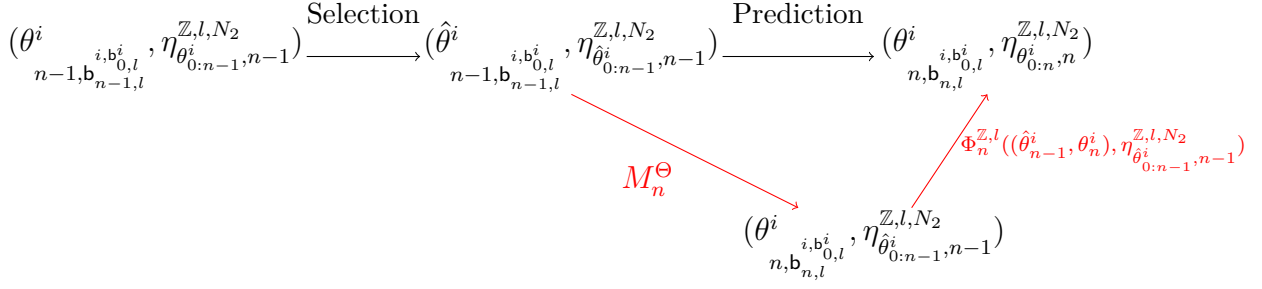
Figure 2.10: Evolution scheme of the Island particle model in a homogeneous random environment

---

Algorithm 6 "Patchwork" Labeled Island particle algorithm - PIP

Require: $\overline{\eta}_0^l$, $((\overline{M}_p^l)_{l=1}^k)_{p=0}^n$, $((\overline{\Psi}_p^l)_{l=1}^k)_{p=0}^n$ and Υ

Ensure: Particle approximation of $\overline{\eta}_n^l$ and $\hat{\overline{\eta}}_n^l$

$\boxed{\text{Begin}}$

1. INITIALIZATION $p = 0$

for $i = 1, \ldots, N_1$ **do**

   Sample $\theta_0^i \sim \eta_0^\Theta$

   $\chi(\mathsf{D}, \theta_0^i) = \{\mathsf{b}_{0,l}^i, l \in [\![1, k]\!]\}$

   for $j = 1, \ldots, N_2$ **do**

      Sample $\xi_0^{i,j} \sim \eta_{\theta_0}^\mathbb{Z}$

   end for

end for

for $p = 0, \ldots, n$ **do**

   2. SELECTION OF ISLANDS

   for $l = 1, \ldots, k$ **do**

      Sample $I_{p,l} = (I_{p,l}^i)_{i=1}^{N_1}$ according to a multinomial distribution with probability

      $\propto \left(\frac{1}{N_2} \sum_{j=1}^{N_2} \tilde{G}_p^{\mathsf{b}_{p,l}^{\mathsf{b}_{0,l}}}(\theta_p^i, \xi_p^{i,j}) \right)_{i=1}^{N_1}$

      for $i = 1, \ldots, N_1$ **do**

         3. SELECTION OF PARTICLES INSIDE EACH ISLAND

         Sample $J_{p,l}^i = (J_{p,l}^{i,j})_{j=1}^{N_2}$ according to a multinomial distribution with probability

         $\propto \left(\tilde{G}_p^{\mathsf{b}_{p,l}^{\mathsf{b}_{0,l}}}(\theta^{I_{p,l}}, \xi_p^{I_{p,l}^i,j}) \right)_{j=1}^{N_2}$

         4. MUTATION OF ISLAND

         Sample independently $\theta_{p+1,\mathsf{b}_{p+1,l}^{\mathsf{b}_{0,l}}}^i$ according to $M_n^\Theta(\theta_{n,l}^{I_{n,l}^i}, .)$

         for $j = 1, \ldots, N_2$ **do**

            5. MUTATION OF PARTICLES

            Sample $\xi_{p+1}^{i,j}$ according to $M_{\theta_{p+1}^i,p+1}^\mathbb{Z}(\xi_{p,l}^{I_{p,l}^i, J_{p,l}^{i,j}}, .)$

         end for

      end for

   end for

end for

$\boxed{\text{End}}$

Acquisition processes for aircraft evolving in a decomposed random atmosphere

As we have seen in the precedent paragraph, the random media Θ_n can be decomposed in homogeneous sub-domains $\mathsf{B}_{n,l}^{\mathsf{B}_{0,l}}$ for $l \in [\![1, k]\!]$. Let consider that the random atmospheric field can be decomposed in such a way, and that the atmospheric evolution kernel verify the conditions (C_1), (C_2), (C_3) and (τ). These assumptions make sense in our case as the time characteristic of the atmosphere phenomenon we are interested in is greater than the aircraft ones. This remark being made, we define k Lagrangian acquisition processes given by $(\mathsf{B}_{n,l}^{\mathsf{B}_{0,l}}, \Theta_{n,\mathsf{B}_{n,l}^{\mathsf{B}_{0,l}}})_{l=1}^{k}$, where $\mathsf{B}_{n,l}^{\mathsf{B}_{0,l}}$ corresponds to the initial atmospheric ball $\mathsf{B}_{0,l}$ transported after n time-steps using the global atmospheric evolution kernels $(M_p^{\Theta})_{p=0}^{n}$. Then consider that we have an air-traffic process, that is several aircraft processes which are supposed to be Markovian, denoted by $\mathbb{X}_n = (X_n^i)_{i=1}^{M} \in \mathsf{E}_n^{X,M}$, where the state space E_n^X encapsulates the characteristics of the aircraft, including their kinetics parameters but also their positions respectively denoted by $\mathbb{Z}_n = (Z_n^i)_{i=1}^{M} \in \mathsf{E}^M$. The transition kernel of each aircraft process is denoted by $M_{\theta_{n,n}}^X$ As one may think here, the number of aircraft in E may vary with time n. Indeed, aircraft can enter and leave the area E. This problem is well known for target tracking problems. In this work, we do not treat this problem for which a modelization is given in the target tracking literature, see Caron et al. (2011a,b,c) for example. Thus we consider that the number of aircraft in E remains the same, M is fixed during the whole horizon of time. However this hypothesis does not represent a strong limitation as for the numerical application we are going to consider, the configuration space E will be the European area. This remark being made, we consider M acquisition processes given by $(Z_n^i, \Theta_{n,Z_n^i})_{i=1}^{M}$.

Then as suggested in the precedent paragraph, we put our interest on the estimation of two measures: χ_n^l and $\hat{\chi}_n^l$, using the observations of the air-traffic process $\mathbb{X}_n$, denoted by $\mathbb{Y}_n = (Y_n^i)_{i=1}^{M}$. That is we want to estimate the following quantities defined for any $f_n \in \mathcal{B}_b(\mathsf{E}_n^{X,M}, \mathsf{E}_n^{\Theta})$ by:

$$\chi_n^l(f_n) \triangleq \mathbb{E}\left[f_n(\mathbb{X}_n, \Theta_{n,\mathsf{B}_{n,l}^{\mathsf{B}_{0,l}}}) | \mathbb{Z}_{0:n-1} \in \mathsf{B}_{0:n-1,l}^{\mathsf{B}_{0,l}}, \mathbb{Y}_{0:n-1} = y_{0:n-1} \right] \tag{2.105}$$

and

$$\hat{\chi}_n^l(f_n) \triangleq \mathbb{E}\left[f_n(\mathbb{X}_n, \Theta_{n,\mathsf{B}_{n,l}^{\mathsf{B}_{0,l}}}) | \mathbb{Z}_{0:n} \in \mathsf{B}_{0:n,l}^{\mathsf{B}_{0,l}}, \mathbb{Y}_{0:n} = y_{0:n} \right]. \tag{2.106}$$

As one may see here, we have a double estimation problem. The first one concerns the estimation of the air-traffic process $\mathbb{X}_n$, the second one concern the estimation of the random field where the aircraft are located. That is, we can estimate the random field in every sub-domains where there are aircraft. In such cases, this filtering problem can be cast into the class of a random process evolving in a random environment. Where the random process is given by $\mathbb{X}_n$, the environment $\Theta_{n,\mathsf{B}_{n,l}^{\mathsf{B}_{0,l}}}$ with l the domain indexes for which aircraft are present. Now we have explained what is the quantity to estimate, we present the Feynman-Kac formulation of this problem. Indeed using the same reasoning as in the computation (2.66), we have that $\hat{\chi}_n^l$ and χ_n^l can be reformulated for any

$f_n \in \mathcal{B}_b(\mathsf{E}_n^{X,M}, \mathsf{E}_n^{\Theta})$ as follow:

$$\chi_n^l(f_n) = \frac{\mathbb{E}\left[f_n(\mathbb{X}_n, \Theta_{n, \mathsf{B}_{n,l}^{\mathsf{B}_{0,l}}}) \prod_{p=0}^{n-1} \mathbb{1}_{\mathsf{B}_{p,l}^{\mathsf{B}_{0,l}}}(\mathbb{Z}_p) | \mathbb{Y}_{0:n-1} = y_{0:n-1}\right]}{\mathbb{E}\left[\prod_{p=0}^{n-1} \mathbb{1}_{\mathsf{B}_{p,l}^{\mathsf{B}_{0,l}}}(\mathbb{Z}_p) | \mathbb{Y}_{0:n-1} = y_{0:n-1}\right]}$$

$$= \frac{\mathbb{E}\left[f_n(\mathbb{X}_n, \Theta_{n, \mathsf{B}_{n,l}^{\mathsf{B}_{0,l}}}) \prod_{p=0}^{n-1} \mathbb{1}_{\mathsf{B}_{p,l}^{\mathsf{B}_{0,l}}}(\mathbb{Z}_p) \prod_{p=0}^{n-1} G_p(\Theta_{p, \mathsf{B}_{p,l}^{\mathsf{B}_{0,l}}}, \mathbb{X}_p)\right]}{\mathbb{E}\left[\prod_{p=0}^{n-1} \mathbb{1}_{\mathsf{B}_{p,l}^{\mathsf{B}_{0,l}}}(\mathbb{Z}_p) \prod_{p=0}^{n-1} G_p(\Theta_{p, \mathsf{B}_{p,l}^{\mathsf{B}_{0,l}}}, \mathbb{X}_p)\right]} \tag{2.107}$$

where $G_p(\Theta_{p, \mathsf{B}_{p,l}^{\mathsf{B}_{0,l}}}, \mathbb{X}_p)$ corresponds to

$$G_p(\Theta_{p, \mathsf{B}_{p,l}^{\mathsf{B}_{0,l}}}, \mathbb{X}_p) \propto \prod_{i=1}^{M} G_p(\Theta_{p, \mathsf{B}_{p,l}^{\mathsf{B}_{0,l}}}, X_p^i)$$

and

$$\hat{\chi}_n^l(f_n) = \frac{\mathbb{E}\left[f_n(\mathbb{X}_n, \Theta_{n, \mathsf{B}_{n,l}^{\mathsf{B}_{0,l}}}) \prod_{p=0}^{n} \mathbb{1}_{\mathsf{B}_{p,l}^{\mathsf{B}_{0,l}}}(\mathbb{Z}_p) | \mathbb{Y}_{0:n} = y_{0:n}\right]}{\mathbb{E}\left[\prod_{p=0}^{n} \mathbb{1}_{\mathsf{B}_{p,l}^{\mathsf{B}_{0,l}}}(\mathbb{Z}_p) | \mathbb{Y}_{0:n} = y_{0:n}\right]}$$

$$= \frac{\mathbb{E}\left[f_n(\mathbb{X}_n, \Theta_{n, \mathsf{B}_{n,l}^{\mathsf{B}_{0,l}}}) \prod_{p=0}^{n} \mathbb{1}_{\mathsf{B}_{p,l}^{\mathsf{B}_{0,l}}}(\mathbb{Z}_p) \prod_{p=0}^{n} G_p(\Theta_{p, \mathsf{B}_{p,l}^{\mathsf{B}_{0,l}}}, \mathbb{X}_p)\right]}{\mathbb{E}\left[\prod_{p=0}^{n} \mathbb{1}_{\mathsf{B}_{p,l}^{\mathsf{B}_{0,l}}}(\mathbb{Z}_p) \prod_{p=0}^{n} G_p(\Theta_{p, \mathsf{B}_{p,l}^{\mathsf{B}_{0,l}}}, \mathbb{X}_p)\right]}. \tag{2.108}$$

Finally, we end up with a random process evolving in an area decomposed in homogeneous domains. Then the reasoning used in the precedent section can be applied here, and Algorithm 6 can be used to solve the precedent estimation problem with a modified potential to take into account the observations.

This chapter was devoted to the development of adapted tools in order to estimate the atmospheric field along the path of aircraft processes. Depending on the atmospheric condition, two particle-based algorithms were developed. The first one, given by Algorithm 3, is able to tackle the estimation problem of an homogeneous atmospheric condition using several aircraft or the estimation of the surrounding atmosphere of one aircraft. The second one, given by Algorithm 6, can deals with random fields which can be decomposed in homogeneous sub-domains. For the first one we have presented some convergence results. The second algorithm still have to be studied.

3

Aircraft Dynamics

So far we have developed a stochastic algorithm which ables one to estimate the random atmospheric field but also the air-traffic process. However we did not detailed yet what was the kernel transition used to make evolute the air-traffic process. This is the scope of this chapter. We present a model that simulates the dynamics of commercial aircraft from the point of view of an air-traffic controller during cruise phase.

Indeed flight can be separated into three phases, the first one is the climb phase. This phase starts after the aircraft's take-off and ends as soon as the aircraft meets the cruise altitude. Then the aircraft enters in what is called the cruise phase. Cruise is the level portion of aircraft travel where flight is most fuel efficient. It occurs between climb and descent phases and is usually the majority of a journey. Technically, cruising consists of heading (direction of flight) changes only at a constant airspeed and altitude. It ends as the aircraft approaches the destination where the descent phase of flight begins in preparation for landing. For most commercial passenger aircraft, the cruise phase of flight consumes the majority of fuel. As this lightens the aircraft considerably, higher altitudes are more efficient for additional fuel economy. However, for operational and air traffic control reasons it is necessary to stay at the cleared flight level. On long haul flights, the pilot may climb from one flight level to a higher one as clearance is requested and given from air traffic control. This manoeuvre is called a step climb. Commercial or passenger aircraft are usually designed for optimum performance at their cruise speed or what is called green dot speed. For a given aircraft type, its optimum cruising altitude depends on many parameters including payload weight, center of gravity of an aircraft, air temperature, humidity, and speed. This altitude is usually where the higher ground speeds, the increase in aerodynamic drag power, and the decrease in engine thrust and efficiency at higher altitudes are balanced. Typical cruising air speed for long-distance

commercial passenger flights is 475-500 knots (880-926 $km.h^{-1}$). The third phase of a flight corresponds to the descent phase. It corresponds to any portion of the flight where the aircraft decreases its altitude. It is the opposite of a climb. Intentional descents might be undertaken to land, avoid other air traffic or poor flight conditions (turbulence, icing conditions, or bad weather), clouds (particularly under visual flight rules), to see something lower, to enter warmer air (see adiabatic lapse rate), or to take advantage of wind direction of a different altitude.

In this work we put our interest on the cruising phase as it is the phase where the most fuel quantity is consumed and as it constitutes the longest part of a journey. Moreover, air-traffic controller do not step in as much as in other phases. Then the model we develop do not need to take air-traffic controller's actions into account.

Aircraft dynamics have been well studied over the last four decades, some works can be used as references in the domain : Boiffier (1998); Hull (2007); Peters and Konyak (2003). The model developed in Boiffier (1998) is similar to our model but does not provide control laws to close the dynamic system. In Peters and Konyak (2003), the model is a full 6 degree of freedom model. Then it is a more complete model not fully adapted to our simpler problem. In Hull (2007), the model corresponds to our model except that the kinematics equations are not derived on a ellipsoidal Earth. Moreover, the control laws developed to close the dynamical system are made such that the aircraft trajectories are optimal, in some sense. In Glover and Lygeros (2004), a stochastic hybrid system has been developed, but as we want to use ensemble weather forecast, the aircraft kinematics has to be expressed in the ellipsoidal Earth. Further, we present the point mass model that describes the motion of commercial aircraft. It is able to deal with several aircraft at the same time, each one with a different flight plan. The dynamic model gives rise to a continuous time model for which we present an integration scheme. The flight plan and the logic variable embedded in the control part give rise to discrete variables. The weather uncertainties are treated as a stochastic disturbance which has its own dynamics. Thus, the model we developed is framed in the context of stochastic hybrid system, likewise in Lymperopoulos (2010). All the model components as well as their relation are resumed in Figure 3.1.

The model we develop in this chapter is used in Chapter 4 as the evolution kernel of the air-traffic process inside the stochastic algorithms developed in **??**.

3.1 Deterministic model for aircraft dynamics

This section is devoted to the development of a deterministic model able to predict the future aircraft's states ($\mathbf{x}$) during cruise phase. The basic idea is to create an hybrid system to generate trajectory. The model allows one to capture many flights taking place at the same time. In the simulation, each flight is represented by an instance of the class *Aircraft*. With each *Aircraft*, we associate the following model components:

- The flight plan.
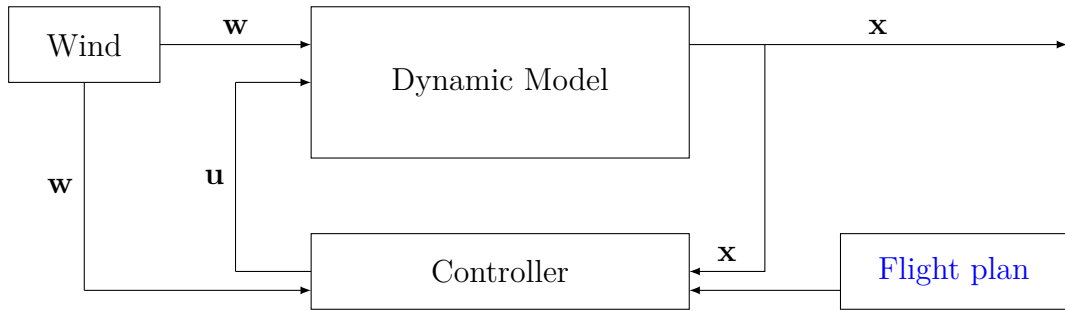
Figure 3.1: Block diagram of Multi Aircraft model components

- The aircraft dynamics.

- The controller.

The evolution of the aircraft state, $\mathbf{x}$, is influenced by the surrounding atmosphere $\mathbf{w}$. Indeed the atmosphere impacts the aircraft dynamics through the controls $\mathbf{u}$ computed to respect the flight plan but also inside the dynamic model itself. The relations between the flight plan, the aircraft dynamics and the controller are summarized in Figure 3.1. In the rest of this section, we provide some details of the model developed for each component listed in Figure 3.1.

3.1.1 Flight Plan

As we have already mention, the flight plan consists in a sequence of way-points, $\{O_i\}_{i=1}^M$ where for $i = 1, \ldots, M$ we have $O_i \in \mathbb{R}^3$. To this sequence, a cruise speed is attached. Therefore, aircraft are assumed to maintain a Calibrated Air Speed (CAS) or a Mach number during the whole cruise phase. Typically this cruise speed corresponds to the green dot speed we have mentioned. That is the optimum speed for the aircraft type which is at stake. The sequence of way points defines a sequence of straight lines joining each way point to the next. We refer to this sequence of straight lines as the reference path. For each way-point, O_i, we also define the reference heading ψ_g^i as the angle that the lines segment joining O_i to O_{i+1} makes with the $\hat{x}_i$-axis of the frame in which the way point coordinates are given, see Figure 3.2. Conclusion, the flight plan considered is a 3D way-point model.

3.1.2 Dynamic model

In this section we derive the aircraft equations of motion that are used in the simulation tool we develop. As a first step, we define reference frames in order to describe the movement of the aircraft with respect to the Earth. Then, several assumptions are made to end up with a point mass model and its associated state equation representation. This section is not a complete review on aircraft dynamics, we recall some basics results and try to make clear modelization choice we made. For a full treatise on the subject, several
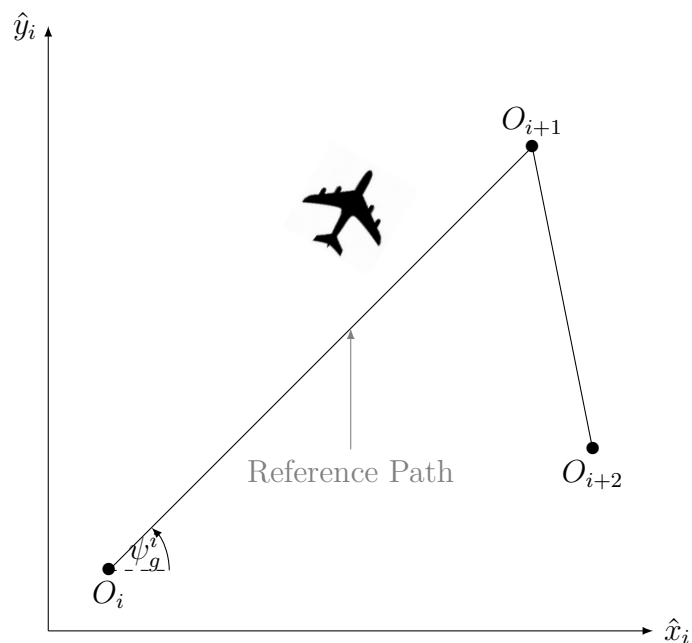
Figure 3.2: Top view of a typical flight plan showing way-points

books are available, see Boiffier (1998), Peters and Konyak (2003) or Hull (2007) for example.

Frames

All frames used to derive mechanical equations for air-plane are three dimensional, orthogonal and right-handed. Denoting by $F_i(O_i, \hat{x}_i, \hat{y}_i, \hat{z}_i)$, the frame F_i, unitary vectors of each axis are marked as follow: $\hat{x}_i, \hat{y}_i, \hat{z}_i$. The origin of the frame F_i is O_i. To derive the aircraft equations of motion, several reference frames are needed. First an inertial reference frame (denoted with a i subscript) in order to apply mechanical equations, the body fixed reference frame (denoted with a b subscript) more convenient to express external efforts and the Air-path reference frame or the aerodynamic reference frame (denoted by a a subscript) more convenient to express aerodynamic forces. Once these frames are defined, we give the transformations matrix used to go from one frame to another defined using Euler angles.

Reference frames definitions

- **Inertial reference frame**: The inertial reference frame is a geocentric inertial axis system, for which we give an illustration on Figure 3.3. The origin of the frame, O_i, is located at the center of the Earth. The axis $\hat{z}_i$ is carried by the axis of the Earth's rotation, $\hat{x}_i$ and $\hat{y}_i$ keeping a fixed direction in space.

- **The Normal Earth reference frame**: The origin is an arbitrary point on the Earth's surface O_e. The $\hat{x}_e$ axis points towards the true North direction (North magnetic pole) and $\hat{y}_e$ points towards the true East direction. $\hat{z}_e$ points down and
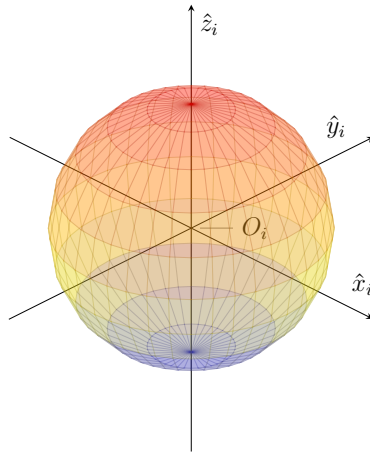
Figure 3.3: The Inertial reference frame
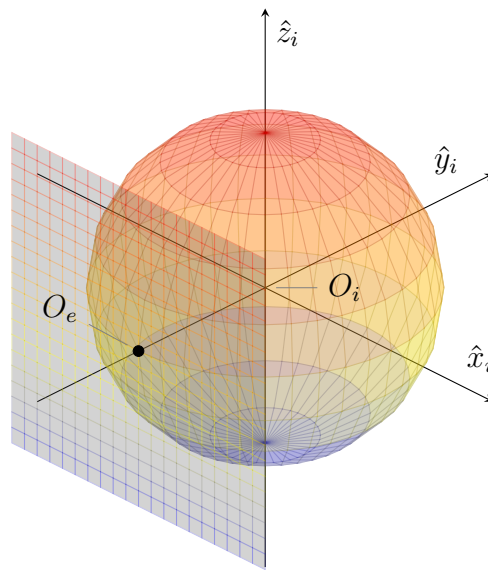
Figure 3.4: The Normal Earth fixed reference frame at O_e and inertial reference frame

is normal to the Earth's surface see Figure 3.4. As this reference frame is supposed to be tangent to the Earth surface The Earth's shape is rather important. In this document, the Earth is always assumed to be ellipsoidal, that is $O_iO_e = R_e$, with R_e the Earth radius which is not constant. More details on the model choice for the Earth is given in Section 3.1.3.

- **Body-fixed reference frame**: As the aircraft body is supposed to be rigid, it can be modelled by its gravitational center (Hypothesis 1). Then, the aircraft body frame's origin is fixed at the aircraft's center of gravity. The $\hat{x}_b$ axis lies in the symmetry plane of the aircraft and points forward the nose of the aircraft. The $\hat{z}_b$ axis lies also in the symmetry plane of the aircraft, is perpendicular to $\hat{x}_b$ and points downwards. The $\hat{y}_b$ axis is obtained using the right-hand rule. Figure 3.5 shows the body fixed reference frame.

- **The Air reference frame**: The Air reference frame origin is the same as the
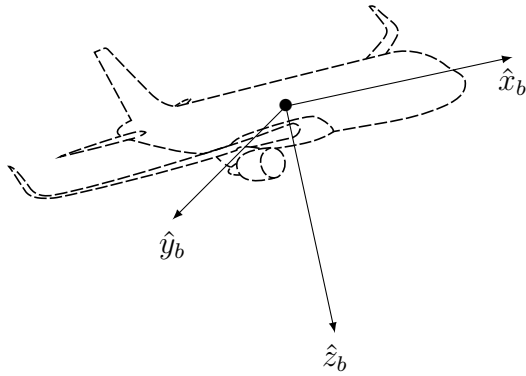
Figure 3.5: Body fixed reference frame aligned with an aircraft
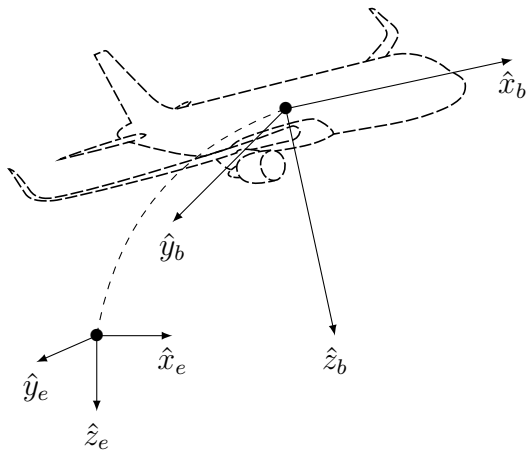
Figure 3.6: Relationship between body and Normal-Earth fixed reference frames

body-fixed reference frame, the axis $\hat{x}_a$ is carried and oriented by the aerodynamic velocity vector $\mathbf{v}_a$. It characterizes the relationship of the aerodynamic angle of attack, denoted by α_a, and the side-slip angle β_a, to the body frame velocity. These aerodynamic angles are defined by means of coordinate rotations.

Angles between frames   As we have now several frames defined, it is useful to know their relative positions by means of angles. The relationship between the body-fixed reference frame and the Normal Earth fixed reference frame is illustrated in Figure 3.6. The orientation of the body-fixed frame with respect to the Normal Earth fixed reference frame is usually described by an Euler angle sequence of rotations. The Figure 3.7 shows the Euler sequence of rotations which is used to quantify the aircraft's orientation. The first rotation is through the azimuth angle or the heading, denoted by ψ, about the $\hat{z}_e$
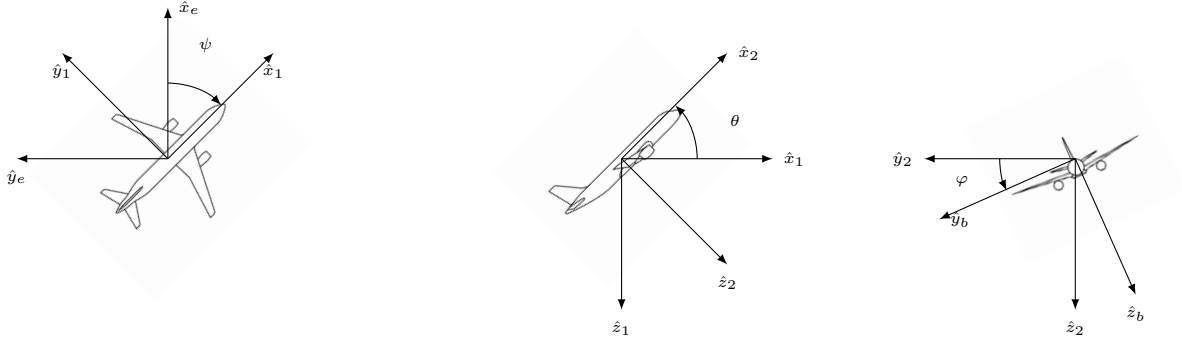
Figure 3.7: The angles Euler sequence of rotations used to quantify the aircraft's orientation

axis to an intermediate reference frame, say 1. The second rotation is through the angle θ, the inclination angle or pitch, about the $\hat{y}_1$ intermediate axis to another intermediate frame, say 2. The final rotation is through the angle φ, the bank angle or roll angle, about the $\hat{x}_2$ axis to the body-fixed frame.

Transformation matrices The conversion between the Normal Earth fixed frame and the body frame of the aircraft is accomplished using transformation matrix denoted by $\mathbb{T}_{e\to b}$. To compute this matrix, we used the same decomposition as in the Euler angles:

$$
\mathbb{T}_{e\to b} = \begin{pmatrix} 1 & 0 & 0 \\ 0 & \cos\varphi & \sin\varphi \\ 0 & -\sin\varphi & \cos\varphi \end{pmatrix} \begin{pmatrix} \cos\theta & 0 & -\sin\theta \\ 0 & 1 & 0 \\ \sin\theta & 0 & \cos\theta \end{pmatrix} \begin{pmatrix} \cos\psi & \sin\psi & 0 \\ -\sin\psi & \cos\psi & 0 \\ 0 & 0 & 1 \end{pmatrix}
$$

$$
= \begin{pmatrix} \cos\theta\cos\psi & \cos\theta\sin\psi & -\sin\theta \\ \sin\varphi\sin\theta\cos\psi - \cos\varphi\sin\psi & \sin\varphi\sin\theta\sin\psi + \cos\varphi\cos\psi & \sin\varphi\cos\theta \\ \cos\varphi\sin\theta\cos\psi + \sin\varphi\sin\psi & \cos\varphi\sin\theta\sin\psi - \sin\varphi\cos\psi & \cos\varphi\cos\theta \end{pmatrix}.
$$

We have also the matrix $\mathbb{T}_{b\to e}$ which is the matrix allowing one to go from the body frame to the Normal Earth fixed frame. Say it in other terms, it is the inverse transformation, then $\mathbb{T}_{b\to e} = \mathbb{T}_{e\to b}^{-1} = \mathbb{T}_{e\to b}^{T}$.

To get from the body fixed reference frame to the aerodynamic one, we define the transformation matrix $\mathbb{T}_{b\to a}$.

$$
\mathbb{T}_{b\to a} = \begin{pmatrix} \cos\alpha_a & 0 & \sin\alpha_a \\ 0 & 1 & 0 \\ -\sin\alpha_a & 0 & \cos\alpha_a \end{pmatrix} \begin{pmatrix} \cos\beta_a & \sin\beta_a & 0 \\ -\sin\beta_a & \cos\beta_a & 0 \\ 0 & 0 & 1 \end{pmatrix}
$$

$$
= \begin{pmatrix} \cos\beta_a\cos\alpha_a & \sin\beta_a & \cos\beta_a\sin\alpha_a \\ -\sin\beta_a\cos\alpha_a & \cos\beta_a & -\sin\beta_a\sin\alpha_a \\ -\sin\alpha_a\cos\beta_a & -\sin\alpha_a\sin\beta_a & \cos\alpha_a \end{pmatrix}.
$$

Moreover $\mathbb{T}_{a\to b} = \mathbb{T}_{b\to a}^{-1} = \mathbb{T}_{b\to a}^{T}$.

To go from the Normal Earth fixed reference frame to the Air reference frame, three Euler angles are needed: the aerodynamic bank angle, the aerodynamic climb angle, and the aerodynamic azimuth angle, denoted respectively by μ_a, γ_a and χ_a. When performing the rotations described above to obtain the air reference frame from the Normal Earth fixed frame, $(\mu_a, \gamma_a, \chi_a)$ are analogous to (φ, θ, ψ), respectively. The azimuth angle χ_a is the angle between the north and the horizontal component of the velocity vector $\mathbf{v}_a$, which describes which direction the aircraft is moving relative to cardinal directions. The climb angle γ_a is the angle between horizontal and the velocity vector, which describes whether the aircraft is climbing or descending. The bank angle μ_a represents a rotation of the lift force around the velocity vector, which may indicate whether the air-plane is turning. Then it is also possible to define the transformation matrix $\mathbb{T}_{e \to a}$ equals to:

$$
\mathbb{T}_{e \to a} = \begin{pmatrix} \cos\chi_a & -\sin\chi_a & 0 \\ \sin\chi_a & \cos\chi_a & 0 \\ 0 & 0 & 1 \end{pmatrix} \begin{pmatrix} \cos\gamma_a & 0 & \sin\gamma_a \\ 0 & 1 & 0 \\ -\sin\gamma_a & 0 & \cos\gamma_a \end{pmatrix} \begin{pmatrix} 1 & 0 & 0 \\ 0 & \cos\mu_a & -\sin\mu_a \\ 0 & \sin\mu_a & \cos\mu_a \end{pmatrix}
$$

$$
= \begin{pmatrix} \cos\chi_a \cos\gamma_a & -\sin\chi_a \cos\mu_a + \cos\chi_a \sin\gamma_a \sin\mu_a & \sin\chi_a \sin\mu_a \cos\chi_a \sin\gamma_a \cos\mu_a \\ \sin\chi_a \cos\gamma_a & \cos\chi_a \cos\mu_a + \sin\chi_a \sin\gamma_a \sin\mu_a & -\cos\chi_a \sin\mu_a + \sin\chi_a \sin\gamma_a \cos\mu_a \\ -\sin\gamma_a & \cos\gamma_a \sin\mu_a & \cos\gamma_a \cos\mu_a \end{pmatrix}.
$$

$$(3.1)$$

Assumptions

Now we have defined all the reference frames which are convenient to express the dynamic equations, we will state some basic and realistic assumptions which are used to simplify our model. Indeed, in this document, we want to describe the flight dynamics with equations. This is however a really complex system. Then, to simplify the model we assume that:

- the pilot maintains "coordinated flight", that is the side-slip angle is always zero, $\beta_a = 0$ (Hypothesis 2),

- the flight is always assumed to be symmetrical, we are not in an approach phase: $\alpha_a \ll 1$ (Hypothesis 3).

By direct inspection, the implication of a coordinated flight combined with a symmetrical flight is that aerodynamic angles are equivalent to body angles. That is $\theta = \gamma_a$, $\psi = \chi_a$ and $\varphi = \mu_a$.

Dynamic equations taking wind into account

Fundamental relationship of kinematics When taking derivatives where different reference frames are involved, it is important to clearly state the reference frame used to express the derivative and the reference frame that is used to express the coordinates of a given vector.

Let's examine some point P. This point is described by a vector $\mathbf{r}_E$ in the reference frame F_E and by $\mathbf{r}_b$ in the reference frame F_b. Also the origin of F_b (with respect to F_E)

is described by the vector $\mathbf{r}_{b \to E}$. So, we have $\mathbf{r}_E = \mathbf{r}_{b \to E} + \mathbf{r}_b$.

Now let us examine the time derivative of $\mathbf{r}_E$ in F_E, denoted by $\left. \frac{d\mathbf{r}_E}{dt} \right|_E$:

$$
\begin{aligned}
\left. \frac{d\mathbf{r}_E}{dt} \right|_E &= \left. \frac{d\mathbf{r}_{b \to E}}{dt} \right|_E + \left. \frac{d\mathbf{r}_b}{dt} \right|_E \\
&= \left. \frac{d\mathbf{r}_{b \to E}}{dt} \right|_E + \left. \frac{d\mathbf{r}_b}{dt} \right|_b + \Omega_{bE} \wedge \mathbf{r}_b
\end{aligned}
$$

where Ω_{bE} denotes the rotation vector of F_b with respect to F_E.

This is quite an important relation, held for every vector. It will be useful to derive the flight dynamics equations.

Newton's second law   Before deriving the equations of motion of an aircraft, we make the hypothesis that the Earth is flat and fixed, thus the Normal Earth reference frame is Galilean (Hypothesis 4). These assumptions are valid for flight with Mach number below to 2 (see Boiffier (1998) for further details), which is an enough large speed value to include all commercial aircraft. Therefore, the Newton's second law can be used in the Normal Earth fixed reference frame. By Newton's second law, one has that:

$$
\begin{aligned}
\sum \mathbf{F}_e &= \left. \frac{d}{dt}(m\mathbf{v}_e^e) \right|_e \\
&= \left. m \frac{d\mathbf{v}_e^e}{dt} \right|_e
\end{aligned}
\tag{3.2}
$$

where $\mathbf{v}_e^e$ is the velocity of the aircraft center of gravity expressed in the Normal Earth reference frame. The sum of all external forces, $\sum \mathbf{F}_e$, is also expressed in the Normal Earth reference frame. The mass of the aircraft, m, is considered as a constant parameter as its variation influence is negligible for small period of time (Hypothesis 5). However, as time goes the mass of the aircraft evolves with the fuel consumption. Therefore an additional equation is added to model the mass evolution with respect to time, see Section 3.1.4.

As we consider only cruise phase, one can consider that rotation rates are negligible and the effect of control surface deflections on aerodynamic forces can be neglected (Hypothesis 6). Therefore the Newton's second law is reduced to translational movement (3.2). If we express now this equation in the Air reference frame coordinate, we obtain:

$$
\begin{aligned}
\sum \mathbf{F}_a &= \left. \frac{dm\mathbf{v}_a^e}{dt} \right|_i \\
&= \left. m \frac{d\mathbf{v}_a^e}{dt} \right|_i \\
&= \left. m \frac{d(\mathbf{v}_a^a + \mathbf{w}_a^e)}{dt} \right|_i \\
&= m \left[\left. \frac{d\mathbf{v}_a^a}{dt} \right|_a + \Omega_{ea} \wedge \mathbf{v}_a^a + \left. \frac{d\mathbf{w}_a^e}{dt} \right|_i \right],
\end{aligned}
\tag{3.3}
$$

where Ω_{ea} is the rotation vector of the Air reference frame with respect to the Normal Earth reference frame. The time derivative, $\frac{d\mathbf{w}_a^e}{dt}\big|_i$ takes into account the acceleration of the air mass, $\mathbf{w}_a^e$ being the wind vector seen from the Normal Earth reference frame projected into the Air reference frame.

As we already say, the aircraft is reduced to a point, then all the external efforts are applied at the center of gravity of the aircraft.

External efforts   Three types of forces can act on an aircraft: the aerodynamics forces denoted by $\mathbf{F}^a$, the propulsive forces denoted by $\mathbf{F}^p$ and the gravitational force $\mathbf{P}$.

Concerning the aerodynamic forces, we make the assumption that the side-slip β_a can be neglected, that means that the only forces which can be considered are the Lift (L) and the Drag (D). In the Air reference frame, these forces are easily expressed by the following vector:

$$\mathbf{F}_a^a = \begin{pmatrix} -D \\ 0 \\ -L \end{pmatrix}.$$

Regarding the propulsive forces, the thrust is aligned with the body-fixed reference frame. But as far as we make the assumption that the aerodynamic angle of attack (α_a) can be neglected, we have that in the Air reference frame, the propulsive force $\mathbf{F}_a^p$ is given by:

$$\mathbf{F}_a^p = \mathbb{T}_{b \to a} \begin{pmatrix} T \\ 0 \\ 0 \end{pmatrix}$$

$$= I_3 \begin{pmatrix} T \\ 0 \\ 0 \end{pmatrix}, \quad \text{since } \alpha_a, \beta_a \approx 0. \tag{3.4}$$

Concerning the gravitational force $\mathbf{P}$, we have in the Normal Earth reference frame that:

$$\mathbf{P}_e = \begin{pmatrix} 0 \\ 0 \\ mg \end{pmatrix}.$$

Then using the transformation matrix $\mathbb{T}_{e \to a}$ and recording that $\mathbb{T}_{b \to a} = I_3$ since $\alpha_a = \beta_a = 0, \mathbb{T}_{e \to a} = \mathbb{T}_{e \to b} I_3$, we have that:

$$\mathbf{P}_a = \mathbb{T}_{e \to a} \begin{pmatrix} 0 \\ 0 \\ mg \end{pmatrix}$$

$$= \begin{pmatrix} -mg\sin\theta \\ mg\sin\varphi\cos\theta \\ mg\cos\varphi\cos\theta \end{pmatrix}. \tag{3.5}$$

Finally we have expressed all the external efforts in the aerodynamic reference frame which is more convenient to express them. Now we focus on the right hand side of (3.3).

Dynamic equations Before we make the force balance in the Air reference frame, we have to express the rotation vector Ω_{ea} of the Air reference frame with respect to the Earth reference frame. We know that the rotation vector in the Earth reference frame is given by: $(\dot{\varphi},\ \dot{\theta},\ \dot{\psi})$. Then using the definition of each of these angles, we have that:

$$
\begin{aligned}
\Omega_{ea} &= \begin{pmatrix} \dot{\varphi} \\ 0 \\ 0 \end{pmatrix} + \begin{pmatrix} 1 & 0 & 0 \\ 0 & \cos\varphi & -\sin\varphi \\ 0 & \sin\varphi & \cos\varphi \end{pmatrix} \begin{pmatrix} 0 \\ \dot{\theta} \\ 0 \end{pmatrix} \\
&\quad + \begin{pmatrix} 1 & 0 & 0 \\ 0 & \cos\varphi & -\sin\varphi \\ 0 & \sin\varphi & \cos\varphi \end{pmatrix} \begin{pmatrix} \cos\theta & 0 & \sin\theta \\ 0 & 1 & 0 \\ -\sin\theta & 0 & \cos\theta \end{pmatrix} \begin{pmatrix} 0 \\ 0 \\ \dot{\psi} \end{pmatrix} \\
&= \begin{pmatrix} \dot{\varphi} - \dot{\psi}\sin\theta \\ \dot{\theta}\cos\varphi + \dot{\psi}\cos\theta\sin\varphi \\ -\dot{\theta}\sin\varphi + \dot{\psi}\cos\theta\cos\varphi \end{pmatrix}
\end{aligned}
\tag{3.6}
$$

Now, we have to express the wind in the Air reference frame and also its derivative seen from the Earth reference frame. In the Earth reference frame, the wind vector is easily expressed by its North and East components (the vertical wind is neglected, Hypothesis 7):

$$
\mathbf{w}_e^e = \begin{pmatrix} w_n \\ w_e \\ 0 \end{pmatrix}.
$$

Then we express it in the Air reference frame, using the transformation matrix $\mathbb{T}_{e\to a}$, we obtain:

$$
\begin{aligned}
\mathbf{w}_a^e &= \mathbb{T}_{e\to a}\mathbf{w}_e^e \\
&= \mathbb{T}_{e\to b}\mathbb{T}_{b\to a}\mathbf{w}_e^e \\
&= \mathbb{T}_{e\to b}I_3\mathbf{w}_e^e \\
&= \begin{pmatrix} w_n\cos\theta\cos\psi + w_e\cos\theta\sin\psi \\ w_n(\sin\varphi\sin\theta\cos\psi - \cos\varphi\sin\psi) + w_e(\sin\varphi\sin\theta\sin\psi + \cos\varphi\cos\psi) \\ w_n(\cos\varphi\sin\theta\cos\psi + \sin\varphi\sin\psi) + w_e(\cos\varphi\sin\theta\sin\psi - \sin\varphi\cos\psi) \end{pmatrix}.
\end{aligned}
\tag{3.7}
$$

Concerning the wind derivative, it is given in the Earth reference frame by:

$$
\left.\frac{d\mathbf{w}_e^e}{dt}\right|_e = \begin{pmatrix} \dot{w}_n \\ \dot{w}_e \\ 0 \end{pmatrix}.
$$

Using the transformation matrix $\mathbb{T}_{e\to a}$, we express it in the Air reference frame:

$$
\left.\frac{d\mathbf{w}_a^e}{dt}\right|_i = \mathbb{T}_{e\to a} \left.\frac{d\mathbf{w}_e^e}{dt}\right|_e
$$

$$
= \begin{pmatrix} \dot{w}_n \cos\theta\cos\psi + \dot{w}_e\cos\theta\sin\psi \\ \dot{w}_n(\sin\varphi\sin\theta\cos\psi - \cos\varphi\sin\psi) + \dot{w}_e(\sin\varphi\sin\theta\sin\psi + \cos\varphi\cos\psi) \\ \dot{w}_n(\cos\varphi\sin\theta\cos\psi + \sin\varphi\sin\psi) + \dot{w}_e(\cos\varphi\sin\theta\sin\psi - \sin\varphi\cos\psi) \end{pmatrix}
$$

$$(3.8)$$

where $\dot{w}_n$ and $\dot{w}_e$ are the total derivatives of wind with respect to time. Assuming wind is a function of time and location, we have:

$$
\begin{cases} \dot{w}_n &= \frac{\partial w_n}{\partial x}\dot{x} + \frac{\partial w_n}{\partial y}\dot{y} + \frac{\partial w_n}{\partial t} \\ \dot{w}_e &= \frac{\partial w_e}{\partial x}\dot{x} + \frac{\partial w_e}{\partial y}\dot{y} + \frac{\partial w_e}{\partial t} \end{cases}
$$

We assume here that the time derivative is negligible. Then the previous system of equation is transformed to:

$$
\begin{cases} \dot{w}_n &= \frac{\partial w_n}{\partial x}\dot{x} + \frac{\partial w_n}{\partial y}\dot{y} \\ \dot{w}_e &= \frac{\partial w_e}{\partial x}\dot{x} + \frac{\partial w_e}{\partial y}\dot{y} \end{cases}
$$

We still need the expression of the velocity vector into the Air reference frame. We can express it thanks to the quantity v_a denoting the true airspeed of the aircraft, *i.e* the relative air to aircraft velocity:

$$
\mathbf{v_a^a} = \begin{pmatrix} v_a \\ 0 \\ 0 \end{pmatrix}. \tag{3.9}
$$

Substituting (3.4), (3.5), (3.6), (3.7), (3.8), and (3.9) into Eq. (3.3), gives us:

$$
\begin{pmatrix} T - D - mg\sin\theta \\ mg\sin\varphi\cos\theta \\ -L + mg\cos\varphi\cos\theta \end{pmatrix} = m\left[\begin{pmatrix} \dot{v}_a \\ 0 \\ 0 \end{pmatrix} + \begin{pmatrix} 0 \\ -v_a(\dot\psi\cos\theta\cos\varphi - \dot\theta\sin\varphi) \\ v_a(\dot\theta\cos\varphi + \dot\psi\cos\theta\sin\varphi) \end{pmatrix} \right.
$$

$$
\left. \begin{pmatrix} \dot{w}_n\cos\theta\cos\psi + \dot{w}_e\cos\theta\sin\psi \\ \dot{w}_n(\sin\varphi\sin\theta\cos\psi - \cos\varphi\sin\psi) + \dot{w}_e(\sin\varphi\sin\theta\sin\psi + \cos\varphi\cos\psi) \\ \dot{w}_n(\cos\varphi\sin\theta\cos\psi + \sin\varphi\sin\psi) + \dot{w}_e(\cos\varphi\sin\theta\sin\psi - \sin\varphi\cos\psi) \end{pmatrix} \right].
$$

$$(3.10)$$

Rearranging all the terms we obtain (see Section A.2 for computation details):

$$
\begin{cases}
\dot{v}_a &= \dfrac{T-D}{m} - g\sin\theta - \cos\theta(\dot{w}_n\cos\psi + \dot{w}_e\sin\psi) \\[2ex]
\dot{\theta} &= \dfrac{1}{v_a}\left[\dfrac{L}{m}\cos\varphi - g\cos\theta + \sin\theta\left[\dot{w}_n\cos\psi + \dot{w}_e\sin\psi\right]\right] \\[2ex]
\dot{\psi} &= \dfrac{1}{v_a\cos\theta}\left[\dfrac{L}{m}\sin\varphi + (\dot{w}_n\sin\psi - \dot{w}_e\cos\psi)\right]
\end{cases}
\qquad (3.11)
$$

Finally, the aircraft dynamic equations are given by the system (3.11). They describe the behaviour of the aircraft in terms of its motion as a function of time. It remains to study the evolution of the aircraft position in the configuration space.

3.1.3 Aircraft kinematics

As wind was taken into account into the dynamics of the aircraft, the velocity of the aircraft with respect to the inertial frame is given by:

$$
\begin{pmatrix}
\dot{x}_i^i \\
\dot{y}_i^i \\
\dot{z}_i^i
\end{pmatrix} =
\begin{pmatrix}
v_a\cos\theta\cos\psi + w_n \\
v_a\cos\theta\sin\psi + w_e \\
v_a\sin\theta
\end{pmatrix}
\qquad (3.12)
$$

Now we propagate the aircraft's trajectories on the surface of the Earth. To do so, we need to relate change in velocity to latitude/longitude change. That is developing kinematic equations in latitude longitude coordinates. In order to get those equations, first we define an additional frame which is commonly used to define latitude longitude coordinates. Then we model the Earth as an Ellipsoid and finally we end up with kinematics equations in latitude longitude coordinates. More details can be found in Peters and Konyak (2003).

Reference frames definitions

To derive the dynamic equations of the aircraft, we made the assumption that the Earth was flat. That means that the Earth's eccentricity was ignored in the force balance. To propagate the trajectory on the Earth, we cannot assume a flat Earth any more. To take into account the Earth eccentricity, we define two additional reference frames. They are used to describe the latitude/longitude kinematics:

- the Earth centered Earth fixed (ECEF) (inertial) reference frame denoted by the subscript "i",

- the North-East-Down (NED) reference frame defined as a surface tangent to the Earth which moves along with the aircraft, denoted by the subscript "e".

Figure 3.8: Latitude and longitude rotations given by latitude and longitude angles (respectively denoted by μ and l).

ECEF reference frame The ECEF reference frame's origin is fixed at the center of the Earth. The $\hat{x}_e$-axis points out the North pole. The plane $(\hat{y}_e O \hat{z}_e)$ lies in the equator plane with the reverse $\hat{z}_e$ axis pointing at zero degrees longitude as it is illustrated in Figure 3.3

The NED reference frame The NED reference frame is centred in an object propagating along the Earth's surface and tangent to it at this point, as it is illustrated in Figure 3.4. The $\hat{z}_e$ axis points downwards and is perpendicular to the surface of the Earth. The longitude and latitude angle, respectively denoted by l and μ are used to describe the rotation between these two frames. The NED frame is oriented in a way such that at zero longitude and latitude the ECEF and NED frames coincide.

Rotation matrix with latitude and longitude To go from ECEF frame to NED frame, the first rotation consist in a positive rotation of angle μ (latitude) about the $\hat{x}_i$-axis to an intermediate reference frame denoted by *int* subscript. The second rotation consist in a positive rotation of angle l (longitude) about the $\hat{y}_{int}$ - axis to the reference frame NED.

We illustrate these two rotations through Figure 3.8. The conversion between the ECEF frame and the NED frame is accomplished using the transformation matrix denoted by $\mathbb{T}_{i \to e}$, defined by:

$$
\begin{aligned}
\mathbb{T}_{i \to e} &= \begin{pmatrix} \cos l & 0 & -\sin l \\ 0 & 1 & 0 \\ \sin l & 0 & \cos l \end{pmatrix} \begin{pmatrix} 1 & 0 & 0 \\ 0 & \cos \mu & \sin \mu \\ 0 & -\sin \mu & \cos \mu \end{pmatrix} \\
&= \begin{pmatrix} \cos l & \sin l \sin \mu & \sin l \cos \mu \\ 0 & \cos \mu & \sin \mu \\ \sin l & -\cos l \sin \mu & \cos l \cos \mu \end{pmatrix}
\end{aligned}
\tag{3.13}
$$

The inverse matrix denoted by $\mathbb{T}_{e \to i}$ allowing us to transform from NED coordinates to ECEF coordinates is given by:

$$
\mathbb{T}_{e \to i} = \mathbb{T}_{i \to e}^{-1} = \mathbb{T}_{i \to e}^{T}.
$$
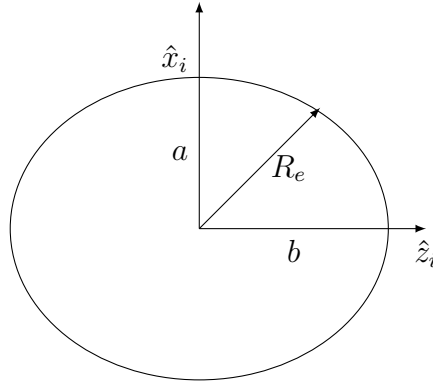
Figure 3.9: Ellipsoidal Earth model

Now we define the reference frames convenient to describe the aircraft movement on the Earth surface, it is left to describe how the Earth is modelled in our simulation setting. Indeed we say that the NED reference frame is tangent to the Earth surface, but the Earth form was not detailed yet. Then, we describe the Earth model used in the next paragraph.

Elliptic Earth's model

The real Earth is not a perfect sphere as the radius changes with the latitude. Therefore we will use an ellipsoidal Earth model where the semi-axis lengths are given by the Earth model WGS-84, Mularie (2000). This model is illustrated on Figure 3.9, with:

- the equatorial radius b equals to $2.092565 \times 10^7 ft$,

- the semi minor axis length a given by $a = b(1 - f)$ where f stands for the Earth flattening parameter sets to $f = \frac{1}{298.257}$.

As the Earth is modelled as an ellipsoid, the position vector which points out at a point on the Earth surface does not have a constant norm. That is $r_e = \|R_e\|$ is not constant. Moreover, it is not normal to the Earth surface as we can see on Figure 3.9.

As in this document we defined the NED frame to be normal to the Earth surface, this vector cannot be used to derived the latitude. To tackle this issue, we introduce the geodetic and geocentric latitude.

Geocentric and Geodetic latitude   The geocentric latitude, λ, is defined as the angle made by the position vector R_e and the $\hat{y}_i$-axis. The geodetic latitude μ is the angle made by the $\hat{y}_i$ axis and the line which intersects the equatorial plane and which is normal to the Earth surface. We illustrate the difference between these two angles on Figure 3.10. As one may observe on Figure 3.10, the geodetic latitude is normal to the Earth surface, but it is not related to the Earth center. Nevertheless we choose to derive the position in terms of the geodetic latitude. Therefore we have to derive a relation between the geodetic and geocentric latitude, illustrated on Figure 3.11. Using the notations of Figure 3.11,
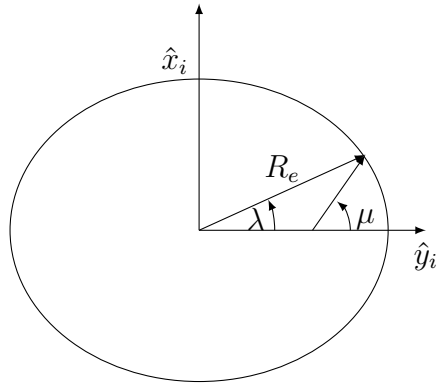
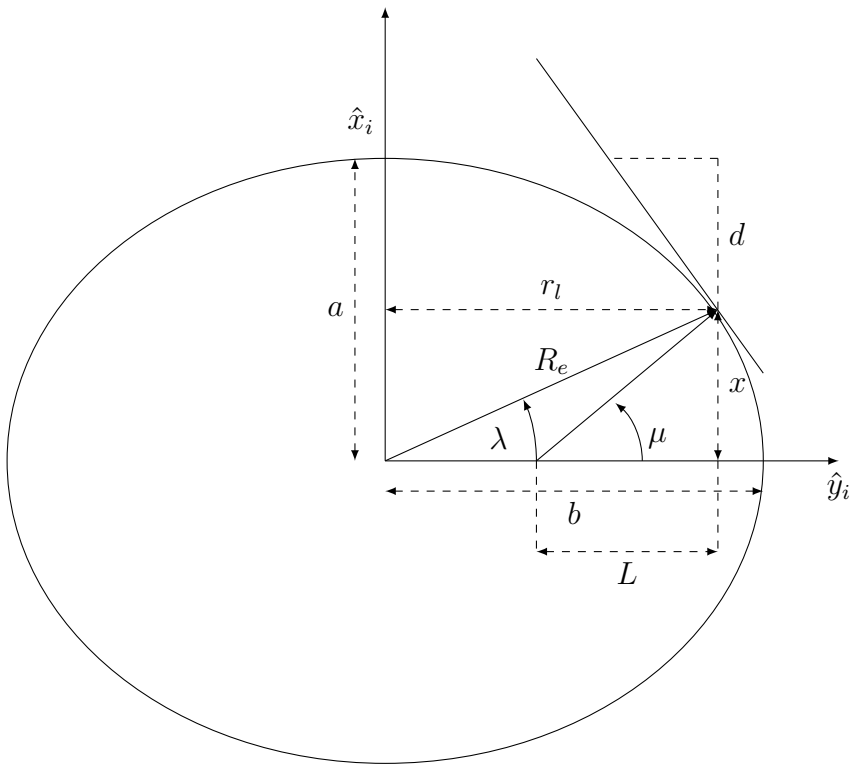Figure 3.10: Geodetic and Geocentric latitude (respectively denoted by μ and λ)

Figure 3.11: Relation between Geodetic and Geocentric latitude (respectively denoted by μ and λ)

the equation for the ellipse is given by:

$$\frac{x^2}{a^2} + \frac{r_l^2}{b^2} = 1$$

$$\iff \frac{b^2x^2 + a^2r_l^2}{a^2b^2} = 1$$

$$\iff x = \sqrt{\frac{a^2b^2 - a^2r_l^2}{b^2}}, \text{ as } x > 0.$$

Looking at Figure 3.11, one can find that:

$$\tan\lambda = \frac{x}{r_l} \quad \text{and} \quad \tan\mu = \frac{x}{L}. \tag{3.14}$$

Taking the derivative of x with respect to r_l to get the slope of the ellipse, we obtain:

$$\frac{dx}{dr_l} = \frac{1}{\cancel{2}}\left(\frac{a^2b^2 - a^2r_l^2}{b^2}\right)^{-\frac{1}{2}} \times \left(-\frac{\cancel{2}a^2}{b^2}r_l\right)$$

$$= \frac{-\frac{a^2}{b^2}r_l}{\sqrt{\frac{a^2b^2 - a^2r_l^2}{b^2}}}$$

$$= \frac{-\frac{a^2}{b^2}r_l}{\sqrt{a^2 - \frac{a^2}{b^2}r_l^2}}.$$

The slope of the line normal to the ellipse is the opposite of the inverse of the slope of the ellipse. That is:

$$d = \frac{\sqrt{a^2 - \frac{a^2r_l^2}{b^2}}}{\frac{a^2}{b^2}r_l} = \frac{x}{\frac{a^2}{b^2}r_l}.$$

Observing that $L = \frac{a^2}{b^2}r_l$, we can write μ as a function of d:

$$\tan\mu = \frac{x}{\frac{a^2}{b^2}r_l}.$$

That is:

$$r_l\frac{a^2}{b^2}\tan\mu = x$$

and finally we obtain the relation between μ and λ:

$$\frac{a^2}{b^2}\tan\mu = \tan\lambda.$$

Geocentric Earth surface As one can have observed, the position vector R_e is not aligned with any reference frame we have defined. Therefore we define a new reference frame: the geocentric Earth surface frame denoted with a "c" subscript. This reference frame is defined such that the opposite of the position vector R_e is aligned with the $\hat{z}_c$-axis and obtained thanks to a rotation of angle ε about the $\hat{y}_e$-axis. The transformation from

91
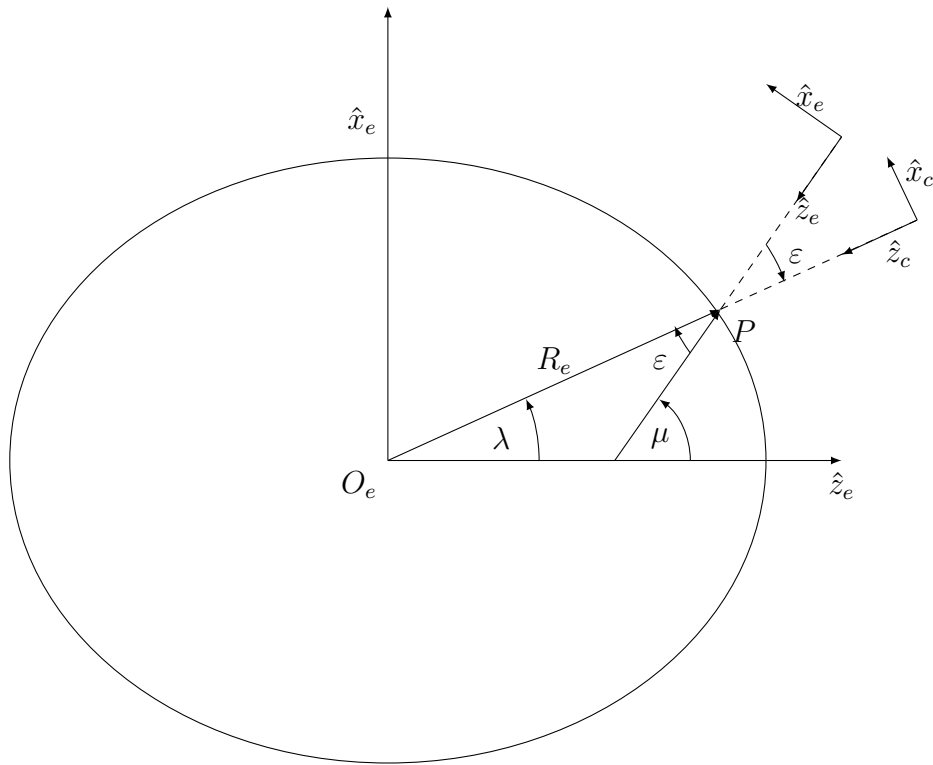
Figure 3.12: Relation between Geocentric Earth surface frame and NED reference frame

the NED reference frame to the geocentric surface frame is illustrated on Figure 3.12.

The angle ε is defined by the following relation:

$$\varepsilon = \mu - \lambda.$$

The rotation matrix from the reference frame "c" to "e", denoted $\mathbb{T}_{c \to e}$, is given by:

$$\begin{pmatrix} \hat{x}_e \\ \hat{y}_e \\ \hat{z}_e \end{pmatrix} = \mathbb{T}_{c \to e} \begin{pmatrix} \hat{x}_c \\ \hat{y}_c \\ \hat{z}_c \end{pmatrix}$$

$$= \begin{pmatrix} \cos \varepsilon & 0 & -\sin \varepsilon \\ 0 & 1 & 0 \\ \sin \varepsilon & 0 & \cos \varepsilon \end{pmatrix} \begin{pmatrix} \hat{x}_c \\ \hat{y}_c \\ \hat{z}_c \end{pmatrix}.$$

Therefore the position vector R_e can now be expressed in terms of the axis of the new reference frame: $R_e = -r_e \hat{z}_c$, where $r_e = \|R_e\|$.

Aircraft kinematics for an ellipsoidal Earth

Now, we have defined the latitude, the longitude and the position vector R_e, the position of the aircraft with respect to the center of the Earth expressed in the NED reference

frame, denoted by R, can be expressed by the following formula:

$$R = O_e P = -r_e \hat{z}_c - h\hat{z}_e$$
$$= -r_e(-\sin\varepsilon\hat{x}_e + \cos\varepsilon\hat{z}_e) - h\hat{z}_e$$
$$= r_e \sin\varepsilon\hat{x}_e - (r_e\cos\varepsilon + h)\hat{z}_e.$$

Therefore the kinematics of the aircraft expressed in the Earth centered reference frame can be derived taking the time derivative of the position vector in the Earth centered reference frame. That is:

$$\left.\frac{dR}{dt}\right|_i = (\dot{r}_e\sin\varepsilon + r_e\dot{\varepsilon}\cos\varepsilon)\hat{x}_e + (r_e\dot{\varepsilon}\sin\varepsilon - \dot{r}_e\cos\varepsilon + \dot{h})\hat{z}_e + \Omega_{ie}\wedge R$$

where Ω_{ie} the rotation vector of the NED reference frame with respect to the Earth. It is given by:

$$\Omega_{ie} = \dot{l}\hat{x}_i + \dot{\mu}\hat{y}_e$$
$$= \dot{l}\cos\mu\hat{x}_e + \dot{\mu}\hat{y}_e + \dot{l}\sin\mu\hat{z}_e.$$

Therefore:

$$\Omega_{ie}\wedge R = (\dot{l}\cos\mu\hat{x}_e + \dot{\mu}\hat{y}_e + \dot{l}\sin\mu\hat{z}_e)\wedge(r_e\sin\varepsilon\hat{x}_e - (r_e\cos\varepsilon + h)\hat{z}_e)$$
$$= (-r_e\dot{\mu}\cos\varepsilon - h\dot{\mu})\hat{x}_s + (\dot{l}\sin\mu\ r_e\sin\varepsilon + \dot{l}\cos\mu(r_e\cos\varepsilon + h))\hat{y}_e + \dot{\mu}r_e\sin\varepsilon\hat{z}_e.$$

And finally we obtain:

$$\left.\frac{dR}{dt}\right|_i = \begin{pmatrix} \dot{r}_e\sin\varepsilon + r_e\dot{\varepsilon}\cos\varepsilon - r_e\dot{\mu}\cos\varepsilon - h\dot{\mu} \\ \dot{l}\sin\mu\ r_e\sin\varepsilon + \dot{l}\cos\mu(r_e\cos\varepsilon + h) \\ r_e\dot{\varepsilon}\sin\varepsilon - \dot{r}_e\cos\varepsilon + \dot{\mu}r_e\sin\varepsilon + \dot{h} \end{pmatrix}. \tag{3.15}$$

The remaining problem is that we do not know the quantities: r_e, $\dot{r}_e$, ε and $\dot{\varepsilon}$, then we have to express them in terms of l, μ, $\dot{l}$ and $\dot{\mu}$. Recording that the ellipse equation is given by:

$$\frac{x^2}{a^2} + \frac{r_l^2}{b^2} = 1$$

and as one can observe on Figure 3.13, we have:

$$\begin{cases} r_l & = & r_e\cos\lambda \\ x & = r_e\sin\lambda \end{cases},$$

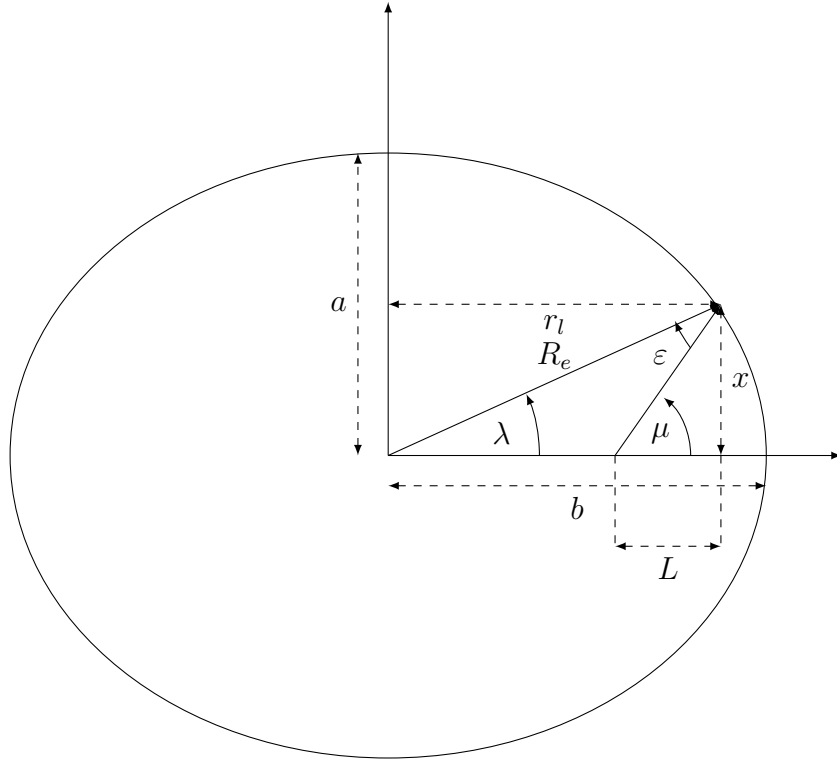Figure 3.13: Relation between derivatives

then we have:

$$\frac{r_e^2 \cos^2 \lambda}{b^2} + \frac{r_e^2 \sin^2 \lambda}{a^2} = 1$$

$$\Rightarrow \frac{a^2 r_e^2 \cos^2 \lambda + b^2 r_e^2 \sin^2 \lambda}{a^2 b^2} = 1$$

$$\Rightarrow r_e^2 (a^2 \cos^2 \lambda + b^2 \sin^2 \lambda) = a^2 b^2$$

$$\Rightarrow r_e = \sqrt{\frac{a^2 b^2}{a^2 \cos^2 \lambda + b^2 \sin^2 \lambda}}.$$

As λ is a derived angle, we use the relation (3.14) to replace its expression in the previous equation. Thanks to (3.14), we find that:

$$\lambda = \arctan\left(\frac{a^2}{b^2} \tan \mu\right).$$

Then,

$$\varepsilon = \mu - \lambda$$

$$= \mu - \arctan\left(\frac{a^2}{b^2} \tan \mu\right)$$

94

Therefore using the chain rule, we have that $\dot{r}_e$ is given by:

$$
\begin{aligned}
\dot{r}_e &= \frac{dr_e}{dt} \\
&= \frac{dr_e}{d\lambda}\frac{d\lambda}{d\mu}\frac{d\mu}{dt},
\end{aligned}
$$

where:

$$
\begin{aligned}
\frac{dr_e}{d\lambda} &= \frac{1}{2}\left(\frac{a^2 b^2}{a^2\cos^2\lambda + b^2\sin^2\lambda}\right)^{-\frac{1}{2}} \times \left(-a^2 b^2 \frac{-2a^2\cos\lambda\sin\lambda + 2b^2\sin\lambda\cos\lambda}{(a^2\cos^2\lambda + b^2\sin^2\lambda)^2}\right) \\
&= \frac{1}{2}\frac{(a^2\cos^2\lambda + b^2\sin^2\lambda)^{\frac{1}{2}}}{\cancel{ab}} \times \left(-\cancel{a^2 b^2}\frac{-\cancel{2}(b^2 - a^2)\cos\lambda\sin\lambda}{(a^2\cos^2\lambda + b^2\sin^2\lambda)^2}\right) \\
&= -\frac{ab(b^2 - a^2)\cos\lambda\sin\lambda}{(a^2\cos^2\lambda + b^2\sin^2\lambda)^{\frac{3}{2}}}
\end{aligned}
$$

and

$$
\frac{d\lambda}{d\mu} = \frac{a^2}{b^2} \times \frac{1}{\cos^2\mu} \times \frac{1}{1 + \frac{a^4}{b^4}\tan^2\mu}.
$$

Then, $\dot{r}_e$ is given by:

$$
\begin{aligned}
\dot{r}_e &= -\frac{ab(b^2 - a^2)\cos\lambda\sin\lambda}{(a^2\cos^2\lambda + b^2\sin^2\lambda)^{\frac{3}{2}}} \times \frac{a^2}{b^2} \times \frac{1}{\cos^2\mu} \times \frac{1}{1 + \frac{a^4}{b^4}\tan^2\mu}\dot{\mu} \\
&= K_{\dot{r}_e}\dot{\mu}
\end{aligned}
\tag{3.16}
$$

and $\dot{\varepsilon}$ is given by:

$$
\begin{aligned}
\dot{\varepsilon} &= \left(1 - \frac{a^2}{b^2} \times \frac{1}{\cos^2\mu} \times \frac{1}{1 + \frac{a^4}{b^4}\tan^2\mu}\right)\dot{\mu} \\
&= K_{\dot{\varepsilon}}\dot{\mu}.
\end{aligned}
\tag{3.17}
$$

Then, recording the definition of $\dot{x}_i^i$, $\dot{y}_i^i$, assuming $\dot{z}_i^i = 0$, and using (3.15) we have that:

$$
\begin{cases}
\dot{\mu} &= \dfrac{\dot{x}_i^i}{K_{\dot{r}_e}\sin\varepsilon + r_e K_{\dot{\varepsilon}}\cos\varepsilon - (r_e\cos\varepsilon + h)} \\
\dot{l} &= \dfrac{\dot{y}_i^i}{\cos\mu(r_e\cos\varepsilon + h) + r_e\sin\varepsilon\sin\mu}
\end{cases}
\tag{3.18}
$$

We finally get the kinematic equations which describe the aircraft motion around the Earth. However to represent the kinematics, and dynamics of the aircraft as a state-space vector, we still have to deal with the mass variation of the aircraft.

3.1.4 Mass variation

As we have already mention, the mass of the aircraft is considered as a fixed quantity to make the force balance. Indeed its influence is negligible for the short dynamics. However

the mass evolves during the cruise phase as the fuel is consumed. The rate of change of the aircraft's mass is given by the quantity of fuel burned. Therefore, in order to take into account its dynamic, another state equation is added. The usual modelization consists in considering it as a linear function of thrust. That is:

$$\dot{m} = -\eta T \tag{3.19}$$

where η is a coefficient relating thrust to fuel consumption see (3.35) for more details on this coefficient.

3.1.5 State space representation

In previous subsections, we derived all the quantities needed to obtain a state space representation of the aircraft. Indeed state space representation represents a convenient mean to model the aircraft dynamics. Indeed the state-variables are defined as a set of variables such that the knowledge of the state vector at a particular time, and the control vector after this time, completely defines the motion (state trajectory) from that time on. In other words, the state variables shall be any set of variables that completely define the state of the system at any time. As we are dealing mainly with commercial airliners, we can simplify the model further by assuming that the aircraft always operates near trimmed flight conditions and treat the flight path angle as an input instead of a state (Hypothesis 8). That is θ is now a control variable. Let us define the state and control vectors as:

$$\dot{\mathbf{x}} = [\dot{\mu}, \ \dot{l}, \ \dot{h}, \ \dot{v}_a, \ \dot{\psi}, \ \dot{m}] \tag{3.20}$$

$$\mathbf{u} = [T, \ \varphi, \ \theta] \tag{3.21}$$

Gathering up all the computation we made so far, we end up with the state space representation:

$$
\begin{cases}
\dot{\mu} &= \dfrac{v_a \cos\theta \cos\psi + w_n}{K_{\dot{r}_e} \sin\varepsilon + r_e K_{\dot{\varepsilon}} \cos\varepsilon - (r_e \cos\varepsilon + h)} \\[2ex]
\dot{l} &= \dfrac{v_a \cos\theta \sin\psi + w_e}{\cos\mu(r_e \cos\varepsilon + h) + r_e \sin\varepsilon \sin\mu} \\[2ex]
\dot{h} &= v_a \sin\theta \\[2ex]
\dot{v}_a &= \dfrac{T - D}{m} - g \sin\theta - \cos\theta(\dot{w}_n \cos\psi + \dot{w}_e \sin\psi) \\[2ex]
\dot{\psi} &= \dfrac{1}{v_a \cos\theta}\left[\dfrac{L}{m}\sin\varphi + (\dot{w}_n \sin\psi - \dot{w}_e \cos\psi)\right] \\[2ex]
\dot{m} &= -\eta T
\end{cases}
\tag{3.22}
$$

with initial conditions:

$$\mathbf{x}_0 = (\mu_0, l_0, h_0, v_{a,0}, \psi_0, m_0). \tag{3.23}$$

To stay in the flight envelope the state and control parameters are subject to the following constraints:

$$\begin{cases} h \in [0, h_{max}] \\ v_a \in [v_{min}, v_{max}] \\ m \in [m_{min}, m_{max}] \\ T \in [T_{min}, T_{max}] \\ |\varphi| < \varphi_{max} \\ |\theta| < \theta_{max} \end{cases} \tag{3.24}$$

The values of the state and control bounds and the values of the parameter C_D, S_w can be obtained from the BADA database, see Section Section 3.1.8 for more details.

3.1.6 Aerodynamic and propulsive forces

As it has been seen in Section 3.1.2, an air-plane flying through the atmosphere experiments gravitational, aerodynamic and propulsive forces. These forces enter in the aircraft dynamic equations. But we did not detailed yet how they are defined. The interested reader can refer to Boiffier (1998) for a detailed presentation of the aerodynamic forces acting on the aircraft.

To sum up, a fluid flowing past the surface of a body exerts a force on it. Lift, denoted by L is the component of this force that is perpendicular to the oncoming flow direction. It contrasts with the drag force, denoted by D, which is the component of the surface force parallel to the flow direction. Summing up, the aerodynamic components L and D can be modelled as a function of the aerodynamic coefficients C_L and C_D:

$$L = qS_wC_L \tag{3.25}$$

$$D = qS_wC_D \tag{3.26}$$

where S_w stands for the wing reference area, q for the dynamic pressure and C_D, C_L for the drag and lift coefficient respectively.

The dynamic pressure q is the kinetic energy per unit volume of a fluid particle, this quantity is defined by:

$$q = \frac{1}{2}\rho(h)v_a^2, \tag{3.27}$$

where $\rho(h)$ stands for the air density which depends on the pressure altitude h and v_a the true airspeed of the aircraft. As one may note here, the dynamic pressure can be used to determine the true airspeed of the aircraft knowing the air density (directly given by the altitude) and q. Aircraft are equipped by a pitot-static tube (Prandtl tube) which can

measure the dynamic pressure. Then the airspeed of an aircraft can be determined. This remark being made, we still have to detail what are the aerodynamic coefficient C_D and C_L. In first approximation, C_D is modelled as a quadratic function of C_L:

$$C_D = (C_{D_0} + KC_L^2) \tag{3.28}$$

where C_{D_0} is the zero lift drag coefficient and K the induced drag coefficient. Equation (3.28) is valid for all situations except for the approach and landing phase where others relations are used. As we are only interesting in cruise phase we just need this relation.

By using Eq. (3.25), (3.26), (3.27) and (3.28), we can express the aerodynamic drag force as a function of the airspeed and air density:

$$D = \frac{1}{2}\rho(h)v_a^2 S_w(C_{D_0} + KC_L^2). \tag{3.29}$$

Finally concerning the propulsive force, T, it usually depends on the pressure altitude h, the velocity of the aircraft and on thrust setting σ:

$$T = T(\sigma, h, v_a) \tag{3.30}$$

3.1.7 ISA model

As we have seen in the previous section, the propulsive and aerodynamic forces depends on different atmospheric parameters, such as the air density ρ which depends itself on the pressure altitude h. Therefore a description of these atmospheric quantities is needed. As we mention in the introduction of this chapter, the ISA model is used to describe these quantities as well as their relations. The ISA is an atmospheric model of how the pressure, temperature, density, and viscosity of the Earth's atmosphere change over a wide range of altitudes or elevations. It has been established to provide a common reference for temperature and pressure and consists of tables of values at various altitudes, plus some formulas by which those values were derived. The ISA model divides the atmosphere into layers with linear temperature distributions. The other values are computed from basic physical constants and relationships. Thus, let us define the conditions which occurs at the Mean Sea Level (MSL).

Definitions

ISA conditions at MSL   MSL atmosphere conditions are those which occur in the ISA at the point where the pressure altitude h is zero. The temperature, pressure, density and speed of sound respectively denoted by: T_0, p_0, ρ_0 and a_0 are given by:

- $T_0 = 288.15$, in $[K]$

- $p_0 = 101325$, in $[Pa]$

- $\rho_0 = 1.225$, in $[kg.m^{-3}]$

- $a_0 = 340.294$, in $[m.s^{-1}]$

Non-ISA atmospheres and MSL However, it may happen that this value are not the ones which actually occurs, therefore we introduce the non-ISA atmospheres. They differ from ISA in the sense that at MSL either one or both following parameters is not zero:

- ΔT temperature difference between temperature at MSL for the ISA atmosphere and Non-ISA atmosphere.

- Δp pressure difference between pressure at MSL for the ISA atmosphere and Non-ISA atmosphere.

That is the temperature and pressure, respectively denoted by: $T_{0,NI}$ and $p_{0,NI}$ are given by:

- $T_{0,NI} = T_0 + \Delta T$

- $p_{0,NI} = p_0 + \Delta p$

Expressions

These quantities being defined, we give the relationship between the atmospheric pressure p, the temperature T, and the pressure altitude h for any ISA and non-ISA atmosphere.

Physical constants Before stating the different relationships, we need to define some atmospheric constants which are involved in the relations.

- the adiabatic index of air, $\kappa = 1.4$

- the real gas constant for air, $R = 287.05287 \; [m^2.(K^{-1}s^{-2})]$

- the gravitational acceleration, $g_0 = 9.80665 \; [m.s^{-2}]$

- the ISA temperature gradient with altitude below the tropopause (also called lapsrate), $K = -0.0065 \; [K.m^{-1}]$

- the tropopause elevation, $h_{11} = 11000 \; [m]$

- the Earth's mean radius, $r_e = 6371 \; [m]$

Temperature The temperature can be expressed as a function of pressure altitude:

$$T = f(h, \Delta T) = \begin{cases} T_0 + \Delta T + Kh, & h < h_{11} \\ T_{11}, & h \geq h_{11} \end{cases} \tag{3.31}$$

where T_{11} is the temperature at h_{11} which is equal to 216.5 $[K]$.

Pressure   The air pressure is a function of temperature:

$$p = f(T, \Delta T) = \begin{cases} p_0 \left(\frac{T - \Delta T}{T_0}\right)^{-\frac{g_0}{KR}}, & h \leq h_{11} \\ p_{11} \exp\left(-\frac{g_0}{RT_{11}}(h - h_{11})\right), & h > h_{11} \end{cases}$$

with $p_{11} = 22632 [Pa]$

Air density   The air density, denoted by ρ, is calculated from the pressure p and the temperature T at altitude h using the perfect gas law:

$$\rho = \frac{p}{RT}. \tag{3.32}$$

Pressure altitude   Pressure altitude h has been introduced such that the hydrostatic equation is given by:

$$dp = -\rho g_0 dh$$

That is, we make the assumption that the gravitational acceleration does not vary with altitude. Therefore,

$$dp = -\rho g_0 dh$$
$$\frac{dp}{p} = \frac{-\rho g_0}{\rho RT} dh, \text{ using (3.32)}$$
$$= -\frac{g_0}{RT} dh.$$

For $h \leq h_{11}$ the hydrostatic equation becomes:

$$\frac{dp}{p} = -\frac{g_0}{R} \frac{dh}{T_0 + Kh}, \text{ using (3.31)}.$$

Integrating yield us,

$$\int_{p_0}^{p} \frac{dp}{p} = -\frac{g_0}{R} \int_{0}^{h} \frac{dh}{T_0 + Kh}$$
$$\ln\left(\frac{p}{p_0}\right) = -\frac{g_0}{RK} \ln\left(\frac{T_0 + Kh}{T_0}\right)$$
$$\frac{p}{p_0} = \left(\frac{T_0 + Kh}{T_0}\right)^{-\frac{g_0}{KR}}.$$

Solving now for h, gives us:

$$\frac{T_0 + Kh}{T_0} = \left(\frac{p}{p_0}\right)^{-\frac{RK}{g_0}}$$
$$h = \frac{T_0}{K}\left[\left(\frac{p}{p_0}\right)^{-\frac{RK}{g_0}} - 1\right].$$

Now if we have that $h > h_{11}$, then:

$$\frac{dp}{p} = -\frac{g_0}{R}\frac{dh}{T_{11}}, \text{ using (3.31)}.$$

Integrating yield us,

$$\int_{p_{11}}^{p} \frac{dp}{p} = -\frac{g_0}{R}\int_{h_{11}}^{h} \frac{dh}{T_{11}}$$

$$\ln\left(\frac{p}{p_{11}}\right) = -\frac{g_0}{RT_{11}}(h - h_{11}).$$

Solving now for h, gives us:

$$-\frac{RT_{11}}{g_0}\ln\left(\frac{p}{p_{11}}\right) = h - h_{11}$$

$$h = h_{11} - \frac{RT_{11}}{g_0}\ln\left(\frac{p}{p_{11}}\right).$$

Wrapping it up, we have the following relation between pressure altitude and pressure:

$$h = \begin{cases} \frac{T_0}{K}\left[\left(\frac{p}{p_0}\right)^{-\frac{RK}{g_0}} - 1\right], & h \leq h_{11} \\ h_{11} - \frac{RT_{11}}{g_0}\ln\left(\frac{p}{p_{11}}\right), & h > h_{11} \end{cases} \tag{3.33}$$

Pressure altitude and geometrical altitude As we make the assumption that g does not vary with altitude and that we are under ISA conditions we have that the geopotential altitude is the same as the geometric altitude.

Air speed of sound The speed of sound is the speed at which the pressure waves travel through a fluid and is given by the expression:

$$a = \sqrt{\kappa RT}.$$

Finally we obtain all the relations relating the different atmospheric quantities which are needed to set all the aerodynamic parameters entering in the aircraft equations of motion. However, we did not detailed yet how the coefficients such as C_L, C_D, η are set. These quantities depend on the aircraft type, the phase of the flight and also the aircraft configuration. They can be obtained using the BADA database, see Nuic (2011). In this work we choose to use this database to derive all the aerodynamic parameter values.

3.1.8 Using BADA

As we have already mentioned in this document, we are going to use the BADA database, see Nuic (2011) for details on the database, to set all the aircraft parameters. The purpose of this section is to explain how we use them. Indeed as we have said, the aerodynamic parameters depend on the aircraft types, the phase of the flight and the

configuration of the aircraft. Therefore we define variables which are going to be use during the simulation to retrieve the value from the BADA database depending on the aircraft, and its configuration.

Discrete parameters

As we want to simulate several type of aircraft trajectories in the same monitored area, we attached to each *Aircraft* a discrete aircraft type, for example: Airbus 330, Boeing 747, *etc.*... To this end, we use a discrete parameter *Aircraft_type* to store it. All the possible values that the parameter *Aircraft_type* can take are listed in the BADA documentation. This parameter is used in our simulator to retrieve values from the BADA database for parameters such as drag coefficient and bounds.

BADA provides also for each *Aircraft_type* an engine type. This is used by the controller to set the maximum climb thrust. In this document, to denote the engine type we use a separate discrete parameter *Engine_type* which can take one of the three values: *Jet, Turboprop* and *Piston.*

Aerodynamic parameters

The two aerodynamic coefficients C_L and C_D are set following the same procedure as in the BADA documentation. That is C_L is set to ensure that the vertical component of the lift projected into the body reference frame exactly balances the weight of the aircraft:

$$C_L = \frac{2mg}{\rho(h)v_a^2 S_w \cos \varphi}. \tag{3.34}$$

The coefficient C_D depends on the lift coefficient as we have already mention in Eq. (3.28). The parameter C_{D_0} and K depend on *Aircraft_type* and can be obtained from the BADA database.

Fuel consumption

The parameter η represents the thrust specific fuel consumption, that is the rate at which the fuel is consumed. This quantity depends on the *Engine_type*, the true airspeed v_a, the flight mode of the aircraft and some other coefficients which depends on the *Aircraft_type*. Concerning the cruise phase, the thrust specific fuel consumption is defined by the following relation:

$$\eta_{cr} = \begin{cases} C_{f1}(1 + \frac{v_a^2}{C_{f2}}) & \text{if } Engine\_type{=}Jet \\ C_{f1}(1 - \frac{v_a^2}{1000C_{f2}}) & \text{if } Engine\_type{=}Turboprop \\ C_{f1} & \text{if } Engine\_type{=}Piston \end{cases} \tag{3.35}$$

where the coefficients C_{f1} and C_{f2} are obtained from the BADA database.

Bounds

As we have already mention, the state and control variables are bounded. In this section we explain how they are defined.

Mass   The maximum and the minimum mass, respectively denoted by m_{max} and m_{min} are given by aircraft performance reference data available in the BADA database.

Altitude   The maximum altitude $h_{max}(m)$, which is a function of the *Aircraft*'s mass m, is expressed in terms of the following parameters:

- h_{MO} which stands for the maximum operating altitude (in ft) above the mean sea level is given by the BADA database.

- h_m which stands for the maximum altitude (in ft) above mean sea level at maximum take off weight under ISA conditions is given by the BADA database

- G_w mass gradient on h_m which is positive

- G_t temperature gradient on h_m which is negative

The maximum altitude for any given mass is:

$$h_{max}(m) = \min\{h_{MO}, h_m + G_t(\Delta T - C_{T,4}) + G_w(m_{max} - m)\}$$

where ΔT is the temperature deviation from ISA (in K) and m stands for the actual mass (in kg),$C_{T,4}$ is given by the BADA database . If $\Delta T - C_{T,4} < 0$ then we set $\Delta T - C_{T,4} = 0$. We will prevent our model to overcome this value using an altitude less than that one.

Speed   The maximum speed for an aircraft is given by the BADA database in terms of CAS or Mach number, depending on the pressure altitude, respectively by V_{MO} and M_{MO}.

In cruise (clean) configuration, that is:

- in climb above the maximum pressure altitude above ground level of initial climb $H_{max,IC}$ $(2000ft)$,

- in descent above the maximum pressure altitude above ground level of approach $H_{max,AP}$ $(8000ft)$,

- or in descent below the maximum pressure altitude above ground level of approach and $v_a > v_{min} + 10$

As it is not convenient for pilot to fly at maximum speed as they have to report if this event occurs, we will prevent the model to overcome not the maximum speed but maximum speed minus 10 knots in case of CAS speed and minus 0.5 in case of Mach speed.

The minimum speed is given in function of aircraft stall speed V_{stall} (in CAS) which depends on the configuration. For $Engine\_type \in \{Turboprop, Piston\}$,the minimum speed is specified as follow:

$$v_{min} = C_{v_{min}} V_{stall} \tag{3.36}$$

where $C_{v_{min}}$ is set to 1.3 for all the *Aircraft_types*.

For $Engine\_type = Jet$, an other limit, the low speed buffeting limit v_{min} depending on M_b and $v_{min,stall}$ (where $v_{min,stall}$ is given by Eq (3.36)) and expressed in terms of Mach number is determined using the following equation

$$\begin{cases} v_{min} &= \max\{v_{min,stall}, M_b\} & h \geq 15000 ft \\ v_{min} &= v_{min,stall} & h < 15000 ft \end{cases}$$

with M_b the solution of the following equation:

$$kM_b^3 - C_{Lbo(M=0)} M_b^2 + \frac{mg}{0.583 S_w p}$$

where k is a lift coefficient gradient, $C_{Lbo(M=0)}$ the initial buffet onset lift coefficient for $M = 0$, p the actual pressure (in Pa), M the Mach number, S_w the wing surface area m^2 and m the actual mass (in kg). As the minimum speed will not be reached during cruise phase, we use another minimum speed related to the green dot speed (most economical speed during cruise phase).

Thrust   Depending on the climbing mode, the *Engine_type*, the pressure altitude h (in ft), the TAS v_a (in kt) and the temperature deviation from ISA atmosphere ΔT (in K), the maximum thrust can be calculated.

When climbing, the maximum climb thrust denoted by $T_{max,C}$ is given by:

$$T_{max,C} = T_{max,C,ISA}(1 - C_{T_5} \Delta T_{eff})$$

where $\Delta T_{eff} = \Delta T - C_{TC,4}$ with the limits $0 \leq C_{T_5} \Delta T_{eff} \leq 0.4$ and $C_{T_5} \geq 0$.The coefficient $T_{max,C,ISA}$ is given by:

$$T_{max,C,ISA} = \begin{cases} C_{Tc,1}\left(1 - \frac{h}{C_{TC,2}} + C_{TC,3} h^2\right) & Engine\_type=Jet \\ \frac{C_{Tc,1}}{v_a}\left(1 - \frac{h}{C_{TC,2}}\right) + C_{TC,3} & Engine\_type=Turboprop \\ C_{Tc,1}\left(1 - \frac{h}{C_{TC,2}}\right) + \frac{C_{TC,3}}{v_a} & Engine\_type=Piston \end{cases}$$

where $C_{T_c,1}$, $C_{T_C,2}$, $C_{T_C,3}$ and C_{T_5} are set using the BADA database. When descending, the maximal descent trust, denoted by $T_{max,D}$, is calculated as a ratio of the maximum climb thrust with different correction factors used for high and low altitudes, that is:

$$T_{max,D} = \begin{cases} C_{T,D,H} T_{max,C} & h > H_{p,D} \\ C_{T,D,L} T_{max,C} & h \leq H_{p,D} \end{cases}$$

where $H_{p,D}$ is the the transition altitude for calculation of descent thrust. When cruising, the maximum of thrust available $T_{max,L}$ is limited and its limitation is given in terms of the maximum climb thrust:

$$T_{max,L} = C_{T,L} T_{max,C}$$

where $C_{T,L}$ is set to 0.95 for all the *Aircraft_types*.

Bank angle   The maximum bank angle φ_{max} is given for all the *Aircraft_types* and set to the value of 25 deg.

Pitch angle   The maximum pitch angle θ_{max} is given for all the *Aircraft_types* and set to the value of 3 deg.

3.1.9   Controller

So far we have developed the dynamic model able to simulate the dynamics of several aircraft. However, as we said in the preamble of this chapter, aircraft have to follow their flight plan. To this end, we need to develop a controller, in the automatic sense of the word. The controller measures the state of the aircraft dynamics, and uses it together with the flight plan to determine the values for the inputs T, φ and θ. The controller is divided into two components, one controlling vertical motion through the thrust and the flight path angle and the other controlling the horizontal motion through the bank angle. The controls we have developed are inspired from the work developed in Verhoeven et al. (2014); Prats et al. (2014) and adapted to the cruise phase. The thrust and the flight path angle are used to set the Rate of Climb/Descent (ROCD). Following current practice, the controller tries to track a desired speed, V_{ref}, which is a function of altitude and *Aircraft_type* and which is determined by the airline see Section 3.1.9.

Discrete State

The discrete states of the model describe the different flight modes. The discrete dynamics are coming from the flight plan of the aircraft and the logic variables embedded in the controller to retrieve values from the BADA database. The discrete states of the controller are stored in 6 discrete variables: way-point index (WP), flight level (FL), climb mode (CM), flight phase (FP), troposphere mode (TrM) and the speed hold mode (SHM).

These discrete quantities evolve depending on the values of the continuous state of the aircraft. In the reverse angle, a different discrete state affects both the continuous

dynamics and the outputs of the controller.

Way-point index   The discrete variable representing the way point index takes integer values:

$$WP \in \{0, 1, \ldots, M\}$$

If $WP = i$, that means that the aircraft is on its way from the ith-way point locate at $O(i)$ and the $(i+1)^{th}$-way point located at $O(i+1)$. To determine WP, we use the horizontal position of the aircraft given by (x, y). To determine when the variable switches from one way point to the next one, we have to adopt a method for modeling how the aircraft are performing turns. In practice, aircraft have two ways of executing turns: fly-by and fly-over model.

- **Fly-by**: The aircraft starts turning before it reaches the next way point and "cuts the corner". This appears to be the most commonly used method to execute turns by modern aircraft.

- **Fly-over**: The aircraft reaches the next way-point before turning. It appears that it was the most commonly used method before the Global Positioning System became standard.

Therefore we adopt the fly-by method. Then, WP switches at the beginning of the turn. That is when the aircraft crosses a vertical plane which location depends on the maximum bank angle and the location of the way points. To determine when this happens, we have to determine the equation of the vertical plane. This step will be described in details in the next paragraph.

Flight Level   The discrete variable representing the flight level (FL) takes on values representing the following altitude discretization:

$$\{250ft, 260ft, \ldots 440ft, 450ft\}$$

This discrete variable is used to set the desired speed, see .

Climb mode   The climb mode reflects whether the aircraft is climbing, descending or flying level:

$$CM \in \{C, D, L\}$$

The value is reset whenever the aircraft starts a new segment of the reference path. If $WP = i$ and $O_{i+1} = (x, y, z)$, the difference between the present altitude and z is used to determine whether to climb ($CM = C$), descent ($CM = D$) or stay at the same level ($CM = L$). The state returns to L when the aircraft reaches its desired altitude. A tolerance of 1 m is introduced.

Flight Phase   From the point of view of the controller, the en-route portion of flight is divided into two phases: cruise phase and level change phase. We use the variable FP to store this information:

$$FP \in \{C, LC\}$$

The rules for changing the value of FP are as follow, if $WP = i$ and $O_{i+1} = (x, y, z)$, the difference between the present altitude and z is used to determine whether to change of flight level ($FP = LC$) or stay at the same level ($FP = C$). The state returns to C when the aircraft reaches its desired altitude,z. A tolerance of $1m$ is introduced.

Troposphere mode   The troposphere mode represents whether the aircraft is above or below tropopause, the boundary between the troposphere and the stratosphere. This affects some variables in the atmosphere model such as air density. The troposphere mode can take two values:

$$TrM \in \{L, H\}$$

To set its value, we use the altitude, z. If $z < 11000ft$, $TrM = L$ else $TrM = H$.

Speed Hold Mode   The speed hold mode represents whether the aircraft is holding a CAS or holding a constant Mach number. The change takes place at the transition altitude, which is the altitude where the True Air Speed (TAS) of the aircraft determined by CAS is equal to the desired TAS determined by the Mach number, see Section 3.1.9 for more details.

$$SHM \in \{C, M\}$$

The value i then exclusively determined by the geopotential altitude of the aircraft.

V_{CAS}, Mach and V_a conversion

The reference speed is given by the BADA database and depends on the flight level, the pressure altitude and also the *Aircraft_type*. Indeed depending on the pressure altitude, the aircraft hold a constant CAS, V_{CAS}, or a constant Mach number, M. The crossover altitude denoted by h_{tr} between a given CAS, V_{CAS}, and a Mach number, M, is defined to be the pressure altitude at which V_{CAS} and M represent the same TAS value. Given v_a, we can obtain the CAS using the following relation:

$$V_{CAS} = \left(\frac{2p_0}{\mu \rho_0} \left(\left(1 + \frac{p}{p_0} \left(\left(1 + \frac{\mu \rho_0 v_a^2}{2p} \right)^{\frac{1}{\mu}} - 1 \right) \right)^{\mu} - 1 \right) \right)^{\frac{1}{2}} \tag{3.37}$$

where p and ρ are the ambient pressure and air density respectively, p_0 the mean sea level pressure, ρ_0 the air density at the mean sea level and $\mu = \frac{\kappa-1}{\kappa}$ with κ corresponding to the adiabatic index of air. We also can obtain the Mach number corresponding to the

TAS using the following relation:

$$M = \frac{1}{\sqrt{\kappa R T}} v_a \tag{3.38}$$

where R is the real gas constant for air and T the ambient temperature.

Now we can give the formula to calculate the crossover altitude depending on V_{CAS} and M:

$$h_{tr} = \frac{1}{0.3048 K} (T_0(1 - \theta_{tr})) \tag{3.39}$$

where K is the lapse rate and the value 0.3048 is used to convert feet to meters and θ_{tr} is the temperature ratio at the crossover altitude, that is:

$$\theta_{tr} = \delta_{tr}^{-\frac{KR}{g_0}}$$

and δ_{tr} is the pressure ratio at the crossover altitude:

$$\delta_{tr} = \frac{\left(1 + \frac{(\kappa-1)V_{CAS}^2}{2a_0^2}\right)^{\frac{\kappa}{\kappa-1}} - 1}{\left(1 + \frac{(\kappa-1)M^2}{2}\right)^{\frac{\kappa}{\kappa-1}} - 1}$$

with the coefficient a_0 corresponding to the speed of sound. Therefore depending at which altitude we are, constant speed does not mean systematically that v_a is constant but that either M or V_{CAS} are remained constant. Then v_a is constant only if we are above the crossover altitude or if the pressure is constant and that we are below the crossover altitude.

Once we know the relation between these quantities, V_{ref} is set based on the discrete parameter *Aircraft_type* and on the discrete states FL, CM, and SHM. These data are obtained from the BADA airline procedure model. Therefore the crossover altitude can be deduced.

Working in the ground reference frame to control the state variable

We have to note that the body heading angle ψ cannot be an output of the state system as it depends on the actual wind vector but also on the true airspeed. Therefore, we define a new angle ψ_g standing for the ground heading angle (the track angle). This angle will be used to control the horizontal movement of the aircraft.

We now define $\mathbf{u}_a$ which is the projection of $\mathbf{v}_a^a$ in the horizontal plane that is $\mathbf{u}_a = (v_a \cos \theta, \ 0, \ 0)$.

We define a new reference frame called the trajectory frame, illustrated on Figure 3.14, denoted by a g subscript, which is a rotation of angle ψ_g of the Earth reference frame
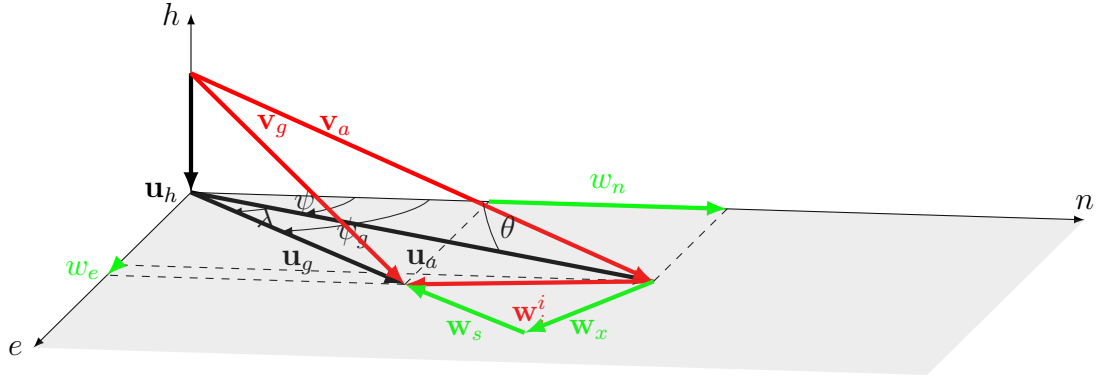
Figure 3.14: Relation between the different aircraft speed vectors with presence of horizontal wind

about the z-axis. We express in this reference frame the wind:

$$
\mathbf{w}_g^i = \begin{pmatrix} \cos \psi_g & \sin \psi_g & 0 \\ -\sin \psi_g & \cos \psi_g & 0 \\ 0 & 0 & 1 \end{pmatrix} \mathbf{w}_i^i
$$

$$
= \begin{pmatrix} w_s \\ w_x \\ 0 \end{pmatrix} = \begin{pmatrix} w_n \cos \psi_g + w_e \sin \psi_g \\ -w_n \sin \psi_g + w_e \cos \psi_g \\ 0 \end{pmatrix}. \tag{3.40}
$$

Therefore we get for $\dot{w}_x$:

$$
\dot{w}_x = -(\dot{w}_n \sin \psi_g + w_n \dot{\psi}_g \cos \psi_g) + \dot{w}_e \cos \psi_g - w_e \dot{\psi}_g \sin \psi_g. \tag{3.41}
$$

Then considering $\lambda = \psi_g - \psi$, the crab angle, we have the following relation:

$$
\sin \lambda = \frac{w_x}{u_a} = \frac{v_a \overline{w_x}}{v_a \cos \theta} = \frac{\overline{w_x}}{\cos \theta} \tag{3.42}
$$

$$
\cos \lambda = \frac{u_g - w_s}{u_a} = \frac{v_a \sqrt{\cos^2 \theta - \overline{w_x}^2}}{v_a \cos \theta} = \frac{\sqrt{\cos^2 \theta - \overline{w_x}^2}}{\cos \theta} \tag{3.43}
$$

Indeed, by Pythagoras theorem, we have that:

$$
\|\mathbf{u}_a\|^2 = \|\mathbf{u}_g - \mathbf{w}_s\|^2 + \|\mathbf{w_x}\|^2
$$

$$
\Leftrightarrow \|\mathbf{u}_a\|^2 - \|\mathbf{w_x}\|^2 = \|\mathbf{u}_g - \mathbf{w}_s\|^2
$$

$$
\Leftrightarrow \|\mathbf{u}_g - \mathbf{w}_s\| = \sqrt{\|\mathbf{u}_a\|^2 - \|\mathbf{w_x}\|^2}.
$$

Therefore:

$$\dot\psi = \dot\psi_g - \dot\lambda$$

$$= \dot\psi_g - \frac{d}{dt}\left[\arcsin\left[\frac{w_x}{v_a\cos\theta}\right]\right]$$

$$= \dot\psi_g - \frac{\dfrac{d}{dt}\{\dfrac{w_x}{v_a\cos\theta}\}}{\sqrt{1-\left(\dfrac{w_x}{v_a\cos\theta}\right)^2}}$$

$$= \dot\psi_g - \frac{\dot w_x v_a\cos\theta - w_x(\dot v_a\cos\theta - v_a\dot\theta\sin\theta)}{v_a^2\cos^2\theta\cos\lambda}. \tag{3.44}$$

Indeed

$$\sqrt{1-\left(\frac{w_x}{v_a\cos\theta}\right)^2} = \sqrt{\frac{v_a^2\cos^2\theta - w_x^2}{v_a^2\cos^2\theta}}$$

$$= \frac{\sqrt{\cos^2\theta - \overline{w_x}^2}}{\cos\theta}$$

$$= \cos\lambda.$$

Then replacing into (3.44) the expression of $\dot\psi$ gives us:

$$\frac{1}{v_a\cos\theta}\left[\frac{L}{m}\sin\varphi + (\dot w_n\sin\psi - \dot w_e\cos\psi)\right].$$

$$= \dot\psi_g - \frac{1}{v_a^2\cos^2\theta\cos\lambda}\Big[\dot w_x v_a\cos\theta - \underbrace{w_x}_{v_a\cos\theta\sin\lambda}\underbrace{(\dot v_a\cos\theta - v_a\dot\theta\sin\theta)}_{(a)}\Big]. \tag{3.45}$$

Decomposing (a) and replacing $\dot v_a$ and $\dot\theta$ gives us:

$$\dot v_a\cos\theta - v_a\dot\theta\sin\theta = \left(\frac{T-D}{m} - g\sin\theta\right)\cos\theta - \cos^2\theta(\dot w_n\cos\psi + \dot w_e\sin\psi)$$

$$- \sin\theta\left[\frac{L\cos\varphi}{m} - g\cos\theta + \sin\theta\,(\dot w_n\cos\psi + \dot w_e\sin\psi)\right].$$

That is:

$$\dot v_a\cos\theta - v_a\dot\theta\sin\theta = \frac{T-D}{m}\cos\theta - \frac{L}{m}\cos\varphi\sin\theta - (\dot w_n\cos\psi + \dot w_e\sin\psi)(\cos^2\theta + \sin^2\theta).$$

So,

$$\dot v_a\cos\theta - v_a\dot\theta\sin\theta = \frac{T-D}{m}\cos\theta - \frac{L}{m}\cos\varphi\sin\theta - \underbrace{(\dot w_n\cos\psi + \dot w_e\sin\psi)}_{(b)}.$$

110

Now going back to equation (3.45), we have:

$$u_a\dot{\psi}_g - \frac{1}{\cancel{v_a\cos\theta}\cos\lambda}\left(\dot{w}_x\cancel{v_a\cos\theta} - \cancel{v_a\cos\theta}\sin\lambda(a)\right) = \frac{L}{m}\sin\varphi + \dot{w}_n\sin\psi - \dot{w}_e\cos\psi.$$

That is:

$$u_a\dot{\psi}_g\cos\lambda - \dot{w}_x + \sin\lambda(a) = \frac{L}{m}\sin\varphi\cos\lambda + \underbrace{\dot{w}_n\sin\psi\cos\lambda - \dot{w}_e\cos\psi\cos\lambda}_{(d)}.$$

Developing $\sin\lambda(b)$ gives us:

$$\begin{aligned}
\sin\lambda(b) &= -\dot{w}_n\cos\psi\sin\lambda - \dot{w}_e\sin\psi\sin\lambda \\
&= -\dot{w}_n\cos(\psi_g + \lambda)\sin\lambda - \dot{w}_e\sin(\psi_g + \lambda)\sin\lambda \\
&= -\dot{w}_n\sin\lambda(\cos\lambda\cos\psi_g + \sin\lambda\sin\psi_g) - \dot{w}_e\sin\lambda(\cos\lambda\sin\psi_g - \sin\lambda\cos\psi_g) \\
&= -\dot{w}_n\sin\lambda\cos\lambda\cos\psi_g - \dot{w}_n\sin^2\lambda\sin\psi_g - \dot{w}_e\sin\lambda\cos\lambda\sin\psi_g + \dot{w}_e\sin^2\lambda\cos\psi_g
\end{aligned}$$

and now developing (d), gives us:

$$\begin{aligned}
(d) &= \dot{w}_n\sin\psi\cos\lambda - \dot{w}_e\cos\psi\cos\lambda \\
&= \dot{w}_n\sin(\psi_g + \lambda)\cos\lambda - \dot{w}_e\cos(\psi_g + \lambda)\cos\lambda \\
&= \dot{w}_n\cos\lambda(\cos\lambda\sin\psi_g - \sin\lambda\cos\psi_g) - \dot{w}_e\cos\lambda(\cos\psi_g\cos\lambda + \sin\psi_g\sin\lambda) \\
&= \dot{w}_n\cos^2\lambda\sin\psi_g - \dot{w}_n\cos\lambda\sin\lambda\cos\psi_g - \dot{w}_e\cos^2\lambda\cos\psi_g - \dot{w}_e\cos\lambda\sin\lambda\sin\psi_g.
\end{aligned}$$

Then subtracting from $(d)\sin\lambda(b)$ gives us:

$$\begin{aligned}
(d) - \sin\lambda(b) &= \dot{w}_n\sin\psi_g(\cos^2\lambda + \sin^2\lambda) - \dot{w}_e\cos\psi_g(\cos^2\lambda + \sin^2\lambda) \\
&= \dot{w}_n\sin\psi_g - \dot{w}_e\cos\psi_g.
\end{aligned}$$

Recording that $\dot{w}_x$ is given by Eq (3.41), we have:

$$u_a\cos\lambda\dot{\psi}_g + (\dot{w}_n\sin\psi_g + w_n\dot{\psi}_g\cos\psi_g) - \dot{w}_e\cos\psi_g + w_e\dot{\psi}_g\sin\psi_g$$

$$+\sin\lambda\left(\frac{T-D}{m}\cos\theta - \frac{L}{m}\cos\varphi\sin\theta\right) = \frac{L}{m}\sin\varphi\cos\lambda + (d) - \sin\lambda(b)),$$

which is equivalent to:

$$\dot{\psi}_g\underbrace{(u_a\cos\lambda + w_n\cos\psi_g + w_e\sin\psi_g)}_{(f)} = \frac{L}{m}(\sin\varphi\cos\lambda + \cos\varphi\sin\theta\sin\lambda) - \frac{T-D}{m}\cos\theta\sin\lambda.$$

Calculating (f) we have:

$$(f) = u_a \cos \lambda + w_n \cos \psi_g + w_e \sin \psi_g$$
$$= u_a \left(\frac{u_g - w_s}{u_a} \right) + w_s$$
$$= u_g.$$

Then going back to Eq (3.45) gives us:

$$u_g \dot{\psi}_g = \frac{L}{m} (\sin \varphi \cos \lambda + \cos \varphi \sin \theta \sin \lambda) - \frac{T - D}{m} \cos \theta \sin \lambda. \qquad (3.46)$$

Therefore, we are now able to control the ground track angle as we obtain its expression.

Controlling the vertical movement

To control vertical movement, we decide to separate level change scenarios into two categories: positive level change (the aircraft has to climb) and negative level change (the aircraft has to descent).

Indeed, when an aircraft has to climb during cruise phase, most of the time, it climbs at constant throttle and constant Mach/CAS speed (see Section 3.1.9 for more details), the ensuing flight path angle is then deducted.

While performing a descent, the Rate of Descent (ROD) is fixed and either the Mach/CAS speed remains constant, from there we can deduce the flight path angle θ and then the thrust.

The ROCD (Rate of Climb/Descent) is defined as the variation with time of the aircraft pressure altitude h. That is:

$$ROCD = \frac{dh}{dt} = \dot{h}. \qquad (3.47)$$

Thanks to ISA model, we have that h is given by (3.33). Therefore using chains rules, the time derivative of h is given by the following relation:

$$\dot{h} = \frac{\partial h}{\partial p} \dot{p}$$
$$= \frac{\partial h}{\partial p} \frac{\partial p}{\partial z} \dot{z}$$

as p only varies with altitude under ISA conditions. Moreover h is z, then we have that:

$$\dot{h} = \dot{z}.$$

When cruising at constant pressure altitude When cruising at constant pressure altitude, the aircraft is achieving zero Rate of Climb/Descent (ROCD): $\dot{h} = 0$. Therefore, to achieve a constant pressure altitude, we have to achieve a constant geometric altitude, $\dot{z} = 0$. Then, as $\dot{z} = v_a \cos \theta$ (3.12), we get $\theta = 0$.

Moreover we supposed that either Mach or CAS speed remains constant that is $\dot{v}_a = 0$ as $\dot{h}$ is zero. Therefore, we have that:

$$T = D + m(\dot{w}_n \cos \psi + \dot{w}_e \sin \psi).$$

When climbing at a given throttle From (3.22), we have that:

$$\dot{v}_a = \frac{T - D}{m} - g \sin \theta - \cos \theta (\dot{w}_n \cos \psi + \dot{w}_e \sin \psi).$$

Recording from section Section 3.1.9 that we have:

$$w_x = -w_n \sin \psi_g + w_e \cos \psi_g,$$
$$\text{and } w_s = w_n \cos \psi_g + w_e \sin \psi_g.$$

Let denote by $\overline{w_x} = \frac{w_x}{v_a}$ and $\overline{w}_s = \frac{w_s}{v_a}$.
We denote by $\dot{w}_v$ the wind derivative contribution to speed variation:

$$\dot{w}_v = \cos \theta (\dot{w}_n \cos \psi + \dot{w}_e \sin \psi).$$

Recording that:

$$\sin \lambda = \frac{w_x}{u_a} = \frac{w_x}{v_a \cos \theta} = \frac{\overline{w}_x}{\cos \theta},$$
$$\text{and } \cos \lambda = \frac{u_g - w_s}{u_a} = \frac{\sqrt{\cos^2 \theta - \overline{w}_x^2}}{\cos \theta}.$$

We can rewrite $\dot{w}_v$ as:

$$
\begin{aligned}
\dot{w}_v &= \dot{w}_n \cos \theta \cos \psi + \dot{w}_e \cos \theta \sin \psi \\
&= \dot{w}_n \cos \theta \cos(\psi_g - \lambda) + \dot{w}_e \cos \theta \sin(\psi_g - \lambda) \\
&= \dot{w}_n \cos \theta (\cos \psi_g \cos \lambda + \sin \psi_g \sin \lambda) + \dot{w}_e \cos \theta (\sin \psi_g \cos \lambda - \sin \lambda \cos \psi_g) \\
&= \dot{w}_n \cancel{\cos \theta} \left(\cos \psi_g \frac{\sqrt{\cos^2 \theta - \overline{w}_x^2}}{\cancel{\cos \theta}} + \sin \psi_g \frac{\overline{w}_x}{\cancel{\cos \theta}} \right) \\
&\quad + \dot{w}_e \cancel{\cos \theta} \left(\sin \psi_g \frac{\sqrt{\cos^2 \theta - \overline{w}_x^2}}{\cancel{\cos \theta}} - \frac{\overline{w}_x}{\cancel{\cos \theta}} \cos \psi_g \right).
\end{aligned}
$$

Then:

$$
\begin{aligned}
\dot{v}_a &= \frac{T - D}{m} - g \sin \theta - \dot{w}_n \left(\cos \psi_g \sqrt{\cos^2 \theta - \overline{w}_x^2} + \sin \psi_g \overline{w}_x \right) \\
&\quad - \dot{w}_e \left(\sin \psi_g \sqrt{\cos^2 \theta - \overline{w}_x^2} - \overline{w}_x \cos \psi_g \right) \\
&= \frac{T - D}{m} - \overline{w}_x (\dot{w}_n \sin \psi_g + \dot{w}_e \cos \psi_g) - g \sin \theta \\
&\quad - \sqrt{\cos^2 \theta - \overline{w}_x^2} (\dot{w}_n \cos \psi_g + \dot{w}_e \sin \psi_g).
\end{aligned}
$$

In general, $\dot{v}_a$ can be split into three terms:

$$\dot{v}_a = A_v + B_v \sin\theta + C_v\sqrt{\cos^2\theta - \overline{w}_x^2}.$$

Case 1: $\overline{w}_x \neq 0$

If $\overline{w}_x \neq 0$, we define ϵ such that $\cos\epsilon = \frac{\overline{w}_x}{\cos\theta}$, then:

$$\sin\theta = \sqrt{1 - \cos^2\theta}$$

$$= \sqrt{1 - \frac{\overline{w}_x^2}{\cos^2\epsilon}}, \text{ by def of } \epsilon$$

$$= \sqrt{1 - \overline{w}_x^2(1 + \tan^2\epsilon)}, \text{ as } \frac{1}{\cos^2\epsilon} = 1 + \tan^2\epsilon$$

and

$$\sqrt{\cos^2\theta - \overline{w}_x} = \sqrt{\overline{w}_x^2 \left(\frac{1}{\cos^2\epsilon} - 1 \right)}$$

$$= \overline{w}_x \tan\epsilon.$$

Using these expressions, we find:

$$\dot{v}_a = \frac{T - D}{m} - \overline{w}_x(\dot{w}_n \sin\psi_g + \dot{w}_e \cos\psi_g) - g\sqrt{1 - \overline{w}_x^2(1 + \tan^2\epsilon)}$$

$$\overline{w}_x \tan\epsilon(\dot{w}_n \cos\psi_g + \dot{w}_e \sin\psi_g)$$

and

$$\dot{v}_a = A_v + B_v\sqrt{1 - \overline{w}_x^2(1 + \tan^2\epsilon)} + C_v\overline{w}_x \tan\epsilon.$$

Subtracting those 2 equations, we have:

$$\left[\frac{T - D}{m} - \overline{w}_x(\dot{w}_n \sin\psi_g + \dot{w}_e \cos\psi_g) - A_v\right] - \overline{w}_x\left(\dot{w}_n \cos\psi_g + \dot{w}_e \sin\psi_g + C_v\right)\tan\epsilon$$

$$- (g + B_v)\sqrt{1 - \overline{w}_x^2(1 + \tan^2\epsilon)} = 0.$$

Denote now by A', B' and C' the following quantities:

$$A' = \frac{T - D}{m} - \overline{w}_x(\dot{w}_n \sin\psi_g + \dot{w}_e \cos\psi_g) - A_v$$

$$B' = g + B_v$$

$$C' = \dot{w}_n \cos\psi_g + \dot{w}_e \sin\psi_g + C_v$$

we have:

$$A' - C' \tan\epsilon - B'\sqrt{1 - \overline{w}_x^2(1 + \tan^2\epsilon)} = 0,$$

which is equivalent to:

$$A' - C' \tan\epsilon = B'\sqrt{1 - \overline{w}_x^2(1 + \tan^2\epsilon)}.$$

Taking the square on both side we have:

$$A'^2 - 2A'C' \tan \epsilon + C'^2 \tan^2 \epsilon = B'^2(1 - \overline{w}_x^2(1 + \tan^2 \epsilon)).$$

That is:

$$(C'^2 + B'^2\overline{w}_x^2) \tan^2 \epsilon - 2A'C' \tan \epsilon + A'^2 - B'^2 + B'^2\overline{w}_x^2 = 0.$$

Denoting by A, B, C the following quantities:

$$A = C'^2 + B'^2\overline{w}_x^2$$
$$B = -2A'C'$$
$$C = A'^2 - B'^2 + B'^2\overline{w}_x^2$$

we have:

$$A \tan^2 \epsilon + B \tan \epsilon + C = 0.$$

Solving this second degree equation in $\tan \epsilon$ allows us to retrieve the value of θ.

Case 2: $\overline{w}_x = 0$

If $\overline{w}_x = 0$, we still have:

$$\dot{v}_a = A_v + B_v \sin \theta + C_v \sqrt{\cos^2 \theta - \overline{w}_x^2}$$

and

$$v_a = \frac{T - D}{m} - \cos \theta (\dot{w}_n \cos \psi_g + \dot{w}_e \sin \psi_g).$$

Recalling that:

$$a \sin x = b \cos x = \sqrt{a^2 + b^2} \sin \left(x + \arctan \frac{b}{a} \right),$$

then

$$\frac{T - D}{m} - A_v - (g + B_v) \sin \theta - (\dot{w}_n \cos \psi_g + \dot{w}_e \sin \psi_g + C_v) \cos \theta = 0$$

$$\Leftrightarrow \frac{T - D}{m} - A_v = (g + B_v) \sin \theta - (\dot{w}_n \cos \psi_g + \dot{w}_e \sin \psi_g + C_v) \cos \theta$$

$$\Leftrightarrow \frac{T - D}{m} - A_v = \sqrt{(g + B_v)^2 + (\dot{w}_n \cos \psi_g + \dot{w}_e \sin \psi_g + C_v)^2}$$
$$\sin \left(\theta + \arctan \left(\frac{\dot{w}_n \cos \psi_g + \dot{w}_e \sin \psi_g + C_v}{g + B_v} \right) \right). \quad (3.48)$$

Finally we have,

$$\theta = \arcsin \left(\frac{\frac{T-D}{m} - A_v}{\sqrt{(g + B_v)^2 + (\dot{w}_n \cos \psi_g + \dot{w}_e \sin \psi_g + C_v)^2}} \right) - \arctan \left(\frac{\dot{w}_n \cos \psi_g + \dot{w}_e \sin \psi_g + C_v}{g + B_v} \right).$$

At a given Mach

We have that:

$$v_a = M\sqrt{\kappa R T}$$

$$\Rightarrow \dot{v}_a = \frac{M\kappa R K \dot{h}}{2\sqrt{\kappa r T}},$$

replacing $\dot{h}$ by $\dot{z}$, we have:

$$\dot{v}_a = \frac{M^2 \kappa R K \sin\theta}{2}.$$

That is in this case, we have $A_v = 0$, $B_v = \frac{M^2\kappa R K}{2}\sin\theta$ and $C_v = 0$. Then if $\overline{w}_x \neq 0$, we solve the second degree equation:

$$A\tan^2\epsilon + B\tan\epsilon + C = 0,$$

where

$$
\begin{cases}
A &= C'^2 + B'^2\overline{w}_x^2 \\
B &= -2A'C' \\
C &= A'^2 - B'^2(1-\overline{w}_x^2)
\end{cases}
\quad\text{and}\quad
\begin{cases}
A' &= \frac{T-D}{m} - \overline{w}_x(\dot{w}_n\sin\psi_g + \dot{w}_e\cos\psi_g) \\
B' &= g + \frac{M^2\kappa R K}{2} \\
C' &= \overline{w}_x(\dot{w}_n\cos\psi_g + \dot{w}_e\sin\psi_g)
\end{cases}
$$

If $\overline{w}_x = 0$, we have:

$$\theta = \arcsin\left(\frac{\frac{T-D}{m}}{\sqrt{(g+\frac{M^2\kappa R K}{2})^2 + (\dot{w}_n\cos\psi_g + \dot{w}_e\sin\psi_g)^2}}\right) - \arctan\left(\frac{\dot{w}_n\cos\psi_g + \dot{w}_e\sin\psi_g}{g + \frac{M^2\kappa R K}{2}}\right)$$

At a given CAS As we assume a ISA atmosphere, we have that

$$v_a = f(v_{CAS}, h),$$

as pressure depends only on the altitude. That implies

$$\dot{v}_a = \frac{\partial f}{\partial v_{CAS}}\dot{v}_{CAS} + \frac{\partial f}{\partial h}\dot{h}.$$

As $\dot{v}_{CAS} = 0$, we have that:

$$\dot{v}_a = \frac{\partial f}{\partial h}\dot{h} := f_h\dot{h}.$$

That is:

$$v_a(h) = \sqrt{\frac{2\rho}{\mu\rho_0}\left[\frac{p_0}{p}A + 1\right]^\mu - 1}$$

with $A = \left[\frac{1}{2}\mu v_{CAS}^2 \left(\frac{\rho_0}{p_0} + 1\right)\right]^{\frac{1}{\mu}} - 1$.

Then:

$$v_a(h) = \sqrt{\frac{2p_0}{\mu\rho_0}}\sqrt{\theta_{tr}\left[\left(\theta_{tr}^{g/KR}A + 1\right)^\mu - 1\right]}$$

with θ_{tr} the temperature ratio (see Section Section 3.1.9).

Then

$$f_h = \frac{1}{2}\sqrt{\frac{2p_0}{\mu\rho_0}}\frac{\frac{d}{dh}\left[\theta_{tr}\left[\left(\theta_{tr}^{g/KR}A + 1\right)^\mu - 1\right]\right]}{\sqrt{\theta_{tr}\left[\left(\theta_{tr}^{g/KR}A + 1\right)^\mu - 1\right]}}$$

$$= \frac{p_0}{\mu\rho_0 v_a(h)}\frac{d}{dh}\left[\theta_{tr}\left[\left(\theta_{tr}^{g/KR}A + 1\right)^\mu - 1\right]\right]$$

$$= \frac{p_0}{\mu\rho_0 v_a(h)}\left[\theta_{tr}\frac{d}{dh}\left[\left(\theta_{tr}^{g/KR}A + 1\right)^\mu - 1\right] + \theta_h\left[\left(\theta_{tr}^{g/KR}A + 1\right)^\mu - 1\right]\right]$$

with θ_h given by:

$$\theta_h = \frac{d}{dh}\theta_h$$
$$= \frac{dT(h)}{dhT_0}$$
$$= \frac{d}{dh}\frac{T_0 + Kh}{T_0}$$
$$= \frac{K}{T_0}.$$

Then it follows that:

$$f_h = \frac{p_0}{\mu\rho_0 v_a(h)}\left[\theta_{tr}\frac{d}{dh}\left[\left(\theta_{tr}^{g/KR}A + 1\right)^\mu - 1\right] + \frac{K}{T_0}\left[\left(\theta_{tr}^{g/KR}A + 1\right)^\mu - 1\right]\right].$$

As $\frac{d}{dh}\left[\left(\theta_{tr}^{g/KR}A + 1\right)^\mu - 1\right] = \mu\left(\theta_{tr}^{g/KR}A + 1\right)^{\mu-1}A\frac{d}{dh}\left[\theta_{tr}^{g/KR}\right]$, we have:

$$f_h = \frac{p_0}{\mu\rho_0 v_a(h)}\left[\theta_{tr}\mu\left(\theta_{tr}^{g/KR}A + 1\right)^{\mu-1}A\frac{d}{dh}\left[\theta_{tr}^{g/KR}\right] + \frac{K}{T_0}\left[\left(\theta_{tr}^{g/KR}A + 1\right)^\mu - 1\right]\right]$$

$$= \frac{\cancel{p_0}}{\cancel{mu\rho_0}v_a(h)}\left[\frac{g\cancel{\theta_{tr}}\cancel{\mu}\cancel{K}}{\cancel{K}\cancel{R}\cancel{T_0}}(\theta_{tr}^{g/KR}A + 1)^{\mu-1}A\theta_{tr}^{g/KR-1} + \frac{KR}{\cancel{T_0}\mu}(\theta_{tr}^{g/KR}A + 1)^\mu - \frac{KR}{\cancel{T_0}\mu}\right]$$

$$= \frac{1}{v_a(h)}\underbrace{\left[g(\theta_{tr}^{g/KR}A + 1)^{\mu-1}A\theta_{tr}^{g/KR} + \frac{KR}{\mu}(\theta_{tr}^{g/KR}A + 1)^\mu - \frac{KR}{\mu}\right]}_{F}$$

$$= \frac{F}{v_a(h)}.$$

Then:

$$\dot{v}_a = \frac{F}{v_a(h)}\dot{h} = F\sin\theta.$$

That is in this case, we have $A_v = 0$, $B_v = F$ and $C_v = 0$.

If $\overline{w}_x \neq 0$, $A \tan^2 \epsilon + B \tan \epsilon + C = 0$ with:

$$
\begin{cases}
A &= C'^2 + B'^2 \overline{w}_x^2 \\
B &= -2A'C' \\
C &= A'^2 - B'^2(1 - \overline{w}_x^2)
\end{cases}
\quad \text{and} \quad
\begin{cases}
A' &= \frac{T-D}{m} - \overline{w}_x(\dot{w}_n \cos \psi_g + \dot{w}_e \sin \psi_g) \\
B' &= g + F \\
C' &= \overline{w}_x(\dot{w}_n \cos \psi_g + \dot{w}_e \sin \psi_g)
\end{cases}
$$

If $\overline{w}_x = 0$,

$$
\theta = \arcsin \left(\frac{\frac{T-D}{m}}{\sqrt{(g+F)^2 + (\dot{w}_n \cos \psi_g + \dot{w}_e \sin \psi_g)^2}} \right) - \arctan \left(\frac{\dot{w}_n \cos \psi_g + \dot{w}_e \sin \psi_g}{g + F} \right).
$$

Iterative algorithm As one may have noticed, to calculate θ, we need to know the wind derivative: $\dot{w}_n$ and $\dot{w}_e$. Indeed, recording their definition here:

$$
\begin{cases}
\dot{w}_n &= \frac{\partial w_n}{\partial x} \dot{x} + \frac{\partial w_n}{\partial y} \dot{y} \\
\dot{w}_e &= \frac{\partial w_e}{\partial x} \dot{x} + \frac{\partial w_e}{\partial y} \dot{y}
\end{cases}
$$

and knowing that:

$$
\begin{cases}
\dot{x} &= v_a \cos \theta \cos \psi \\
\dot{y} &= v_a \cos \theta \sin \psi
\end{cases}
$$

means that θ is needed to compute the wind derivatives. Therefore, we propose here to use an iterative algorithm to compute θ as it has to verify two equations using a tolerance error θ_{tol} (see Algorithm 7).

Algorithm 7 Iterating algorithm calculating a feasible flight path angle θ

Require: θ_{init}, θ_{tol}
Ensure: Computation of θ

> Begin

$i \leftarrow 0$
$\theta_{error} \leftarrow \infty$
while $\theta_{error} > \theta_{tol}$ **do**
  $\theta_{guess} \leftarrow \theta_i$
  Compute Drag
  Compute kinematics
  Compute wind derivatives
  $i \leftarrow i + 1$
  Compute θ_i
  $\theta_{error} = |\theta_{i+1} - \theta_i|$
end while

> End

When descending at a given Mach with a given ROD Descending at a given ROD means that: $\dot{h}_p = \alpha$. Then we have $\theta = \sin^{-1}\left(\frac{\alpha}{v_a}\right)$. As

$$\dot{v}_a = \frac{M}{2\sqrt{\kappa RT}}\kappa RK\dot{h}$$

and

$$\dot{v}_a = \frac{T - D}{m} - g\sin\theta - \cos\theta(\dot{w}_n\cos\psi + \dot{w}_e\sin\psi),$$

we have that:

$$\frac{M}{2\sqrt{\kappa RT}}\kappa RK\dot{h} = \frac{T - D}{m} - g\sin\theta - \cos\theta(\dot{w}_n\cos\psi + \dot{w}_e\sin\psi)$$

$$\Rightarrow T = \frac{mM}{2\sqrt{\kappa RT}}\kappa RK\dot{h} + mg\sin\theta + m\cos\theta(\dot{w}_n\cos\psi + \dot{w}_e\sin\psi) + D.$$

When descending at a given CAS with a given ROD Descending at a given ROD means that: $\dot{h}_p = \alpha$. Then we obtain $\theta = \sin^{-1}\left(\frac{\alpha}{v_a}\right)$. As

$$\dot{v}_a = \frac{F}{v_a}\dot{h}$$

and

$$\dot{v}_a = \frac{T - D}{m} - g\sin\theta - \cos\theta(\dot{w}_n\cos\psi + \dot{w}_e\sin\psi),$$

we have that:

$$\frac{F}{v_a}\dot{h} = \frac{T - D}{m} - g\sin\theta - \cos\theta(\dot{w}_n\cos\psi + \dot{w}_e\sin\psi)$$

$$\Rightarrow T = \frac{mF}{v_a}\dot{h} + mg\sin\theta + m\cos\theta(\dot{w}_n\cos\psi + \dot{w}_e\sin\psi) + D.$$

Controlling the ground track angle and the horizontal position

As we have already mention in this document we adopt the fly-by method to compute turn trajectories. We assume here that ground trajectories are describing an arc of circle tangent to tracks. It should be noted here that, in presence of wind, air trajectories differ from ground trajectories and are not an arc of circle. Let us denoted by $\Delta\psi_g^i$ the orientation change of the track between way-point O_i and O_{i+1}.

By definition of the fly-by method, aircraft start turning before reaching their next way point such that their trajectory describe an arc of circle tangent to the ground tracks. The distance at which the aircraft starts turning depends only on the radius of the turn and on the track change angle $\Delta\psi_g^i$. On Figure 3.15, this distance is denoted by d_i and
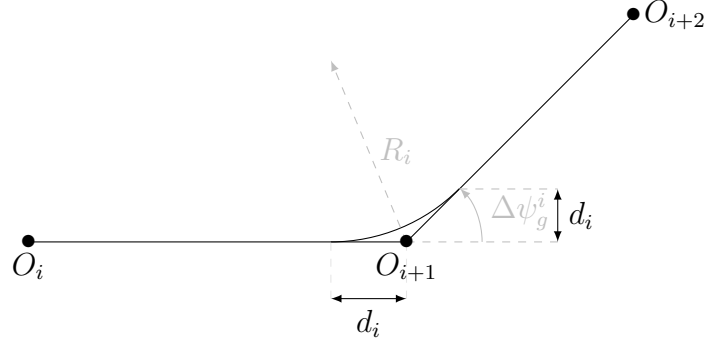
Figure 3.15: Geometry of turn between two way points

we can see from this figure that:

$$d_i = R_i \tan\left(\frac{\Delta\psi_g^i}{2}\right). \tag{3.49}$$

The distance from the way point O_{i+1} to the point at which the aircraft is going to intercept the following track is the same as the distance between the way point and the point at which the aircraft is starting to turn. The aircraft starts to turn when the distance between its along-track position and the way point is less than or equal to d_i.

The radius of the turn depends essentially on the bank angle and on the aircraft ground speed. As we assume that the ground trajectory is an arc of circle, the radius as to be kept constant. Therefore the bank angle have to be adjusted during the turn as long as the ground speed changes.

When predicting the trajectory of the aircraft, as ground speed is a derived state variable, the ground speed is not known beforehand. Therefore, the turn radius is not known neither the starting point nor the ending point. In this work, we have decided to use an iterative method to determine all the turn characteristics.

Turn dynamics   Taking into account the wind, the ground turn dynamics can be written as follow (see Section 3.1.9 for more details):

$$u_g\dot{\psi}_g = \frac{L}{m}(\sin\varphi\cos\lambda + \cos\varphi\sin\theta\sin\lambda) - \frac{T-D}{m}\cos\theta\sin\lambda. \tag{3.50}$$

We make the assumption that during turn, θ remains 0, that is Eq. (3.50) can be rewritten as follow:

$$u_g\dot{\psi}_g = \frac{L}{m}\sin\varphi\cos\lambda - \frac{T-D}{m}\sin\lambda$$

with $\cos \lambda = \sqrt{1 - \overline{w}_x^2}$ and $\sin \lambda = \overline{w}_x$.

Instead of using L, we use the vertical load factor which is defined by the following relation:

$$n_z = \frac{L}{mg}. \tag{3.51}$$

Using (3.51) into Eq. (3.50) we obtain:

$$u_g \dot{\psi}_g = g n_z \sin \varphi \cos \lambda - \frac{T - D}{m} \sin \lambda.$$

Using the forth equation of system (3.22) we have that:

$$\frac{T - D}{m} = \dot{v}_a + (\dot{w}_n \cos \psi + \dot{w}_e \sin \psi).$$

Replacing $\frac{T-D}{m}$ by the previous expression, we obtain:

$$u_g \dot{\psi}_g = g n_z \sin \varphi \cos \lambda - (\dot{v}_a + \dot{w}_n \cos \psi + \dot{w}_e \sin \psi) \sin \lambda$$
$$= g n_z \sin \varphi \cos \lambda - \dot{v}_a \sin \lambda - (\dot{w}_n \cos \psi + \dot{w}_e \sin \psi) \sin \lambda. \tag{3.52}$$

As $\dot{\theta} = 0$, we have by the second equation of the system (3.11) that:

$$0 = \frac{1}{v_a} \left[\frac{L}{m} \cos \varphi - g \right].$$

Therefore we obtain for n_z:

$$n_z = \frac{1}{\cos \varphi}. \tag{3.53}$$

Furthermore, we assume that turns are executed at constant ground radius R_i, that is:

$$\dot{\psi}_g^i = u_g \kappa_i \tag{3.54}$$

where $\kappa_i = \frac{1}{R_i}$ if the aircraft is turning right and $-\frac{1}{R_i}$ if it is turning left.

Using Eqs. (3.54) and (3.53) into Eq. (3.52) we obtain:

$$u_g^2 \kappa_i = \frac{g}{\cos \varphi} \sin \varphi \cos \lambda - \dot{v}_a \sin \lambda - (\dot{w}_n \cos \psi + \dot{w}_e \sin \psi) \sin \lambda$$
$$= \tan \varphi \underbrace{g \cos \lambda - [\dot{v}_a + (\dot{w}_n \cos \psi + \dot{w}_e \sin \psi)] \sin \lambda}_{(a)}. \tag{3.55}$$

This equation can be used to compute the bank angle if the state variables and the

curvature are known (Eq (3.56)):

$$\varphi = \arctan\left(\frac{u_g^2 \kappa_i}{(a)}\right). \tag{3.56}$$

On the reverse angle, if the bank angle and all the state variables are known we can use it to calculate the curvature:

$$\kappa_i = \frac{\tan\varphi g \cos\lambda - [\dot{v}_a + (\dot{w}_n \cos\psi + \dot{w}_e \sin\psi)]\sin\lambda}{u_g^2}. \tag{3.57}$$

We describe in the next section how to find a suitable radius of turn to not exceed the maximum bank angle and also reach the next leg with the good track angle.

Iterative algorithm   As we have seen, a maximum bank angle is specified for all *Aircraft_type*. For each turning point, an initial bank angle (say $\varphi_{max}/2$) is supposed.

With this initial guess, the curvature of the trajectory is computed using (3.55) at each step of the integration scheme. Having the radius of the turn, the turn initiation distance d_i is also computed using (3.49). Then we check if the distance to the next way point is greater than or less than the initiation distance. In the former case the turn does not start, and we make another integration step.

When the distance is less than or equal to the initiation distance computed with the guess bank angle, the turn starts and we store the time index. From now on, the turn radius is kept constant and using (3.56), we compute φ as long as u_g changes for each integration step and we store all the values of it. We also compute at this step the instantaneous rate of turn $\dot{\psi}_g$ at each integration step using (3.54).

When the turn ends, that is when the instantaneous turn radius reach $\Delta\psi_g^i$, the set of historic bank angle is examined and if φ_{max} is not met neither $\dot{\psi}_{max}$, that means that the initial φ was an acceptable guess and we stop the algorithm. If one of these bound is reached then we start with a smaller initial bank angle. We resume this algorithm in the Algorithm 8.

Once we have found the φ, we use equation 1 and 2 of the system (3.22) to compute the horizontal position of the aircraft.

Finally, we derive all the control laws needed for the aircraft to follow the prescribed flight plan. However we did not take into account any disturbances coming from the environmental uncertainties yet. The next section is devoted to the development of a stochastic model for the aircraft motion based on the deterministic tool we have just developed.

3.2   Stochastic model

So far, we have developed a simulation tool based on numerical models for aerodynamics. Predicted trajectories may not behave as they would if experimentally measured. Reasons for this can be several :

Algorithm 8 Iterating algorithm calculating a feasible bank angle

Require: φ_{init}, φ_{max}, $\dot{\psi}_{max}$, $\Delta\varphi$
Ensure: Computation of turn characteristics
  Begin
  starting_turn = **false**
  $j \leftarrow j_0$
  $\varphi_j \leftarrow \varphi_{init}$
  while starting_turn == **false do**
    repeat
      Make an integration step
      $j \leftarrow j + 1$
      Compute κ_i using φ_{init}
      Compute d_i using φ_{init}
    until $d_i \leq s_i - s(t_j)$
    $index\_starting\_turn \leftarrow j$
    repeat
      Make an integration step
      $j \leftarrow j + 1$
      Compute φ_j
      Store φ_j in $\varphi_{history}$
      Compute $\dot{\psi}_g(t_j)$
    until $\dot{\psi}_g(t_j) \leq \Delta\psi_g^i$
    if $\max_j\{\varphi_{history}\} > \varphi_{max}$ **then**
      $j \leftarrow j_0$
      $\varphi_{init} \leftarrow \varphi_{init} - \Delta\varphi$
    else
      starting_turn==**true**
    end if
  end while
  End
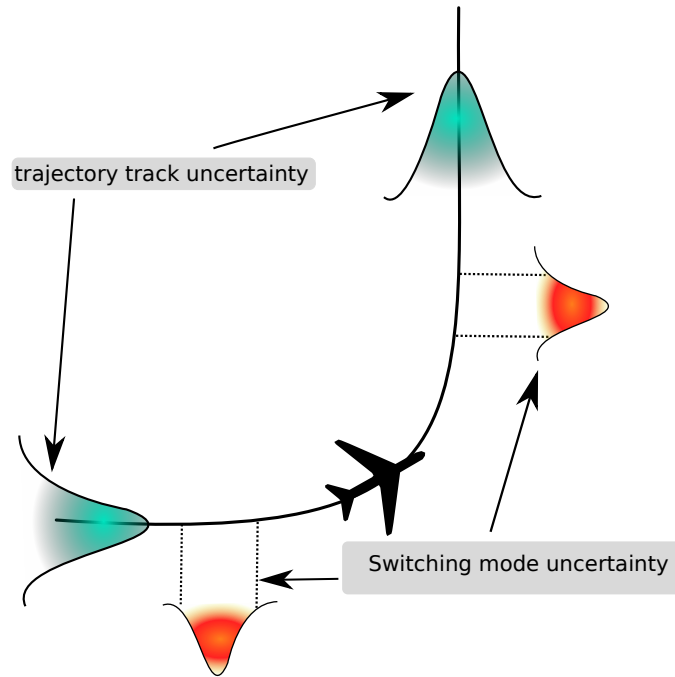
Figure 3.16: Pilot intents and trajectory uncertainties

- The model (3.22) is simplified in comparison with the reality,

- neither input parameters nor the initial states are fully known,

- measurements used for calibration are characterized by noise.

To take into account this lack of knowledge, we add uncertainty into the model. That is we reformulate (3.22) as further described in this section.

For sake of convenience we rewrite the system (3.22) as :

$$
\begin{cases}
\dot{\mathbf{x}}_t & = & \mathbf{f}_t(\mathbf{x}_t(\mathbf{u}_t, \mathbf{p}_t), \mathbf{u}_t(\mathbf{x}_t, \mathbf{p}_t), \mathbf{p}_t(\mathbf{x}_t, \mathbf{u}_t)), \quad t > t_0 \\
\mathbf{x}_0 & = & x(t_0) \\
\mathbf{x}_t & \in & [\mathbf{x}_{min}, \mathbf{x}_{max}] \\
\mathbf{u}_t(\mathbf{x}_t, \mathbf{p}_t) & \in & [\mathbf{u}_{min}, \mathbf{u}_{max}]
\end{cases}
$$

where $\mathbf{p}_t$ denotes the set of parameters and $\mathbf{u}_t$ the controls used to integrate this equation which depends on the state of the system.

3.2.1   Navigation deviation

We did not mention that the aircraft can derive from its initial flight plan. Indeed we make different modelization choices for the aircraft to follow the flight plan. Actually, the person who takes these decisions are the pilots of the aircraft. So a deviation can be observed on the actual aircraft trajectory. We represent these uncertainties on Figure 3.16.

In this work we choose to not model the pilots intents. Indeed, we take the decision to assume that the pilot will always follow the flight plan. Nevertheless, to integrate the uncertainties induced by the pilot intent, we presume that two modifications to the model should be added. The first one is to integrate a Markov switching model to the model we developed. Indeed, in our simulation tool we have different flight modes, for each mode of the flight we have a different control law. The uncertainties are then concentrated on the time the decision are going to be made. That is when the switch is made between modes. The second pilot deviation from the flight plan is its willingness to actually follow the straight lines between way-points. Therefore the ground tack angle, which have been previously considered as a fixed parameter should be modelled as random variable to account for these deviations.

3.2.2 Parameters, initial conditions and controls uncertainties

In this section three kinds of uncertainties are introduced to the state space equation (3.22), one in the parameter, $\mathbf{p}(\omega^{\mathbf{p}})$, one in the initial condition $\mathbf{x}_0(\omega^x)$ and one in the control law $\mathbf{u}(\omega^{\mathbf{u}})$ which are used to integrate the state equations and derived the control law of the system.

As we said, the uncertainties in the control vector $\omega^{\mathbf{u}}$ are neglected in the rest of the document since we do not model aircraft trajectories deviation. Indeed we do not take into into account the possibility for the pilot to do not respect the flight plan. This uncertainty would be modelled by a probability whose density is concentrated on the ground leg but spread around it. Moreover he has the possibility to turn before or after the point we calculate, this uncertainty would be modelled by a probability whose density is concentrated on the turning point and a double tail modelling its propensity to follow or not the flight plan. We illustrate this on Figure 3.16.

Then, only parameter uncertainties remain. Concerning them, we distinguish whether they are environment parameters such as wind, temperature and pressure whether there are intrinsic to the aircraft model, *i.e* all the parameters which were fit thanks to BADA database. We denote by Θ the atmospheric parameters and by p the aircraft parameters. Therefore, parameter uncertainties are modelled as a $(P, \mathcal{E})$-valued random variable : $p_t(\omega_t^p)$. The environment uncertainties are modelled as a $(\mathsf{E}_t^\Theta, \mathcal{E}')$- valued random variable denoted by $\Theta_t(\omega_t^\theta, \mathbf{x}_t)$. The aircraft initial state uncertainty is a $(\mathsf{E}_0^X, \mathcal{E})$-valued random variable, denoted by $\mathbf{x}_0(\omega_0^x)$.

Introducing these notations into (3.22), the deterministic model is transformed to :

$$
\begin{cases}
d\mathbf{x}_t = \mathbf{f}_t\left(\mathbf{x}_t(\mathbf{u}_t, p_t), \mathbf{u}_t(p_t, \mathbf{x}_t, \Theta_t), p_t(\omega_t^p, \mathbf{x}_t, \mathbf{u}_t, \Theta_t), \Theta_t(\omega_t^\theta, \mathbf{x}_t, \mathbf{u}_t)\right) dt, \quad t > t_0, \\
\mathbf{x}_0(\omega_0^x) = x(\omega_0^x, t_0) \\
\mathbf{x}_t \in [\mathbf{x}_{min}, \mathbf{x}_{max}] \\
\mathbf{u}(x_t, p_t, x_t^\theta) \in [\mathbf{u}_{min}, \mathbf{u}_{max}]
\end{cases}
\tag{3.58}
$$

Now it becomes clear that the aircraft process is a random process evolving in a random media and justifies the developments made in Chapter 2. Nonetheless, we developed in Chapter 2 techniques able to estimate both the random process and the random media in discrete time. Then we propose in the next section the integration scheme which turns the continuous dynamics of the aircraft into discrete ones.

3.3   Integration scheme

The multi Aircraft model we have developed so far requires the real time integration of a series of non linear differential equations. Since they cannot be solved analytically, we have to use a numerical integration method.

In our case the first order Euler method is adequate for the time step of 4 seconds we are interested in. Using the state vector $\mathbf{x}_k$ at time step t_k, the next time step state vector $\mathbf{x}_{k+1}$ is calculated using the following relation :

$$\mathbf{x}_{k+1} = \mathbf{x}_k + \nabla f(\mathbf{x}_k)\Delta t$$

A study on the integration scheme error was not held in this work. But it would be necessary to complete this work, a reference paper which gives details on the error introduced by the Euler discretization scheme is Bally and Talay (1996).

This chapter was dedicated to the construction of an aircraft model able to track an imposed flight plan, but also taking into account the atmospheric uncertainties. To this end, we established the dynamic equations starting from the Newton second law expressed in the aerodynamic reference frame. Then we express the kinematics equations of the aircraft around the ellipsoidal Earth. Further we explain how the aerodynamic parameters entering inside the model are set using the BADA database. Finally we explain how we derive the control laws and turn the deterministic set of equations into a stochastic hybrid systems. In the subsequent chapter, the deterministic model is used inside the particle filters we developed in **??**.

"A pessimist is an optimist who has plenty of experience."

André Bapst

4

Numerical experiments and applications

This chapter deals with the application of the algorithm we have developed in **??** in order to enhance the trajectory prediction tool we have built in Chapter 3. As we mention several times, aircraft parameters but also environmental ones are unknown. In order to improve the accuracy of the trajectory prediction, one basic idea consists in using observations delivers by civil radar equipments to learn these parameters. That is filtering out the noise from the radar measurements and learn the aircraft and environmental parameters using estimation techniques developed in **??**. Here we proceed step by step and we present several results obtained on different examples.

First, we present the results obtained on two pedagogical filtering problems using either Algorithm 2 or Algorithm 3. Then, the theoretical results, presented in Section 2.2.3 and Section 2.2.4, to qualify the estimate given by Algorithm 3 are illustrated. Algorithm 5 performance is also illustrated for a simple numerical experiment. After, results obtained thanks to the labeled island particle filter (Algorithm 3) to estimate the air traffic process when the aircraft model is simplified and the wind field synthetic are presented. From there, we gradually increase the complexity level of the model towards the final application: a point mass model for the aircraft and actual weather forecast for the wind field.

4.1   Application on toy models

In order to give an illustration of Algorithm 3, Algorithm 2 and of the theoretical results obtained to qualify the subsequent estimator, we present two estimation problems on toy-models. Then we present the results obtained thanks to Algorithm 5 on a simple filtering problem.

4.1.1 Applications of the labeled island particle filter

First let us introduce the example of a mobile whose evolution is influenced by an unknown force. Noisy observations of this physical systems are available. We resume the dynamics by the following system of equations :

$$
\begin{cases}
X_{n+1} &= X_n + V_n \begin{pmatrix} \cos\alpha \\ \sin\alpha \end{pmatrix} \Delta t + \Theta_{n+1}\Delta t + B_n^X \\
V_{n+1} &= V_n + B_n^V \\
Y_n &= h(X_n, V_n) + B_n^Y
\end{cases}
\tag{4.1}
$$

where X_{n+1} denotes the position of the mobile in the plane, V_n the proper speed of the mobile and Y_n their noisy observations through the observation function h, with $B_n^Y \sim \mathsf{N}(0, \Sigma^Y)$. The course track of the mobile α is constant over time. The vector Θ_n is a random variable and denotes the unknown force acting on the position of the mobile. Its equation of evolution is given by

$$
\Theta_{n+1} = \begin{pmatrix} \Theta_{n+1}^1 \\ \Theta_{n+1}^2 \end{pmatrix} = \begin{pmatrix} \cos\Theta_n^1 \\ \sin\Theta_n^2 \end{pmatrix} + B_n^\Theta
$$

with $B_n^\Theta \sim \mathsf{N}(0, \Sigma^\Theta)$. The initial condition of the system is given by $X_0 \sim \mathsf{N}(m_{\theta_0,0}^X, \Sigma_{\theta_0,0}^X)$, $V_0 \sim \mathsf{N}(m_0^V, \Sigma_0^V)$ and $\alpha = \pi/2$. We are interested in the estimation of the position of the mobile, which depends on the parameter Θ_n. We thus need to learn both the force, the speed and the position of the mobile. The tricky part is that there is no observation of the force. Here we will consider that the speed is a Poisson process, that is B_n^V is a Poisson process of intensity 0.03 where the jumps height is given by a standard normal distribution of variance 3. Concerning B_n^X, it is a Gaussian random variable such that $B_n^X \sim \mathsf{N}(0, \Sigma^X)$. We present now the results obtained for a simulating time of 125 minutes with $\Delta t = 15s$. The value of the different variances are set to

$$
\Sigma^\theta = \begin{pmatrix} 1 & 0 \\ 0 & 1 \end{pmatrix}, \ \Sigma^X = \Sigma_{\theta_0,0}^X = \begin{pmatrix} 1.5 & 0 \\ 0 & 1.5 \end{pmatrix}, \ \text{and } \Sigma^Y = \begin{pmatrix} 0.5 & 0 & 0 \\ 0 & 0.5 & 0 \\ 0 & 0 & 1 \end{pmatrix}.
$$

As one can notice, to estimate the law of the couple $(\Theta_n, \eta_{\Theta_{0:n},n}^X)$ given the observations $Y_{0:n}$, one can use Interacting Kalman filters and labeled island particle filters (LIPFs), detailed respectively in Algorithm 2 and Algorithm 3. We present comparative results obtained thanks to both methods.

Concerning the labeled version, the potential of each particle is given by the density of the observations, that is for all $x_n \in \mathsf{E}_n^X$ and for all $\theta_n \in \mathsf{E}_n^\Theta$:

$$
G_n(\theta_n, x_n) \propto \exp\left(-\frac{1}{2}(y_n - h(x_n, v_n))^T (\Sigma^Y)^{-1}(y_n - h(x_n, v_n))\right).
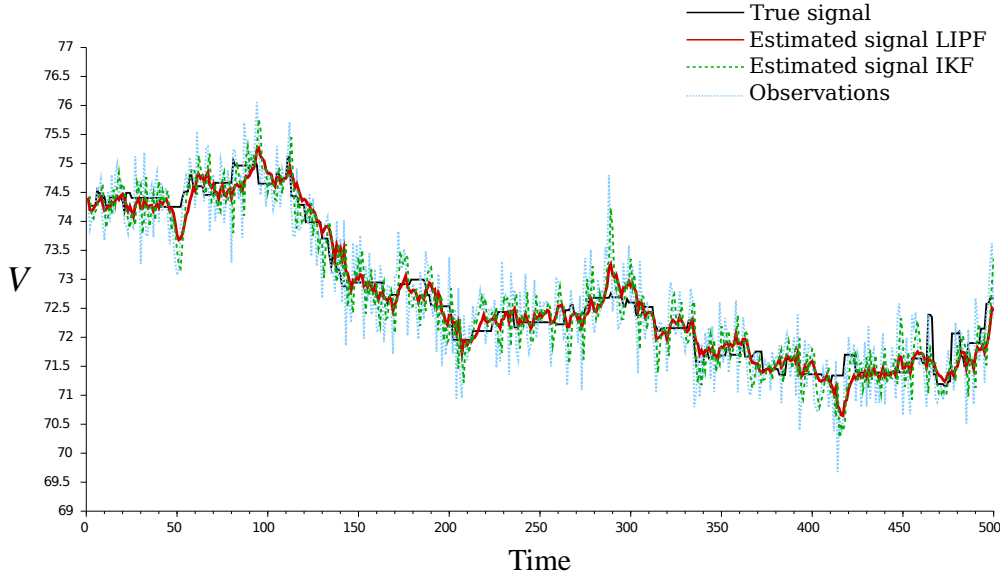$$

Figure 4.1: Temporal evolution (horizontal axis) of the reference mobile's speed given in $m.s^{-1}$ (black line), its observed (blue dotted line) and filtered counterparts (red obtained by the labeled island particle algorithm or green line obtained by IKF).In spite of the strong perturbation on the observations, the estimation of the speed is quite efficient with an absolute error smaller than 0.5 kt.

On all the figures the realization of the true signal is represented by the color black, the observations Y are represented by the color blue, the filtered signal obtained thanks to Algorithm 3 with $N_1 = 100$ and $N_2 = 300$ in red and results obtained using Algorithm 2 in green with $N_1 = 100$. On Figure 4.1, one realization of the signal V_n, its observed and its estimations counterparts are represented with respect to time. As one may observe, the true signal is well estimated by the technique we develop. Indeed, here the Interacting Kalman filter is not optimal as the noise sequence is not Gaussian. On Figure 4.3, we represent the temporal evolution of the force strength estimation. One can notice that even if no observation is available, we are able to find back the value of the true signal thanks to Algorithm 3 whereas Algorithm 2 retrieves only a global trend. Figure 4.2 represents the temporal evolution of one realization of the force orientation and its estimated counterparts. Results obtained thanks to Algorithm 3 give a better estimation of the true signal than the results obtained thanks to the Algorithm 2. From this example we can conclude that the labeled island particle filter is able to filter observations of the process while estimating the environment where the process evolves. Moreover the comparison with the Interacting Kalman filter algorithm shows that the labeled island particle filter is more effective to treat this double level estimation problem.

Let us consider the 2-D filtering problem inspired from the growth model Kitagawa (1987). This model, which is a standard benchmark example in the particle filtering literature, is
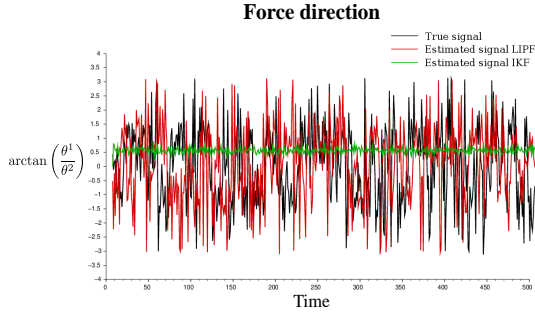
129

Figure 4.2: Temporal evolution (horizontal axis) of the reference force orientation (vertical axis) in *rad* (black line) and its estimated counterpart (red obtained by the labeled island particle algorithm or green line obtained by IKF). The estimation obtained thanks to IKF gives a mean trends whereas the labeled island particle algorithm retrieves the dynamics of the signal.
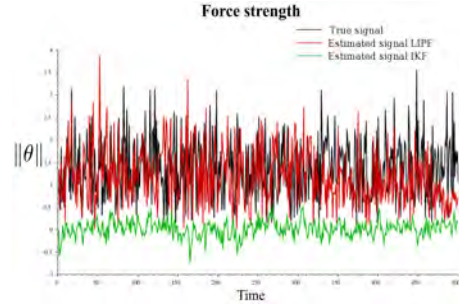

Figure 4.3: Temporal evolution (horizontal axis) of the reference force strength (vertical axis) in $m.s^{-1}$ (black line) and its estimated counterpart (red obtained by the labeled island particle algorithm or green line obtained by IKF). The estimation obtained thanks to IKF gives an underestimate mean trends whereas the labeled island particle algorithm retrieves the dynamics of the signal.

given by the following system of equations :

$$\begin{cases} \Theta_{n+1} &= 8\cos(1.2(n+1)) + B^\theta_{n+1} \\ X_{n+1} &= \dfrac{X_n}{2} + 25\dfrac{X_n}{1+X_n^2} + \Theta_{n+1} + B^X_{n+1} \\ Y_n &= X_n + B^Y_n \end{cases}$$

where $\Theta_0 \sim \mathsf{N}(0,\sigma_\theta^2)$, $X_0 \sim \mathsf{N}(0,\sigma_X^2)$, $B^\theta_{n+1} \sim \mathsf{N}(0,\sigma_\theta^2)$, $B^X_{n+1} \sim \mathsf{N}(0,\sigma_X^2)$ and $B^Y_n \sim \mathsf{N}(0,\sigma_Y^2)$.

We use the labeled island particle model to estimate the law of the couple $(\Theta_n, \eta^X_{\Theta_{0:n},n})$ given the observations $Y_{0:n}$, where the potential functions G_n are given by the likelihood of the observations, that is for all $x_n \in \mathsf{E}^X_n$ and $\theta_n \in \mathsf{E}^\Theta_n$:

$$G_n(\theta_n, x_n) \propto \exp\left(-\frac{(Y_n - x_n)^2}{2\sigma_Y^2}\right).$$

We present the results obtained for a simulating time of 1000 time steps. The different variances are set to $\sigma_\theta^2 = 1$, $\sigma_X^2 = 1$ and $\sigma_Y^2 = 10$. On all the figures the realization of the reference signal (also called true) is represented in black color, the observations Y are represented in blue, and the filtered signal obtained thanks to Algorithm 3 with $N_1 = 200$ and $N_2 = 100$ is represented in red. On Figure 4.4, one realization of the signal Θ and its estimation obtained thanks to the labeled island particle algorithm are represented on a small period of time. As one may observe, the true signal is well estimated even if no observations are available. On Figure 4.5, one realization of the process X is represented, its observed and its estimation counterparts. Even if the observations are really noisy, one is able to filter out the noise to find back the value of the true signal.
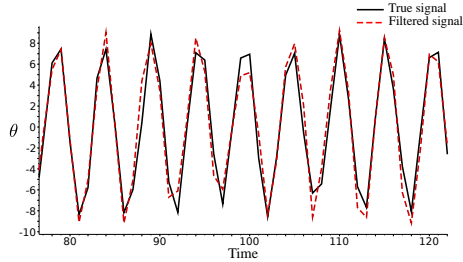
130

Figure 4.4: Temporal zoom (horizontal axis) on one realization of the Θ process (black line) and its estimated counterpart (red dashed line). The filter signal obtained thanks to the labeled island particle algorithm is really close to the reference signal.
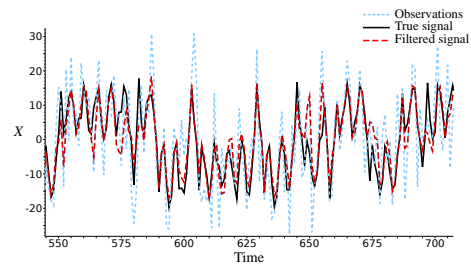

Figure 4.5: Temporal zoom (horizontal axis) on one realization of the X process (black line), its observed (blue dotted line) and estimated counterparts (red dashed line). The estimated signal obtained thanks to the labeled island particle algorithm retrieves the reference value even if the observations where really noisy.
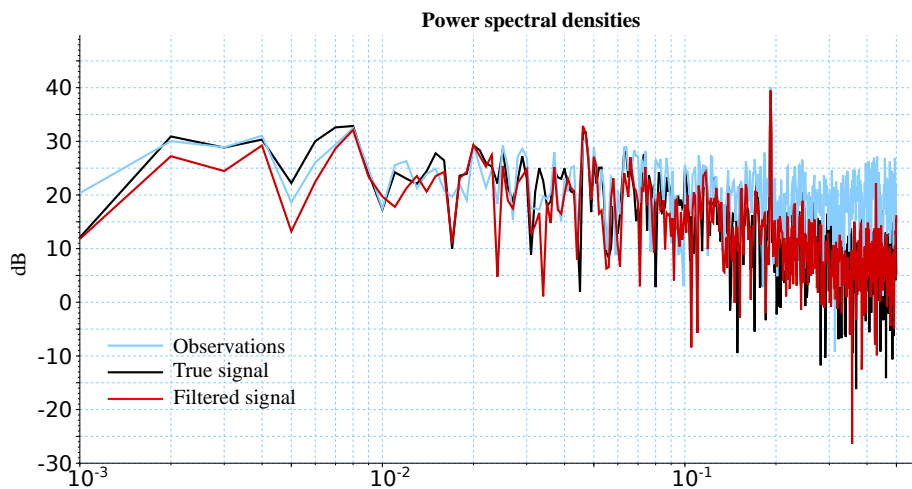
Figure 4.6: Reference (black line), filtered (red line) and observed (blue line) power spectral densities for one realization of the process X over 1000 time steps. The observed spectral densities has the same shape as a white noise for high frequencies. The filtered spectral density has the same shape as the reference signal and retrieves frequencies which are not present in the observed signal.
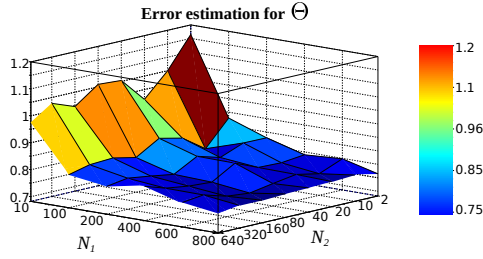
Figure 4.7: Evolution of the estimation's error (vertical axis, color-scale) for the law of Θ for 100 realizations of the process in function of N_1 and N_2. The error decreases as N_1 tends to infinity whatever the value of N_2 is.
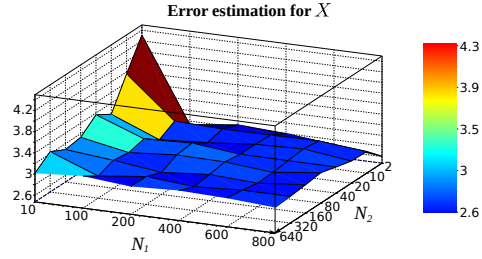

Figure 4.8: Evolution of the estimation's error (vertical axis, color-scale) for the law of X for 100 realizations of the process in function of N_1 and N_2. The error decreases as N_1 tends to infinity whatever the value of N_2 is.

Indeed, as one may have noticed, on Figure 4.6, the filtered power spectral density (in red) is closer to the black line, representing the "true" signal, than the observed power spectral density which has the same shape as a white noise for the high frequencies. Moreover, some frequencies are found even if there are not present in the observed signal. These two observations illustrate the convergence of the estimator constructed by the labeled island particle algorithm detailed in Algorithm 3.

Then we run 100 times the same experiment to get a sample of realizations for the true signal and the filtered signal. In that way one can illustrate the theoretical results obtained for the $\mathbb{L}^p$ error bound. On Figure 4.7 and Figure 4.8 are presented the $\mathbb{L}^2$ errors between the estimated law and the true law at one time step respectively for Θ and X in function of the number of islands N_1 and the number of particles inside each island N_2. This error decreases both with the number of particles and the number of islands as it was suggested by the Theorem 2.2.1. Concerning the variance of the error made between the true law and the filtered one, on Figure 4.9 and Figure 4.10 for Θ and X respectively, one can observe that the results obtained in Theorem 2.2.3 are confirmed. Moreover one can notice that the variance is more influenced by the number of islands than the number of particles inside each island. Indeed as in Figure 4.10, the variance obtained for a fixed time step is varying with respect to the number of islands and number of particles inside each islands. But if the number of islands influences the variance, we can observe that the number of particles inside each island does not seem to be really influent for a given number of islands.
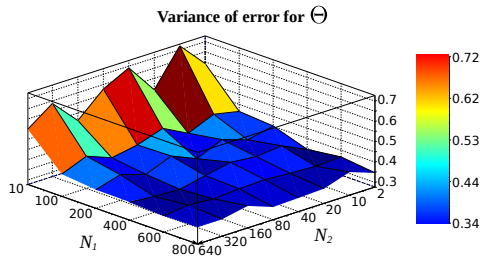
Figure 4.9: Evolution of the variance estimation's error (vertical axis, color-scale) for the law of Θ for 100 realizations of the process in function of N_1 and N_2. The variance decreases as N_1 tends to infinity whatever the value of N_2 is.
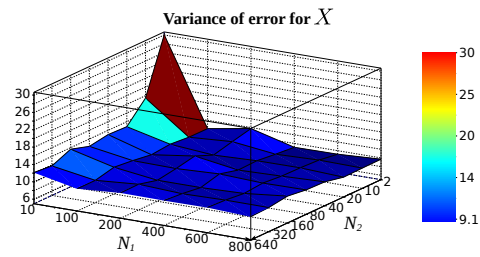

Figure 4.10: Evolution of the variance estimation's error (vertical axis, color-scale) for the law of X for 100 realizations of the process in function of N_1 and N_2. The variance decreases as N_1 tends to infinity whatever the value of N_2 is.

4.1.2 Application of the labeled island MCMC method

In order to illustrate Algorithm 5, we go back to the following dynamical system:

$$
\begin{cases}
\Theta_{n+1} &= \begin{pmatrix} \Theta_{n+1}^1 \\ \Theta_{n+1}^2 \end{pmatrix} = \begin{pmatrix} \cos \Theta_n^1 \\ \sin \Theta_n^2 \end{pmatrix} + B_n^\Theta \\
X_{n+1} &= X_n + V_n \begin{pmatrix} \cos \alpha \\ \sin \alpha \end{pmatrix} \Delta t + \Theta_{n+1} \Delta t + B_n^X \\
V_{n+1} &= V_n + B_n^V \\
Y_n &= h(X_n, V_n) + B_n^Y
\end{cases}
\tag{4.2}
$$

where as before X_{n+1} denotes the position of the mobile in the plane, V_n the proper speed of the mobile and Y_n their noisy observations through the observation function h, with $B_n^Y \sim \mathsf{N}(0, \Sigma^Y)$. The vector Θ_n is a random variable and denotes the unknown force acting on the position of the mobile, with $B_n^\Theta \sim \mathsf{N}(0, \Sigma^\Theta)$. Then the simulation set up is the same as in the first example used to illustrate the labeled island particle algorithm. Nevertheless, this time α is not known. The initial condition of the system is given by $X_0 \sim \mathsf{N}(m_{\theta_0,0}^X, \Sigma_{\theta_0,0}^X)$ and $V_0 \sim \mathsf{N}(m_0^V, \Sigma_0^V)$. We are interested in the estimation of the position of the mobile, which depends on the parameter Θ_n and α. We thus need to learn both the force, the speed, the direction and the position of the mobile. The tricky part is that there is no observation of the force. Here we will consider that the speed is a Poisson process, that is B_n^V is a Poisson process of intensity 0.3 where the jumps high is given by a standard normal distribution of variance 0.2. Concerning B_n^X, it is a Gaussian random variable such that $B_n^X \sim \mathsf{N}(0, \Sigma^X)$. We present now the results obtained for a simulating time of 25 minutes with $\Delta t = 15s$. The value of the different variances are set to

$$
\Sigma^\theta = \begin{pmatrix} 0.6 & 0 \\ 0 & 0.6 \end{pmatrix}, \ \Sigma^X = \Sigma_{\theta_0,0}^X = \begin{pmatrix} 0.1 & 0 \\ 0 & 0.1 \end{pmatrix}, \ \text{and} \ \Sigma^Y = \begin{pmatrix} 0.5 & 0 & 0 \\ 0 & 0.5 & 0 \\ 0 & 0 & 0.3 \end{pmatrix}.
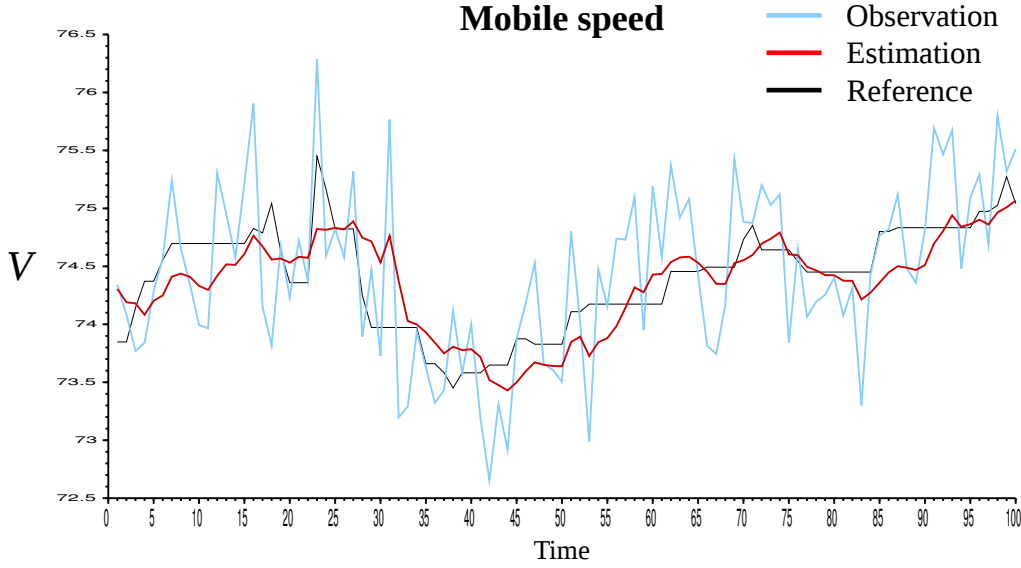$$

Figure 4.11: Temporal evolution (horizontal axis) of the reference mobile speed (black line), its observed (blue line) and filtered counterparts (red line) using Algorithm 5, given in $m.s^{-1}$ (vertical axis). The filtered signal obtained retrieves the Poissonian jumps even if the observations were really noisy.

As one can notice, to estimate the law of the couple $(\Theta_n, \eta^X_{\Theta_{0:n},n})$ and α given the observations $Y_{0:n}$, one can use Algorithm 5. We present here the results obtained thanks to this method where the potential of each particle is given by the density of the observations. That is for all $\alpha \in \mathbb{R}$, $(x_n, v_n) \in \mathsf{E}^X_n$ and for all $\theta_n \in \mathsf{E}^\Theta_n$:

$$G_{n,\alpha}(\theta_n, x_n) \propto \exp\left(-\frac{1}{2}(y_n - h(x_n, v_n))^T(\Sigma^Y)^{-1}(y_n - h(x_n, v_n))\right).$$

The MCMC iterations are obtained thanks to the Gaussian transition kernel. In other terms, the new proposition is obtained thanks to the following recursion :

$$\alpha^* = \alpha_{p-1} + B^\alpha_p$$

where $B^\alpha_p = \mathsf{N}(0,1)$. The first proposition for α is set to 0.

On all the figures the realization of the true signal is represented by the color black, the observations Y are represented by the color blue, the filtered signal obtained thanks to Algorithm 5 with $N_1 = 100$ and $N_2 = 200$ and in red with the number of MCMC iterations fixed to $n_{sample} = 1000$. On Figure 4.11, one realization of the signal V_n, its observed and its estimations counterparts are represented with respect to time. As one may observe, the true signal is well estimated by the technique we develop. On Figure 4.13, we represent the temporal evolution of the force strength estimation. One can notice that even if no observations are available, we are able to find back the value of the true signal thanks to Algorithm 5. Furthermore we see that with the MCMC iteration steps, the algorithm gives an estimation of the parameter α even if on this graph the MCMC algorithm does not converge yet towards the true value.
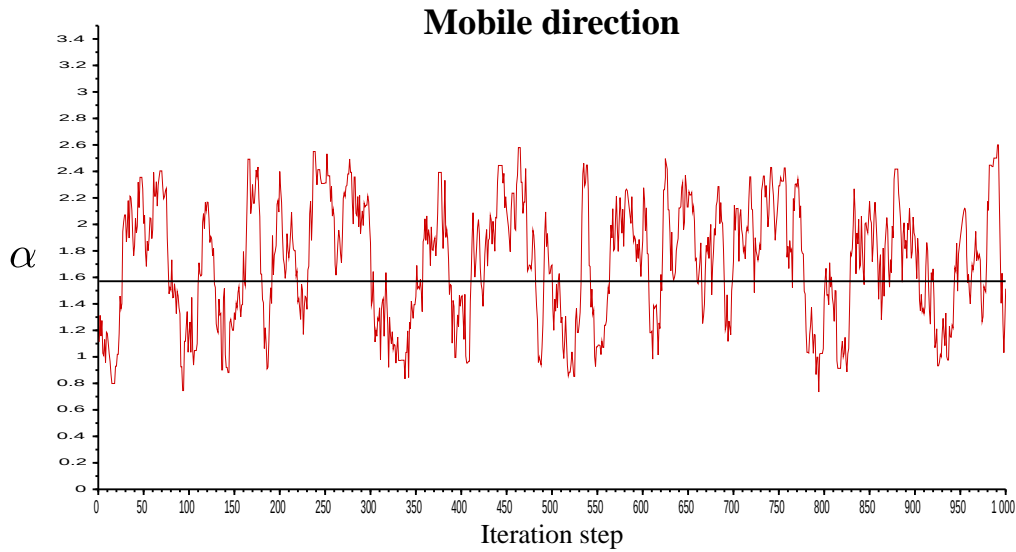
134

Mobile direction

Figure 4.12: Evolution of the mobile direction estimation (red line) and the reference one (black line) given in *rad* (vertical axis) along the MCMC algorithm iteration (horizontal axis). The evolution of the estimated parameter along the MCMC steps, shows that the algorithm has not yet converged towards the true parameter value.
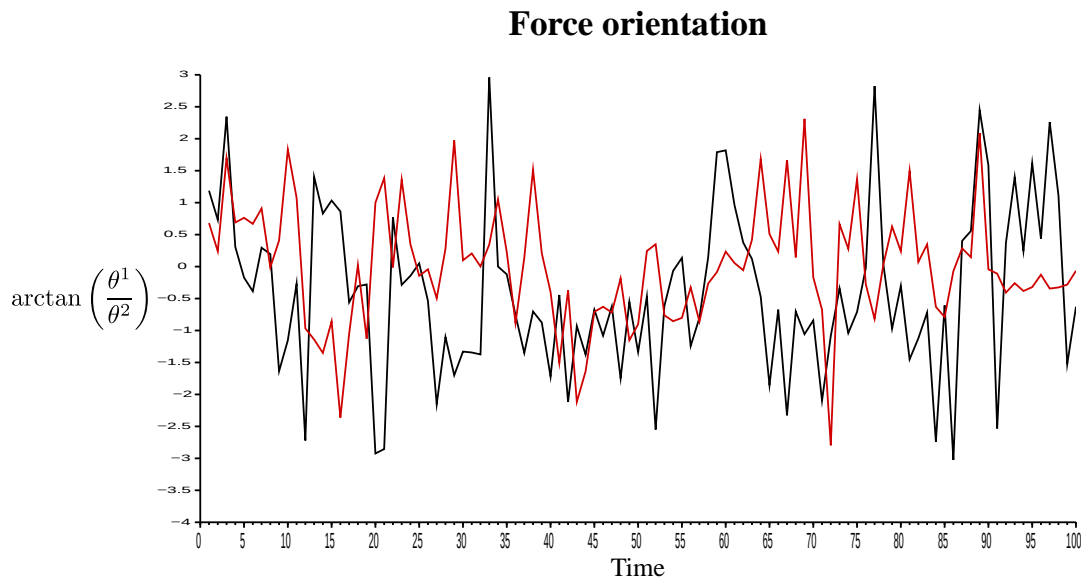

Force orientation

Figure 4.13: Temporal evolution (horizontal axis) of the reference force orientation (black line) and its estimated counterpart (red line) using lipMCMC in *rad* (vertical axis). Although no observations on this process were available, the filtered signal obtained thanks to the Algorithm 5 is quite close to the reference signal.
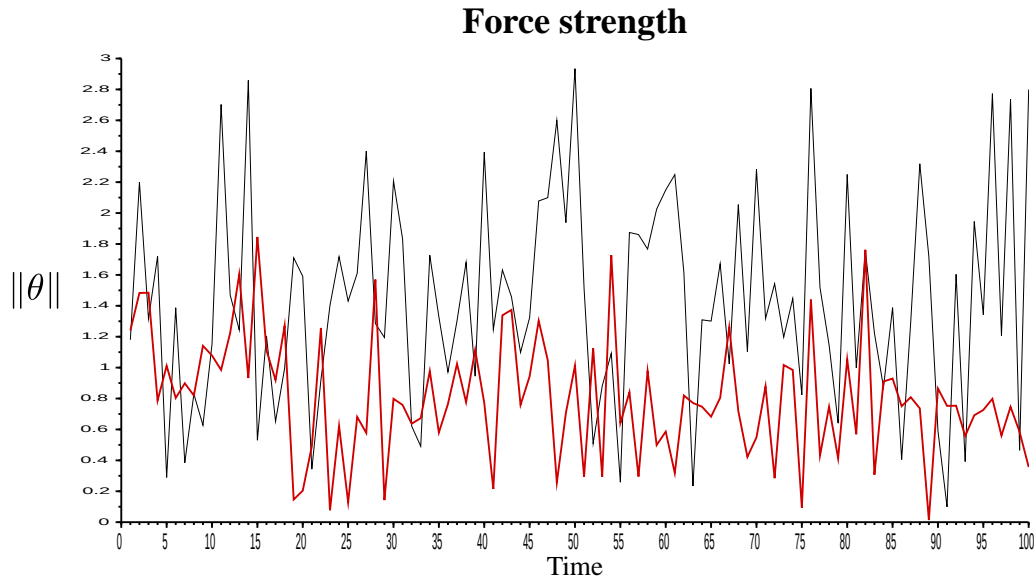
135

Force strength

Figure 4.14: Temporal evolution (horizontal axis) of the reference force strength (black line) and its estimated counterpart (red line) using lipMCMC in $m.s^{-1}$ (vertical axis). Although no observations on this process were available, the filtered signal obtained thanks to the Algorithm 5 is quite close to the reference signal

4.2 Learning a synthetic wind field with a simulated air-traffic using simplified aircraft model

As we said we are going step by step towards the final aim of this work: estimating the wind forecast error using observations delivered by aircraft along their trajectories. So far we have illustrated the effectiveness of the algorithm developed in Chapter 2 on toy-models. Now we apply the algorithm developed in Chapter 2 for random processes evolving in a random field on two simple experiments. That is we are going to use the acquisition processes formalism and their particle approximations introduced in Section 2.4 to estimate the air-traffic process and the wind field. By simple experiment, we mean that the aircraft model is a much simpler model than the one we have developed in Chapter 3 and that the wind field is synthetic. In the first case it is uniform in space and constant over time. In the second case it is decomposed in two uniform sub-domains which remain constants over time.

A uniform wind field is a field where the wind value is the same at every point of the configuration space. That means that each aircraft experiment the same wind. In this case we present the estimation of the air-traffic process and the wind field.

In the second case, when the wind field can be decomposed in two uniform sub-domains, we estimate the air-traffic but also the wind field on each uniform sub-domain.

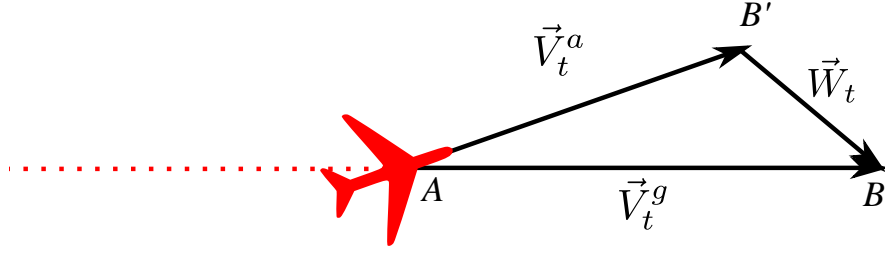Let us present the simplified model which is used in this section to simulate the air-traffic process.

Figure 4.15: Illustration of wind triangle at time t. The aircraft follows the trajectory represented by red dots, oriented along $\vec{AB}$ with an air-speed vector oriented along $\vec{AB'}$ which compensates the wind force $\vec{W}_t$.

4.2.1 Simplified aircraft model

The simplified model considers only the kinematics of the aircraft model in Cartesian coordinates and supposes that aircraft can only move along straight lines between two points in $\mathbb{R}^2$, say A and B with the air-speed at time t denoted by V_t^a.

Denote by $\vec{W}_t$ the wind at time t. It is possible to determine which ground speed the aircraft has along its prescribed ground trajectory. Let B' denotes the point in the air-mass that the aircraft should aim at to follow the prescribed ground trajectory. Define also the ground velocity vector of the aircraft at time t, denoted by $\vec{V_t^g}$ as follows:

$$\vec{V_t^g} = \alpha_t \frac{\vec{AB}}{\|\vec{AB}\|}, \text{ with } \alpha_t > 0 \tag{4.3}$$

where α_t is the ground speed of the aircraft. Using the wind triangle illustrated on Figure 4.15, we have:

$$\vec{V_t^g} = V_t^a \frac{\vec{AB'_t}}{\|\vec{AB'_t}\|} + \vec{W}_t. \tag{4.4}$$

Combining (4.3) with (4.4), and using Al-Kashi relation we obtain:

$$(V_t^a)^2 = \alpha_t^2 + \|\vec{W}_t\|^2 - 2\alpha_t \langle \frac{\vec{AB}}{\|\vec{AB}\|}, \vec{W}_t \rangle$$

where $\langle .,. \rangle$ signs for the scalar product. Then the precedent equation is equivalent to:

$$\alpha_t^2 - 2\alpha_t \langle \frac{\vec{AB}}{\|\vec{AB}\|}, \vec{W}_t \rangle + \|\vec{W}_t\|^2 - (V_t^a)^2 = 0. \tag{4.5}$$

Solving for α_t, (4.5), we have:

$$\alpha_t = \langle \frac{\vec{AB}}{\|\vec{AB}\|}, \vec{W}_t \rangle \pm \sqrt{\langle \frac{\vec{AB}}{\|\vec{AB}\|}, \vec{W}_t \rangle^2 - \left(\|\vec{W}_t\|^2 - (V_t^a)^2 \right)}. \tag{4.6}$$

We retrieve the aircraft ground speed along the straight line joining point A and B in presence of wind.

The discrete time evolution of the dynamic system from time step n to time step $n+1$ formed by the aircraft position in the ground frame, Z_{n+1}, and the air-speed V^a_{n+1}, is given by:

$$\begin{cases} Z_{n+1} &= Z_n + \alpha_n \Delta t \frac{\overrightarrow{AB}}{\|\overrightarrow{AB}\|} \\ V^a_{n+1} &= f_n(V^a_n, B_n) \end{cases} \tag{4.7}$$

where α_n is obtained using (4.6) and f_n is the evolution dynamic of V^a which is supposed to be given and dependent on a random process B_n.

4.2.2 Aircraft evolving in a random uniform environment

In this section we try to evaluate the uniform wind field denoted by $\Theta_n = \overrightarrow{W}$ using three independent aircraft processes, denoted by $\mathbb{X}_n = (Z^i_n, V^{a,i}_n)^3_{i=1}$.

These processes evolve using (4.7) with f^i_n defined for all $i = 1, 2, 3$ by:

$$V^{a,i}_{n+1} = V^{a,i}_n + B^i_n$$

where $B^i_n \sim \mathsf{N}(0, \sigma^V) \times \mathcal{P}(\lambda)$. The speed is a Poisson process, of intensity 0.03 where the jumps height is given by a standard normal distribution of variance 1, for every $i = 1, 2, 3$.

The initial distribution of each aircraft position process Z^i_0, denoted by $\eta^{Z^i}_{\Theta_{0,0}}$ is given by:

$$\eta^{Z^i}_0(\mathrm{d}z) = \delta_{A^i}(\mathrm{d}z)$$

where $A^1 = (-100, 400)$, $A^2 = (0, 0)$ and $A^3 = (400, 400)$. The initial distribution of each true air-speed process is given by:

$$\eta^{V^i}_0(\mathrm{d}v) = \mathsf{N}(0, \sigma^V) \times \mathcal{P}(\lambda)(\mathrm{d}v).$$

The aircraft are following the straight lines between their initial position and their final destination given respectively by:

$$B^1 = (0, 400), \ B^2 = (-400, 400) \text{ and } B^3 = (-400, -200).$$

The uniform wind field used to simulate the air-traffic reference process is given by the 2D-vector: $\overrightarrow{W} = (0, 75)$. That is, at each point of the configuration space E, the wind is given by this value. From the reference air-traffic process, we generate the observation process $\mathbb{Y}_n \triangleq (Y^i_n)^3_{i=1}$ thanks to the following equation:

$$Y^i_n = \begin{pmatrix} Z^i_n \\ V^{a,i}_n \end{pmatrix} + B^Y_n$$

where $B^Y_n \sim \mathsf{N}(0, \Sigma^Y)$, and $\Sigma^Y = \begin{pmatrix} 0.1 & 0 & 0 \\ 0 & 0.1 & 0 \\ 0 & 0 & 0.5 \end{pmatrix}$.

We use the labeled island particle model to estimate the law of the couple $(\Theta_n, \eta^{\mathbb{X}}_{\theta_{0:n}, n})$

given the observations $\mathbb{Y}_{0:n}$, where the potential functions G_n are given by the likelihood of the observations, that is for all $x_n \in (\mathsf{E}_n^X)^3$ and $\theta_n \in \mathsf{E}_n^\Theta$:

$$G_{\theta_n,n}(\mathbb{X}_n) \propto \prod_{i=1}^{3} \exp\left(-\frac{(Y_n^i - (Z_n^i, V_n^{a,i}))^T (\Sigma^Y)^{-1}(Y_n^i - (Z_n^i, V_n^{a,i}))}{2}\right).$$

We present the results obtained for a simulating time of 45 minutes, with $\Delta t = 4s$. Let the number of island $N_1 = 1000$ and the particle inside each island given by $N_2 = 100$. The wind propositions (or islands) are obtained thanks to:

- the normal distribution for its strength $\|W_n^i\|$ around the true value: 75, that is $\|W_n^i\| \sim \mathsf{N}(75, 1)$, for $i \in [\![1, 10]\!]$

- the uniform distribution for the direction β_n^i between $[\frac{\pi}{4}, \frac{3\pi}{4}]$, that is $\beta_n^i \in [\frac{\pi}{4}, \frac{3\pi}{4}]$, for $i \in [\![1, 100]\!]$.

Then we built $\theta_n^i = (\|W_n^i\|, \beta_n^i)_{i=1}^{1000}$ by pairing all the possibilities. On Figure 4.16, we present the evolution of the direction proposal's weight value (represented by the color scale) obtained thanks to the labeled island particle algorithm. The island number is given by the x-coordinate, and the time evolution on the y-coordinate. As one can observe, at the beginning of the experiment all the weight seems to be uniformly distributed. As time goes, one may observe that one island appears to have a highest value till it becomes the only one with a positive potential. It turns out that this island corresponds to the island for which the wind value is the closest to the wind used to create the reference air-traffic process. On Figure 4.17 and Figure 4.18, one realization of the processes $V_n^{a,1}$ and $V_n^{a,2}$ are respectively represented, its observed and its estimation counterparts. Even if observations are really noisy, one is able to filter out the noise to find back the value of the true signal.

Finally, we can say that the labeled island particle algorithm shows its ability to overcome the double estimation problem.

4.2.3 Aircraft evolving in a random decomposed uniform environment

We increase again the complexity of the simulation setting by using a synthetic wind field which is decomposed into two uniform domains remaining constant over time. That is we consider the situation where the wind is equal to one value on one side of the domain and to another one on the other side. Therefore, there are two domains $\mathsf{B}_{0,1}$ and $\mathsf{B}_{0,2}$ where the wind field has to be estimated. We resume the wind field value by the following equation:

$$\overrightarrow{W}_{x,y} = \begin{cases} (0, 75), & \text{for } x < 100 \\ \frac{45}{\sqrt{2}} \times (1, 1), & \text{for } x \geq 100 \end{cases}$$

The wind situation is represented on Figure 4.19. Then using three aircraft whose evolutions are given by the set of equations (4.7), we try to estimate the wind field and the

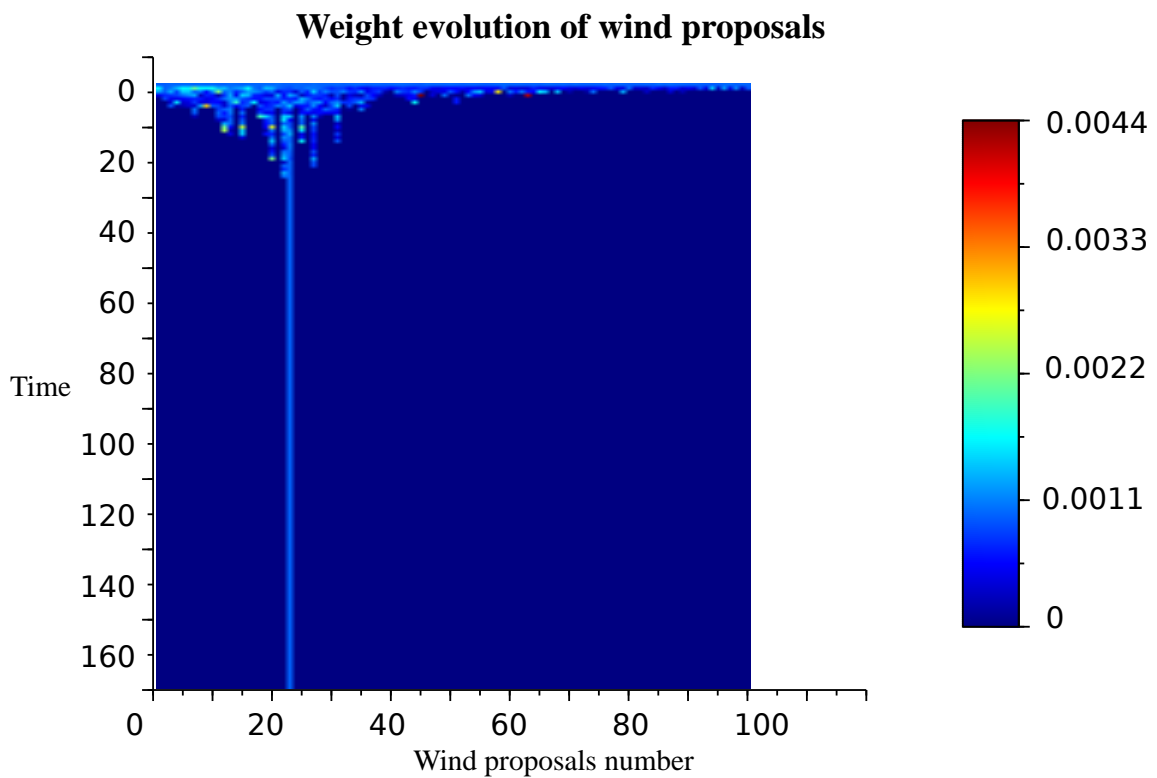**Weight evolution of wind proposals**

Figure 4.16: Time evolution (vertical axis) of the wind direction proposals likelihood (color-scale) with respect to the wind proposal number (horizontal axis). Using Algorithm 3,the maximum of weight is quickly concentrate over one direction giving the best forecast regarding to the air-traffic radar observations. In this example, the best forecast corresponds to the real direction.

Mobile airspeed for aircraft 1

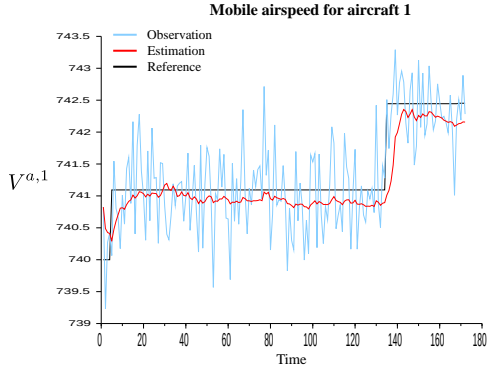**Mobile airspeed for aircraft 2**

Figure 4.17: Time evolution (horizontal axis) of the speed (vertical axis) reference process $V^{a,1}$ (black line), its observed (blue line) and estimated (red line) counterparts in $m.s^{-1}$. Estimated aircraft true airspeed by labeled island particle method. In spite of the strong perturbation on the observations, the estimation of the TAS is quite efficient with an absolute error smaller than 1 $m.s^{-1}$.
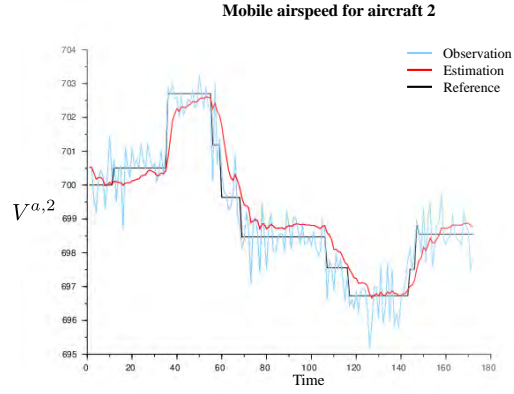
Figure 4.18: Time evolution (horizontal axis) of the speed (vertical axis) reference process $V^{a,2}$ (black line), its observed (blue line) and estimated (red line) counterparts in $m.s^{-1}$. Estimated aircraft true airspeed by labeled island particle method. In spite of the strong perturbation on the observations, the estimation of the TAS is quite efficient with an absolute error smaller than 1 $m.s^{-1}$.

air-traffic process using Algorithm 6. The reference process is obtained using the same parameters setting: $\sigma^V = 1$, $\lambda = 0.03$ and the air-traffic process has to follow the same flight plans as in the last section. The observations are obtained using the same scheme as in the last section, with the standard deviation matrix given by:

$$\Sigma^Y = \begin{pmatrix} 0.1 & 0 & 0 \\ 0 & 0.1 & 0 \\ 0 & 0 & 0.5 \end{pmatrix}.$$

In order to estimate the air-traffic process law and the wind field in each homogeneous domain, we use Algorithm 6. Then the parameters N_1 and N_2 are set as follow.

To estimate the wind field we use 5^5 proposals, or labeled islands. The proposals are obtained using the same procedure as in the last section. That is, first a proposal is made on the limit where the wind field value change. We assume here that we already know how the limit is but we do not know where it is located. That means that we know that it is vertical but we do not know at which x-coordinate the wind value switch takes place. The limit proposals are obtained using a uniform distribution between $[50, 150]$. Then a wind direction proposal is made using a uniform distribution on $[\frac{\pi}{4}, \frac{7\pi}{8}]$. For the wind strength, a normal distribution centered on the true value with standard deviation 1 is used. Concerning the second wind zone, direction proposals are uniformly distributed on $[0, \frac{\pi}{2}]$ and strength proposals are obtained using a normal distribution centered on the true value with standard deviation 1. Then combining all the proposals we have $N_1 = 5^5$. To estimate the air-traffic process, we set $N_2 = 100$.
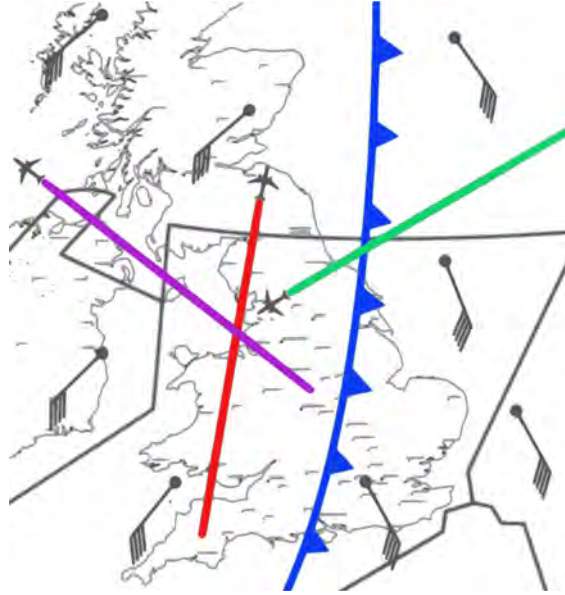
Figure 4.19: Example of possible numerical experiment. Crossing a sector control, there are a cold front and three En-Route aircraft moving with different speeds. The cold front is a limit of two domains with different wind directions. The purpose of the experiment is to estimate the likelihood of the weather and the aircraft airspeed using an ensemble of weather forecasts and radar observations.

We use the patchwork labeled island particle model to estimate the law of the couple $(\Theta_{n,\mathsf{B}_{0,l}}, \eta^{\mathbb{X}}_{\theta_{0:n},n}(\mathbb{1}_{\mathsf{B}_{0,l}}))^2_{l=1}$ given the observations $\mathbb{Y}_{0:n}$, where the potential functions $(G^l_n)^2_{l=1}$ are given by the likelihood of the observations, that is for all $x_n \in \mathsf{E}^X_n$ and $\theta_n \in \mathsf{E}^\Theta_n$:

$$G^l_{\theta_n,n}(\mathbb{X}_n) \propto \prod_{i=1}^{M} \exp\left(-\frac{(Y^i_n - (Z^i_n, V^{a,i}_n))^T (\Sigma^Y)^{-1} (Y^i_n - (Z^i_n, V^{a,i}_n))}{2}\right).$$

where M is given by the number of aircraft present at time n in the domain $\mathsf{B}_{0,l}$.

We present the results obtained for a simulating time of 45 minutes, with $\Delta t = 4s$.

The numerical results are quite good both for the learning of the Met environment and for the TAS of the aircraft. First we put our attention to the Met situation. As regards the limit, as soon as an aircraft experiment the limit, the true limit is perfectly determined. Figure 4.21 represents the likelihood evolution of the vertical limit proposals over time. First all the limit proposals are equivalent as no aircraft experiment the limit yet. Therefore the likelihood of all the proposal are the same. In the experiment only one aircraft is crossing the limit from the right to the left. When the aircraft is crossing a wrong proposal, the likelihood of the proposal decreases down to zero and gradually all the wrong limits obtain a weak likelihood. At the end, the highest likelihood limit proposal are concentrated on the left where the real limit is.

Once the limit between the two domains is known, we can put our interest on the meteorological parameters, for instance for the left area. First the likelihood of the wind direction forecasts is examined. As it might be noticed on Figure 4.20, the weight evolution of the direction proposals for the uniform domain on the left is concentrated over one proposition. At the beginning of the experiment the direction weights are distributed. Then
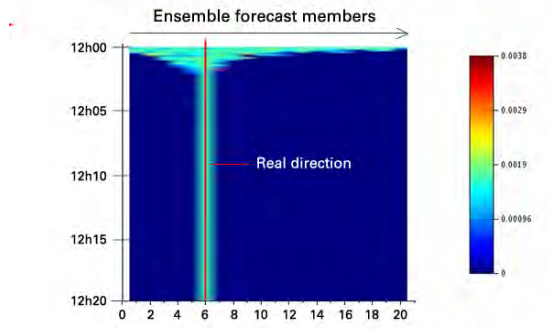
Figure 4.20: Likelihood evolution (in color) over time (y-axis from top to bottom) of direction proposals (x-axis) obtained with Algorithm 6 for the left uniform area. Using the algorithm, the maximum of weight is quickly concentrate over one direction giving the best forecast regarding to the air-traffic radar observations. In this example, the best forecast corresponds to the real direction.
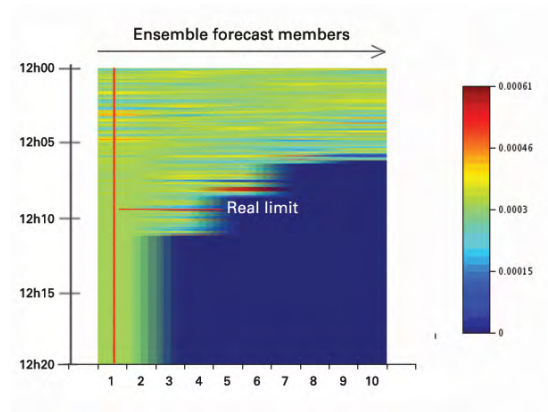
Figure 4.21: Time evolution (y-axis from top to bottom) of weight (color scale) of the different limit proposals (x-axis) between the two domain. The algorithm gives gradually the maximum of likelihood to the forecast which has the most probable limit. The other limit are excluded as soon as an aircraft experiment the border.
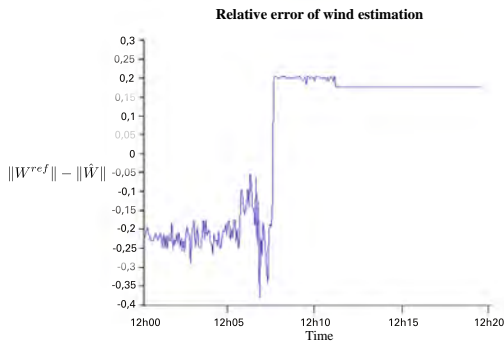
Figure 4.22: Evolution in time (x-axis) of the relative error of the estimated wind force using Algorithm 6 for one area to the real wind force. During the first third of the series, the error computed with two aircraft is not very stable. When a new aircraft is entering into the zone, the estimation is better and more stable. The relative errors on the wind force stay about 2%, i-e less than 1 kt.

Figure 4.23: Estimated aircraft true airspeed by Algorithm 6. In spite of the strong perturbation on the TAS observations, the estimation of the TAS is quite efficient with an absolute error smaller than 0.5 kt.

143

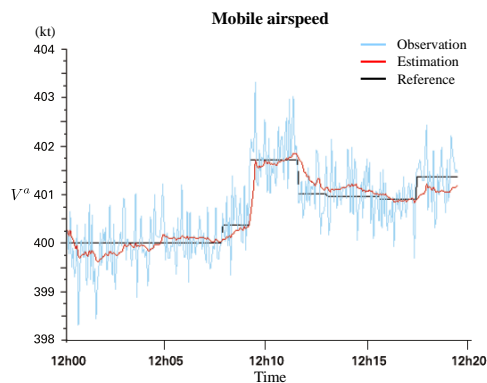using the Mode-S information, the weight starts to concentrate on only one direction till the end of the experiment. This weight concentration on one direction corresponds to the real direction which has been successfully learned.

The direction of the wind being learned, Figure 4.22 presents the wind force relative errors. One can see that this relative error is about 2%. Concerning the wind force, it seems to have two periods. The second period and the jump in the error values correspond to the entry of the right aircraft in the left area. In the first one, the relative errors are quite unstable showing the learning phase with two aircraft. While in the second period the relative error is very stable showing the end of the learning process with the three aircraft in the same domain.

While the environment parameters are learned by the patchwork labeled island particle system, the aircraft parameters are also estimated. In our experiment we only have to estimate the true airspeed of each aircraft about 400 kt. The airspeed estimation of one of these aircraft is represented in Figure 4.23. On this graphic, the black line represents the true airspeed which needs to be estimated (knots), the blue line the mode-S radar observations and the red line the reconstructed signal by the labeled island particle algorithm. Even if the perturbations of the TAS observation are strong, the estimation of the TAS is efficient picking out the Poissonian jump.

In this numerical experiment, we have shown the capability of our method to estimate the likelihood of an ensemble of Met forecasts while learning some aircraft parameters. For further experiments, we intend to work with multiple areas and more realistic meteorological forecasts. These results were presented during the ISIATM conference held in Toulouse in 2013 (see Ichard et al. (2013)), and in Stockholm for the 3rd Edition of the Sesar Innovation Days (see Baehr and Ichard (2013)).

4.3 Estimating a synthetic wind field using a simulated air-traffic using a 3DDL aircraft model

As we have said in the preamble of this section the difficulty of the numerical experiments increases gradually. This paragraph is devoted to the results obtained using the aircraft model we have developed in Chapter 3.

The principle of the aircraft model is illustrated in Figure 3.1 and the time evolution of the aircraft state is resumed by the set of equations (3.22) with initial conditions given by (3.23) and the constraints resumed in (3.24). Chapter 3 ended with a stochastic model for the aircraft dynamics. Implementing the stochastic version needs stochastic controls laws to be developed so that aircraft stay along their flight plans. This was out of the scope of this thesis project. A project named IMET was launched to answer this question in collaboration with the NLR and the UK MET office, Jacob et al. (2014). The core component will be a probabilistic trajectory predictor able to deals with uncertain aircraft parameters but also stochastic control laws.

This remark being made, it turns out that aircraft processes measures are reduced to

Aircraft		O_1	O_2	O_3
1	Lat	-39	40	50
	Long	-7	-2	10
2	Lat	52	45	45
	Long	12	10	-5
3	Lat	52.6	46	
	Long	8.5	-7	
4	Lat	42	42	
	Long	-8	10	
5	Lat	52.5	39	
	Long	1.5	1.5	
6	Lat	42	53	
	Long	11	11	
7	Lat	39	47	52
	Long	12	-0.5	-6.5

Table 4.1: Flight plans of the seven aircraft given in degrees

Dirac measures. Nevertheless as we aim to estimate the wind field using the aircraft processes, we use the labeled island particle algorithm (Algorithm 3) developed in Chapter 2.

In this section two numerical experiments are held. For both applications, the air-traffic process are the same but the wind conditions differ. In the first case, the wind is uniform on the configuration space. In the second case, we consider an homogeneous wind field. We apply in both cases the labeled island particle algorithm (Algorithm 3) to estimate the wind using seven independent aircraft processes, denoted by $\mathbb{X}_n = (X_n^i)_{i=1}^7$ which encapsulates the aircraft position process $\mathbb{Z}_n = (Z_n^i)_{i=1}^7$.

The air-traffic process is composed of seven independent aircraft processes. These processes evolve independently using (3.22) and the controls laws developed in Section 3.1.9. All the aircraft are Airbus $A320$, we set the aerodynamics parameters using the BADA database. The Mach speed is set for all the aircraft to 0.78. Aircraft are assumed to be on the flight level $FL350$, the initial masses are set to 70% of the maximum pay-load. The flight plans are given for each aircraft in Table 4.1 where Lat refers to latitudes and Long to longitudes in degrees.

The initial distribution of each aircraft position process Z_0^i, denoted by $\eta_{\Theta_0,0}^{Z^i}$ is given by:

$$\eta_0^{Z^i}(\mathrm{d}z) = \delta_{O_1^i}(\mathrm{d}z).$$

The air-traffic process observations $\mathbb{Y} = (Y_n^i)_{i=1}^7$ are reduced to the aircraft $3D$-positions $\mathbb{Z}_n = (Z_n^i)_{i=1}^7$. They are obtained thanks to the following equation:

$$Y_n^i = Z_n^i + B_n^Y$$

where $B_n^Y \sim \mathsf{N}(0, \Sigma^Y)$, and $\Sigma^Y = 1.5 \times 10^{-5} \begin{pmatrix} 1 & 0 & 0 \\ 0 & 1 & 0 \\ 0 & 0 & 1 \end{pmatrix}$. The standard deviation of the observation process was set using the radar specifications which deliver aircraft positions

with an error of approximatively 200 meters.

4.3.1 Estimating a uniform wind field

In this section we try to evaluate the wind field denoted by $\Theta_n = \vec{W}$, illustrated on Figure 4.24. We use Algorithm 3 to estimate the law of the couple $(\Theta_n, \eta^{\mathbb{X}}_{\theta_{0:n},n})$ given the observations $\mathbb{Y}_{0:n}$, where the potential functions G_n are given by the likelihood of the observations, that is for all $\mathbb{X}_n \in (\mathsf{E}_n^X)^7$ and $\theta_n \in \mathsf{E}_n^\Theta$:

$$G_{\theta_n,n}(\mathbb{X}_n) \propto \prod_{i=1}^{7} \exp\left(-\frac{(Y_n^i - Z_n^i)^T (\Sigma^Y)^{-1} (Y_n^i - (Z_n^i, V_n^{a,i})))}{2} \right).$$

We present the results obtained for a simulating time of 20 minutes, with $\Delta t = 4s$. Let the number of wind proposals $N_1 = 200$. The wind propositions (or islands) are obtained thanks to:

- the normal distribution for its strength $\|W_n^i\|$ around the true value : 20.8, that is $\|W_n^i\| \sim \mathsf{N}(20.8, 3)$, for $i \in [\![1, 20]\!]$

- the uniform distribution for the direction β_n^i between $[0, \frac{\pi}{4}]$, that is $\beta_n^i \sim \mathcal{U}_{[0,\frac{\pi}{4}]}$, for $i \in [\![1, 10]\!]$.

Then we built $\theta_n^i = (\|W_n^i\|, \beta_n^i)_{i=1}^{200}$ by pairing all the possibilities. On Figure 4.25, we present the evolution of the island's weight value (represented by the z-coordinate) obtained thanks to the labeled island particle algorithm. The island number is given by the x-coordinate, and the time evolution on the y-coordinate. As one can observe, at the beginning of the experiment all the weight seems to be uniformly distributed. As time goes, one may observe on Figure 4.26 that there is a periodic pattern for the weight value. We explain this periodicity by the redundancy in the wind proposals. Indeed we have 10 direction's proposals repeated 20 times. On each segment of ten proposals, the wind direction which appears to have the highest potential corresponds to the closest direction of the wind field used to simulate the reference aircraft process. Regarding now over all segments, it appears that the wind force which has the highest potential is given by the strength's proposals closest to the actual wind.

4.3.2 Estimating an homogeneous wind field

Since we have presented the results obtained for a uniform wind field, we propose to do the same experiment but this time with a wind field varying along the space location. The wind field shape is illustrated on Figure 4.27. The simulation setting is the same as in the precedent section. Nevertheless the wind proposals are built in a different manner. We assume here that the wind proposals are made knowing the field structure. That is how it varies in function of the location. That is knowing the direction and the strength at one point will able one to built the whole field. Then, the wind propositions (or islands) are obtained as follows:
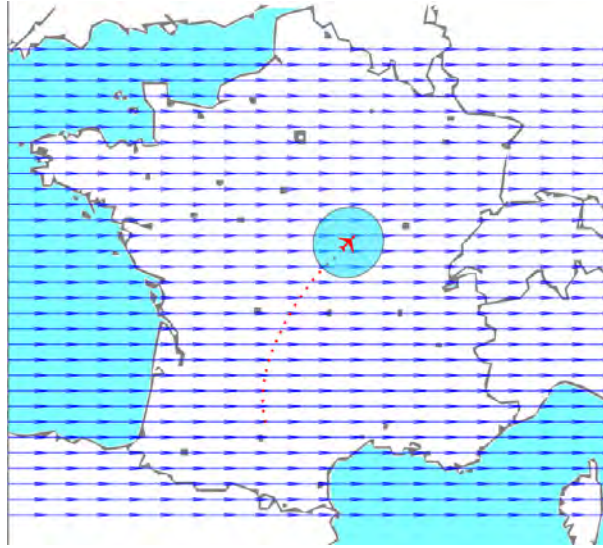
Figure 4.24: Reference wind field where the reference air-traffic is evolving, arrows represents the wind direction and their length are proportional to the wind strength

- the normal distribution for its strength $\|W_n^i\|$ around the true value : 20.8, that is $\|W_n^i\| \sim \mathsf{N}(75, 1)$, for $i \in [\![1, 10]\!]$

- the uniform distribution for the direction β_n^i between $[0, \pi]$, that is $\beta_n^i \in \left[\frac{\pi}{4}, \frac{3\pi}{4}\right]$, for $i \in [\![1, 10]\!]$.

Then we built $\theta_n^i = (\|W_n^i\|, \beta_n^i)_{i=1}^{200}$ by pairing all the possibilities. On Figure 4.29, we present the evolution of the island's weight value (represented by z-coordinate) obtained thanks to the labeled island particle algorithm. The island number is given by the x-coordinate, and the time evolution on the y-coordinate. As one can observe, at the beginning of the experiment all the weight seems to be uniformly distributed. As time goes, on may observe that the same pattern repeats every 10 proposals, as before we introduce redundancy in the wind proposals by pairing all the possibilities for the strength and direction proposals. Nevertheless, examining each group of ten proposals, we can see that the weights are concentrated on the same wind direction which appears to be the closest to the one used to generate the actual wind field. Then observing over all the groups, one strength proposition has the highest potential which corresponds to the closest strength value to the reference wind field. To put it in a nutshell, Algorithm 3 provide good estimation results for synthetic wind field.

4.4 Weighting ensemble wind forecast using a 3DDL aircraft model and air-traffic observations

The aim of this study was to develop an adapted framework in order to estimate the wind field where the aircraft are evolving: enhancing the accuracy level of the aircraft trajectory prediction by reducing the wind uncertainty. So far, we have presented the results obtained using the methods developed in Chapter 2 on simple experiments. We are now close to
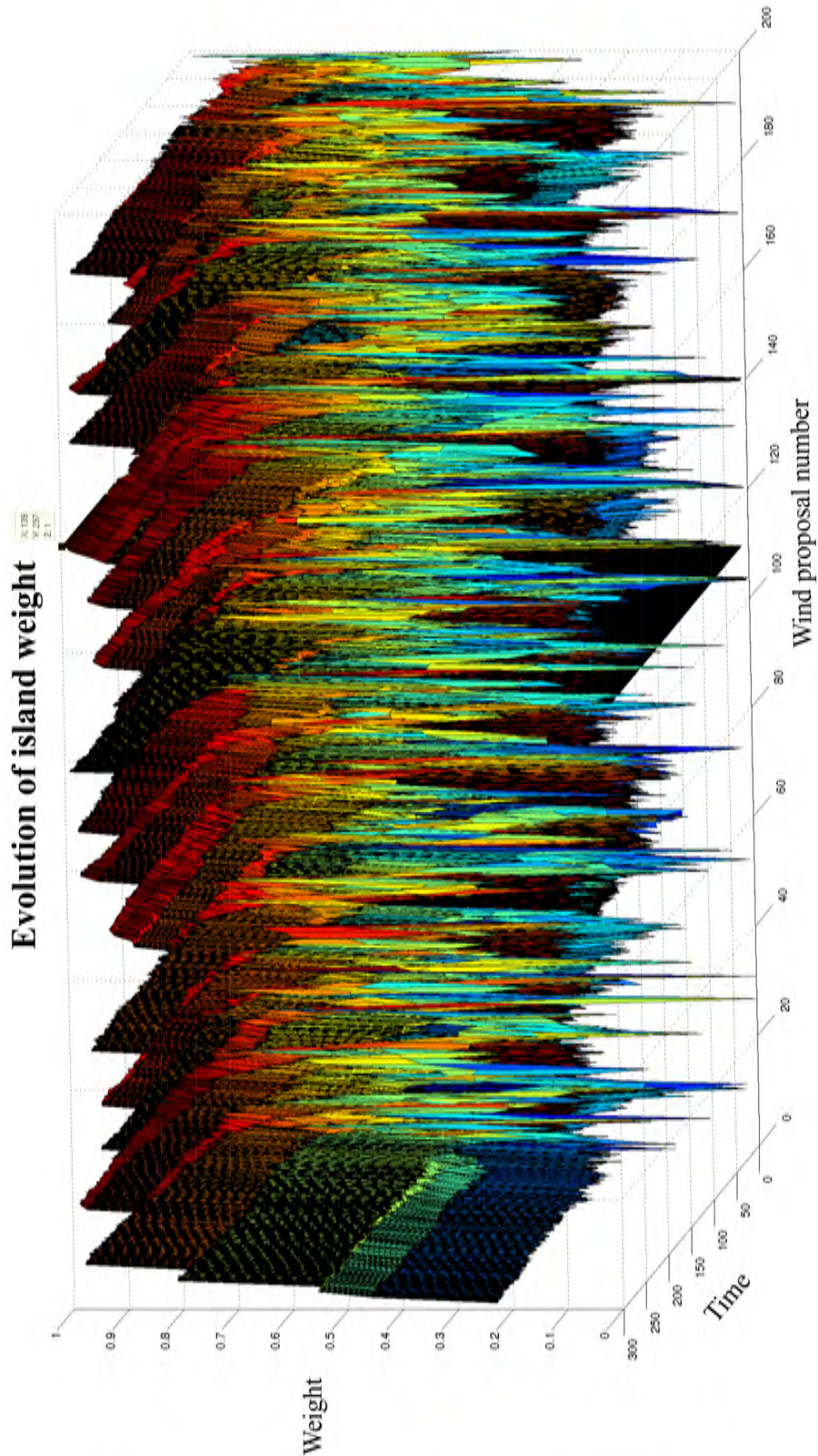
Figure 4.25: Time evolution (y axis) of the wind proposals weights (vertical axis, and colorscale) with respect to the wind proposal number (*x* axis) obtained using Algorithm 3. Weight repartition over all members is periodic with a period of 10 due to the redundancy introduced inside the wind proposals. However, at the end of the time period, the wind proposal which has the highest weight (identified with the label) corresponds to the wind proposal with the closest direction and the closest strength to the reference wind.

Figure 4.26: Time evolution (vertical axis) top view of the wind proposals weights (colorscale) with respect to the wind proposition number (horizontal axis) obtained using Algorithm 3. Weight repartition over all members is periodic with a period of 10 due to the redundancy introduced inside the wind proposals. However, at the end of the time period, the wind proposal which has the highest weight (identified with the label) corresponds to the wind proposal with the closest direction and the closest strength to the reference wind.
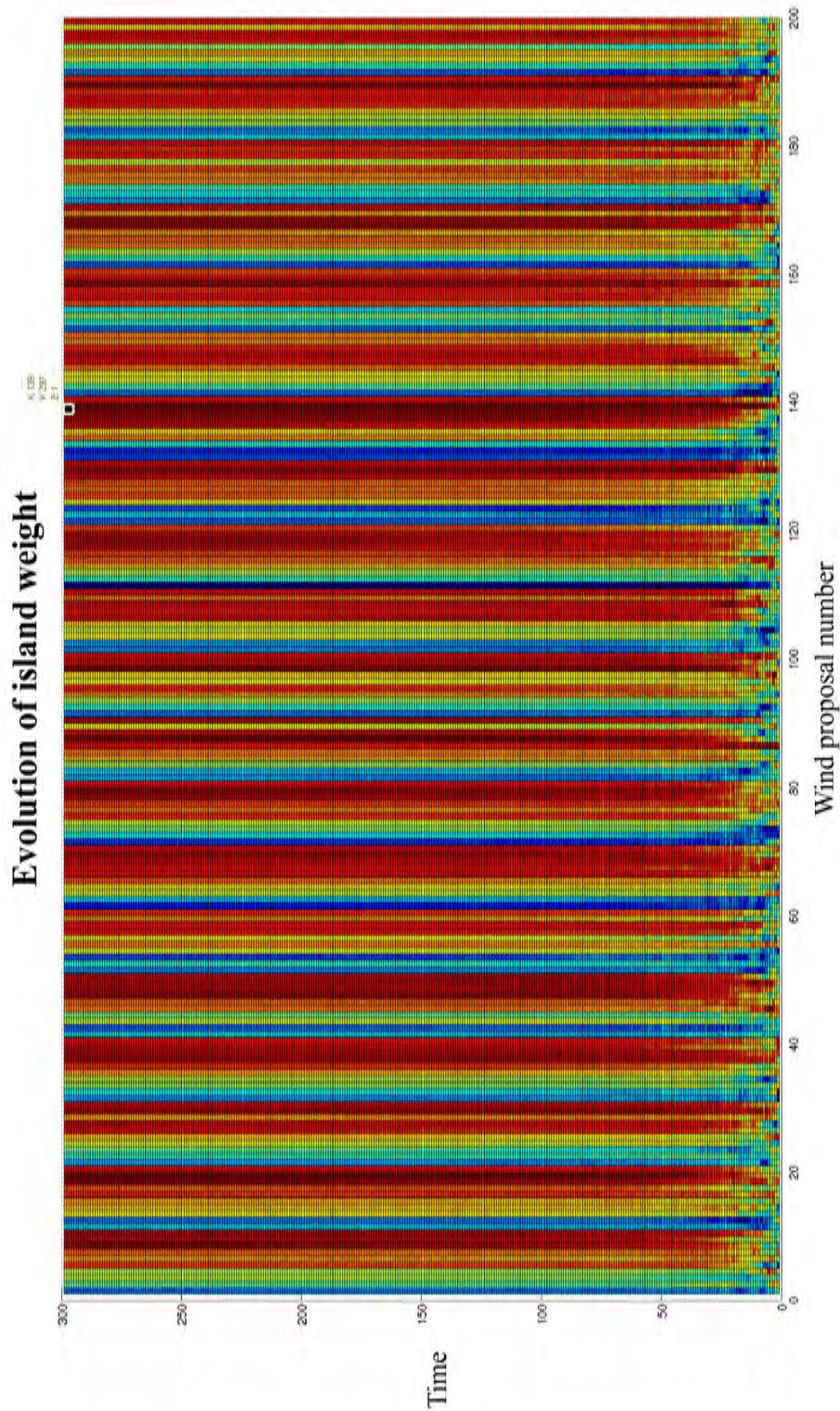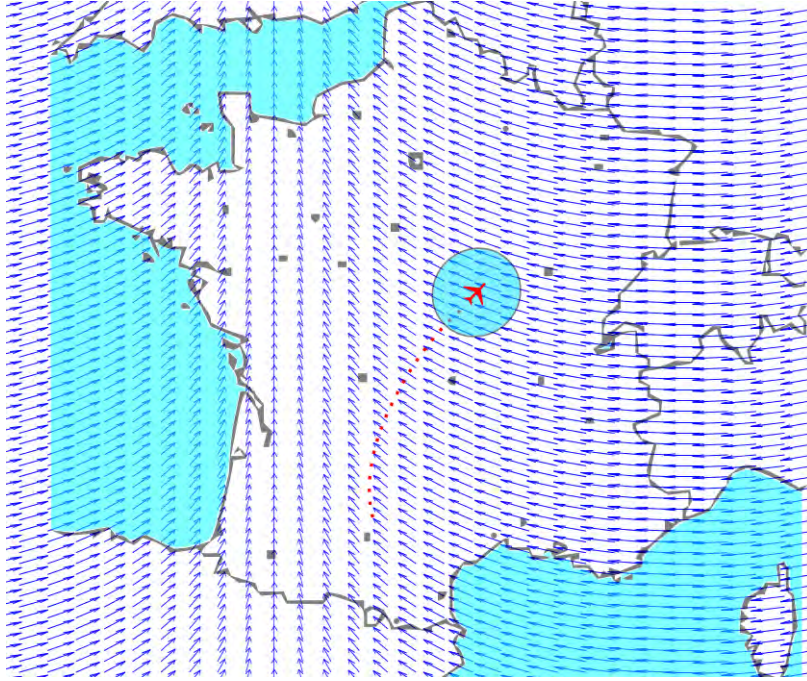
Figure 4.27: Reference wind field where the seven aircraft processes evolve, arrows represents the wind direction and their length are proportional to the wind strength.

our main goal: estimating the wind field using aircraft trajectory predictions.

For synthetic wind field, we have seen that the island number was already really high even if the atmosphere scenarios under consideration were really simple. In the case of the atmosphere, the cost to proceed to a classical Monte-Carlo strategy is too important, even prohibitive. To tackle this issue, we propose to use ensemble weather forecasts which are multi-model forecasts containing N_1 members which propose N_1 realizations of the atmosphere. Using ensemble weather forecasts enables one to have access to the wind value at every point of the configuration space E, but it leads us to consider the filtering problem in model space.

Then, we present the estimation results for the filtering problem of the air-traffic process evolving in a small random environment using the labeled island particle algorithm (described by Algorithm 3). Indeed, the random field under consideration in the experiment is the weather forecasting error and as the configuration space being small, the homogeneous hypothesis is reasonable.

In Section 2.4, we have developed the framework adapted to deal with environment which can be decomposed in several homogeneous domains. We explain here one possible method to get the configuration space decomposition, such that the weather forecasting error is homogeneous in each sub-domain.

Finally we present the results obtained on realistic simulations (realistic for the wind field and for the aircraft model) using Algorithm 6 .

150
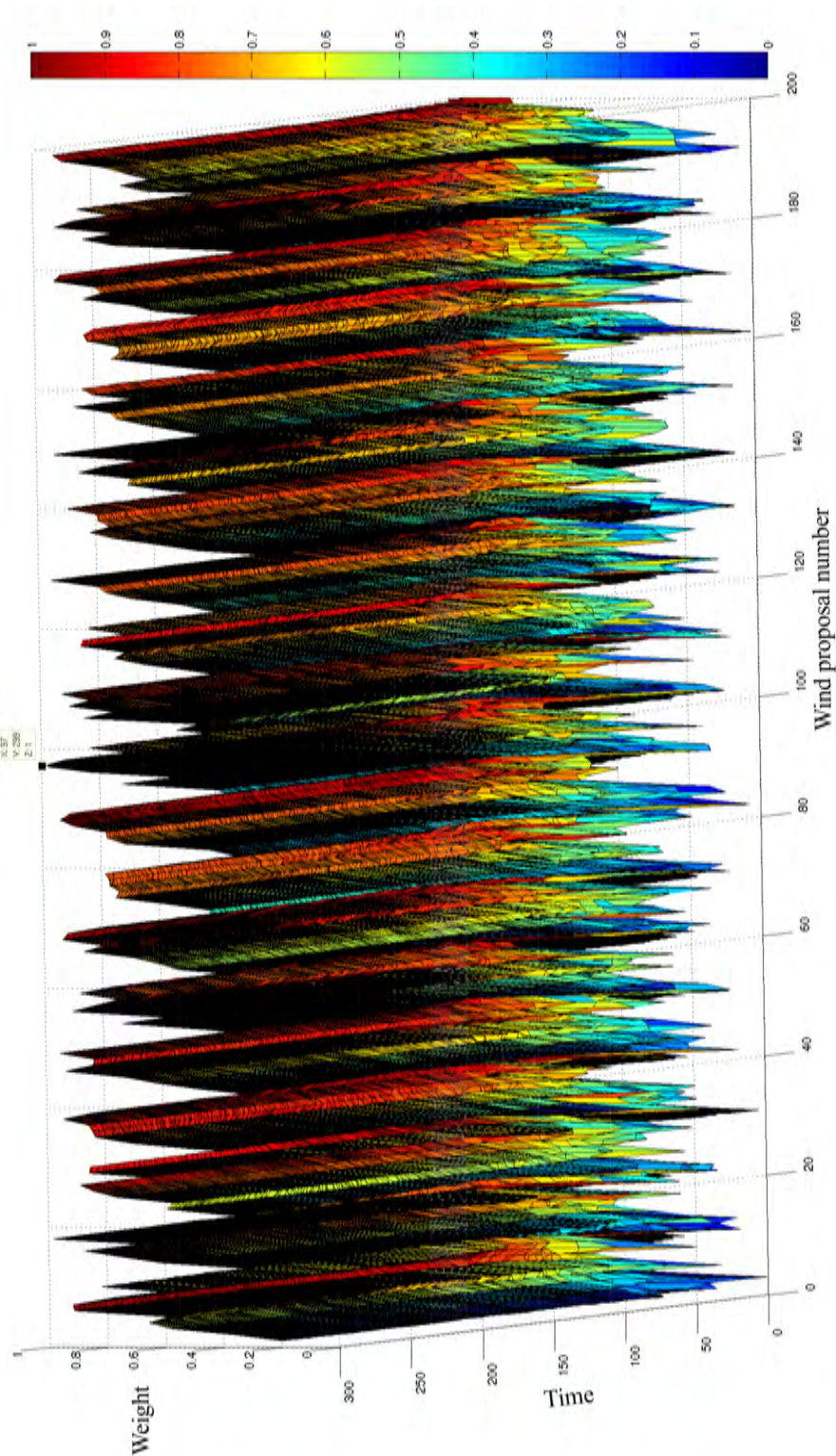
Figure 4.28: Time evolution (y axis) of the wind proposals weights (vertical axis, and colorscale) with respect to the wind proposal number (*x* axis) using Algorithm 3. Weight repartition over all members is periodic with a period of 10 due to the redundancy introduced inside the wind proposals. However, at the end of the time period, the wind proposal which has the highest weight (identified with the label) corresponds to the wind proposal with the closest direction and the closest strength to the reference wind.

151
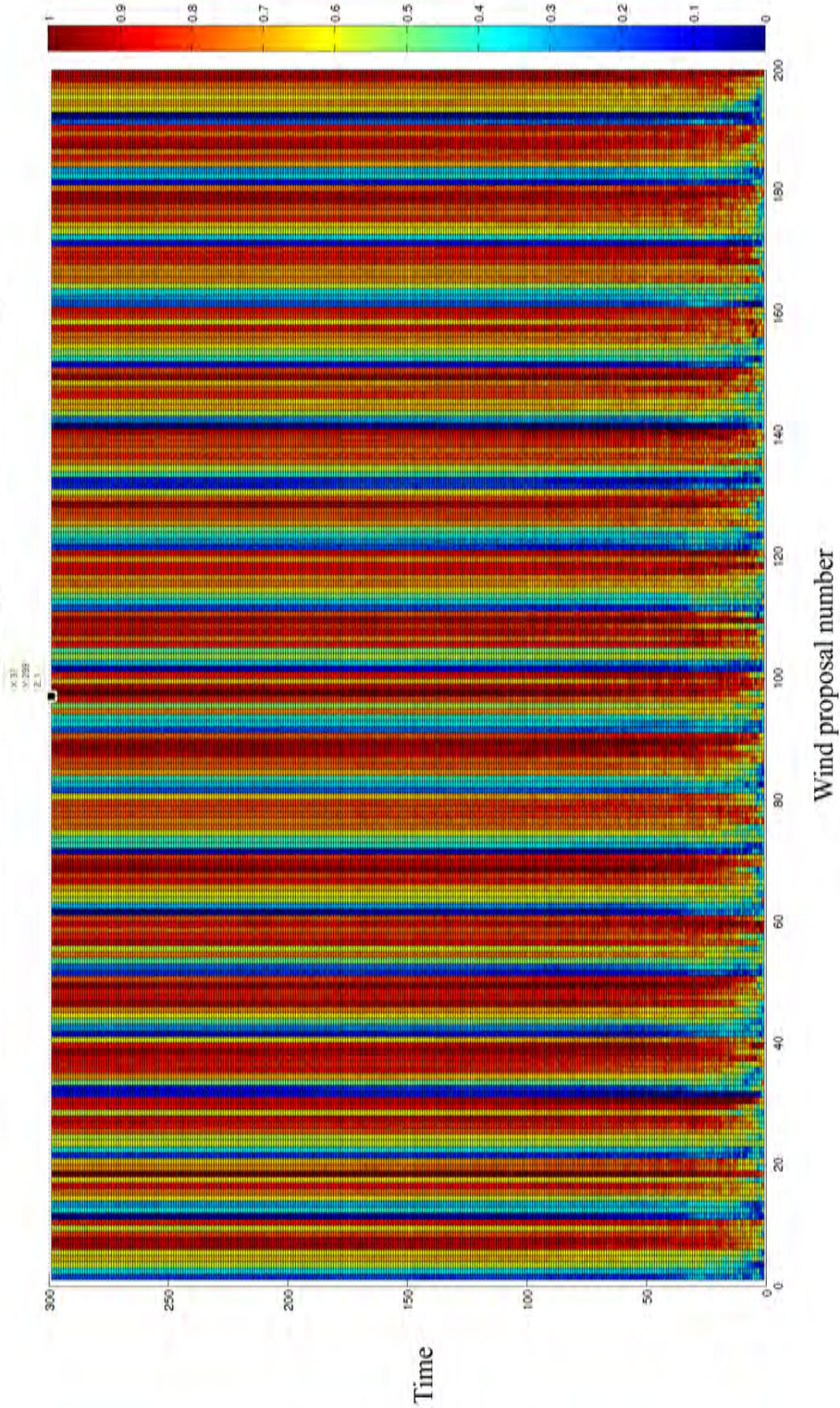
Figure 4.29: Time evolution (vertical axis) top view of the wind proposals weights (colorscale) with respect to the wind proposition number (horizontal axis) using Algorithm 3. Weight repartition over all members is periodic with a period of 10 due to the redundancy introduced inside the wind proposals. However, at the end of the time period, the wind proposal which has the highest weight (identified with the label) corresponds to the wind proposal with the closest direction and the closest strength to the reference wind.

4.4.1 Wind forecast and Monte Carlo methods

The atmosphere state takes its value in a high-dimensional space, dimension is 10^5 at least. It turns out that Monte Carlo strategies are not adapted to effectively sample from a distribution in a such high dimension space. To overcome this problem, we propose in this work to use ensemble weather forecasts. There are produced by national weather forecast centres and deliver several scenarios for the atmosphere evolution.

Using ensemble weather forecast Prévision d'Ensemble Arome (PE AROME)

Numerical weather prediction uses mathematical models of the atmosphere and oceans to predict the weather based on current weather conditions. In 1963, Edward Lorenz discovered the chaotic nature of the fluid dynamics equations involved in weather forecasting. Extremely small errors in temperature, winds, or other initial inputs given to numerical models will amplify and double every five days, making it impossible for long-range forecasts–those made more than two weeks in advance–to predict the state of the atmosphere with any degree of forecast skill. Furthermore, existing observation networks have poor coverage in some regions (for example, over large bodies of water such as the Pacific Ocean), which introduces uncertainty into the true initial state of the atmosphere. While a set of equations, known as the Liouville equations, exists to determine the initial uncertainty in the model initialization, the equations are too complex to run in real-time, even with the use of supercomputers. These uncertainties limit forecast model accuracy to about five or six days into the future.

Edward Epstein recognized in 1969 that the atmosphere could not be completely described with a single forecast run due to inherent uncertainties, and proposed a stochastic dynamic model that produced means and variances for the state of the atmosphere, see Epstein (1969). Although these Monte Carlo simulations showed skill, in 1974 Cecil Leith revealed that they produced adequate forecasts only when the ensemble probability distribution was a representative sample of the probability distribution in the atmosphere, Leith (1974).

Ensemble forecasting is a numerical prediction method that is used to attempt to generate a representative sample of the possible future states of a dynamical system. It is a multiple numerical predictions conducted using slightly different initial conditions that are all plausible given the past and current set of observations, or measurements. Sometimes the ensemble of forecasts may use different forecast models for some different members, or different formulations of a forecast model. The multiple simulations are conducted to account for the two usual sources of uncertainty in forecast models: the errors introduced by the use of imperfect initial conditions, amplified by the chaotic nature of the evolution equations of the dynamical system, which is often referred to as sensitive dependence on the initial conditions; and errors introduced because of imperfections in the model formulation, such as the approximate mathematical methods to solve the equations. Ideally, the verified future dynamical system state should fall within the predicted ensemble spread, and the amount of spread should be related to the uncertainty (error) of the forecast.

It was not until 1992 that ensemble forecasts began being prepared by the European Centre for Medium-Range Weather Forecasts and the National Centres for Environmental Prediction. The ECMWF model, the Ensemble Prediction System, uses singular vectors to simulate the initial probability density, while the NCEP ensemble, the Global Ensemble Forecasting System, uses a technique known as vector breeding, see Toth and Kalnay (1997); Molteni et al. (1996)

On its side, Météo-France has implemented an ensemble prediction system known as Prévision d'Ensemble ARPEGE (PEARP). This system is a global ensemble performing forecasts up to 4/5 days. It uses the operational global numerical weather prediction model Action de Recherche Petite Echelle Grande Echelle (ARPEGE) and benefits from variable horizontal resolution, so that it is comparable to some limited-area mesoscale systems over France. Perturbations to the initial conditions are computed by combining an ensemble data assimilation system with singular vectors of the manifold. Model uncertainties are represented through a "multiphysics" with ten different physical parametrization sets, Descamps et al. (2014).

Since 2008, weather forecasters have at their disposition a high resolution regional model named Applications de la Recherche à l'Opérationnel à Méso-Echelle (AROME). It provides detailed weather forecasts over France with a range forecast from 3 hours to 36 hours. Since then, weather forecasters are better positioned to forecast small scale meteorological phenomenon potentially hazardous such as thunderstorms and heavy rainfall. Another major advantage of this model is that it takes into account violent small scale vertical movements associated to the cumulonimbus developments (thunderstorms clouds). Hence it is able to simulate convective phenomenon and rainy-stormy systems.

Currently, a stochastic physics scheme is tested in the AROME short-range convection-permitting ensemble prediction system, Bouttier et al. (2012), called PE AROME. It is an adaptation of ECMWF's stochastic perturbation of physics tendencies scheme. The main improvement from PEARP lies in the ensemble reliability and the spread-skill consistency.

Hence in this work, we use the most recent ensemble weather forecast developed at Météo-France as its high resolution suits the air-traffic application demands. The ensemble forecast we used was made up of 34 members, that is 34 possible evolution scenarios for the atmosphere built on the basis of 10 different physic models. Nevertheless, we would like to highlight here that the work we are conducting does not depend on the ensemble weather forecast we choose. We can also choose to use ensemble weather forecasts coming from the UK Met Office or any other national centres as well as superEnsemble which are currently under study for the SESAR project.

Working in the model space

In order to use the filtering techniques we have developed, a switch into the model space for the random field Θ_n has to be made. By switch to the model space, we mean that the the random field used to make the aircraft-trajectory predictions is given by ensemble weather forecasts instead of realization of the random field Θ_n. As we said in the previous

section, Météo-France provide ensemble weather forecasts. In this work, we consider that members of the weather forecast ensemble are a sample of the random atmospheric field projected into the model space. We denote the projected random atmospheric field in the model space, $\mathsf{E}_n^{\Theta,P}$, by Θ_n^P. We decompose Θ_n, the random atmospheric field, in a sum of two processes: the predicted process Θ_n^P and the unpredicted process Θ_n^U such that for all $n \in \mathbb{N}$:

$$\Theta_n = \Theta_n^P + \Theta_n^U$$

where Θ_n^P a $(\mathsf{E}_n^{\Theta,P}, \mathcal{E})$-random variable and Θ_n^U a $(\mathsf{E}_n^{\Theta,U}, \mathcal{E})$-random variable, with $\mathsf{E}_n^{\Theta,P} \perp \mathsf{E}_n^{\Theta,U}$ and $\mathsf{E}_n^{\Theta} = \mathsf{E}_n^{\Theta,P} \oplus \mathsf{E}_n^{\Theta,U}$.

Then in order to forecast the positions of aircraft, we use the predicted process Θ_n^P instead of Θ_n as it is not accessible. This predicted air-traffic process is then denoted by $\mathbb{X}_n^P = (X_n^{P,i})_{i=1}^M$, with M the number of aircraft. It is obtained by using the random atmospheric field projected inside the model space through the flight mechanics model developed in Chapter 3, resumed by (3.22). For notation simplicity, let denote by f the evolution scheme of each aircraft state, then we have:

$$X_n^{P,i} = f(\Theta_n^P, X_{n-1}^{P,i})$$

As one can notice the function f (defined by (3.22)) is linear with respect to the wind variable, then we can notice that the real air-traffic process evolution can be decomposed into two terms: one consists in the evolution of the predicted traffic process $\mathbb{X}_n^P$ and the other one concerns the evolution of $\mathbb{X}_n^U$. We have for each aircraft :

$$\begin{aligned}
X_n^i &= f(\Theta_n, X_{n-1}^i) \\
&= f(\Theta_n^P + \Theta_n^U, X_{n-1}^i) \\
&= f(\Theta_n^P, X_{n-1}^i) + f(\Theta_n^U, X_{n-1}^i) \\
&= f(\Theta_n^P, X_{n-1}^{P,i} + X_{n-1}^{U,i}) + f(\Theta_n^U, X_{n-1}^{P,i} + X_{n-1}^{U,i}) \\
&= f(\Theta_n^P, X_{n-1}^{P,i}) + \varepsilon_n
\end{aligned}$$

where the term ε_n is an error term representing the error made by using weather forecasts to predict the air-traffic process. However, the air-traffic observations, denoted by $\mathbb{Y}_n = (Y_n^i)_{i=1}^M$, are observations of the real air-traffic process, in the sense that they are produced by the real atmospheric random field Θ_n. For each aircraft, the observations are given by the following equation:

$$Y_n^i = h(X_n^i, \Theta_n)$$

Therefore, using air-traffic radar observations gives one information about the quality of the weather forecast we use. Indeed the potential function G_n is defined as the likelihood

of the observations with respect to the environment and real air-traffic realization

$$G_n(\Theta_n, \mathbb{X}_n) \propto \prod_{i=1}^{M} G_n(\Theta_n, X_n^i) \tag{4.8}$$

Then it follows that we are in a Hidden Markov model where the hidden state is given by $(\Theta_n, \mathbb{X}_n)$ and we can access through it by $\mathbb{Y}_{0:n}$. .

4.4.2 Meteorological situation

The meteorological situation considered, was the one which took place the 22nd of May in 2014 at midnight. The atmospheric conditions are represented on Figure 4.30. Western Europe is under the influence of close Atlantic trough. In altitude, a minimum of geopotential (a low) is located on the south of Ireland. A upper level jet stream is developed on the east part of the trough over France. And over the South of France many thunderstorms arise below the east part of the outflow jet streak.

This situation leads in altitude to a fair southward to south-westward flux over France. We can distinguish 2 main type of area over the domain of interest:

- An area with close and parallel isobaric lines where the wind is strong and structured (from east of France to Norway, and close east of the low). It correspond to the jet-stream and the stormy outflow part over the south of France.

- An area at the rear of the jet-stream, less organized and with weaker winds on the Northwest of France, without significant meteorological phenomena.

From this interpretation, we justify that we split the domain in 2 areas in which the wind has a different law of probability. In the jet, it will likely be high in mean, with a small variance, especially in direction. Out of the jet, it will likely be lower with a larger variance in both direction and speed.

Therefore, if the whole domain over France is considered, the patchwork labeled island algorithm has to be used. In another case, we can consider only a reduced area and use the labeled island particle algorithm.

4.4.3 Weighting ensemble weather forecasts members using labeled island particle algorithm

When considering a small area of the configuration space E, the meteorological forecast error can be considered homogeneous. Hence the labeled island particle algorithm (Algorithm 3) can be used to weight the ensemble weather forecast regarding the air-traffic predictor performance.

As one can see on Figure 4.31, the random field reduced to the black frame is almost spatially uniform. Then to weight the ensemble wind forecast, we propose to use the labeled island particle algorithm. We hold two experiments for this weather situation. The first one consists in weighting the member of the ensemble wind forecast when the

ANALYSE EN SURFACE DU JEU 22/05/14 12UTC

ANALYSE A 500 hPa DU JEU 22/05/14 12UTC

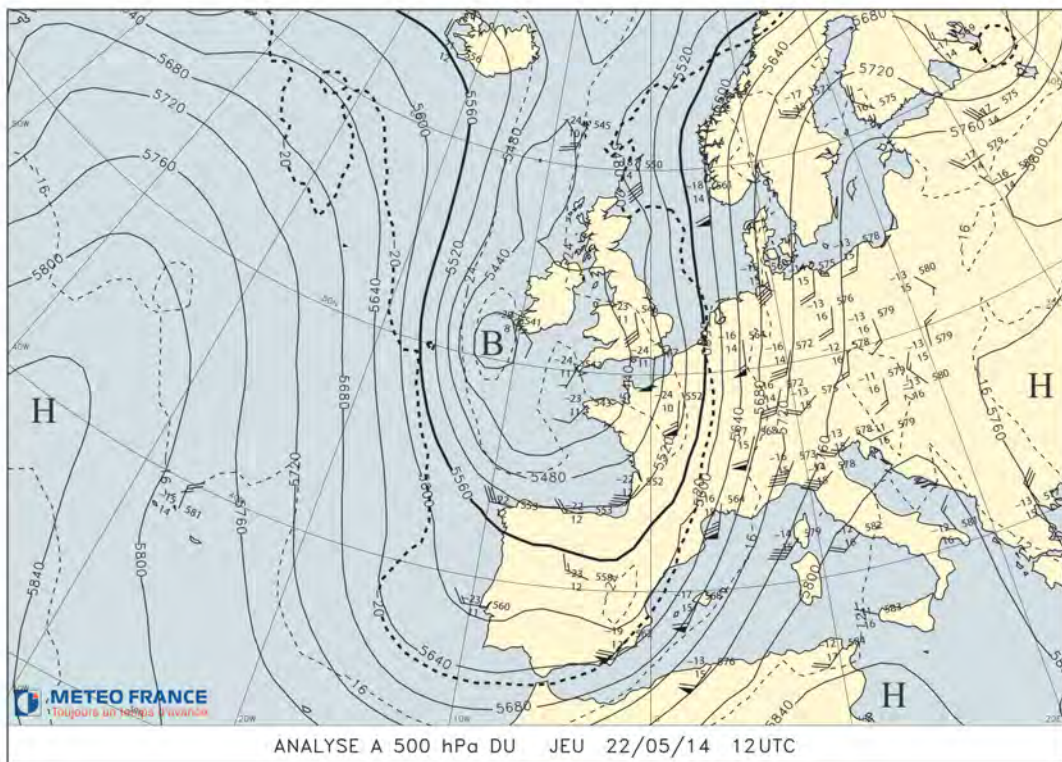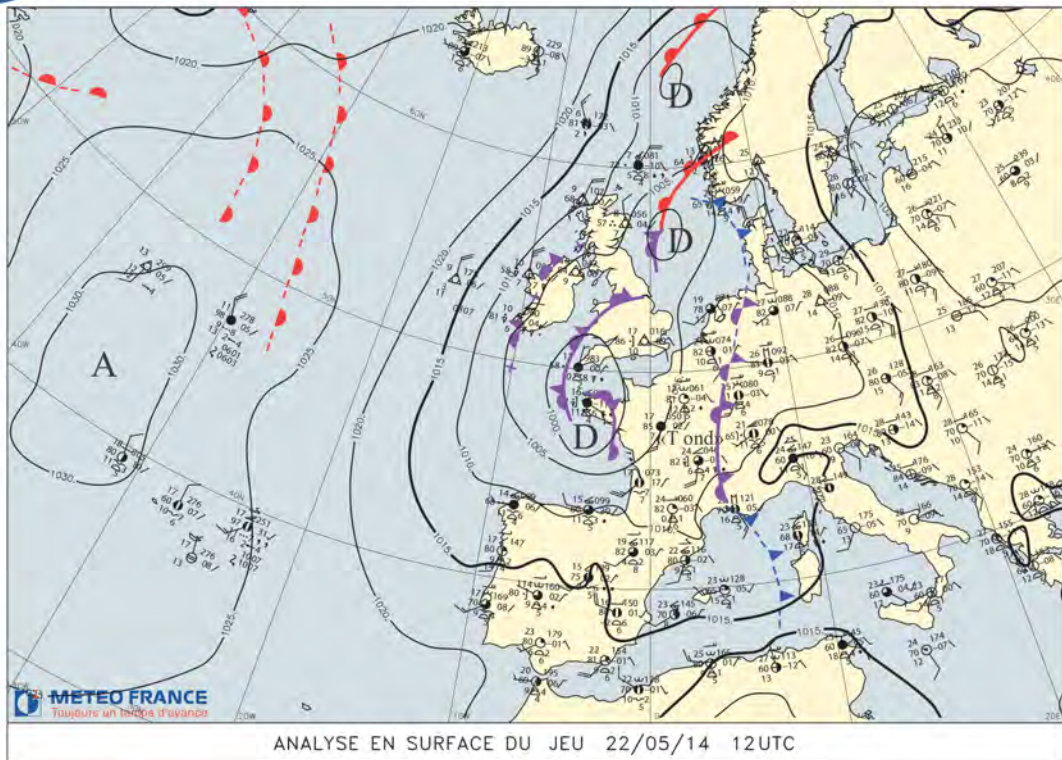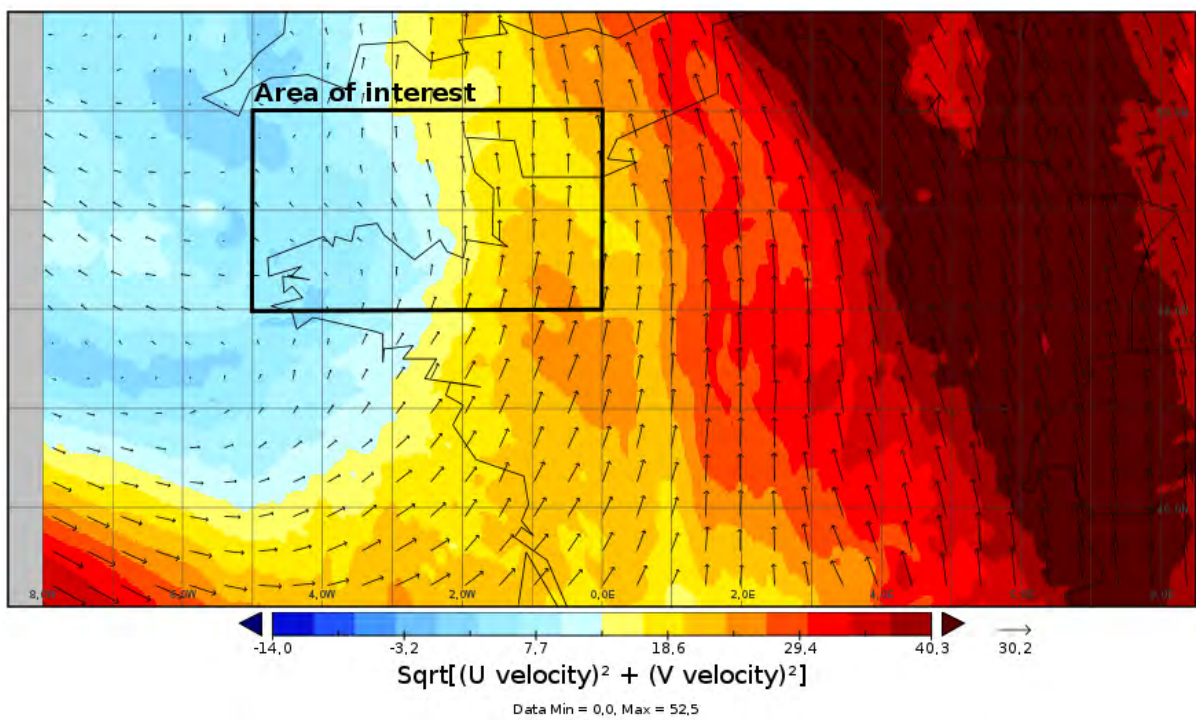Figure 4.30: Meteorological situation over France on the 22nd of May 2014

Figure 4.31: Wind field given by member 10 of the ensemble weather forecast at FL350. The black frame represents the area under consideration for the labeled island particle algorithm application. Arrows represents the wind direction, their length are proportional to the wind speed. The color represents also the wind speed

Aircraft		O_1	O_2	O_3
1	Lat	48	48	50
	Long	-5	-2	0
2	Lat	50	49	49
	Long	-1	-2	-3
3	Lat	48	48	
	Long	-5	0	
4	Lat	48	49	
	Long	-1	-1	
5	Lat	50	49	48
	Long	-4	-1.5	-0.5
6	Lat	49	48	
	Long	0	6	
7	Lat	48.5	50	
	Long	-1.5	-1.5	

Table 4.2: Flight plans of the seven aircraft given in degrees

reference air-traffic is generated with one of the member. The second one is weighting the ensemble wind forecast when the reference air-traffic is simulated with the analysis.

As a first experiment on this meteorological situation, we generate an air-traffic composed of 7 aircraft using the model developed in Chapter 3. We denote it by $\mathbb{X}_n = (X_n^i)_{i=1}^7$ with their positions given by $\mathbb{Z}_n = (Z_n^i)_{i=1}^7$. Their flight plans are given in Table 4.2 where Lat refers to latitudes and Long to longitudes in degrees. We simulate 10 minutes of air-traffic with a time step of 4 seconds. All the aircraft are Airbus $A320$, we set the aerodynamics parameters using the BADA database. The Mach speed is set for all the aircraft to 0.78. aircraft are assumed to be on the flight level $FL350$, the initial masses are set to 70% of the maximum pay-load. In a first place, to simulate the reference air-traffic process, we use the member number 10 of the ensemble weather forecast. It is the wind field represented on Figure 4.31. The initial distribution of each aircraft position process Z_0^i, denoted by $\eta_{\Theta_0^P,0}^{Z^i}$ is given by:

$$\eta_0^{Z^i}(\mathrm{d}z) = \delta_{O_1^i}(\mathrm{d}z).$$

The air-traffic process observations $\mathbb{Y} = (Y_n^i)_{i=1}^7$ are reduced to the aircraft $3D$-positions $\mathbb{Z}_n = (Z_n^i)_{i=1}^7$. They are obtained thanks to the following equation:

$$Y_n^i = Z_n^i + B_n^Y$$

where $B_n^Y \sim \mathsf{N}(0, \Sigma^Y)$, and $\Sigma^Y = 1.5 \times 10^{-5} \begin{pmatrix} 1 & 0 & 0 \\ 0 & 1 & 0 \\ 0 & 0 & 1 \end{pmatrix}$. The standard deviation was set to fit the radar specifications. We use Algorithm 3 to estimate the law of the couple $(\Theta_n, \eta_{\theta_{0:n},n}^{\mathbb{X}})$ given the observations $\mathbb{Y}_{0:n}$, where the potential functions G_n are given by
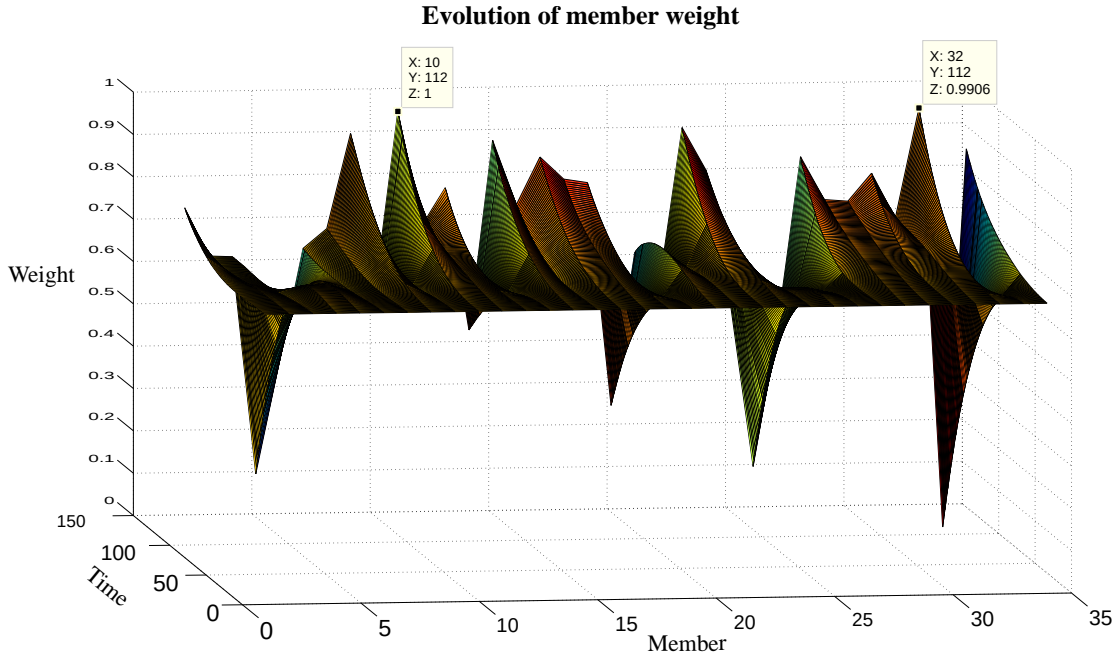
Figure 4.32: Time evolution (y coordinate) of the wind proposal weights (z-coordinate) obtained thanks to the labeled island particle algorithm. At the beginning of the algorithm all the weights are equidistributed, then member 10 (identified by a label) which has been used to simulate the air-traffic reference process concentrates the highest weight. Member 32 has also a high weight. After analysis of the wind field proposal, members 10 and 32 proposed a really close scenario.

the likelihood of the observations, that is for all $\mathbb{X}_n \in (\mathsf{E}_n^X)^7$ and $\theta_n \in \mathsf{E}_n^\Theta$:

$$G_{\theta_n,n}(\mathbb{X}_n) \propto \prod_{i=1}^{7} \exp\left(-\frac{(Y_n^i - Z_n^i)^T(\Sigma^Y)^{-1}(Y_n^i - (Z_n^i, V_n^{a,i})))}{2}\right).$$

The wind proposals are given by the members of the ensemble weather forecast.

Figure 4.32 and Figure 4.33 represents the weight evolution of the wind proposals. On the x-coordinate, the number of the ensemble is represented. The y-coordinate represents the time evolution and the z-coordinate or the color represents the weight-value of the wind proposal. As one may observe weights are the same at the beginning of the experiment for each wind proposal. Then one member seems to be privileged as time goes. For this experiment, the reference air-traffic was simulated with the member number 10, and with no surprise, the labeled island particle algorithm tends to favour this member by giving him a high weight. Nevertheless, two other members (as member 32), see Figure 4.32, appears to have a comparable weight as the member 10. This can be explained by the fact that the 34 members are constructed picking up upon 10 different physical models. Then among 34 propositions almost 3/4 propositions have the same physics, that explains why 3 members have around the same weight. This numerical experiment demonstrate the effectiveness of the labeled island particle algorithm on a realistic toy-model with expected results achieved. Now, we present the results obtained when the reference air-traffic is generated using the analysis.
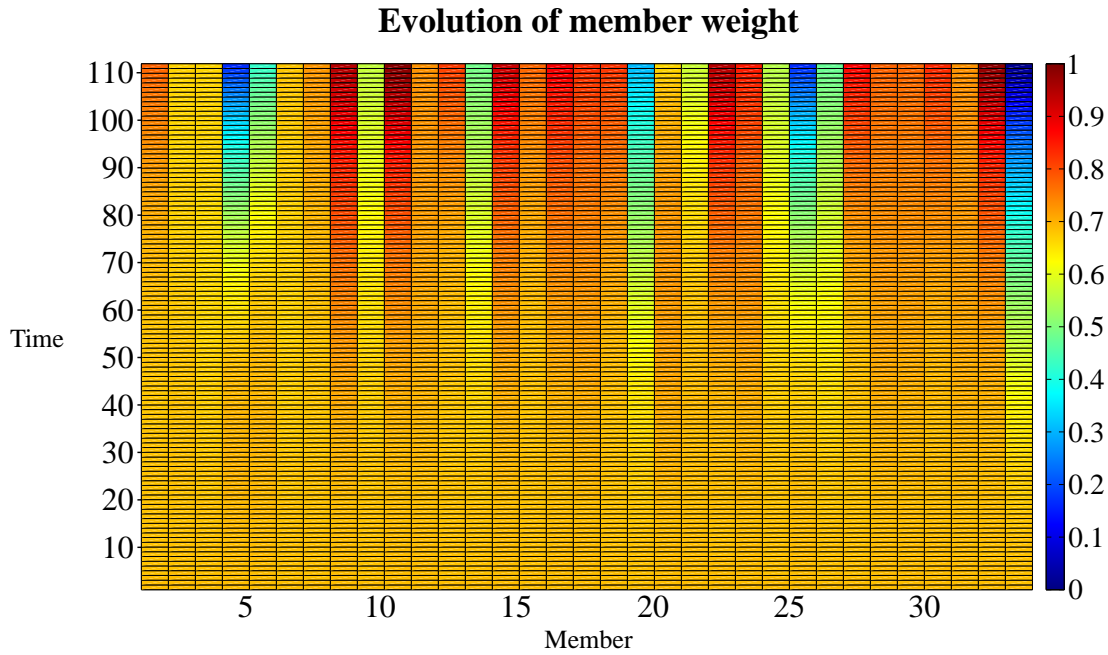
Figure 4.33: Time evolution (vertical axis) of the wind proposal weights (colorscale) with respect to the wind proposal number (horizontal axis) obtained thanks to the labeled island particle algorithm-Top view. At the beginning of the algorithm all the weights are equidistributed, then member 10 which has been used to simulate the air-traffic reference process concentrates the highest weight.

The analysis, in numerical weather forecast, corresponds to the best representation of the atmosphere. It is obtained by making a compromise between the model output for a time t and all the observations available at that time. In this work, we use the analysis based on the AROME model. The wind field analysis at aircraft altitudes is represented on Figure 4.34 The air-traffic situation is the same as in the previous experiment. In Figure 4.35 the weight evolution of the different members of the ensemble with respect to time is represented. As one can note, at the beginning of the experiment, all the members have the same weight. Then as time goes, the weight start to concentrate over 4 members. As we have said in the previous experiment, the different members are obtained using 10 different physics. Then over 34 members between 3 and 4 members will have the same physics. That may explain why 4 members have a high weight at the end of the experiment. Here, we want to make clear that the weight obtained through the labeled island particle algorithm is not a performing score of the weather forecast member itself. It is a performing score of the member through the air-traffic prediction system. Then we cannot interpret this score as a parameter allowing one to evaluate the forecast accuracy directly. The score corresponds to the error made by the wind forecast member through the air-traffic prediction system respectively to the air-traffic observations.

To sum up, the labeled island particle algorithm capability to weight ensemble weather forecast has been demonstrated on realistic experiments when the domain is small and can be considered homogeneous.
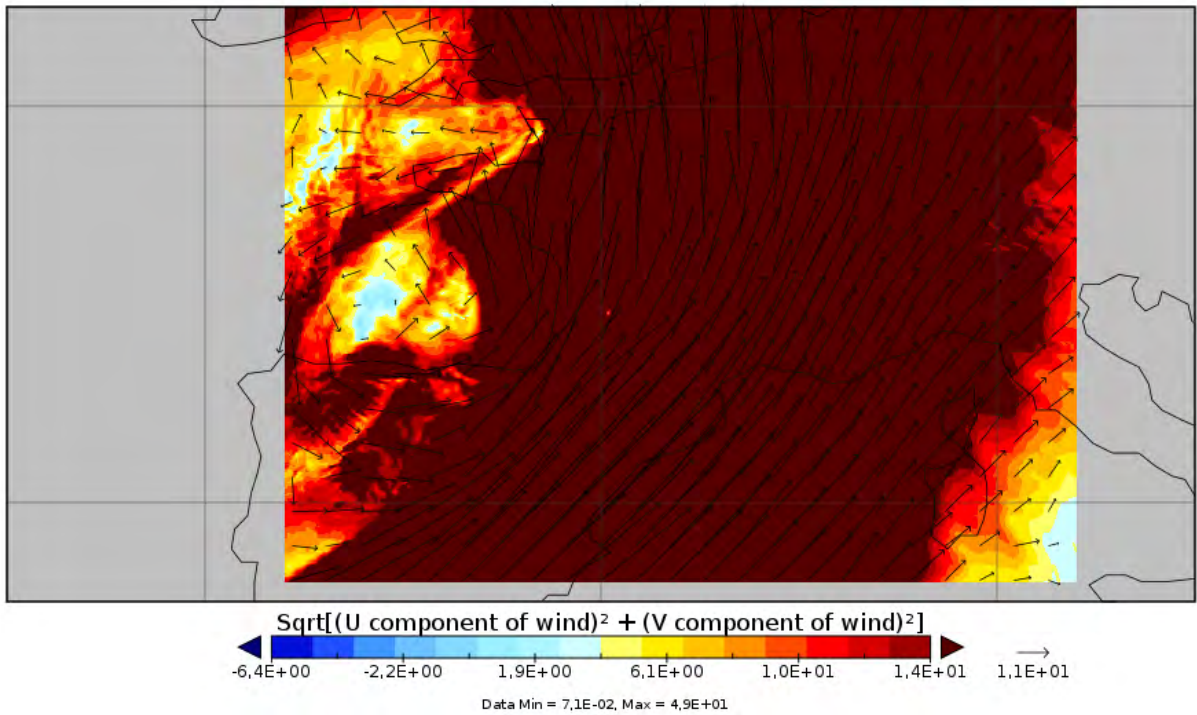
Figure 4.34: Wind field given by AROME analysis over Western Europe at FL350, color-scale gives the wind strength scale, arrows materialize the direction of the wind force and their length are proportional to the strength of the wind.
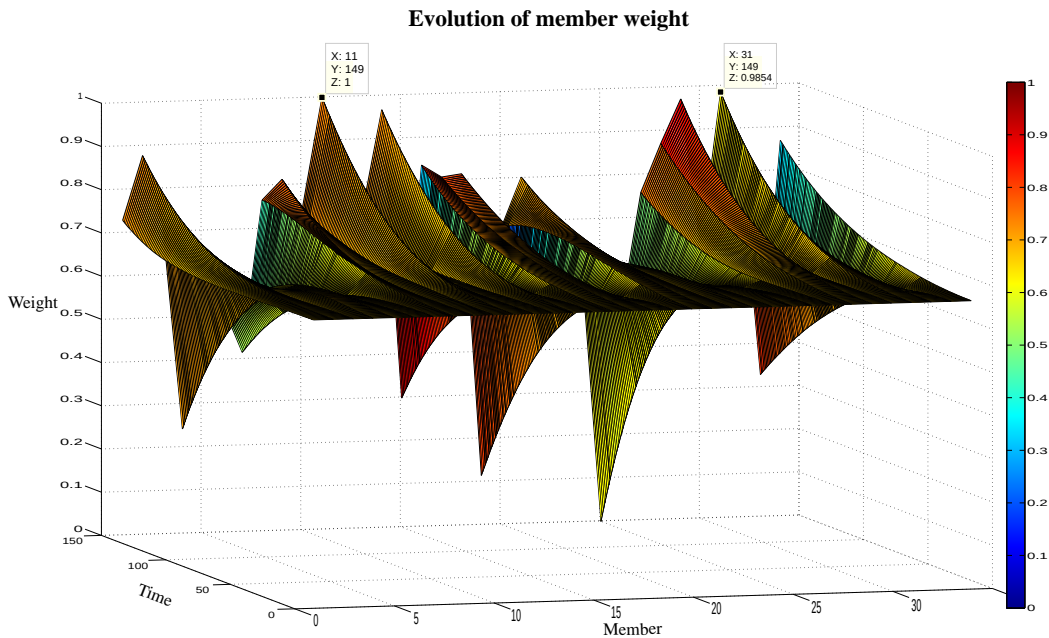
Figure 4.35: Time evolution (y coordinate) of the wind proposal weights (z-coordinate) obtained thanks to the patchwork labeled island particle algorithm. At the beginning of the algorithm all the weights are equidistributed, then the weights concentrates over 4 members (*e.g.* member 11 and 31)

4.4.4 Locally Weighting ensemble weather forecasts using the patchwork labeled island algorithm

Now, we are touching the main goal of the whole study: weighting an ensemble weather forecast using aircraft trajectories and air-traffic observations. The previous section was devoted to the case where the environment, the wind field error, can be considered as an homogeneous random field. However, errors on the weather forecasts are space dependent and it is believed that the error structure depends on the phenomenon being forecast. Then, we assume that the error forecast field can be decomposed in homogeneous sub-domains. Each sub-domain is given by a different meteorological phenomenon.

In Section 2.4, we proposed a stochastic algorithm able to estimate random environment decomposed in an homogeneous cover as well as random processes influenced by this environment. To this end, we suppose that the operator Υ, defined by (2.67), gives us the decomposition of the configuration E in homogeneous sub-domains, $(\mathsf{B}_{0,l})_{l=1}^{k}$. In this numerical experiment, we choose to use cluster analysis method on PE AROME wind forecasts to get such decompositions. This section is devoted to its presentation and implementation. Finally we present the results obtained using the patchwork labeled island particle filters on the segmented wind field to weight ensemble weather forecast and reduce uncertainties on trajectory prediction due to weather forecast uncertainties.

Wind field decomposition using cluster analysis method

"Cluster analysis" regroups techniques used to classify objects into groups called *clusters*. The purpose of cluster analysis is to create these groups without any prior information about the groups or the hypothetical membership of an object to a group. Two points in the same group will be similar, while two points in different groups will be dissimilar. There are many different ways to do a cluster analysis. A good overview of this domain is provided by Jain et al. (1999).

The first paragraph is a general introduction to cluster analysis where the vocabulary and some useful definitions are stated. The second paragraph focuses on the specific algorithm implemented.

Concepts and definitions Cluster analysis is a common tool of data mining. Grouping the data makes it possible to extract useful information from the data set. It is applied in various domains such as pattern recognition (find a specific shape), artificial intelligence (find a relevant among fuzzy input), biology (group similar species), climatology (define a climate), marketing (identify profiles of consumers).

The driven idea is to use cluster analysis to identify the sub-domains where the weather forecast errors are homogeneous. Cluster analysis creates groups, each of them representing an homogeneous sub-domain. This requires homogeneous groups, well separated.

Cluster analysis is now introduced in a more technical way. The following definitions will be used to describe the method with a relevant vocabulary in the next sections.
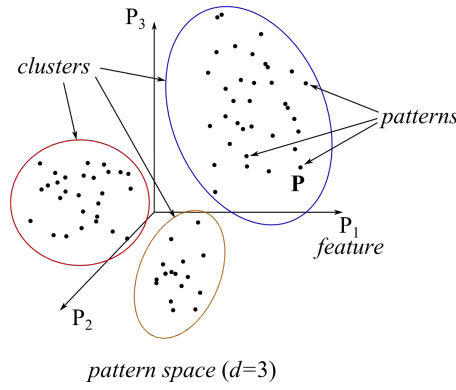
pattern space (d=3)

Figure 4.36: Example of pattern space, with patterns, features and clusters detailed.

Definition 4.4.1 (Pattern, pattern space). *A pattern* $\mathbf{P}$ *is a single data item, an object that will be assigned into a cluster. It is a vector of d points.*

$$\mathbf{P} = \begin{pmatrix} P_1 \\ \vdots \\ P_d \end{pmatrix}$$

A pattern is not modified by the cluster analysis.
All together, the patterns form a pattern set : $\mathcal{P} = \{\mathbf{P}^1, \ldots, \mathbf{P}^n\}$.
The space of dimension d where belong the patterns is called the pattern space, $\mathbb{P}$.

Definition 4.4.2 (Feature). *A feature is a single scalar component* P_j *of a pattern* $\mathbf{P}$. *It corresponds to one type of measurement. Each feature is a dimension of the pattern space. Feature space is a synonym of pattern space.*

In order to avoid confusion between feature indexes and pattern indexes, $\mathbf{P}^i$ indicates the i-th pattern in the pattern set (which is a vector), and P_j indicates the j-th feature of the pattern $\mathbf{P}$ (which is a scalar). So the j-th feature of the pattern $\mathbf{P}^i$ will be noted P_j^i (scalar).

A seed $\mathbf{C}$ is a special pattern that does not come from a data in the pattern set $\mathcal{P}$. It is the centroid of a cluster (created by the program).

Definition 4.4.3 (Cluster, centroid). *A cluster* $\mathcal{C}$ *is a group of patterns close to each other in the pattern space and according to the distance chosen. The clusters form a partition of the pattern set : if we have K clusters, then*

$$\bigcup_{k=1}^{K} \mathcal{C}^k = \mathcal{P}$$

The property $\bigcap_{k=1}^{K} \mathcal{C}^k = \emptyset$ *is also true.*

For each cluster $\mathcal{C}$, we can define (by different manners) a centroid. A centroid of the cluster $\mathcal{C}$ is any pattern $\mathbf{C}$ representative of the whole cluster. A synonym for centroid is seed.

The Figure 4.36 shows a pattern space with 3 features, where several patterns gathered into clusters are drawn.

For this work, the centroid will be the pattern for which each feature is the average feature of the patterns in the cluster.

$$\mathbf{C}^k = \begin{pmatrix} C_1^k \\ \vdots \\ C_d^k \end{pmatrix}, \quad \text{with } C_j^k = \frac{1}{n_k} \sum_{\mathbf{P}^i \in \mathcal{C}^k} P_j^i \, , \ \forall j \in \{1, \dots, d\} \tag{4.9}$$

where n_k is the number of patterns (population) in the cluster $\mathcal{C}^k$ $(1 \leqslant k \leqslant K)$.

The distance $\text{dist}(\cdot, \cdot)$ used to qualify the proximity of the patterns can be any metric defined on the pattern space. The most common distance is the Euclidean distance:

$$\text{dist}(\mathbf{P^j}, \mathbf{P^i}) = \|\mathbf{P^j} - \mathbf{P^i}\|_2 = \sqrt{\sum_{l=1}^{d} (P_l^j - P_l^i)^2}$$

The distance is an important issue in cluster analysis, because it's the metric of dissimilarity that will assess the membership to a cluster. The exact relation between distance and membership may vary in other cluster analysis method. Thus, the next definition is specific to K-means algorithms.

Definition 4.4.4 (Membership)**.** *Let $\mathcal{P} = \{\mathbf{P}^1, \dots, \mathbf{P}^n\}$ denotes a pattern set, and $\mathcal{C}^k$ a cluster where $k \in K$. The coefficient $w_k(\mathbf{P}^i)$ is defined by:*

$$w_k(\mathbf{P}^i) = \begin{cases} 1, & \text{if} \quad dist(\mathbf{P}^i, \mathbf{C}^k) = \min_{\ell=1\dots K} \big\{ dist(\mathbf{P}^i, \mathbf{C}^\ell) \big\} \\ 0, & \text{else} \end{cases} \tag{4.10}$$

signs the membership of the pattern $\mathbf{P}^i$ to the cluster $\mathcal{C}^k$. The coefficients have to verify $\forall i, \quad \sum_{k=1}^{K} w_k(\mathbf{P}^i) = 1$. This property means that a pattern belongs to only one cluster.

The concept of membership allows a more rigorous expression for the centroid definition than in (4.9). Here is the formula to use :

$$\mathbf{C}^k = \begin{pmatrix} C_1^k \\ \vdots \\ C_d^k \end{pmatrix}, \quad \text{with } C_j^k = \frac{\sum_{i=1}^{n} w_k(\mathbf{P}^i) P_j^i}{\sum_{i=1}^{n} w_k(\mathbf{P}^i)} \, , \ \forall j \in \{1, \dots, d\}$$

Here, the objects that will be manipulated and the relevant vocabulary were presented.

Implementation of K-means algorithms This section will focus on the clustering algorithm chosen: the K-means algorithm, and how it was implemented. The K-means algorithm was chosen for this problem because of the simplicity of its implementation and its robustness Jain et al. (1999). The K-means algorithm is a widely used method to gather huge amounts of data into clusters.

Each pattern $\mathbf{P}^i$, $\forall i \in \{1, \ldots, n\}$ is a vector of d variables. In this example, $d = 2 : w_n$ corresponding in Chapter 3 to the north component of the wind, and w_e corresponding to the east component is the other, and the i-th pattern is the vector $\mathbf{P}^i = \begin{pmatrix} w_n{}^i \\ w_e{}^i \end{pmatrix}$. In the K-means algorithm, the number of clusters K is known *a priori*. For each cluster $k, \quad k \in \{1, ..., K\}$, there is one centroid. Clusters are formed around these centroids.

The flowchart of the implemented K-means is given in Figure 4.37. The input of the program is a pattern set $\mathcal{P}$, resulting from the ensemble weather forecast.

The first box, called "Initializations", define the number clusters, the domain of clustering and the initial membership. In K-means, the number of clusters K is an input parameter. The choice of K can be an issue. However, for this work, 2 clusters has been validated as being the best choice. Indeed the point to point variance map, illustrated on Figure 4.39 shows that the ensemble is highly spread where the jet-stream takes place (see Figure 4.30). Then it follows that two sectors can be identified, the first being where the jet-stream takes place and the other being the complementary set,

$$\textit{Number of clusters :} \quad K = 2$$

The initial membership is set randomly, along an uniform law. This is a way to avoid sensitivity to initial conditions. After the initialization, the main loop is entered. It is composed with 3 boxes, corresponding to the 3 steps iterative algorithm. These steps are represented in Figure 4.38.

1. **Define the seeds** as the average point in the cluster.
   This step creates a new pattern for each cluster which features are the average feature of all the points in the clusters. If seeds already exists, the old ones are replaced by the new. It corresponds to the "Step 3" in Figure 4.38.

2. **Compute point-to-seed distances**.
   For each point $\mathbf{P}^i$, the distances from $\mathbf{P}^i$ to every seed $\mathbf{C}^1, \ldots, \mathbf{C}^K$ are calculated. It corresponds to the "Step 1" in Figure 4.38.

3. **Update membership**.
   Here the distances computed at the previous step are used to evaluate the membership of each point. It corresponds to the "Step 2" in Figure 4.38. The formula to calculate the membership from the distances is given on the previous section, with the definition of *membership*.

4. **Test of convergence**.
   The intra-cluster variance V is tested to check if it is of interest to stay in the main loop. The lower is V, the more the clusters are homogeneous and well separated. The criterion to go out of the loop is the trend of V: while it decreases, the loop continues. But as soon as V increase, the loop is stopped. This ensure a local minimum is reached, which is the best K-means can provide. The intra-cluster
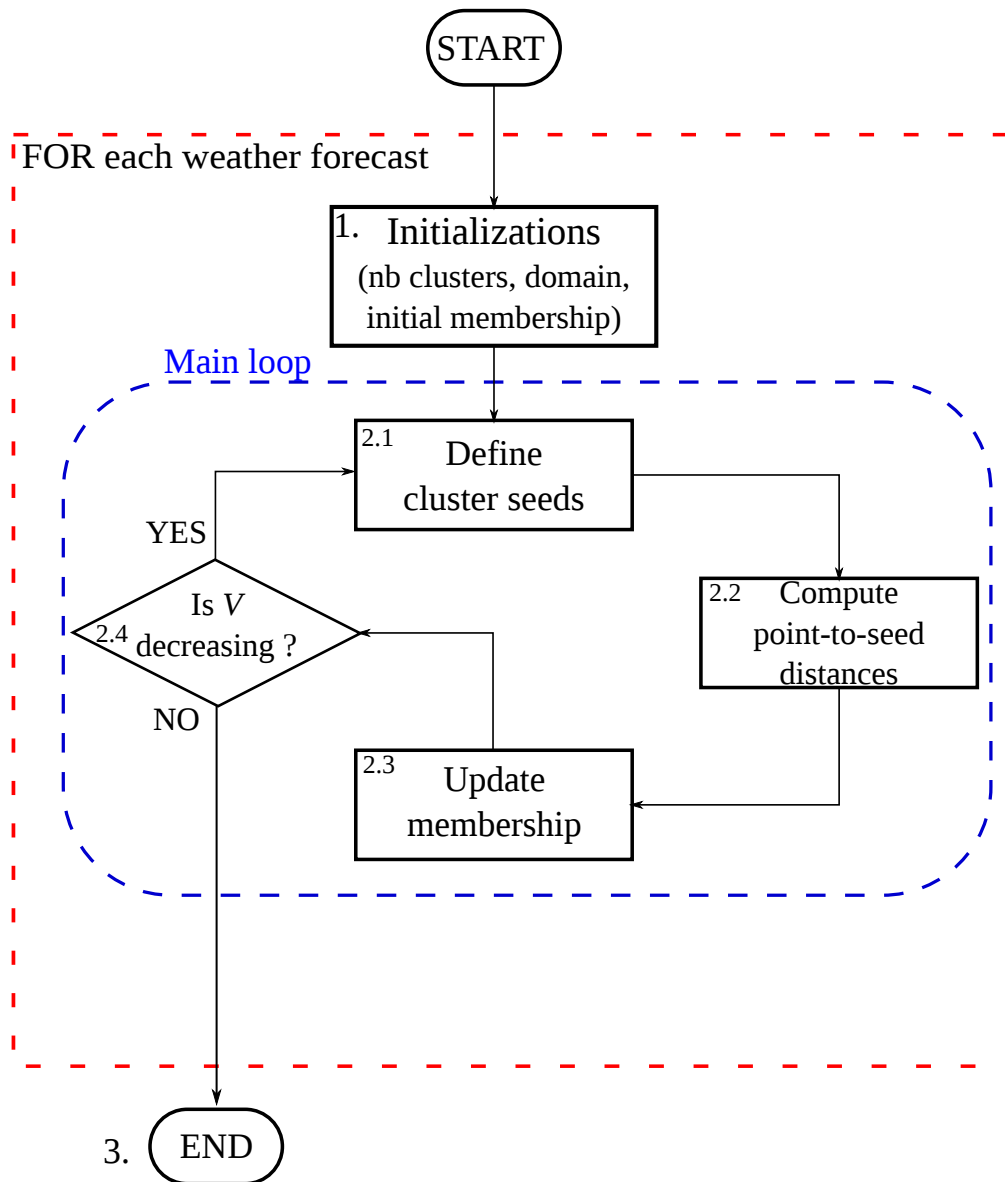
Figure 4.37: Flowchart of the K-means algorithm.
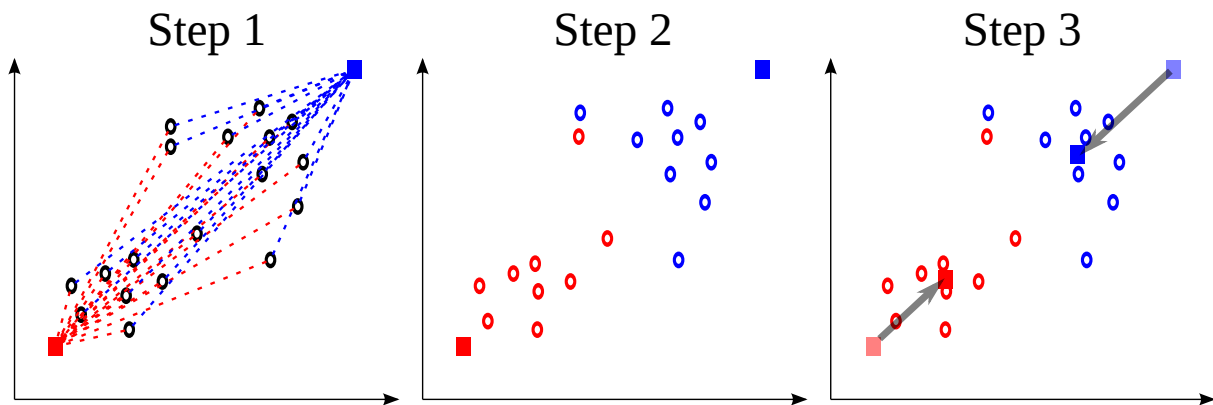
Figure 4.38: Schematic 3 steps in the main loop of the K-means algorithm.
It represents a 2D pattern space, with the patterns (empty circles) and 2 seeds (filled squares). Step 1 shows the "Compute point-to-seed distances". Step 2 is "Update membership", we can see the patterns turning the same color as the closest seed. Step 3 shows the new seeds after the "Define seeds" step, and few point-to-seed distances likely to change the membership at the next step.
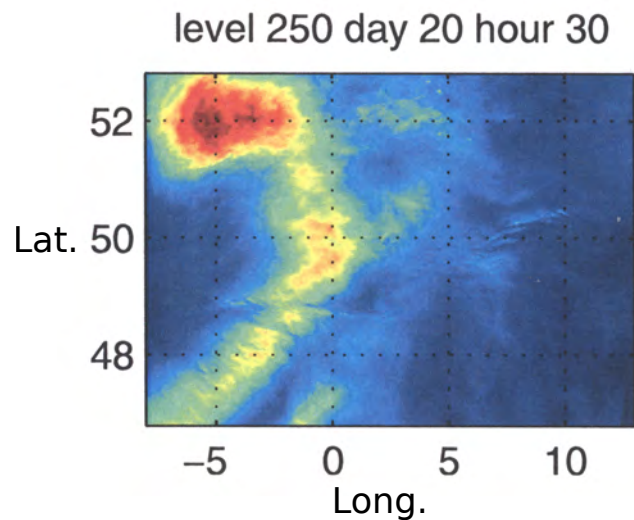
Figure 4.39: Representation of the point to point variance (color-scale from blue to red, blue color corresponds to a low variance and red color to a high variance) of the wind proposals given by the 34 members of the PE AROME forecast at $250Hpa$ for the 22nd of May, midnight, with respect to the latitude (y-axis) and longitude coordinate(x-axis). The forecast was launched 30 hours before. The variance is really high on the high-left corner of the domain. This localization corresponds to the meteorological phenomenon located at the south of Ireland. Then a long strip of higher variance value oriented from South-West to North-East of Europe is present and correspond to the jet-stream localization, see Figure 4.30.

variance is the sum of squared errors:

$$V = \sum_{k=1}^{K} \sum_{i=1}^{n} w_k(\mathbf{P}^i) \mathrm{dist}(\mathbf{P}^i, \mathbf{C}^k)$$

Then, in the box 3, the clusters are formed and the homogeneous sub-domains defined by them.

In summary, the K-means algorithm is an iterative algorithm to create clusters. The cluster are created around centroids called seeds. The homogeneous sub domains are then defined using the clusters. The flowchart can be summarized in the following list:

1. Select the useful features. Initialize clusters randomly (uniform law).

2. Enter the main loop (WHILE loop)

   2.1 A seed is defined as the average pattern of a cluster.

   2.2 We compute the distances from each point to each seed.

   2.3 Each point is assigned to the closest cluster (we update the membership).

   2.4 If the intra-cluster variance reaches a minimum, we stops. If it doesn't, go to step 2.1.

We presents the segmentation results obtained on wind forecast members 2 and 12 for the 22nd of May at midnight. The forecast was launched 30 hours before. The cluster 1 seems to corresponds to the jet stream zone, as one can see comparing Figure 4.30 with Figure 4.40 and Figure 4.41. Cluster 2 is the complementary set of cluster 1.

Results obtained thanks to the patchwork labeled island algorithm

Every ingredients needed to perform the ensemble weather forecast weighting are now ready. The air-traffic scenario used is composed of 11 aircraft using the model developed in Chapter 3. We denote it by $\mathbb{X}_n = (X_n^i)_{i=1}^{11}$ with their positions given by $\mathbb{Z}_n = (Z_n^i)_{i=1}^{11}$. Their flight plans are given in Table 4.3 where Lat refers to latitudes and Long to longitudes in degrees. We simulate 10 minutes of air-traffic with a time step of 4 seconds. All the aircraft are Airbus $A320$, we set the aerodynamics parameters using the BADA database. The Mach speed is set for all the aircraft to 0.78. aircraft are assumed to be on the flight level $FL350$, the initial masses are set to 70% of the maximum pay-load. In a first place, to simulate the reference air-traffic process, we use the analysis. It is the wind field represented on Figure 4.34. The initial distribution of each aircraft position process Z_0^i, denoted by $\eta_{\Theta_0^P,0}^{Z^i}$ is given by:

$$\eta_0^{Z^i}(\mathrm{d}z) = \delta_{O_1^i}(\mathrm{d}z).$$

The air-traffic process observations $\mathbb{Y} = (Y_n^i)_{i=1}^{11}$ are reduced to the aircraft $3D$-
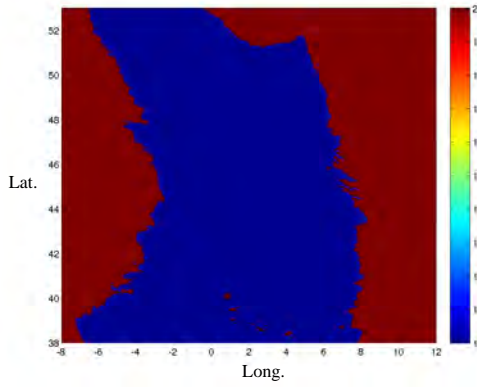
Figure 4.40: Representation of the segmented wind field proposal given by member 2, in blue is represented $\mathsf{b}_{0,1}^1$ and in red $\mathsf{b}_{0,1}^2$. The x-axis represents the longitude coordinates and the y-axis the latitude coordinates. $\mathsf{b}_{0,l}^1$ corresponds to the jet-stream meteorological object. Indeed its localization (see Figure 4.30) is close to the one presented on Figure 4.30.
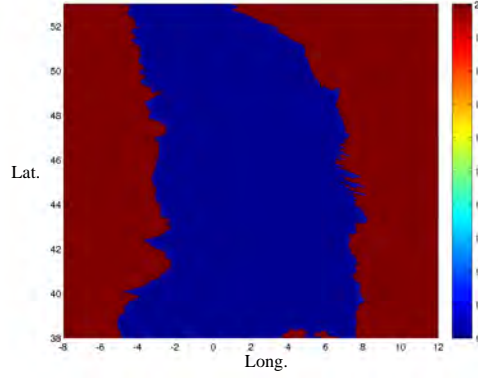
Figure 4.41: Representation of the segmented wind field proposal given by member 12, in blue is represented $\mathsf{b}_{0,1}^1$ and in red $\mathsf{b}_{0,1}^2$. The x-axis represents the longitude coordinates and the y-axis the latitude coordinates. $\mathsf{b}_{0,l}^1$ corresponds to the jet-stream meteorological object. Member 32 propose another realization location for the jet-stream as the one proposed by member 2, even if they are close one to each other, the form differs.

Aircraft		O_1	O_2
1	Lat	39.5	39.5
	Long	-1	-6.5
2	Lat	40	44.5
	Long	1.5	1.5
3	Lat	41.5	45
	Long	-7	0
4	Lat	48	49
	Long	-1	-1
5	Lat	40	46.5
	Long	9.5	2
6	Lat	47	47
	Long	0.5	5.5
7	Lat	48.5	48.5
	Long	3.5	10
8	Lat	52	49.5
	Long	9.5	2
9	Lat	52.5	49.5
	Long	1.5	1.5
10	Lat	52	48
	Long	-7	1.5
11	Lat	47	52.5
	Long	-1.5	-3

Table 4.3: Flight plans of the eleven aircraft in degrees

Figure 4.42: Time evolution (y coordinate) of the wind proposal weights (z-coordinate) for $b_{0,1}^1$ obtained thanks to the patchwork labeled island particle algorithm. At the beginning of the algorithm all the weights are equidistributed

positions $\mathbb{Z}_n = (Z_n^i)_{i=1}^{11}$. They are obtained thanks to the following equation:

$$Y_n^i = Z_n^i + B_n^Y$$

where $B_n^Y \sim \mathsf{N}(0, \Sigma^Y)$, and $\Sigma^Y = 1.5 \times 10^{-5} \begin{pmatrix} 1 & 0 & 0 \\ 0 & 1 & 0 \\ 0 & 0 & 1 \end{pmatrix}$. The standard deviation was set to fit the radar specifications. We use Algorithm 6 to estimate the law of the couple $(\Theta_n, \eta_{\theta_{0:n},n}^{\mathbb{X}})$ given the observations $\mathbb{Y}_{0:n}$, where the potential functions G_n are given by the likelihood of the observations, that is for all $\mathbb{X}_n \in (\mathsf{E}_n^X)^{11}$ and $\theta_n \in \mathsf{E}_n^\Theta$:

$$G_{\theta_n,n}(\mathbb{X}_n) \propto \prod_{i=1}^{11} \exp\left(-\frac{(Y_n^i - Z_n^i)^T (\Sigma^Y)^{-1} (Y_n^i - (Z_n^i, V_n^{a,i})))}{2} \right).$$

The wind proposals are given by the members of the ensemble weather forecast. The reference air-traffic is generated using the wind field produced by the analysis, represented on Figure 4.34. In Figure 4.42 and Figure 4.43 the weight evolution of the different members of the ensemble with respect to time is represented for cluster 1 and 2 respectively. As one can note, at the beginning of the experiment, all the members have the same weight. Then as time goes, the weight start to concentrate over several members. It follows that for cluster 1, that is $b_{0,1}^1$, weights are concentrated over 8 members. Concerning the cluster 2, $b_{0,l}^2$, the weights are less concentrated but discard 4 members. The obtained results are not surprising, indeed as one can see on Figure 4.39 the point to point variance is low which means that members do not propose really different scenarios. Hence the weights which are not concentrated can be explained. To sum up, the numerical experiment led
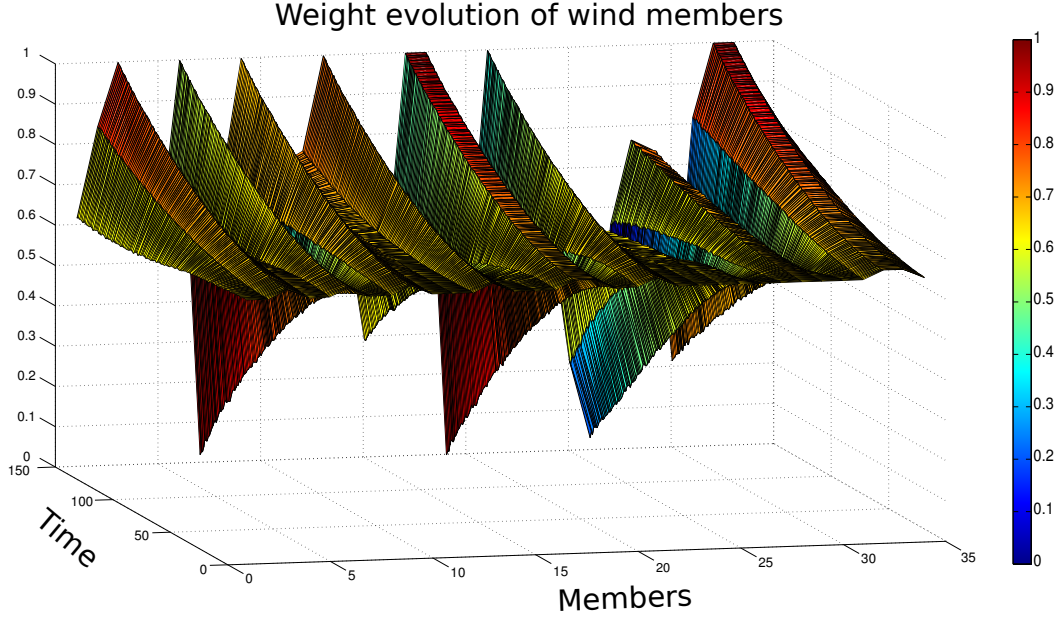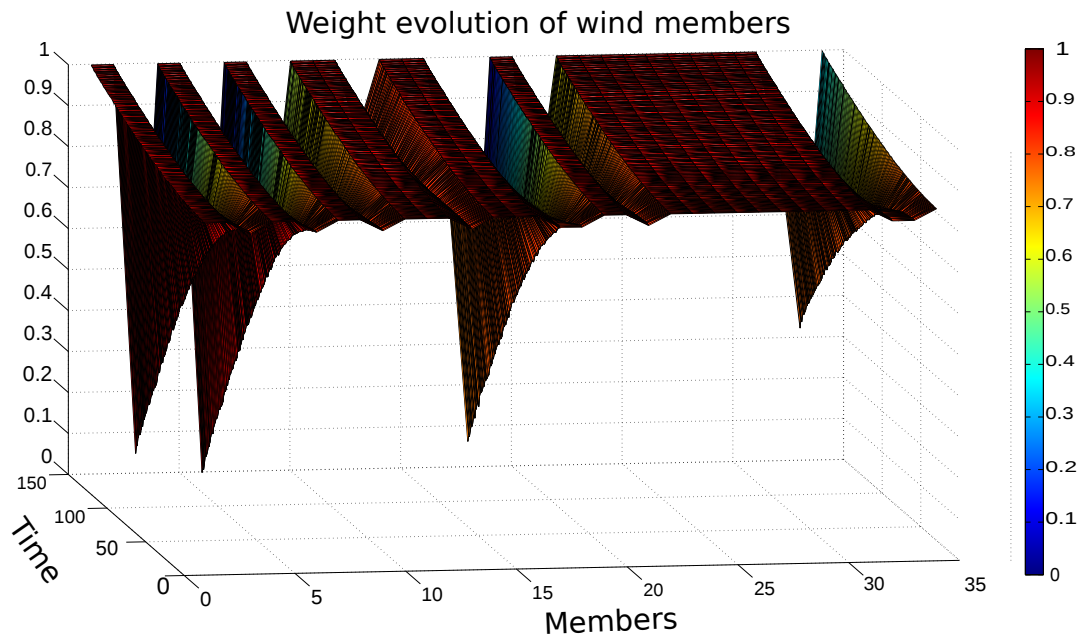
Figure 4.43: Time evolution (y coordinate) of the wind proposal weights (z-coordinate) for $b_{0,1}^2$ obtained thanks to the patchwork labeled island particle algorithm. At the beginning of the algorithm all the weights are equidistributed

with the patchwork labeled island particle filter have shown its ability to locally weight an ensemble weather forecast.

In this chapter we present all the numerical experiments we have conducted. They have been the achievement of the novel filtering techniques we have developed. We have seen their efficiency and their limits. That gives us the possibility to conclude and have new prospectives for future works.

"Begin at the beginning," the King said, gravely, *"and go on till you come to an end; then stop."*

Lewis Carroll, *Alice in Wonderland*

5

Conclusion

The research work we have conducted in this thesis allows us to propose innovative solutions for the ATM community concerning the study of aircraft trajectory prediction uncertainties induced by weather forecast errors. Thanks to the novel methods, we are able to deliver ensemble weather forecast assorted with performing scores. This scores are obtained regarding the performance of each member of the ensemble through the trajectory prediction system with respect to air-traffic observations. This stochastic engineering work have also given us the opportunity to develop more general innovative mathematical models to describe the estimation problem of random punctual processes evolving in a random field decomposed in homogeneous sub-domains.

For two decades, particle filtering techniques have been widely studied in applied mathematics and used in several application domains such as target tracking, robot positioning, finance and ATM. The probability theory is well settled and particle filtering methods are now used for real time systems to filter signals, to track targets or to estimate probability of rare-events. However, to filter signals evolving in a random field decomposed in homogeneous sub-domains, no pre-existing filters were well-adapted. In this thesis work, we have developed and studied methods which can deal with such processes and we have given associated particle approximations.

In Chapter 2, first, we have presented the non-linear filtering problem for random processes on which the development we have made are based. In order to be applied to random processes evolving in a random environment we have extended the filtering problem to distribution space and we have developed an adapted algorithm which propose a way to give an approximation of the couple random environment, conditional law of the random process given the environment. The proposed algorithm has been studied and

first convergence results are provided for the ensuing estimator.

Finally, we have recalled the acquisition process formalism which provides a good framework to model the estimation problem of a random field along a random path. Then, this framework was has been extended to acquisition processes of random field decomposed in homogeneous sub-domains along random paths. This model allows us to couple the Lagrangian evolution of homogeneous sub-domains with the acquisition systems defined by the random paths. This coupling enables us to formulate the estimation problem of the random field for each sub-domain using random processes evolving inside the whole random field. Then weighting an ensemble weather forecast with respect to its performance through the aircraft trajectory prediction system and air-traffic observations is the application of this theoretical work.

We have tested with numerical experiments the efficiency of the developed algorithms in Chapter 4. The numerical experiences are various. As concerns the algorithm developed to estimate random processes in random environment we have tried to highlight its efficiency on simple toy-models and we have illustrated the theoretical results obtained. Gradually, we have increased the level of complexity towards the final aim : weighting ensemble weather forecast with respect to their performance according to air-traffic observations. To this end, we have developed a realistic aircraft model in Chapter 3. The presented algorithm to estimate random field decomposed in homogeneous sub-domains using observations of random processes evolving inside it able us to actually weight ensemble weather forecasts through the performance of the aircraft trajectory prediction systems according to air-traffic observations. In a toy-model experiment, the obtained results are encouraging as the highest weight is affected to the member used to create the reference air-traffic.

However to properly end the numerical work we have made, one should develop stochastic controls for the trajectory predictor we have built in order to turn the deterministic dynamic controlled system into a stochastic one. In this way, all the theoretical work we have developed about estimation will take sense. Another improvement would be also to take temperature as an uncertain parameter inside the dynamic model used to predict aircraft trajectories. More practically, an optimization of the computer code should also be performed in order to deal with the high dimensional data coming from the ensemble weather forecasts, but also with the high number of aircraft present at the same time in the same controlled area.

From there, another theoretical work can be led. Indeed weighting the ensemble weather forecast gives to the ATM actors the opportunity to have a better clue of the future evolution of the atmospheric conditions. To exploit this opportunity one may think at developing an optimization tool to get optimized aircraft trajectories taking into account the environment uncertainties. In Section A.3, we propose a way to model and solve it.

Bibliography

Hajime Akashi and Hiromitsu Kumamoto. Random sampling approach to state estimation in switching environments. *Automatica*, 13(4):429–434, 1977.

Sungbae An and Frank Schorfheide. Bayesian analysis of dsge models. *Econometric reviews*, 26(2-4):113–172, 2007.

Christophe Andrieu, Arnaud Doucet, and Roman Holenstein. Particle markov chain monte carlo methods. *Journal of the Royal Statistical Society: Series B (Statistical Methodology)*, 72(3):269–342, 2010.

Pedro Argüelles, Manfred Bischoff, Philippe Busquin, BAC Droste, Sir Richard Evans, W Kröll, JL Lagardere, A Lina, J Lumsden, D Ranque, et al. European aeronautics: A vision for 2020. *Advisory Council for Aeronautics Research in Europe, Report*, 2001.

GérardBen Arous. Flots et series de taylor stochastiques. *Probability Theory and Related Fields*, 81(1):29–77, 1989. ISSN 0178-8051. doi: 10.1007/BF00343737. URL http://dx.doi.org/10.1007/BF00343737.

Christophe Baehr. Stochastic modeling and filtering of discrete measurements for a turbulent field. application to measurements of atmospheric wind. *International Journal of Modern Physics B*, 23(28-29):5424–5433, 2009.

Christophe Baehr. Nonlinear filtering for observations on a random vector field along a random path. application to atmospheric turbulent velocities. *ESAIM: Mathematical Modelling and Numerical Analysis*, 44(05):921–945, 2010.

Christophe Baehr and Nolwenn Huet. Sesar wp 04.07.02, internal technical note "weather model". Technical report, SESAR, 2011.

Christophe Baehr and Cécile Ichard. Aircraft trajectory prediction in random atmosphere. mathematical background and application to a locally uniform academic case. In Dirk Schaefer, editor, *Proceedings of the SESAR Innovation Days*. EUROCONTROL, 2013. ISBN 978-2-87497-074-0.

Mark G Ballin, Vivek Sharma, Robert A Vivona, Edward J Johnson, and Ermin Ramiscal. A flight deck decision support tool for autonomous airborne operations. In *Proceedings of the AIAA Guidance, Navigation, and Control Conference & Exhibit*, 2002.

Vlad Bally and Denis Talay. The law of the euler scheme for stochastic differential equations. *Probability theory and related fields*, 104(1):43–60, 1996.

Leonard E Baum and Ted Petrie. Statistical inference for probabilistic functions of finite state markov chains. *The annals of mathematical statistics*, pages 1554–1563, 1966.

Leonard E Baum, Ted Petrie, George Soules, and Norman Weiss. A maximization technique occurring in the statistical analysis of probabilistic functions of markov chains. *The annals of mathematical statistics*, pages 164–171, 1970.

Henk AP Blom and Edwin A Bloem. Joint immpda particle filter. In *Proceedings of the 6th International Conference on Information Fusion*, pages 8–11, 2003.

Henk AP Blom and Edwin A Bloem. Tracking multiple maneuvering targets from possibly unresolved, missing or false measurements. In *Information Fusion, 2005 8th International Conference on*, volume 1, pages 8–pp. IEEE, 2005.

LV Bogachev. Random walks in random environments. *Encyclopedia Math. Phys.*, 4 (arXiv : 0707.3160):353–371, 2007.

Jean-Luc Boiffier. *The dynamics of flight: the equations*. Wiley, 1998.

François Bouttier, Benoît Vié, Olivier Nuissier, and Laure Raynaud. Impact of stochastic physics in a convection-permitting ensemble. *Monthly Weather Review*, 140(11):3706–3721, 2012.

O. Cappe, S.J. Godsill, and E. Moulines. An overview of existing methods and recent advances in sequential monte carlo. *Proceedings of the IEEE*, 95(5):899–924, May 2007. ISSN 0018-9219. doi: 10.1109/JPROC.2007.893250.

François Caron, Pierre Del Moral, Arnaud Doucet, and Michele Pace. Particle approximations of a class of branching distribution flows arising in multi-target tracking. *SIAM Journal on Control and Optimization*, 49(4):1766–1792, 2011a.

François Caron, Pierre Del Moral, Arnaud Doucet, Michele Pace, et al. On the conditional distributions of spatial point processes. *Advances in Applied Probability*, 43(2):301–307, 2011b.

Francois Caron, Pierre Del Moral, Michele Pace, and B-N Vo. On the stability and the approximation of branching distribution flows, with applications to nonlinear multiple target filtering. *Stochastic Analysis and Applications*, 29(6):951–997, 2011c.

Georgios Chaloulos and John Lygeros. Effect of wind correlation on aircraft conflict probability. *Journal of Guidance, Control, and Dynamics*, 30(6):1742–1752, 2007.

Rong Chen and Jun S Liu. Mixture kalman filters. *Journal of the Royal Statistical Society: Series B (Statistical Methodology)*, 62(3):493–508, 2000.

Jianye Ching, James L Beck, and Keith A Porter. Bayesian state and parameter estimation of uncertain dynamical systems. *Probabilistic engineering mechanics*, 21(1):81–96, 2006.

N. Chopin. A sequential particle filter method for static models. *Biometrika*, 89:539–552, 2002.

Nicolas Chopin. Central limit theorem for sequential monte carlo methods and its application to bayesian inference. *Annals of statistics*, pages 2385–2411, 2004.

Nicolas Chopin, Pierre E Jacob, and Omiros Papaspiliopoulos. Smc2: an efficient algorithm for sequential analysis of state space models. *Journal of the Royal Statistical Society: Series B (Statistical Methodology)*, 75(3):397–426, 2013.

Rama Cont. Model uncertainty and its impact on the pricing of derivative instruments. *Mathematical Finance*, 16(3):519–547, 2006. ISSN 1467-9965. doi: 10.1111/j.1467-9965. 2006.00281.x. URL http://dx.doi.org/10.1111/j.1467-9965.2006.00281.x.

Dan Crisan and Arnaud Doucet. A survey of convergence results on particle filtering methods for practitioners. *Signal Processing, IEEE Transactions on*, 50(3):736–746, 2002.

Dan Crisan and Joaquin Miguez. Nested particle filters for online parameter estimation in discrete-time state-space markov models. 2013.

Pierre Del Moral. Non-linear filtering: interacting particle resolution. *Markov processes and related fields*, 2(4):555–581, 1996a.

Pierre Del Moral. Non-linear filtering: interacting particle resolution. *Markov processes and related fields*, 2(4):555–581, 1996b.

Pierre Del Moral. *Feynman-Kac formulae: genealogical and interacting particle systems with applications*. Series: Probability & Applications Springer Verlag, 2004.

Pierre Del Moral and Alice Guionnet. On the stability of interacting processes with applications to filtering and genetic algorithms. In *Annales de l'institut Henri Poivaré (B) Probability and Statistics*, volume 37, pages 155–194. Elsevier, 2001.

Pierre Del Moral, Laurent Miclo, and Michael A Kouritzin. On a class of discrete generation interacting particle systems. *Electronic Journal of Probability*, 6(16):1–26, 2001.

Pierre Del Moral, Arnaud Doucet, and Ajay Jasra. An adaptive sequential monte carlo method for approximate bayesian computation. *Statistics and Computing*, 22(5):1009–1020, 2012.

Daniel Delahaye, Stéphane Puechmorel, and Pierre Vacher. Windfield estimation by radar track kalman filtering and vector spline extrapolation. In *Digital Avionics Systems Conference, 2003. DASC'03. The 22nd*, volume 1, pages 5–E. IEEE, 2003.

L Descamps, C Labadie, A Joly, E Bazile, P Arbogast, and P Cébron. Pearp, the météo-france short-range ensemble prediction system. *Quarterly Journal of the Royal Meteorological Society*, 2014.

Randal Douc and Eric Moulines. Limit theorems for weighted samples with applications to sequential monte carlo methods. In *ESAIM: Proceedings*, volume 19, pages 101–107. EDP Sciences, 2007.

Arnaud Doucet. On sequential simulation-based methods for bayesian filtering. Technical report, Department of Engineering, Cambridge University, 1998.

Arnaud Doucet and Adam M Johansen. A tutorial on particle filtering and smoothing: Fifteen years later. *Handbook of Nonlinear Filtering*, 12:656–704, 2009.

Arnaud Doucet, Nando De Freitas, Kevin Murphy, and Stuart Russell. Rao-blackwellised particle filtering for dynamic bayesian networks. In *Proceedings of the Sixteenth conference on Uncertainty in artificial intelligence*, pages 176–183. Morgan Kaufmann Publishers Inc., 2000.

Arnaud Doucet, Nando de Freitas, and Neil Gordon. *Sequential Monte Carlo Methods in Practice.* Springer New York, 2001.

Edward S Epstein. Stochastic dynamic prediction. *Tellus*, 21(6):739–759, 1969.

EU. Sesar joint undertaking, sesar (single european sky atm research), 2007. URL http://www.sesarju.eu/.

Eurocontrol. Challenges of growth, task 7. european air-traffic in 2050. Technical report, European Organization for the Safety of Air Navigation (Eurocontrol), 2013.

FAA. Nextgen, concept of operations for the next generation air transport system, 2007. URL http://www.faa.gov/nextgen/.

Jesús Fernández-Villaverde and Juan F Rubio-Ramírez. Estimating macroeconomic models: A likelihood approach. *The Review of Economic Studies*, 74(4):1059–1087, 2007.

Franco Flandoli, Massimiliano Gubinelli, and Enrico Priola. Well-posedness of the transport equation by stochastic perturbation. *Inventiones mathematicae*, 180(1):1–53, 2010.

Jean-Pierre Fouque, Josselin Garnier, George Papanicolaou, and Knut Solna. *Wave propagation and time reversal in randomly layered media*, volume 56. Springer Science & Business Media, 2007.

William Glover and John Lygeros. A stochastic hybrid model for air traffic control simulation. In *Hybrid Systems: Computation and Control*, pages 372–386. Springer, 2004.

Neil J Gordon, David J Salmond, and Adrian FM Smith. Novel approach to nonlinear/non-gaussian bayesian state estimation. In *IEE Proceedings F (Radar and Signal Processing)*, volume 140, pages 107–113. IET, 1993.

Steven M Green and Robert Vivona. Field evaluation of descent advisor trajectory prediction accuracy. In *Proceedings of the AIAA Guidance Navigation and Control Conference*, volume 8, 1996.

Fredrik Gustafsson, Fredrik Gunnarsson, Niclas Bergman, Urban Forssell, Jonas Jansson, Rickard Karlsson, and P-J Nordlund. Particle filters for positioning, navigation, and tracking. *Signal Processing, IEEE Transactions on*, 50(2):425–437, 2002.

JE Handschin. Monte carlo techniques for prediction and filtering of non-linear stochastic processes. *Automatica*, 6(4):555–563, 1970.

JE Handschin and David Q Mayne. Monte carlo techniques to estimate the conditional expectation in multi-stage non-linear filtering. *International journal of control*, 9(5): 547–559, 1969.

Gustaf Hendeby, Rickard Karlsson, and Fredrik Gustafsson. The rao-blackwellized particle filter: A filter bank implementation. *EURASIP Journal on Advances in Signal Processing*, 2010(724087), 2010.

Jianghai Hu, Maria Prandini, and Shankar Sastry. Optimal coordinated maneuvers for three-dimensional aircraft conflict resolution. *Journal of Guidance, Control, and Dynamics*, 25(5):888–900, 2002.

David G Hull. Fundamentals of airplane flight mechanics. 2007.

ICAO. Global air transport outlook to 2030 and trends to 2040. Technical report, International Civil Aviation Organization (ICAO), 2013.

Cécile Ichard and Christelle Vergé. Introduction to labeled island particle models and their asymptotic properties. *arXiv preprint arXiv:1503.07316*, 2015.

Cécile Ichard, Christophe Baehr, et al. Inference of a random environment from random process realizations: Formalism and application to trajectory prediction. In *ISIATM 2013, 2nd International Conference on Interdisciplinary Science for Innovative Air Traffic Management*, 2013.

Michael R Jackson, Yiyuan J Zhao, and Rhonda A Slattery. Sensitivity of trajectory prediction in air traffic management. *Journal of Guidance, Control, and Dynamics*, 22 (2):219–228, 1999.

Cheung Jacob, Jean-Louis Brenguier, Heijstek Jaap, Adri Marsman, and Helen Wells. Sensitivity of flight durations to uncertainties in numerical weather prediction. In Dirk Schaefer, editor, *Proceedings of the SESAR Innovation Days*. EUROCONTROL, 2014. ISBN 978-2-87497-077-1. URL http://www.sesarinnovationdays.eu/sites/default/files/media/SIDs/SID%202014-32.pdf.

Anil K Jain, M Narasimha Murty, and Patrick J Flynn. Data clustering: a review. *ACM computing surveys (CSUR)*, 31(3):264–323, 1999.

Adam M Johansen, Nick Whiteley, and Arnaud Doucet. Exact approximation of rao-blackwellised particle filters. *System Identification*, 16(1):488–493, 2012.

Rudolph E Kalman and Richard S Bucy. New results in linear filtering and prediction theory. *Journal of Fluids Engineering*, 83(1):95–108, 1961.

Rudolph Emil Kalman. A new approach to linear filtering and prediction problems. *Journal of Fluids Engineering*, 82(1):35–45, 1960.

Rickard Karlsson. *Simulation based methods for target tracking.* Division of Automatic Control & Communication Systems, Department of Electrical Engineering, Linköpings universitet, 2002.

G. Kitagawa. Non-Gaussian state space modeling of nonstationary time series. *jasa*, 82 (400):1023–1063, 1987.

Genshiro Kitagawa. Monte carlo filter and smoother for non-gaussian nonlinear state space models. *Journal of computational and graphical statistics*, 5(1):1–25, 1996.

Genshiro Kitagawa. A self-organizing state-space model. *Journal of the American Statistical Association*, pages 1203–1215, 1998.

Hans R Künsch. Recursive monte carlo filters: algorithms and theoretical analysis. *Annals of Statistics*, pages 1983–2021, 2005.

CE Leith. Theoretical skill of monte carlo forecasts. *Monthly Weather Review*, 102(6): 409–418, 1974.

Ping Li, Roger Goodall, and Visakan Kadirkamanathan. Estimation of parameters in a linear state space model using a rao-blackwellised particle filter. *IEE Proceedings-control theory and applications*, 151(6):727–738, 2004.

Xiangdong Lin, Thiagalingam Kirubarajan, Yaakov Bar-Shalom, and Simon Maskell. Comparison of ekf, pseudomeasurement, and particle filters for a bearing-only target tracking problem. In *AeroSense 2002*, pages 240–250. International Society for Optics and Photonics, 2002.

Jane Liu and Mike West. Combined parameter and state estimation in simulation-based filtering. In *Sequential Monte Carlo methods in practice*, pages 197–223. Springer, 2001.

Lennart Ljung. Asymptotic behavior of the extended kalman filter as a parameter estimator for linear systems. *Automatic control, IEEE Transactions on*, 24(1):36–50, 1979.

Lennart Ljung. *System identification.* Springer, 1998.

Christian Lundquist, Rickard Karlsson, Emre Özkan, and Fredrik Gustafsson. Tire radii estimation using a marginalized particle filter. *IEEE transactions on intelligent transportation systems (Print)*, 15(2):663–672, 2014.

Ioannis Lymperopoulos. *Sequential Monte Carlo methods in air traffic management.* PhD thesis, Diss., Eidgenössische Technische Hochschule ETH Zürich, Nr. 19004, 2010, 2010.

Ioannis Lymperopoulos and John Lygeros. Adaptive aircraft trajectory prediction using particle filters. In *AIAA Guidance, Navigation and Control Conference and Exhibit*, volume 7387, 2008a.

Ioannis Lymperopoulos and John Lygeros. Trajectory prediction by adaptively reducing wind uncertainty. In *10th International Conference on Application of Advanced Technologies in Transportation*, number EPFL-CONF-187519, 2008b.

Ioannis Lymperopoulos and John Lygeros. Improved ground trajectory prediction by multi-aircraft track fusion for air traffic control. In *AIAA Guidance, Navigation and Control Conference and Exhibit*, 2009.

Ioannis Lymperopoulos and John Lygeros. Improved multi-aircraft ground trajectory prediction for air traffic control. *Journal of guidance, control, and dynamics*, 33(2): 347–362, 2010.

Ioannis Lymperopoulos, John Lygeros, and A Lecchini Visintini. Model based aircraft trajectory prediction during takeoff. In *AIAA Guidance, Navigation and Control Conference and Exhibit, Keystone, Colorado*, 2006.

R Mikulevicius and BL Rozovskii. Stochastic navier–stokes equations for turbulent flows. *SIAM Journal on Mathematical Analysis*, 35(5):1250–1310, 2004.

Annie Millet and Marta Sanz-Solé. A stochastic wave equation in two space dimension: smoothness of the law. *Annals of Probability*, pages 803–844, 1999.

Sanjoy K Mitter. *Nonlinear filtering and stochastic control: proceedings of the 3rd 1981 Session of the Centro Internazionale Matematico Estivo (CIME), held at Cortona, July 1-10, 1981.* Number 972-973. Springer Verlag, 1982.

Franco Molteni, Roberto Buizza, Tim N Palmer, and Thomas Petroliagis. The ecmwf ensemble prediction system: Methodology and validation. *Quarterly Journal of the Royal Meteorological Society*, 122(529):73–119, 1996.

Stéphane Mondoloni. Aircraft trajectory prediction errors: Including a summary of error sources and data (version 0.2). *FAA/EUROCONTROL Action Plan*, 16, 2006a.

Stéphane Mondoloni. A multiple-scale model of wind-prediction uncertainty and application to trajectory prediction. In *6th AIAA Aviation Technology, Integration and Operations Conference (ATIO)*, 2006b.

Stephane Mondoloni, Mike Paglione, and Steve Green. Trajectory modeling accuracy for air traffic management decision support tools. In *ICAS 2002 Congress, Toronto, ON*, 2002.

D Montemerlo, Sebastian Thrun, and William Whittaker. Conditional particle filters for simultaneous mobile robot localization and people-tracking. In *Robotics and Automation, 2002. Proceedings. ICRA'02. IEEE International Conference on*, volume 1, pages 695–701. IEEE, 2002.

WM Mularie. Department of defense world geodetic system 1984, its definition and relationships with local geodetic systems. *National Geospatial-Intelligence Agency, Tech. Rep*, 152, 2000.

Per-Johan Nordlund. *Sequential Monte Carlo filters and integrated navigation.* Citeseer, 2002.

A Nuic. User manual for the base of aircraft data (bada). *Eurocontrol Experimental Centre, Cedex, France, revision*, 3, 2011.

Emre Özkan, Vaclav Smidl, Saikat Saha, Christian Lundqvist, and Fredrik Gustafsson. Marginalized adaptive particle filtering for nonlinear models with unknown time-varying noise parameters. *Automatica*, 49(6):1566–1575, 2013.

Szymon Peszat. The cauchy problem for a nonlinear stochastic wave equation in any dimension. *Journal of Evolution Equations*, 2(3):383–394, 2002.

Mark Peters and Michael A Konyak. The engineering analysis and design of the aircraft dynamics model for the faa target generation facility. *Seagull Technology, Inc., Los Gatos, CA*, pages 43–45, 2003.

SB Pope. Pdf methods for turbulent reactive flows. *Progress in Energy and Combustion Science*, 11(2):119–192, 1985.

George Poyiadjis, Arnaud Doucet, and Sumeetpal S Singh. Maximum likelihood parameter estimation in general state-space models using particle methods. In *Proc of the American Stat. Assoc.* Citeseer, 2005.

Xavier Prats, Marc Pérez-Batlle, Cristina Barrado, Santi Vilardaga, Isidro Bas, Florent Birling, Ronald Verhoeven, and Adri Marsman. Enhancement of a time and energy management algorithm for continuous descent operations. In *Proceedings of the Aviation Technology, Integration and Operations (ATIO) conference*, 2014.

Pál Révész. *Random walk in random and non-random environments.* World Scientific, 2005.

Saikat Saha and Fredrik Gustafsson. Particle filtering with dependent noise processes. *IEEE Transactions on Signal Processing*, 60(9):4497–4508, 2012.

Roger D. Schaufele. Aerospace forecast fiscal years 2014-2034. Technical report, Federal Aviation Administration (FAA), 2013.

Thomas Schön, Fredrik Gustafsson, and P-J Nordlund. Marginalized particle filters for mixed linear/nonlinear state-space models. *Signal Processing, IEEE Transactions on*, 53(7):2279–2289, 2005.

Zoltan Toth and Eugenia Kalnay. Ensemble forecasting at ncep and the breeding method. *Monthly Weather Review*, 125(12):3297–3319, 1997.

C. Vergé, C. Dubarry, P. Del Moral, and E. Moulines. On parallel implementation of sequential monte carlo methods: the island particle model. *Statistics and Computing*, 23, 2013. URL http://link.springer.com/article/10.1007%2Fs11222-013-9429-x.

Ronald Verhoeven, Ramon Dalmau Codina, Xavier Prats Menéndez, Nico de Gelder, et al. Real-time aircraft continuous descent trajectory optimization with atc time constraints using direct collocation methods. 2014.

Jaco Vermaak, Simon J Godsill, and Patrick Perez. Monte carlo filtering for multi target tracking and data association. *Aerospace and Electronic Systems, IEEE Transactions on*, 41(1):309–332, 2005.

Mark E Weber, James E Evans, William R Moser, and Oliver J Newell. Decision support during convective weather. *Lincoln Laboratory Journal*, 16(2), 2007.

Steven Wollkind, John Valasek, and Thomas R Ioerger. Automated conflict resolution for air traffic management using cooperative multiagent negotiation. In *AIAA guidance, navigation, and control conference*, pages 1–11, 2004.

Lee C Yang and James K Kuchar. Prototype conflict alerting system for free flight. *Journal of Guidance, Control, and Dynamics*, 20(4):768–773, 1997.

Ofer Zeitouni. Part ii : Random walks in random environment. In *Lectures on probability theory and statistics*, pages 189–312. Springer, 2004.

Meriem Zghal, Laurent Mevel, and Pierre Del Moral. Modal parameter estimation using interacting kalman filter. *Mechanical Systems and Signal Processing*, 47(1-2):139 – 150, 2014. ISSN 0888-3270. doi: http://dx.doi.org/10.1016/j.ymssp.2012.11.005. URL http://www.sciencedirect.com/science/article/pii/S0888327012004633. MSSP Special Issue on the Identification of Time Varying Structures and Systems.

List of Acronyms

AROME Applications de la Recherche à l'Opérationnel à Méso-Echelle 154, 161, 162

ARPEGE Action de Recherche Petite Echelle Grande Echelle 154

ATC Air Traffic Control 4, 5, 7

ATCC Air-Traffic Control Centers 2

ATM Air Traffic Management 1, 2, 10, 173, 174

BADA Base of Aircraft DAta vi, 97, 101–103, 105, 107, 108, 145, 159, 169

CAS Calibrated Air Speed 77, 104, 107, 112, 113, 116, 119

CDR Conflict Detection and Resolution 4

DST Decision Support Tool 4

ECEF Earth centered Earth fixed 87, 88

EKF Extended Kalman Filter 6

FIR Flight Information Region 2, 3

FL Flight Level 2, 3, 158

FMS Flight Management System 4, 5

HMM Hidden Markov Model 11

ICAO International Civil Aviation Organization 5

IKF Interacting Kalman Filters 8

ISA International Standard Atmosphere vi, 98, 99, 101, 103, 104, 112, 116

MCMC Markov Chain Monte-Carlo 9, 42, 43, 45, 47–49, 51–53, 134

MSL Mean Sea Level 98, 99

NED North-East-Down 87–89, 92

NextGen Next Generation Air Transportation System 1, 4

PE AROME Prévision d'Ensemble Arome 153, 154, 163, 168

PEARP Prévision d'Ensemble ARPEGE 154

PMCMC Particle Markov Chain Monte-Carlo v, 42, 47–49

ROCD Rate of Climb/Descent 105

SESAR Single European Sky ATM Research 1, 4, 154

List of terms and notations

A
Appendix

A.1 Convergence results for labeled island particle filters

INTRODUCTION TO LABELED ISLAND PARTICLE MODELS AND THEIR ASYMPTOTIC PROPERTIES

By Cécile Ichard[‡] and Christelle Vergé[§,*,†]

Météo-France[‡] and ONERA[§]

Estimation of stochastic processes evolving in a random environment is of crucial importance, notably to predict aircraft trajectories evolving in an unknown atmosphere. For fixed parameter, interacting particle systems are a convenient way to approximate such stochastic process. But the second level of uncertainty provided by the environment parameters leads us to also consider interacting particles on the parameter space. This novel algorithm is described in this paper. It allows to approximate both a random environment and a stochastic process evolving in this environment, given noisy observations of the process. It is a sequential algorithm that generalizes island particle models including a parameter. We refer to it as labeled island particle algorithm. We prove the convergence of the labeled island particle algorithm and we establish $\mathbb{L}^p$ bound as well as time uniform $\mathbb{L}^p$ bound for the asymptotic error introduced by this double level of approximation. Finally, we illustrate these results on a filtering problem where one learns a dynamical parameter through noisy observations of a stochastic process influenced by the parameter.

Introduction. This paper deals with the estimation of stochastic processes whose evolution is influenced by a random environment. This question is at stake in different areas. In the fields of economy, when one wants to estimate the option price with an unknown volatility using the Black-Scholes model, one can consider that the option price has its evolution influenced by an unknown parameter, the market volatility (see Cont (2006)). In biology, to estimate the number of bacteria with unknown environmental factors (see Augustin and Carlier (2000)), the evolution of the bacteria number can be modeled as a stochastic process whose evolution is influenced by unknown external factors. In air traffic management, this modelization can also be used in order to predict aircraft trajectories evolving in an atmosphere whose state is uncertain. Indeed if pilots' intents and some aircraft parameters are unidentified, actual wind and temperature evolve locally and are not perfectly known either. Those atmospheric parameters which appear in the dynamic equations of the aircraft have a great importance to predict the future position of the aircraft. They are thus both uncertain. In order to improve the trajectory prediction, one has to

---

*CNES - Centre National d'Etudes Spatiales, 18 avenue Edouard Belin, 31 401 Toulouse Cedex 9, France
†CMAP UMR 7641 École Polytechnique CNRS, Route de Saclay, 91128 Palaiseau Cedex France

1

learn aircraft parameters but also atmospheric ones, see Baehr and Ichard (2013). These
examples may be cast in the general framework of random motions in random media. An
example for continuous state space is given in Sznitman (1998) where a review for Brownian
motion among Poissonian obstacles is made. When the state space is discrete, $e.g$ $\mathbb{Z}^d$, these
problems are treated as random walk in random environment. This recent area of applied
probabilities tries to establish conditions under which the random walk shows specific be-
havior such as transience and recurrence. Zeitouni (2004); Révész (2005); Bogachev (2007)
made a broad survey in the domain. However, the question in these works concerns the
influence of the environment on the random process, not their estimations.

The study of wave propagation in random media deals with the estimation of the random
media using time-reversals methods, see Fouque et al. (2007) and references therein. In
this topic, the aim is to infer the environment properties from the propagation of waves.
Nevertheless these methods does not deal with general random process in random media.
In Andreoletti, Loukianova and Matias (2015), the question is to estimate the environment
distribution using the observations of a random path evolving in the environment. To this
end, they considered this problem as a Hidden Markov Model (HMM). However this study
handle Markov chain on discrete state space. Here we put our interest in continuous cases.

Nonetheless, HMM or state space models offer a convenient mean to study stochastic
dynamical systems. When the dynamics are linear with Gaussian densities, the optimal
solution to state estimation is given by Kalman filter, Kalman (1960) and Kalman and
Bucy (1961). When the process can take discrete values, the estimation can be done using
HMM filters, see Baum and Petrie (1966); Baum et al. (1970). When the dynamics are
nonlinear and the state space continuous another method has to be used. Over the last two
decades, particle simulation has been widely used to solve many state estimation problems.
These methods, also known as sequential Monte Carlo methods have been first applied to
state space models by Handschin and Mayne (1969), Handschin (1970) and Akashi and Ku-
mamoto (1977). During the 1990s, several particle filters algorithm which are belonging to
sequential monte carlo methods were proposed. Gordon et al. proposed in Gordon, Salmond
and Smith (1993) a new algorithm given by bootstrap filters. Independently, Kitagawa pro-
posed in Kitagawa (1996) another solution named Monte Carlo filters. In the meantime
Doucet et al. in Doucet (1998) gave a solution through sequential importance sampling
with resampling (SISR). Such filters also known as interacting particle filters have been
first studied by Del Moral in Del Moral (1996) and applied in various domains, see Doucet,
de Freitas and Gordon (2001); Cappe, Godsill and Moulines (2007); Doucet and Johansen
(2009) for a complete survey.

In our problem, a double estimation has to be made. One concerns the environment and
the other one the random process itself. To solve the combined problem of state and fixed
parameter estimation, a wide variety of methods have been studied. For linear dynamic
systems basic estimation techniques are available, see Ljung (1998). For more general state
space models, the classical method used is based on extended Kalman filter. However it has
been shown that this approach may give biased and divergent estimations, Ljung (1979).

Kitagawa in Kitagawa (1998) has first proposed the use of a particle filter to estimate simultaneously the states and the parameters in a general nonlinear non-Gaussian state space model. The idea was to augment the state vector with unknown parameters and then perform particle filter estimation on the augmented state space model. However, the main drawback of considering the parameter as an auxiliary variable is that the number of particles needed to have a rather acceptable estimation explodes with the dimension, see Liu and West (2001). Therefore augmenting the state space dimension can be inefficient. Nevertheless Ching, Beck and Porter (2006) show in their paper comparative results between particle filters and extended Kalman filters on several examples. It indicates that particle filters give better results especially when non linearity cannot be neglected. Another recent solution was given by Andrieu, Doucet and Holenstein (2010) and consists in using sequential Monte Carlo methods inside Markov chain Monte Carlo methods. However this method is not recursive and cannot be performed on-line. For recursive estimation, when models show special substructure such as in linear stochastic state space model with unknown parameters, the idea is to take advantage of the underlying linearity structure using *Rao-Blackwellization* techniques. Such filters have been introduced as mixture Kalman filters in Chen and Liu (2000), Rao-Blackwellized particle filters in Doucet et al. (2000); Li, Goodall and Kadirkamanathan (2004); Schön, Gustafsson and Nordlund (2005) and as interacting Kalman filters (IKF) in Del Moral (2004); Zghal, Mevel and Del Moral (2014).

However when the dynamics are non-linear, as for aircraft dynamics, an analytic resolution is not possible without making further model simplifications. A method based on interacting particle systems, which takes into account the randomness due to the environment and also the randomness coming from the process itself, was proposed by Del Moral in Del Moral (2004). This idealized algorithm would be a sequential Monte Carlo (SMC) algorithm on the couple defined by the random environment and the conditional law of the process evolving in this random environment given the history of the environment. Nonetheless, the calculation of the previous conditional law is not tractable in practice when the dynamics are non-linear. Therefore another approximation level is necessary in order to estimate this conditional law. We propose in this paper to use interacting systems of interacting particles. These interacting systems can be seen as a two-level interacting particle system. The top level particles are composed of an environment proposition and an empirical measure which gives an approximation of the process law evolving in the proposed environment. The empirical measure is obtained by the second level of interacting particles. This nested structure was used in Montemerlo, Thrun and Whittaker (2002) to estimate the pose of a mobile robot and positions of people surrounding it, in Baehr (2010) for mean field processes and in Ichard and Baehr (2013) for air-traffic process in random atmospheric environment.

This algorithm can be seen as a generalization of interacting island particle models where each island is associated with a random parameter. Those island particle models have been introduced in Vergé et al. (2015) and their statistical properties studied in Vergé et al. (2014), but without parameters. The first paper deals with the parallelization of interacting

particle systems, the second one dwells on the asymptotic properties of the ensuing estimator. Concerning filtering problems, Chopin et al. in Chopin, Jacob and Papaspiliopoulos (2013) introduced a kind of island particle models where each island is identified by a parameter proposition. They proposed an algorithm called SMC^2 which is a practical version of the idealized iterated batch importance sampling (IBIS) algorithm introduced by Chopin in Chopin (2002) for exploring a sequence of parameter posterior distributions. The considered parameter did not have any proper dynamic whereas in the present paper the stochastic process evolution scheme depends on a dynamic parameter. Moreover, in the SMC^2 algorithm, islands of particles grow continuously with time as particles ancestral lines are required to estimate the likelihood increments, and by their product to estimate the total likelihood. The algorithm introduced by Crisan et al. in Crisan and Miguez (2013) is a different version of the SMC^2 which also allows the estimation of fixed parameters of a state-space dynamic system using sequential Monte Carlo methods. However, unlike the SMC^2 method, the proposed algorithm by Crisan et al. operates in a purely sequential and recursive manner. In particular, the scheme for the rejuvenation of the particles in the parameter space is simpler, given that it does not need the simulation of the auxiliary particle filter from initial time to evaluate the likelihood. Therefore the algorithm we propose in this paper is similar to the algorithm of Crisan and Miguez (2013) in the sense that it is sequential in time and structured as a nested interacting particle filters, but also different as it deals with dynamic parameters.

In this article, we present a novel algorithm to estimate both a random environment and a process whose evolution depends on this environment, and study the asymptotic properties of the ensuing estimators. This study is of great importance to justify the convergence of this algorithm and also a challenging issue as it deals with error in distribution space. Therefore, as a first step, we establish $\mathbb{L}^p$ bound for the asymptotic error introduced by this double level of approximation at each time step. As a matter of fact, the shape of the bound was suggested by Baehr (2010). Then we obtain a time uniform $\mathbb{L}^p$ bound for the error. From there we deduce the almost sure convergence of the estimator towards the target measure. Afterwards, we compare the labeled island particle algorithm and interacting Kalman filters (IKF) on a filtering example dealing with the evolution of a mobile on a random media. More particularly, it appears that the labeled island particle algorithm gives a better estimation of the position and the speed of the mobile than IKF. Finally, the labeled island particle algorithm is applied to another filtering problem where one learns a dynamical parameter through observations of a stochastic process influenced by the parameter. The theoretical results of this paper are illustrated on this example.

Formalization of the problem through Feynman-Kac measures is given in Section 1, then the labeled island particle algorithm is described in Section 2. $\mathbb{L}^p$ bounds of this algorithm are established in Section 3. Finally, convergence of the labeled island particle algorithm and some results proved in Section 4 are illustrated in Section 5 on two filtering examples.

1. Feynman-Kac models in random media. In this section, we first present an example which motivates our study. Then we introduce notations and models which have been developed by Del Moral in Del Moral (2004) to model stochastic processes evolving in random media.

1.1. *Example of process evolution in random media.* In this article, one always consider stochastic processes whose evolution are influenced by their surrounding environment. When the environment is unknown, one can be interested in estimating both the environment and the law of the stochastic process itself using observations of the last one. Take a really simple example : a mobile evolving in $\mathbb{R}^2$ whose dynamics is influenced by an unknown exterior force. This problem can be modeled by the following system of equations

$$(1) \qquad \begin{cases} X_{n+1} & = X_n + V_n \begin{pmatrix} \cos \alpha \\ \sin \alpha \end{pmatrix} \Delta t + \Theta_{n+1} \Delta t + B_n^X \\ V_{n+1} & = V_n + B_n^V, \end{cases}$$

where X_{n+1} denotes the position of the mobile, which depends on Θ_{n+1}, and B_n^X a Gaussian noise. The proper speed V_n of the mobile, is known up to a Gaussian white noise B_n^V. The course track of the mobile is denoted by the parameter α. The vector Θ_{n+1} is random and represents the unknown force acting on the position of the mobile.
We are interested in the estimation of the state of the mobile, which depends on the parameter Θ_{n+1}. We thus need to learn both the force, the speed and the position of the mobile. Consider now that noisy observations Y_n of the mobile's state are available. One has to estimate the quantity $\mathbb{E}\left[(X_0, V_0, \Theta_0), \ldots, (X_n, V_n, \Theta_n) \mid Y_0, \ldots, Y_n\right]$. Therefore, we need to use a model able to tackle this issue. To this end, the formalism of Feynman-Kac models in random media is well adapted. In Section 1.3, we recall the definitions attached to this model and some important results. For a more detailed review see Del Moral (2004).

1.2. *Notations.* Let us define some notations used in this paper. For $(m, n) \in \mathbb{Z}^2$ such that $m \leq n$ we denote $[\![m, n]\!] \triangleq \{m, m + 1, \ldots, n\} \subset \mathbb{Z}$. We will use the vector notation $a_{m:n} \triangleq (a_m, \ldots, a_n)$. Moreover, $\mathbb{R}_+$ and $\mathbb{R}_+^*$ denote the sets of nonnegative and positive real numbers respectively, and $\mathbb{N}^*$ the set of positive integers.
$\mathsf{N}(\mu, \Sigma)$ denotes a multivariate Gaussian distribution with mean μ and covariance matrix Σ.
In the sequel, we assume that all random variables are defined on a common probability space $(\Omega, \mathcal{F}, \mathbb{P})$. For some given measurable space $(\mathsf{E}, \mathcal{E})$ we denote by $\mathsf{M}(\mathsf{E})$ and $\mathcal{P}(\mathsf{E}) \subset \mathsf{M}(\mathsf{E})$ the set of measures and probability measures on $(\mathsf{E}, \mathcal{E})$, respectively. In addition, we denote by $\mathsf{F}(\mathsf{E})$ the set of real-valued measurable functions on $(\mathsf{E}, \mathcal{E})$ and by $\mathcal{B}_b(\mathsf{E}) \subset \mathsf{F}(\mathsf{E})$ the set of bounded such functions. For any $\nu \in \mathsf{M}(\mathsf{E})$ and $f \in \mathsf{F}(\mathsf{E})$ we denote by $\nu f \triangleq \int f(x) \nu(\mathrm{d}x)$ the Lebesgue integral of f under ν whenever this is well-defined. Now, given also some other $(\mathsf{Y}, \mathcal{Y})$ measurable space, an *unnormalized transition kernel* K from $(\mathsf{E}, \mathcal{E})$ to $(\mathsf{Y}, \mathcal{Y})$ is a mapping from $\mathsf{E} \times \mathcal{Y}$ to $\mathbb{R}$ such that for all $\mathsf{A} \in \mathcal{Y}$, $x \mapsto K(x, \mathsf{A})$

is a nonnegative measurable function on E and for all $x \in \mathsf{E}$, $\mathsf{A} \mapsto K(x, \mathsf{A})$ is a measure on $(\mathsf{Y}, \mathcal{Y})$. If $K(x, \mathsf{Y}) = 1$ for all $x \in \mathsf{E}$, then K is called a *transition kernel* (or simply a *kernel*). The kernel K induces two integral operators, one acting on functions and the other on measures. More specifically, let $f \in \mathsf{F}(\mathsf{E})$ and $\nu \in \mathsf{M}(\mathsf{E})$ and define the measurable function

$$Kf : \mathsf{E} \ni x \mapsto \int f(y) \, K(x, \mathrm{d}y),$$

and the measure

$$\nu K : \mathcal{Y} \ni \mathsf{A} \mapsto \int K(x, \mathsf{A}) \, \nu(\mathrm{d}x),$$

whenever these quantities are well-defined. Finally, let K be as above and let L be another unnormalized transition kernels from $(\mathsf{Y}, \mathcal{Y})$ to some third measurable space $(\mathsf{Z}, \mathcal{Z})$; then we define the *product* of K and L as the unnormalized transition kernel

$$KL : \mathsf{E} \times \mathcal{Z} \ni (x, \mathsf{A}) \mapsto \int K(x, \mathrm{d}y) \, L(y, \mathsf{A}),$$

from $(\mathsf{E}, \mathcal{E})$ to $(\mathsf{Z}, \mathcal{Z})$ whenever this is well-defined.

1.3. *Introduction of Feynman-Kac models.* Let Θ_n be a random process on E_n^Θ which influences the evolution of another random process X_n on E_n^X. In order to avoid any confusion, all the quantities which refer to the random process Θ_n (resp. X_n) may be identified by the exponent Θ (resp. X). Let the couple $(\Theta_n, X_n)_{n \in \mathbb{N}}$ be a $\mathsf{E}_n \triangleq (\mathsf{E}_n^\Theta, \mathsf{E}_n^X)$- valued Markov chain of elementary transition matrix T_n form E_{n-1} to E_n defined by

$$T_n \left((\theta_{n-1}, x_{n-1}), \mathrm{d}(\theta_n, x_n) \right) \triangleq M_n^\Theta(\theta_{n-1}, \mathrm{d}\theta_n) M_{\theta_n, n}^X(x_{n-1}, \mathrm{d}x_n),$$

where M_n^Θ and $M_{\theta_n, n}^X$ are the transition kernels of the Θ_n and X_n processes from E_{n-1}^Θ to E_n^Θ and from E_{n-1}^X to E_n^X respectively.
Its initial distribution is given by

$$\eta_0(\mathrm{d}(\theta_0, x_0)) \triangleq \eta_0^\Theta(\mathrm{d}\theta_0) \eta_{\theta_0}^X(\mathrm{d}x_0),$$

with $\eta_0^\Theta \in \mathcal{P}(\mathsf{E}_0^\Theta)$ and $\eta_{\theta_0}^X \in \mathcal{P}(\mathsf{E}_0^X)$, denoting respectively the initial distributions of Θ_0 and X_0 given $\Theta_0 = \theta_0$.
Let $(G_n)_{n \in \mathbb{N}}$ be a collection of bounded measurable functions from E_n to $]0, \infty[$. We define the Feynman-Kac measure associated to the couple (G_n, T_n) with initial distribution η_0 by

$$(2) \quad \mathbb{Q}_{\eta_0, n} \left(\mathrm{d} \left((\theta_0, x_0), \dots, (\theta_n, x_n) \right) \right)$$

$$\triangleq \frac{1}{\mathcal{Z}_n} \left\{ \prod_{p=0}^{n-1} G_p(\theta_p, x_p) \right\} \mathbb{P}_{\eta_0^\Theta, n}^\Theta \left(\mathrm{d}(\theta_0, \dots, \theta_n) \right) \mathbb{P}_{\theta_{0:n}, n}^X \left(\mathrm{d}(x_0, \dots, x_n) \right),$$

with the normalizing constant $\mathscr{Z}_n$, given by

$$\mathscr{Z}_n \triangleq \mathbb{E}_{\eta_0} \left[\prod_{p=0}^{n-1} G_p(\Theta_p, X_p) \right] > 0,$$

and the two path probabilities

$$\mathbb{P}_{\eta_0^\Theta, n}^\Theta \left(\mathrm{d}(\theta_0, \ldots, \theta_n) \right) \triangleq \eta_0^\Theta(\mathrm{d}\theta_0) M_1^\Theta(\theta_0, \mathrm{d}\theta_1) \ldots M_n^\Theta(\theta_{n-1}, \mathrm{d}\theta_n),$$

and

$$\mathbb{P}_{\theta_{0:n}, n}^X \left(\mathrm{d}(x_0, \ldots, x_n) \right) \triangleq \eta_{\theta_0}^X(\mathrm{d}x_0) M_{\theta_1, 1}^X(x_0, \mathrm{d}x_1) \ldots M_{\theta_n, n}^X(x_{n-1}, \mathrm{d}x_n).$$

As one may have noticed, given $\Theta_{0:n} = \theta_{0:n}$, the sequence X_n is also a Markov chain of transition kernels $(M_{\theta_n, n}^X)_{n \in \mathbb{N}^*}$ and initial distribution $\eta_{\theta_0}^X$. Then one can associate to it another Feynman-Kac path measure which is called quenched.

DEFINITION 1.1. *The quenched Feynman-Kac path measure associated to the realization* $\Theta_{0:n} = \theta_{0:n}$ *is defined by*

$$\mathbb{Q}_{\theta_{0:n}, n}^X \left(\mathrm{d}(x_0, \ldots, x_n) \right) \triangleq \frac{1}{\mathscr{Z}_{\theta_{0:n}, n}^X} \left\{ \prod_{p=0}^{n-1} G_p(\theta_p, x_p) \right\} \mathbb{P}_{\theta_{0:n}, n}^X \left(\mathrm{d}(x_0, \ldots, x_n) \right),$$

where the quenched normalizing constant $\mathscr{Z}_{\theta_{0:n}, n}^X$ *is given by*

$$\mathscr{Z}_{\theta_{0:n}, n}^X \triangleq \mathbb{E}_{\theta_{0:n}} \left[\prod_{p=0}^{n-1} G_p(\theta_p, X_p) \right] > 0.$$

In the rest of the paper the quenched potential functions are denoted by $G_{\theta_p, p}$ and defined as

$$(3) \qquad\qquad G_{\theta_p, p} : x_p \in \mathsf{E}_p^X \mapsto G_{\theta_p, p}(x_p) \triangleq G_p(\theta_p, x_p).$$

To get further into the dynamic, one can define the time marginal of the quenched Feynman-Kac measure also called the quenched Feynman-Kac distribution.

DEFINITION 1.2. *For every realization* $\Theta_{0:n} = \theta_{0:n}$, *the quenched Feynman-Kac distribution flow* $\eta_{\theta_{0:n}, n}^X$ *on* E_n^X *is defined for every* $f_n \in \mathcal{B}_b(\mathsf{E}_n^X)$ *by*

$$\eta_{\theta_{0:n}, n}^X(f_n) \triangleq \gamma_{\theta_{0:n}, n}^X(f_n) / \gamma_{\theta_{0:n}, n}^X(\mathbb{1})$$

with $\gamma_{\theta_{0:n}, n}^X(f_n) \triangleq \mathbb{E}_{\theta_{0:n}} \left[f_n(X_n) \prod_{p=0}^{n-1} G_{\theta_p, p}(X_p) \right].$

The distribution of X_n depends on the trajectory $\theta_{0:n}$ which is emphasized by denoting the unnormalized quenched Feynman-Kac distribution by $\gamma^X_{\theta_{0:n},n}$. An important result taken from [Del Moral (2004), Proposition 2.6.2] is recalled below.

PROPOSITION 1.1.   *The quenched distribution sequence* $(\eta^X_{\theta_{0:n},n})_{n\in\mathbb{N}}$ *satisfies the non linear equation :*

$$(4) \qquad\qquad \eta^X_{\theta_{0:n+1},n+1} = \Psi^X_{\theta_n,n}(\eta^X_{\theta_{0:n},n})M^X_{\theta_{n+1},n+1},$$

where the mapping $\Psi^X_{\theta_n,n} : \mathcal{P}(\mathsf{E}^X_n) \to \mathcal{P}(\mathsf{E}^X_{n+1})$ *is given by*

$$(5) \qquad\qquad \Psi^X_{\theta_n,n}(\eta^X_{\theta_{0:n},n})(\mathrm{d}x_n) \triangleq \frac{1}{\eta^X_{\theta_{0:n},n}(G_{\theta_n,n})}G_{\theta_n,n}(x_n)\eta^X_{\theta_{0:n},n}(\mathrm{d}x_n).$$

Defining the mapping Φ^X_{n+1} *by*

$$(6) \qquad \begin{aligned} \Phi^X_{n+1} : \left(\mathsf{E}^\Theta_n \times \mathsf{E}^\Theta_{n+1}\right) \times \mathcal{P}(\mathsf{E}^X_n) &\rightarrow \mathcal{P}(\mathsf{E}^X_{n+1}) \\ \left((\theta_n,\theta_{n+1}),\eta^X_{\theta_{0:n},n}\right) &\mapsto \Psi^X_{\theta_n,n}(\eta^X_{\theta_{0:n},n})\,M^X_{\theta_{n+1},n+1} \end{aligned}$$

The non linear recursion (4) *can be reformulated as*

$$(7) \qquad\qquad \eta^X_{\theta_{0:n+1},n+1} = \Phi^X_{n+1}\left((\theta_n,\theta_{n+1}),\eta^X_{\theta_{0:n},n}\right).$$

Remind that, for a fixed value $\theta_{0:n}$ of the random process $\Theta_{0:n}$, the probability measures $(\eta^X_{\theta_{0:n},n})_{n\in\mathbb{N}}$ can be approximated recursively thanks to an interacting particle system which evolves successively according to selection step with potentials $G_{\theta_n,n}$ defined in (3) and transition kernels $M^X_{\theta_n,n}$. See Del Moral (2004) for further details. Now, consider that the random environment $\Theta_{0:n}$, where the stochastic process X_n evolves, is not known. Then we focus our interest on the estimation of the couple

$$(8) \qquad\qquad \overline{X}_n \triangleq (\Theta_n, \eta^X_{\Theta_{0:n},n}) \in \overline{\mathsf{E}}_n \triangleq (\mathsf{E}^\Theta_n \times \mathcal{P}(\mathsf{E}^X_n)),$$

made up of the environment and the law of the process evolving in this environment. The tricky part will be to deal with the probability measure space. First, notice that, as it has been shown in Del Moral (2004), the pair process is a Markov chain.

PROPOSITION 1.2 (Del Moral (2004), Proposition 2.6.3). $\overline{X}_n$ *is a Markov chain with transition kernel* $\overline{M}_n$ *defined for every function* $\overline{f}_n \in \mathcal{B}_b(\overline{\mathsf{E}}_n)$ *and* $(u,\eta) \in \overline{\mathsf{E}}_n$ *by*

$$\overline{M}_n(\overline{f}_n)(u,\eta) \triangleq \int_{\mathsf{E}^\Theta_n} M^\Theta_n(u,\mathrm{d}v)\overline{f}_n(v, \Phi^X_n((u,v),\eta))$$

and with initial distribution $\overline{\eta}_0 \in \mathcal{P}(\overline{\mathsf{E}}_0)$ *defined by*

$$\overline{\eta}_0(\mathrm{d}(u,\nu)) \triangleq \eta^\Theta_0(\mathrm{d}u)\delta_{\eta^X_{\hat\theta_0}}(\mathrm{d}\nu).$$

To this Markov chain, one may associate the Feynman-Kac distribution flow $\overline{\eta}_n$ defined for every $\overline{f}_n \in \mathcal{B}_b(\overline{\mathsf{E}}_n)$ by

$$\overline{\eta}_n(\overline{f}_n) \triangleq \overline{\gamma}_n(\overline{f}_n)/\overline{\gamma}_n(\mathbb{1}) \tag{9}$$

where

$$\overline{\gamma}_n(\overline{f}_n) \triangleq \mathbb{E}_{\overline{\eta}_0}\left[\overline{f}_n(\overline{X}_n) \prod_{p=0}^{n-1} \overline{G}_p(\overline{X}_p)\right],$$

and the functions $\overline{G}_p$ are non negative functions defined as follows :

$$\begin{array}{rcl} \overline{G}_p : \overline{\mathsf{E}}_p & \to & [0, \infty[\\ (u, \eta) & \mapsto & \overline{G}_p(u, \eta) = \int_{\mathsf{E}_p^X} G_p(u, x)\eta(\mathrm{d}x) = \int_{\mathsf{E}_p^X} G_{u,p}(x)\eta(\mathrm{d}x) = \eta(G_{u,p}). \end{array} \tag{10}$$

PROPOSITION 1.3 (Del Moral (2004), p. 86). *For all $n \in \mathbb{N}$, the sequence $\overline{\eta}_n$ satisfies the following non linear recursive equation :*

$$\overline{\eta}_{n+1} = \overline{\Psi}_n(\overline{\eta}_n)\overline{M}_{n+1} = \overline{\Phi}_{n+1}(\overline{\eta}_n), \tag{11}$$

where for every $\mu \in \mathcal{P}(\overline{\mathsf{E}}_n)$, the application $\overline{\Psi}_n : \mathcal{P}(\overline{\mathsf{E}}_n) \to \mathcal{P}(\overline{\mathsf{E}}_n)$, is defined by

$$\overline{\Psi}_n(\mu)(\overline{f}_n) = \mu(\overline{G}_n\overline{f}_n)/\mu(\overline{G}_n), \quad (\forall \overline{f}_n \in \mathcal{B}_b(\overline{\mathsf{E}}_n)), \tag{12}$$

and the operator $\overline{\Phi}_n$ is defined by

$$\begin{array}{rcl} \overline{\Phi}_{n+1} : \mathcal{P}(\overline{\mathsf{E}}_n) & \to & \mathcal{P}(\overline{\mathsf{E}}_{n+1}) \\ \mu & \mapsto & \overline{\Psi}_n(\mu)\overline{M}_{n+1}. \end{array}$$

In the non linear case, (11) cannot be solved analytically. Therefore, in the next section, we introduce an interacting particle system to approximate recursively the sequence of Feynman-Kac probability measures $(\overline{\eta}_n)_{n \in \mathbb{N}}$.

2. Algorithm derivation. This section is about the algorithm associated with the Feynman-Kac distribution flow $\overline{\eta}_n$ defined in (9). One considers the process $\overline{X}_n$ associated with the pair $(\overline{G}_n, \overline{M}_n)$, where the transition kernel $\overline{M}_n$ is defined in Proposition 1.2 and the potential function $\overline{G}_n$ is defined in (10).

2.1. *Idealized interacting particle model.* Let N_1 be some positive integer. A N_1-interacting particle system associated with the sequence $((\overline{G}_n, \overline{M}_n))_{n \in \mathbb{N}}$ and the initial distribution $\overline{\eta}_0$, is a sequence of non-homogeneous Markov chain, denoted by $\overline{X}_n^{[N_1]}$, taking value in the product space $\overline{\mathsf{E}}_n^{N_1}$,

$$\overline{X}_n^{[N_1]} \triangleq (\overline{X}_n^i)_{i=1}^{N_1} = (\overline{X}_n^1, \ldots, \overline{X}_n^{N_1}) \in \overline{\mathsf{E}}_n^{N_1} \triangleq \underbrace{\overline{\mathsf{E}}_n \times \ldots \times \overline{\mathsf{E}}_n}_{N_1 \text{ times}}.$$

The initial state of the Markov chain $\overline{X}_0^{[N_1]}$ consists in N_1 independent random variables with common distribution $\overline{\eta}_0$. The interacting particle system $(\overline{X}_n^i)_{i=1}^{N_1}$ explores the state space $\overline{\mathsf{E}}_n$ and with the dynamic given to it, empirically samples the law $\overline{\eta}_n$. Each particle i of the system consists in a random variable $\overline{X}_n^i = (\theta_n^i, \eta_{\theta_{0:n}^i,n}^X) \in \overline{\mathsf{E}}_n$. Therefore, the empirical process $\overline{\eta}_n^{N_1}$ is defined by

$$(13) \qquad\qquad\qquad \overline{\eta}_n^{N_1} \triangleq \frac{1}{N_1} \sum_{i=1}^{N_1} \delta_{\overline{X}_n^i}.$$

The elementary transition of the Markov chain $\overline{X}_n^{[N_1]}$ from $\overline{\mathsf{E}}_n^{N_1}$ to $\overline{\mathsf{E}}_{n+1}^{N_1}$ is given for any $\overline{x}_n^{[N_1]} \triangleq (\overline{x}_n^1, \ldots, \overline{x}_n^{N_1}) \in \overline{\mathsf{E}}_n^{N_1}$ by

$$\mathbb{P}_{\overline{\eta}_0}^{N_1} \left(\overline{X}_{n+1}^{[N_1]} \in \mathrm{d}\overline{x}_{n+1}^{[N_1]} \,|\, \overline{X}_n^{[N_1]} \right) \triangleq \prod_{i=1}^{N_1} \overline{\Phi}_{n+1}(\overline{\eta}_n^{N_1})(\mathrm{d}\overline{x}_{n+1}^i)$$

$$= \prod_{i=1}^{N_1} \sum_{j=1}^{N_1} \frac{\overline{G}_n(\overline{X}_n^j)}{\sum_{k=1}^{N_1} \overline{G}_n(\overline{X}_n^k)} \overline{M}_{n+1}(\overline{X}_n^j, \mathrm{d}\overline{x}_{n+1}^i), \text{ thanks to (11)}.$$

Thus, the evolution of the particle swarm consists in two steps : a selection and a mutation. In the selection step, the particles $(\overline{X}_n^i)_{i=1}^{N_1}$ are selected multinomially with probability proportional to their potentials $(\overline{G}_n(\overline{X}_n^i))_{i=1}^{N_1}$. Selected particles are identified with a hat on Figure 1. Then the mutation step is performed independently using the kernel $\overline{M}_{n+1}$. The evolution scheme of the particles is illustrated on Figure 1. Using this algorithm one
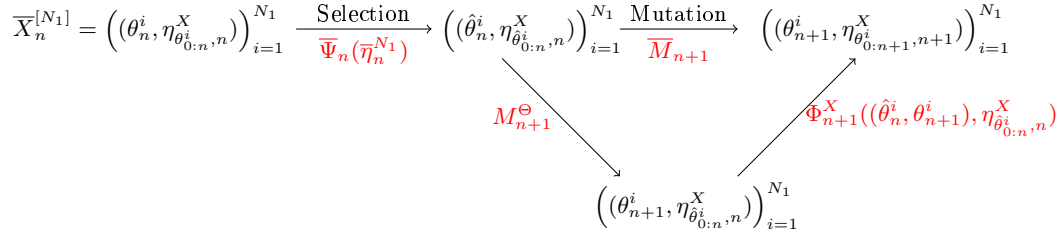
Fig 1: Evolution scheme of the interacting particle system for exact measures.

can empirically sample the measure $\overline{\eta}_n$ at each time step n. Several results are available to qualify the subsequent estimator. However, as one may have noticed, for each θ_n^i the measure $\eta_{\theta_{0:n}^i,n}^X$ corresponds to the quenched distributions defined in (1.2). That means that one should have the exact quenched measure associated with the parameter realization $\theta_{0:n}^i$ to use that standard particle algorithm. This can happen in two special cases.

Firstly, one special case is when the transition kernel $M_{\theta_n,n}^X$ is Gaussian and the initial distribution $\eta_{\theta_0}^X$ is Gaussian. Indeed, it turns out that this particle algorithm corresponds to the interacting Kalman filters (IKF) (see Del Moral (2004), Zghal, Mevel and Del Moral (2014)). That is a N_1-interacting particle model which is composed of N_1 particles where the measure value part are Gaussian distributions. In other words, for each particle θ_n^i, one iterative step of the Kalman filter is run to update the measure, *i.e.* one prediction step and one correction step. Those filters are then competing through the selection step using the transformation $\overline{\Psi}_n$ defined in (12). For example let us consider the case where Θ_n is a E_n^Θ-process with initial distribution η_0^Θ and elementary transition kernel M_n^Θ. For a realization $\theta_{0:n}$ of $\Theta_{0:n}$, consider that (X_n, Y_n) is a $\mathbb{R}^{p+q}$-Markov chain, for positive integers (p, q), defined through the linear Gaussian system :

$$\left\{ \begin{array}{rcl} X_n & = & A_{\theta_n,n} X_{n-1} + a_{\theta_n,n} + B_{\theta_n,n} \varepsilon_n^X, \quad n \geq 1 \\ Y_n & = & C_{\theta_n,n} X_n + c_{\theta_n,n} + D_{\theta_n,n} \varepsilon_n^Y, \quad n \geq 0. \end{array} \right.$$

$(A_{\theta_n,n}, B_{\theta_n,n}, C_{\theta_n,n}, D_{\theta_n,n})$ and $(a_{\theta_n,n}, c_{\theta_n,n})$ are respectively matrices and deterministic vectors of appropriate dimension which may depend on a parameter θ_n. The sequences ε_n^X and ε_n^Y are two independent white noises, independent from the initial condition X_0. There are Gaussian random variables whose mean and variance are given by

$$X_0 \sim \mathsf{N}(m_{\theta_0,0}, \Sigma_{\theta_0,0}), \quad \varepsilon_n^X \sim \mathsf{N}(0, \Sigma_n^X), \quad \text{and } \varepsilon_n^Y \sim \mathsf{N}(0, \Sigma_n^Y).$$

In this framework, $\eta_{\theta_{0:n},n}^X$ corresponds to the conditional law of X_n given the observations $Y_{0:n-1} = y_{0:n-1}$ and the history of the parameter $\theta_{0:n}$, also called optimal predictor. One wants to estimate recursively the law of the couple $(\Theta_n, \eta_{\theta_{0:n},n}^X)$ using observations $Y_{0:n-1} = y_{0:n-1}$. For that purpose, one needs to introduce the optimal filtering which is the conditional law of X_n given the observations $Y_{0:n} = y_{0:n}$ and the history of the parameter $\theta_{0:n}$. It turns out that these previous distributions are Gaussian respectively denoted by $\eta_{\theta_{0:n},n}^X = \mathsf{N}(m_{\theta_n,n}, \Sigma_{\theta_n,n})$ and $\mathsf{N}(\hat{m}_{\theta_n,n}, \hat{\Sigma}_{\theta_n,n})$. Thus,

$$\hat{m}_{\theta_n,n} = \mathbb{E}_{\theta_{0:n}}[X_n \mid Y_{0:n}]$$
$$\hat{\Sigma}_{\theta_n,n} = \mathbb{E}_{\theta_{0:n}} \left[(X_n - \hat{m}_{\theta_n,n})(X_n - \hat{m}_{\theta_n,n})^T \right]$$
$$m_{\theta_{n+1},n+1} = \mathbb{E}_{\theta_{0:n+1}}[X_{n+1} \mid Y_{0:n}]$$
$$\Sigma_{\theta_{n+1},n+1} = \mathbb{E}_{\theta_{0:n+1}} \left[(X_{n+1} - m_{\theta_{n+1},n+1})(X_{n+1} - m_{\theta_{n+1},n+1})^T \right].$$

Moreover, the mapping Φ_{n+1}^X defined in (6) which is used to update the measure valued part $\eta_{\theta_{0:n},n}^X$ corresponds to a complete step of the Kalman filter evolution between predictors. This means that $\Phi_{n+1}^X((\theta_n, \theta_{n+1}), \mathsf{N}(m_{\theta_n,n}, \Sigma_{\theta_n,n}))$ is also a Gaussian distribution whose mean and covariance matrix are obtained recursively through two steps:

$$\mathsf{N}(m_{\theta_n,n}, \Sigma_{\theta_n,n}) \xrightarrow{\text{Correction}} \mathsf{N}(\hat{m}_{\theta_n,n}, \hat{\Sigma}_{\theta_n,n}) \xrightarrow{\text{Prediction}} \mathsf{N}(m_{\theta_{n+1},n+1}, \Sigma_{\theta_n,n}).$$

The first one is a correction step which is given by

$$
\begin{cases}
\hat{m}_{\theta_n,n} & = m_{\theta_n,n} + K_{\theta_n,n}(Y_n - (C_{\theta_n,n}m_{\theta_n,n} + c_{\theta_n,n})) \\
\hat{\Sigma}_{\theta_n,n} & = (I - K_{\theta_n,n}C_{\theta_n,n})\Sigma_{\theta_n,n}
\end{cases}
$$

where I is the identity matrix and $K_{\theta_n,n}$ is the classical gain matrix

$$
K_{\theta_n,n} \triangleq \Sigma_{\theta_n,n}(C_{\theta_n,n})^T \left(C_{\theta_n,n}\Sigma_{\theta_n,n}(C_{\theta_n,n})^T + D_{\theta_n,n}\Sigma_n^Y(D_{\theta_n,n})^T \right)^{-1}.
$$

The second step is the predicting step :

$$
\begin{cases}
m_{\theta_{n+1},n+1} & = A_{\theta_{n+1},n+1}\hat{m}_{\theta_n,n} + a_{\theta_{n+1},n+1} \\
\Sigma_{\theta_{n+1},n+1} & = A_{\theta_{n+1},n+1}\hat{\Sigma}_{\theta_n,n}(A_{\theta_{n+1},n+1})^T + B_{\theta_{n+1},n+1}\Sigma_{n+1}^X(B_{\theta_{n+1},n+1})^T.
\end{cases}
$$

Then all the Kalman filters attached to each realization θ_{n+1}^i for $i \in [\![1, N_1]\!]$ interact through their potential $\bar{G}_{n+1}(\theta_{n+1}^i, \eta_{\theta_{0:n+1}^i,n+1}^X)$ defined in (10) by

$$
\begin{aligned}
\bar{G}_{n+1}(\theta_{n+1}^i, \eta_{\theta_{0:n+1}^i,n+1}^X) &= \eta_{\theta_{0:n+1}^i,n+1}^X(G_{\theta_{n+1}^i,n+1}) \\
&= \mathsf{N}(m_{\theta_{n+1}^i,n+1}, \Sigma_{\theta_{n+1}^i,n+1})(G_{\theta_{n+1}^i,n+1})
\end{aligned}
$$

where $G_{\theta_{n+1}^i,n+1}$ is the likelihood function defined for every $x_{n+1} \in \mathsf{E}_{n+1}^X$ by

$$
G_{\theta_{n+1}^i,n+1}(x_{n+1}) = \frac{\mathrm{d}\mathsf{N}(C_{\theta_{n+1}^i,n+1}x_{n+1}, \Sigma_{n+1}^Y)}{\mathrm{d}\mathsf{N}(0, \Sigma_{n+1}^Y)}.
$$

One finally ends up with the following expression:

$$
\begin{aligned}
(14) \quad &\bar{G}_{n+1}(\theta_{n+1}^i, \eta_{\theta_{0:n+1}^i,n+1}^X) \\
&\quad = \frac{\mathrm{d}\mathsf{N}(C_{\theta_{n+1}^i,n+1}m_{\theta_{n+1}^i,n+1}, C_{\theta_{n+1}^i,n+1}\Sigma_{\theta_{n+1}^i,n+1}(C_{\theta_{n+1}^i,n+1})^T + \Sigma_{n+1}^Y)}{\mathrm{d}\mathsf{N}(0, \Sigma_{n+1}^Y)}.
\end{aligned}
$$

See Del Moral (2004) for further details. The interacting Kalman filter for this general example is given by Algorithm 1.

Data: $\overline{\eta}_0$, $(\overline{M}_p)_{p=0}^n$, $(\overline{\Psi}_p)_{p=0}^n$, $m_{\theta_0^i,0}$ and $\Sigma_{\theta_0^i,0}$
Result: Interacting Kalman approximation of $\overline{\eta}_n$

/* Initialization   */
for $i \leftarrow 1$ **to** N_1 **do**
  Sample $\tilde{X}_0^i = (\theta_0^i, \eta_{\theta_0^i,0}^X) \sim \tilde{\eta}_0$, *i.e.* $\theta_0^i \overset{i.i.d}{\sim} \eta_0^{\Theta}$ and $\eta_{\theta_0^i,0}^X = \mathsf{N}(m_{\theta_0^i,0}, \Sigma_{\theta_0^i,0})$;
end
for $p \leftarrow 0$ **to** $n-1$ **do**
  /* Selection of Kalman filters   */
  Sample $I_p = (I_p^i)_{i=1}^{N_1}$ according to a multinomial distribution with probability
  proportional to $\left(\bar{G}_p(\theta_p^k, \eta_{\theta_{0:p}^k,p}^X) \right)_{k=1}^{N_1}$ given by (14) ;
  for $i \leftarrow 1$ **to** N_1 **do**
    /* Updating step for each Kalman filter   */
    $\begin{cases} \hat{m}_{\theta_p^{I_p^i},p} & = & m_{\theta_p^{I_p^i},p} + K_{\theta_p^{I_p^i},p}(Y_n - C_{\theta_p^{I_p^i},p}\, m_{\theta_p^{I_p^i},p}) \\ \hat{\Sigma}_{\theta_p^{I_p^i},p} & = & \left(I - K_{\theta_p^{I_p^i},p} C_{\theta_p^{I_p^i},p} \right) \Sigma_{\theta_p^{I_p^i},p} \end{cases}$;
    /* Mutation of each island   */
    Sample independently θ_{p+1}^i according to $M_{p+1}^{\Theta}(\theta_p^{I_p^i}, .)$;
    /* Prediction step for each Kalman filter   */
    $\begin{cases} m_{\theta_{p+1}^i,p+1} & = & A_{\theta_{p+1}^i,p+1}\hat{m}_{\theta_p^{I_p^i},p} + a_{\theta_{p+1}^i,p+1} \\ \Sigma_{\theta_{p+1}^i,p+1} & = & A_{\theta_{p+1}^i,p+1}\hat{\Sigma}_{\theta_p^{I_p^i},p}(A_{\theta_{p+1}^i,p+1})^T + B_{\theta_{p+1}^i,p+1}\Sigma_{p+1}^X(B_{\theta_{p+1}^i,p+1})^T \end{cases}$
  end
  $p \longleftarrow p+1$
end

Algorithm 1: Interacting Kalman Filter - IKF

Secondly, when the non linear Equation 6 can be solved analytically *i.e.* when one has access to the exact measure $\eta_{\theta_{0:n},n}^X$, one can apply a simple interacting particle model as described in Figure 1, where each particle corresponds to the pair: parameter and exact measure.

However, in most cases, this equation cannot be solved analytically, so that an additional approximation is needed in order to estimate the measure $\eta_{\theta_{0:n}^i,n}^X$ for each $i \in [\![1, N_1]\!]$. The next subsection is dedicated to the derivation of an algorithm to deal with this constraint.

2.2. *Labeled island particle model.* To tackle the case where $\eta_{\theta_{0:n}^i,n}^X$, $i \in [\![1, N_1]\!]$ is not analytically known, the idea consists in using a particle estimation of $\eta_{\theta_{0:n}^i,n}^X$ inside the previous interacting particle model. The ensuing algorithm will be called *labeled island particle model* in reference to the island particle model developed in Vergé et al. (2015), even if in the present case, each island i have a label θ_n^i whose evolution is given by the

Markov kernel M_n^Θ. The labeled island particle model consists in associating to each term of the sequence $(\theta_n^i)_{i=1}^{N_1}$ a sub N_2-interacting particle system. We call sub N_2-interacting particle system associated with the sequence $((G_{\theta_n^i,n}, M_{\theta_n^i,n}^X))_{n\in\mathbb{N}}$ and the initial distribution $\eta_{\theta_0^i,0}^X$, the sequence of non-homogeneous Markov chain $(\xi_n^{i,j})_{j=1}^{N_2}$ taking value in the product space E_n^{X,N_2}, that is :

$$\xi_n^{i,[N_2]} \triangleq (\xi_n^{i,j})_{j=1}^{N_2} \triangleq (\xi_n^{i,1}, \ldots, \xi_n^{i,N_2}) \in \mathsf{E}_n^{X,N_2} \triangleq \underbrace{\mathsf{E}_n^X \times \ldots \times \mathsf{E}_n^X}_{N_2 \text{ times}}.$$

The initial state of the Markov chain $(\xi_0^{i,j})_{j=1}^{N_2}$ consists in sampling N_2 independent random variables with common distribution $\eta_{\theta_0^i,0}^X$.

The interacting particle system, denoted by $(\xi_n^{i,j})_{j=1}^{N_2}$, explore the state space E_n^X and with the dynamic given to it, empirically sample the law $\eta_{\theta_{0:n}^i,n}^X$.

Denoting the empirical measure

$$(15) \qquad\qquad \eta_{\theta_{0:n}^i,n}^{X,N_2} \triangleq \frac{1}{N_2} \sum_{j=1}^{N_2} \delta_{\xi_n^{i,j}},$$

the elementary transition of the process $\xi_n^{i,[N_2]}$ from E_n^{X,N_2} to E_{n+1}^{X,N_2} is given for any $x_n^{[N_2]} = (x_n^1, \ldots, x_n^{N_2}) \in \mathsf{E}_n^{X,N_2}$ by

$$
\begin{aligned}
\mathbb{P}_{\eta_{\theta_0}^X}^{N_2}\left(\xi_{n+1}^{i,[N_2]} \in \mathrm{d}x_{n+1}^{[N_2]} \,|\, \xi_n^{i,[N_2]}\right) &\triangleq \prod_{j=1}^{N_2} \Phi_{n+1}^X\left((\theta_n^i, \theta_{n+1}^i), \eta_{\theta_{0:n}^i,n}^{X,N_2}\right)(\mathrm{d}x_{n+1}^j) \\
&= \prod_{j=1}^{N_2} \Psi_{\theta_n^i,n}^X(\eta_{\theta_{0:n}^i,n}^{X,N_2}) M_{\theta_{n+1}^i,n+1}^X(\xi_n^{i,j}, \mathrm{d}x_{n+1}^j) \quad \text{using (6)} \\
&= \prod_{j=1}^{N_2} \sum_{k=1}^{N_2} \frac{G_{\theta_n^i,n}(\xi_n^{i,k})}{\sum_{\ell=1}^{N_2} G_{\theta_n^i,n}(\xi_n^{i,\ell})} M_{\theta_{n+1}^i,n+1}^X(\xi_n^{i,k}, \mathrm{d}x_{n+1}^j) \quad \text{by (5).}
\end{aligned}
$$

Define the mapping $\tilde{\Phi}_n^X$ by

$$
\begin{aligned}
\tilde{\Phi}_n^X : \mathsf{E}_{n-1}^\Theta \times \mathsf{E}_n^\Theta \times \mathcal{P}(\mathsf{E}_{n-1}^X) &\rightarrow \mathcal{P}(\mathsf{E}_n^X) \\
((u,v), \nu) &\mapsto \prod_{j=1}^{N_2} \Phi_n^X((u,v), \nu)(\mathrm{d}x_n^j),
\end{aligned}
$$

then

$$(16) \qquad\qquad \eta_{\theta_{0:n+1}^i,n+1}^{X,N_2} = \tilde{\Phi}_{n+1}^X\left((\theta_n^i, \theta_{n+1}^i), \eta_{\theta_{0:n}^i,n}^{X,N_2}\right).$$

So, the evolution of the particle swarm $\xi_n^{i,[N_2]}$ consists in two steps: a selection and a mutation. In the selection step, the particles are selected multinomially with probability proportional to their potentials $\left(G_{\theta_n^i,n}(\xi_n^{i,j})\right)_{j=1}^{N_2}$. Then the mutation step is performed independently using the kernel $M_{\theta_{n+1}^i,n+1}^X$. Hence, at each iteration $n \in \mathbb{N}$, the empirical measure $\eta_{\theta_{0:n}^i,n}^{X,N_2}$ approximates $\eta_{\theta_{0:n}^i,n}^X$ when N_2 tends to ∞. Replacing $\eta_{\theta_{0:n}^i,n}^X$ by $\eta_{\theta_{0:n}^i,n}^{X,N_2}$ inside the first algorithm presented, one gets a nested particle model named *labeled island particle model*. In order to derive precisely this algorithm, first introduce the following sequence $\tilde{X}_n$ on $\overline{\mathsf{E}}_n = \mathsf{E}_n^\Theta \times \mathcal{P}(\mathsf{E}_n^X)$, defined by $\tilde{X}_n \triangleq (\Theta_n, \eta_{\Theta_{0:n},n}^{X,N_2})$, *i.e.* the couple environment and empirical measure of the process X_n conditionally on $\Theta_{0:n}$, where $\eta_{\Theta_{0:n},n}^{X,N_2} \triangleq \sum_{j=1}^{N_2} \delta_{\xi_n^j}/N_2$.

PROPOSITION 2.1. $\tilde{X}_n$ *is a* $\overline{\mathsf{E}}_n$-*Markov chain with transition kernel* $\tilde{M}_n$ *defined for every function* $\overline{f}_n \in \mathcal{B}_b(\overline{\mathsf{E}}_n)$ *and* $(u,\nu) \in \overline{\mathsf{E}}_n$ *by*

$$(17) \qquad \tilde{M}_n(\overline{f}_n)(u,\nu) = \int_{\mathsf{E}_n^\Theta} M_n^\Theta(u,\mathrm{d}v)\overline{f}_n(v, \tilde{\Phi}_n^X((u,v),\nu)),$$

where $\tilde{\Phi}_n^X$ *is defined in* (16), *and with initial distribution* $\tilde{\eta}_0 \in \mathcal{P}(\overline{\mathsf{E}}_0)$ *given by*

$$\tilde{\eta}_0(\mathrm{d}(u,\nu)) \triangleq \eta_0^\Theta(\mathrm{d}u)\delta_{\eta_{\theta_0,0}^{X,N_2}}(\mathrm{d}\nu).$$

PROOF. Let $\sigma(\tilde{X}_0,\ldots,\tilde{X}_n)$ stands for the σ-algebra generated by the random variables $\tilde{X}_p$, $0 \le p \le n$. For all $\overline{f}_n \in \mathcal{B}_b(\overline{\mathsf{E}}_n)$:

$$\mathbb{E}_{\tilde{\eta}_0}[\overline{f}_n(\tilde{X}_n) \mid \sigma(\tilde{X}_0,\ldots,\tilde{X}_{n-1})]$$
$$= \mathbb{E}_{\tilde{\eta}_0}[\overline{f}_n(\Theta_n, \eta_{\Theta_{0:n},n}^{X,N_2}) \mid \sigma(\tilde{X}_0,\ldots,\tilde{X}_{n-1})]$$
$$= \mathbb{E}_{\tilde{\eta}_0}[\overline{f}_n(\Theta_n, \tilde{\Phi}_n^X((\Theta_{n-1},\Theta_n), \eta_{\Theta_{0:n-1},n-1}^{X,N_2}) \mid \sigma(\tilde{X}_0,\ldots,\tilde{X}_{n-1})] \quad \text{by (16).}$$

Recalling that $\tilde{X}_{n-1} = (\Theta_{n-1}, \eta_{\Theta_{0:n-1},n-1}^{X,N_2})$, one can conclude that

$$\mathbb{E}_{\tilde{\eta}_0}[\overline{f}_n(\tilde{X}_n) \mid \sigma(\tilde{X}_0,\ldots,\tilde{X}_{n-1})]$$
$$= \mathbb{E}_{\tilde{\eta}_0}[\overline{f}_n(\tilde{X}_n) \mid \tilde{X}_{n-1}]$$
$$= \int_{\mathsf{E}_n^\Theta} \overline{f}_n(\theta_n, \tilde{\Phi}_n^X((\Theta_{n-1},\theta_n), \eta_{\Theta_{0:n-1},n-1}^{X,N_2})M_n^\Theta(\Theta_{n-1},\mathrm{d}\theta_n).$$

$\square$

To the Markov chain $\tilde{X}_n$, one may associate the Feynman-Kac distribution defined for every $\overline{f}_n \in \mathcal{B}_b(\overline{\mathsf{E}}_n)$ by

$$(18) \qquad\qquad \tilde{\eta}_n(\overline{f}_n) \triangleq \tilde{\gamma}_n(\overline{f}_n)/\tilde{\gamma}_n(\mathbb{1}),$$

where $\tilde{\gamma}_n$ is defined such that

$$\tilde{\gamma}_n(\overline{f}_n) \triangleq \mathbb{E}_{\tilde{\eta}_0}\left[\overline{f}_n(\tilde{X}_n)\prod_{p=0}^{n-1}\overline{G}_p(\tilde{X}_p)\right],$$

with $\overline{G}_p$ defined in (10).

In a similar way to $\overline{\eta}_n$, the measure $\tilde{\eta}_n$ satisfies a recursive equation $\tilde{\eta}_n = \overline{\Psi}_{n-1}(\tilde{\eta}_{n-1})\tilde{M}_n$, with $\overline{\Psi}_{n-1}$ the application defined in Proposition 1.3. This non linear equation can be rewritten as

$$(19) \qquad\qquad\qquad \tilde{\eta}_n = \tilde{\Phi}_n(\tilde{\eta}_{n-1}),$$

where the mapping $\tilde{\Phi}_n$ is defined as follows :

$$(20) \qquad\qquad \begin{aligned} \tilde{\Phi}_n : \mathcal{P}(\overline{\mathsf{E}}_{n-1}) &\rightarrow \mathcal{P}(\overline{\mathsf{E}}_n) \\ \eta &\mapsto \overline{\Psi}_{n-1}(\eta)\tilde{M}_n. \end{aligned}$$

As in Section 2.1, when this equation cannot be solved analytically one may use a particle model to approximate the probability measure $\tilde{\eta}_n$. In this case, the particles $\{\tilde{X}_n^i \triangleq (\theta_n^i, \eta_{\theta_{0:n}^i,n}^{X,N_2}), i \in [\![1, N_1]\!]\}$, would be testing points on the state space $\overline{\mathsf{E}}_n$, for $(N_1, N_2) \in (\mathbb{N}^*)^2$. These particles explore the state space $\overline{\mathsf{E}}_n$ and their dynamics empirically sample the law $\tilde{\eta}_n$ when N_1 gets large. An interacting particle system associated with the couple $(\overline{G}_n, \tilde{M}_n)$ and the initial distribution $\tilde{\eta}_0$, is a sequence of non-homogeneous Markov chain, $\tilde{X}_n^{[N_1]}$, taking value in the product space $\overline{\mathsf{E}}_n^{N_1}$, defined by

$$\tilde{X}_n^{[N_1]} \triangleq (\tilde{X}_n^i)_{i=1}^{N_1} = (\tilde{X}_n^1, \ldots, \tilde{X}_n^{N_1}) \in \overline{\mathsf{E}}_n^{N_1}.$$

The initial state of the Markov chain $\tilde{X}_0^{[N_1]}$ consists in N_1 independent random variables with common distribution $\tilde{\eta}_0$. Denote by $\tilde{\eta}_n^{N_1}$ the empirical measure at time n, which is defined by

$$(21) \qquad\qquad\qquad \tilde{\eta}_n^{N_1} \triangleq \frac{1}{N_1}\sum_{i=1}^{N_1}\delta_{\tilde{X}_n^i}.$$

The elementary probability transition, is given for any $\overline{x}_{n+1}^{[N_1]} \in \overline{\mathsf{E}}_{n+1}^{N_1}$ by

$$\mathbb{P}_{\tilde{\eta}_0}^{N_1}(\tilde{X}_{n+1}^{[N_1]} \in \mathrm{d}\overline{x}_{n+1}^{[N_1]} \,|\, \tilde{X}_n^{[N_1]}) = \prod_{i=1}^{N_1}\overline{\Psi}_n(\tilde{\eta}_n^{N_1})\tilde{M}_{n+1}(\tilde{X}_n^i, \mathrm{d}\overline{x}_{n+1}^i).$$

The particle evolution is summarized in Figure 2 where by definitions (10) and (15),

$$\overline{G}_n(\tilde{X}_n^i) = \frac{1}{N_2}\sum_{j=1}^{N_2}G_n(\theta_n^i, \xi_n^{i,j}) = \frac{1}{N_2}\sum_{j=1}^{N_2}G_{\theta_n^i,n}(\xi_n^{i,j}).$$
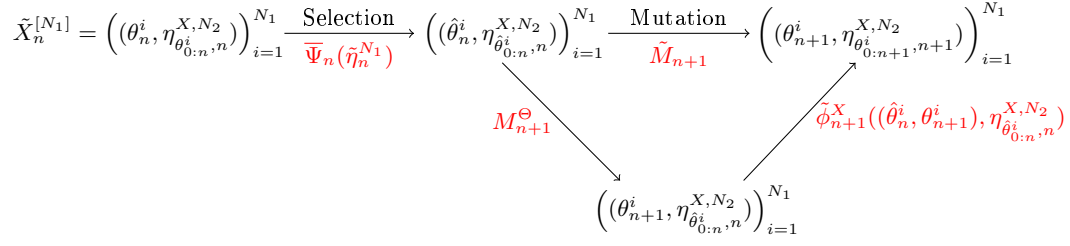
$$\tilde{X}_n^{[N_1]} = \left((\theta_n^i, \eta_{\theta_{0:n}^i,n}^{X,N_2}) \right)_{i=1}^{N_1} \xrightarrow[\overline{\Psi}_n(\tilde{\eta}_n^{N_1})]{\text{Selection}} \left((\hat{\theta}_n^i, \eta_{\hat{\theta}_{0:n}^i,n}^{X,N_2}) \right)_{i=1}^{N_1} \xrightarrow[\tilde{M}_{n+1}]{\text{Mutation}} \left((\theta_{n+1}^i, \eta_{\theta_{0:n+1}^i,n+1}^{X,N_2}) \right)_{i=1}^{N_1}$$

$$M_{n+1}^{\Theta} \searrow \qquad \nearrow \tilde{\phi}_{n+1}^X((\hat{\theta}_n^i, \theta_{n+1}^i), \eta_{\hat{\theta}_{0:n}^i,n}^{X,N_2})$$

$$\left((\theta_{n+1}^i, \eta_{\hat{\theta}_{0:n}^i,n}^{X,N_2}) \right)_{i=1}^{N_1}$$

Fig 2: Evolution scheme of the labeled island particle model.

The ensuing algorithm is described in Algorithm 2.

Data: $\tilde{\eta}_0$, $(\tilde{M}_p)_{p=0}^n$ and $(\overline{\Psi}_p)_{p=0}^n$
Result: Particle approximation of $\tilde{\eta}_n$

/* Initialization   */
for $i \leftarrow 1$ **to** N_1 **do**

 Sample $\tilde{X}_0^i = (\theta_0^i, \eta_{\theta_0^i,0}^{X,N_2}) \sim \tilde{\eta}_0$, that is

$$\theta_0^i \overset{i.i.d}{\sim} \eta_0^\Theta, \ \xi_0^{i,j} \overset{i.i.d}{\sim} \eta_{\theta_0^i,0}^X \text{ and } \eta_{\theta_0^i,0}^{X,N_2} = \frac{1}{N_2} \sum_{j=1}^{N_2} \delta_{\xi_0^{i,j}}.$$

end
for $p \leftarrow 0$ **to** $n-1$ **do**

 /* Selection of islands   */
 Sample $I_p = (I_p^i)_{i=1}^{N_1}$ according to a multinomial distribution with probability

 proportional to $\left(\frac{1}{N_2} \sum_{j=1}^{N_2} G_p(\theta_p^i, \xi_p^{i,j}) \right)_{i=1}^{N_1}$;

 for $i \leftarrow 1$ **to** N_1 **do**

  /* Selection of particles inside each island   */
  Sample $J_p^i = (J_p^{i,j})_{j=1}^{N_2}$ according to a multinomial distribution with probability

  proportional to $\left(G_p(\theta_p^{I_p^i}, \xi_p^{I_p^i,j}) \right)_{j=1}^{N_2}$;

  /* Mutation of each island   */
  Sample independently θ_{p+1}^i according to $M_{p+1}^\Theta(\theta_p^{I_p^i}, .)$;
  for $j \leftarrow 1$ **to** N_2 **do**

   /* Mutation of particles   */
   Sample $\xi_{p+1}^{i,j}$ according to $M_{\theta_{p+1}^i,p+1}^X(\xi_p^{I_p^i,J_p^{i,j}}, .)$;

  end

 end

 $p \longleftarrow p+1$

end

Algorithm 2: Labeled island particle algorithm

For every $n \geq 0$, $\tilde{\eta}_n^{N_1}$ is an estimator of $\tilde{\eta}_n$, obtained through the labeled island particle model, i.e. for every $\overline{f}_n \in \mathcal{B}_b(\overline{\mathsf{E}}_n)$,

$$\tilde{\eta}_n^{N_1}(\overline{f}_n) = \frac{1}{N_1} \sum_{i=1}^{N_1} \overline{f}_n(\theta_n^i, \eta_{\theta_{0:n}^i,n}^{X,N_2})$$

converges to $\tilde{\eta}_n(\overline{f}_n)$ when $N_1 \rightarrow +\infty$.

3. $\mathbb{L}^p$ bounds . We are interested in this section in the $\mathbb{L}^p$ bounds of the difference between the estimator $\tilde{\eta}_n^{N_1}$ and the measure $\overline{\eta}_n$. To get these bounds we will use several

notations. We define them before going further.

3.1. *Notations.* Let $(\mathsf{E}, \mathcal{E})$ be a measurable space. For a real-valued measurable function $h \in \mathcal{B}_b(\mathsf{E})$, we denote the oscillator norm $\mathrm{osc}(h) \triangleq \sup_{(x,x') \in \mathsf{E}^2} |h(x) - h(x')|$, and $\mathrm{Osc}_1(\mathsf{E})$ the convex set of $\mathcal{E}$-measurable functions with oscillations less than one. The sup norm of h is noted $\|h\|_\infty \triangleq \sup_{x \in \mathsf{E}} |h(x)|$ and the $\mathbb{L}^p$-norm $\|.\|_p$. $\mathcal{B}_1(\mathsf{E}) \subset \mathcal{B}_b(\mathsf{E})$ refers to the set of functions whose sup norm is less than one. For two probability measures $(\mu, \eta) \in \mathcal{P}(\mathsf{E})^2$, the Zolotarev semi-norm $\|.\|_{\mathfrak{F}}$ attached to $\mathfrak{F}$ a countable collection of bounded measurable functions in $\mathcal{B}_1(\mathsf{E})$ is defined by

$$\|\mu - \eta\|_{\mathfrak{F}} \triangleq \sup_{f \in \mathfrak{F}} |\mu(f) - \eta(f)|.$$

To measure the size of a given class $\mathfrak{F}$, one considers the covering numbers $\mathcal{N}(\varepsilon, \mathfrak{F}, \mathbb{L}^p(\mu))$ defined as the minimal number of $\mathbb{L}^p(\mu)$-balls of radius $\varepsilon > 0$ needed to cover $\mathfrak{F}$. Let $\mathcal{N}(\varepsilon, \mathfrak{F})$ and $I(\mathfrak{F})$ denote respectively the uniform covering numbers and entropy integral given by

$$(22) \qquad \mathcal{N}(\varepsilon, \mathfrak{F}) \triangleq \sup_{\mu \in \mathcal{P}(\mathsf{E})} \mathcal{N}(\varepsilon, \mathfrak{F}, \mathbb{L}^2(\mu))$$

$$(23) \qquad I(\mathfrak{F}) \triangleq \int_0^1 \sqrt{\log(1 + \mathcal{N}(\varepsilon, \mathfrak{F}))} \mathrm{d}\varepsilon.$$

Let $\wedge$ denote the minimum operator and $\vee$ denote the maximum operator. For a kernel M defined on E, the Dobrushin coefficient of M is

$$\beta(M) \triangleq \sup_{f \in \mathrm{Osc}_1(\mathsf{E})} \mathrm{osc}(M(f)).$$

Let $(d(n))_{n \geq 0}$ be a sequence defined for every $m \geq 0$ by

$$\begin{cases} d(2m)^{2m} \triangleq (2m)_m 2^{-m} \\ d(2m+1)^{2m+1} \triangleq \frac{(2m+1)_{m+1}}{\sqrt{m+1/2}} 2^{-m+1/2}, \end{cases}$$

where for any positive integers $(p, q) \in (\mathbb{N}^*)^2$, $(q + p)_p \triangleq (q + p)!/q!$.
For $n \in \mathbb{N}$, introduce the Feynman-Kac semi-groups $\overline{Q}_n$ (resp. $Q^X_{\theta_{n-1:n},n}$) such that for all $(\overline{x}_n, \overline{x}_{n+1}) \in \overline{\mathsf{E}}_n \times \overline{\mathsf{E}}_{n+1}$ (resp. $(x_n, x_{n+1}) \in \mathsf{E}^X_n \times \mathsf{E}^X_{n+1}$),

$$\overline{Q}_{n+1}(\overline{x}_n, \mathrm{d}\overline{x}_{n+1}) \triangleq \overline{G}_n(\overline{x}_n) \overline{M}_{n+1}(\overline{x}_n, \mathrm{d}\overline{x}_{n+1}),$$

$$\left(\text{resp. } Q^X_{\theta_{n:n+1},n+1}(x_n, \mathrm{d}x_{n+1}) \triangleq G_{\theta_n,n}(x_n) M^X_{\theta_{n+1},n+1}(x_n, \mathrm{d}x_{n+1}) \right).$$

For every $(p,n) \in (\mathbb{N})^2$ such that $p < n$, set

$$\overline{Q}_{p,n} \triangleq \overline{Q}_{p+1} \dots \overline{Q}_n, \quad \text{and} \quad \overline{P}_{p,n} \triangleq \overline{Q}_{p,n} / \overline{Q}_{p,n}(\mathbb{1}),$$

$$\left(\text{resp.} Q^X_{\theta_{p:n},p,n} \triangleq Q^X_{\theta_{p:p+1},p+1} \dots Q^X_{\theta_{n-1:n},n} \text{ and } P^X_{\theta_{p:n},p,n}(f_n) \triangleq Q^X_{\theta_{p:n},p,n}(f_n) / Q^X_{\theta_{p:n},p,n}(\mathbb{1}) \right),$$

and set the normalizing constant

$$\overline{G}_{p,n} \triangleq \overline{Q}_{p,n}(\mathbb{1}), \quad (\text{resp.} G_{\theta_{p:n},p,n} \triangleq Q^X_{\theta_{p:n},p,n}(\mathbb{1})).$$

Finally, set

$$\overline{g}_{p,n} \triangleq \sup_{(\overline{x}_p, \overline{y}_p) \in (\overline{\mathsf{E}}_p)^2} \frac{\overline{G}_{p,n}(\overline{x}_p)}{\overline{G}_{p,n}(\overline{y}_p)}, \quad \left(\text{resp.} \ g_{\theta_{p:n},p,n} \triangleq \sup_{(x_p, y_p) \in (\mathsf{E}^X_p)^2} \frac{G_{\theta_{p:n},p,n}(x_p)}{G_{\theta_{p:n},p,n}(y_p)} \right).$$

In order to study the difference between $\tilde{\eta}_n^{N_1}$ and $\overline{\eta}_n$, we use several results taken from Del Moral (2004). Then, we will always assume that for all $n \in \mathbb{N}$, the potential functions $G_{\theta_n,n}$ defined in (3) satisfy the following condition (G_θ):
there exists a sequence of strictly positive number $\epsilon_n(G_\theta) \in (0,1]$ such that for any $(x_n, y_n) \in (\mathsf{E}^X_n)^2$:

$$(G_\theta) \qquad\qquad G_{\theta_n,n}(x_n) \geq \epsilon_n(G_\theta) G_{\theta_n,n}(y_n) > 0$$

Therefore, for all $n \in \mathbb{N}$, the potential functions $\overline{G}_n$ satisfy the following condition $(\overline{G})$:
there exists a sequence of strictly positive number $\epsilon_n(\overline{G}) \in (0,1]$ such that for any $(\overline{x}_n, \overline{y}_n) \in (\overline{\mathsf{E}}_n)^2$:

$$(\overline{G}) \qquad\qquad \overline{G}_n(\overline{x}_n) \geq \epsilon_n(\overline{G}) \overline{G}_n(\overline{y}_n) > 0$$

Moreover we always assume that the collection of distributions $\left(\overline{M}_{n+1}(\overline{x}_n, .) \right)_{\overline{x}_n \in \overline{\mathsf{E}}_n}$ are absolutely continuous with one another. That is for every $n \geq 0$ and $(\overline{x}_n, \overline{y}_n) \in (\overline{\mathsf{E}}_n)^2$, one has

$$\overline{M}_{n+1}(\overline{x}_n, .) \ll \overline{M}_{n+1}(\overline{y}_n, .).$$

In addition, we assume that the collection of distributions $\left(M^X_{\theta_{n+1},n+1}(x_n, .) \right)_{x_n \in \mathsf{E}^X_n}$ are absolutely continuous with one another. That is for every $n \geq 0$, $\theta_{n+1} \in \mathsf{E}^\Theta_{n+1}$ and $(x_n, y_n) \in (\mathsf{E}^X_n)^2$, one has :

$$M^X_{\theta_{n+1},n+1}(x_n, .) \ll M^X_{\theta_{n+1},n+1}(y_n, .).$$

Note that for time homogeneous models on finite spaces condition those conditions are met as soon as the Markov chain is aperiodic and irreducible. Some examples are illustrated by typical examples in Del Moral (2004).

3.2. $\mathbb{L}^p$ *bound.* Consider that for all $n \in \mathbb{N}$, the product space $\overline{\mathsf{E}}_n = \mathsf{E}_n^\Theta \times \mathcal{P}(\mathsf{E}_n^X)$ is equipped with the norm $\|\cdot\|_{\overline{\mathsf{E}}_n}$ such that for all $(u,v) \in (\mathsf{E}_n^\Theta)^2$ and $(\nu, \eta) \in (\mathcal{P}(\mathsf{E}_n^X))^2$,

$$\|(u,\eta) - (v,\nu)\|_{\overline{\mathsf{E}}_n} = |u-v| + \|\eta - \nu\|_{\mathfrak{F}_n}.$$

where $\mathfrak{F}_n$ is a countable collection of functions in $\mathcal{B}_1(\mathsf{E}_n^X)$.

THEOREM 3.1.   *For any $p \in \mathbb{N}^*$, $n \in \mathbb{N}$, let $\overline{f}_n \in \mathrm{Osc}_1(\overline{\mathsf{E}}_n)$ be a k_n-Lipschitz function. Assume that for any $\theta_n \in \mathsf{E}_n^\Theta$, the kernel transition $M_{\theta_n,n}^X$ can be written as $M_{\theta_n,n}^X(x_{n-1}, \mathrm{d}x_n) = m_{\theta_n,n}^X(x_{n-1}, x_n) p_{\theta_n,n}(\mathrm{d}x_n)$ for some measurable function $m_{\theta_n,n}^X$ on $\mathsf{E}_{n-1}^X \times \mathsf{E}_n^X$ and some probability measure $p_{\theta_n,n} \in \mathcal{P}(\mathsf{E}_n^X)$. Furthermore, assume that there exists a collection of mappings $\alpha_{\theta_n,n}$ on E_n^X such that*

$$\sup_{x_{n-1} \in \mathsf{E}_{n-1}^X} |\log m_{\theta_n,n}^X(x_{n-1}, x_n)| \le \alpha_{\theta_n,n}(x_n)$$

with $p_{\theta_n,n}(e^{3\alpha_{\theta_n,n}}) < \infty$.
Then, the $\mathbb{L}^p$ error is bounded by

$$(24) \qquad \|\tilde{\eta}_n^{N_1}(\overline{f}_n) - \overline{\eta}_n(\overline{f}_n)\|_p \le k_n \frac{a(p)}{\sqrt{N_2}} (I(\mathfrak{F}_n) + b(n)) + 2\frac{d(p)}{\sqrt{N_1}} \sum_{q=0}^n \overline{g}_{q,n} \beta(\overline{P}_{q,n}),$$

where the sequence $d(n)$ is defined in (24), $I(\mathfrak{F}_n)$ is defined in (23), $(b(n))_{n\ge 0}$ is defined by

$$b(0) = 0 \text{ and } b(n+1) \le g_{\theta_n,n} p_{\theta_{n+1},n+1}(e^{3\alpha_{\theta_{n+1},n+1}}) \sum_{q=0}^n g_{\theta_{q:n},q,n} \beta(P_{\theta_{q:n},q,n}),$$

and $a(n)$ is a sequence such that for all $n \in \mathbb{N}^*$, $a(n) \le c\,[n/2]!$ with c a universal constant.

PROOF. Let $\overline{f}_n \in \mathrm{Osc}_1(\overline{\mathsf{E}}_n)$ be a k_n-Lipschitz function, and apply triangular inequality:

$$\|\tilde{\eta}_n^{N_1}(\overline{f}_n) - \overline{\eta}_n(\overline{f}_n)\|_p \le \|\tilde{\eta}_n^{N_1}(\overline{f}_n) - \overline{\eta}_n^{N_1}(\overline{f}_n)\|_p + \|\overline{\eta}_n^{N_1}(\overline{f}_n) - \overline{\eta}_n(\overline{f}_n)\|_p,$$

where $\overline{\eta}_n$ is defined in (9). Then using Theorem 7.4.4 from Del Moral (2004), one can bound the second term

$$\|\overline{\eta}_n^{N_1}(\overline{f}_n) - \overline{\eta}_n(\overline{f}_n)\|_p \le 2\frac{d(p)}{\sqrt{N_1}} \sum_{q=0}^n \overline{g}_{q,n} \beta(\overline{P}_{q,n}).$$

Therefore, in order to bound the first term, use the definitions of $\tilde{\eta}_n^{N_1}$ and $\overline{\eta}_n^{N_1}$ in (21) and (13) respectively :

$$\|\tilde{\eta}_n^{N_1}(\overline{f}_n) - \overline{\eta}_n^{N_1}(\overline{f}_n)\|_p = \mathbb{E}_{\overline{\eta}_0}\left[|\tilde{\eta}_n^{N_1}(\overline{f}_n) - \overline{\eta}_n^{N_1}(\overline{f}_n)|^p\right]^{1/p}$$

$$= \mathbb{E}_{\overline{\eta}_0}\left[\left|\frac{1}{N_1} \sum_{i=1}^{N_1} \left\{\overline{f}_n(\theta_n^i, \eta_{\theta_{0:n}^i,n}^{X,N_2}) - \overline{f}_n(\theta_n^i, \eta_{\theta_{0:n}^i,n}^X)\right\}\right|^p\right]^{1/p}$$

$$\le \mathbb{E}_{\overline{\eta}_0}\left[\left(\frac{1}{N_1} \sum_{i=1}^{N_1} |\overline{f}_n(\theta_n^i, \eta_{\theta_{0:n}^i,n}^{X,N_2}) - \overline{f}_n(\theta_n^i, \eta_{\theta_{0:n}^i,n}^X)|\right)^p\right]^{1/p}$$

As $\overline{f}_n$ is k_n-Lipschitz, it follows

$$\left| \overline{f}_n(\theta_n^i, \eta_{\theta_{0:n}^i,n}^{X,N_2}) - \overline{f}_n(\theta_n^i, \eta_{\theta_{0:n}^i,n}^X) \right| \le k_n \left\| (\theta_n^i, \eta_{\theta_{0:n}^i,n}^{X,N_2}) - (\theta_n^i, \eta_{\theta_{0:n}^i,n}^X) \right\|_{\overline{\mathsf{E}}_n}$$
$$\le k_n \left\| \eta_{\theta_{0:n}^i,n}^{X,N_2} - \eta_{\theta_{0:n}^i,n}^X \right\|_{\mathfrak{F}_n}.$$

where $\mathfrak{F}_n$ is a countable collection of functions in $\mathcal{B}_1(\mathsf{E}_n^X)$ Therefore one gets

$$\|\tilde{\eta}_n^{N_1}(\overline{f}_n) - \overline{\eta}_n^{N_1}(\overline{f}_n)\|_p \le \mathbb{E}_{\overline{\eta}_0} \left[\left(\frac{1}{N_1} \sum_{i=1}^{N_1} k_n \left\| \eta_{\theta_{0:n}^i,n}^{X,N_2} - \eta_{\theta_{0:n}^i,n}^X \right\|_{\mathfrak{F}_n} \right)^p \right]^{1/p}.$$

Denoting by θ^* the value at which the maximum of the Zolotarev semi-norms for $i \in [\![1, N_1]\!]$ is reached, yields to

$$\|\tilde{\eta}_n^{N_1}(\overline{f}_n) - \overline{\eta}_n^{N_1}(\overline{f}_n)\|_p \le k_n \mathbb{E}_{\overline{\eta}_0} \left[\|\eta_{\theta_{0:n}^*,n}^{X,N_2} - \eta_{\theta_{0:n}^*,n}^X\|_{\mathfrak{F}_n}^p \right]^{1/p}.$$

But, according to [Del Moral (2004), Corollary 7.4.4] (p. 247),

$$\mathbb{E}_{\overline{\eta}_0} \left[\|\eta_{\theta_{0:n}^*,n}^{X,N_2} - \eta_{\theta_{0:n}^*,n}^X\|_{\mathfrak{F}_n}^p \right]^{1/p} \le \frac{a(p)}{\sqrt{N_2}} (I(\mathfrak{F}_n) + b(n)),$$

where $I(\mathfrak{F}_n)$ is the entropy of $\mathfrak{F}_n$ defined in (23). Finally one ends up with

$$\|\tilde{\eta}_n^{N_1}(\overline{f}_n) - \overline{\eta}_n^{N_1}(\overline{f}_n)\|_p \le k_n \frac{a(p)}{\sqrt{N_2}} (I(\mathfrak{F}_n) + b(n)) + 2 \frac{d(p)}{\sqrt{N_1}} \sum_{q=0}^n \overline{g}_{q,n} \beta(\overline{P}_{q,n}).$$

$\square$

3.3. *Time uniform bound.*   Before stating the uniform estimate we define the following two additional conditions.
There exists some integer $\overline{m} \ge 1$ and some numbers $\varepsilon_n(\overline{M}) \in]0,1[$ such that for $n \in \mathbb{N}$ and $(\overline{x}_n, \overline{y}_n) \in \overline{\mathsf{E}}_n^2$, one has :

$$((\overline{M})_{\overline{m}}) \qquad \overline{M}_{n,n+\overline{m}}(\overline{x}_n, .) \triangleq \overline{M}_{n+1} \ldots \overline{M}_{n+\overline{m}}(\overline{x}_n, .) \ge \varepsilon_n(\overline{M}) \overline{M}_{n,n+\overline{m}}(\overline{y}_n, .)$$

For all $i \in [\![1, N_1]\!]$, there exists some integer $m_i \ge 1$ and some numbers $\varepsilon_n(M_{\theta^i}^X) \in]0,1[$ such that for $n \in \mathbb{N}$, $(x_n, y_n) \in (\mathsf{E}_n^X)^2$, and $\theta_{n+1:n+m_i}^i \in \mathsf{E}_{n+1}^\Theta \times \ldots \times \mathsf{E}_{n+m}^\Theta$, one has :

$$((M_{\theta^i}^X)_{m_i}) \quad M_{\theta_{n+1:n+m_i}^i,n,n+m_i}^X(x_n, .) \triangleq M_{\theta_{n+1}^i,n+1}^X \ldots M_{\theta_{n+m_i}^i,n+m_i}^X(x_n, .)$$
$$\ge \varepsilon_n(M_{\theta^i}^X) M_{\theta_{n+1:n+m_i}^i,n,n+m}^X(y_n, .)$$

THEOREM 3.2.   *Suppose that conditions* $(\overline{G})$, $((\overline{M})_{\overline{m}})$ *are met for some integer* $\overline{m} \geq 1$ *and some pair parameters* $(\epsilon_n(\overline{G}), \varepsilon_n(\overline{M}))$ *and set* $\epsilon(\overline{G}) \triangleq \wedge_{n\geq0}\epsilon_n(\overline{G})$ *and* $\varepsilon(\overline{M}) \triangleq \wedge_{n\geq0}\varepsilon_n(\overline{M})$.

Moreover, assume that for all $i \in [\![1, N_1]\!]$ *conditions* (G_θ) *and* $((M_{\theta^i}^X)_{m_i})$ *hold true for some sequence of integer* m_i *and some pair parameters* $(\epsilon_n(G_{\theta^i}), \varepsilon_n(M_{\theta^i}^X))$ *and set* $\epsilon(G_{\theta^i}) \triangleq \wedge_{n\geq0}\epsilon_n(G_{\theta^i})$ *and* $\varepsilon(M_{\theta^i}^X) \triangleq \wedge_{n\geq0}\varepsilon_n(M_{\theta^i}^X)$. *Set* $m \triangleq \vee_i m_i$.

Further assume that for all $n \geq 0$ *and* $\theta_n^i \in \mathsf{E}_n^\Theta$ *the kernel transition* $M_{\theta_n^i, n}^X$ *has the form* $M_{\theta_n^i, n}^X(x_{n-1}, dx_n) = m_{\theta_n^i, n}^X(x_{n-1}, x_n) p_{\theta_n^i, n}(dx_n)$ *for some measurable function* $m_{\theta_n^i, n}^X$ *on* $\mathsf{E}_{n-1}^X \times \mathsf{E}_n^X$ *and some probability measure* $p_{\theta_n^i, n} \in \mathcal{P}(\mathsf{E}_n^X)$.

Also assume that $\sup_{x_{n-1} \in \mathsf{E}_{n-1}^X} |\log m_{\theta_n^i, n}^X(x_{n-1}, x_n)| \leq \alpha_{\theta_n^i, n}(x_n)$ *with* $p_{\theta_n^i, n}(e^{3\alpha_{\theta_n^i, n}}) < \infty$ *for some collection of mappings* $\alpha_{\theta_n^i, n}$ *on* E_n^X, *and set :*

$$p_{\theta^i}(e^{3\alpha_{\theta^i}}) \triangleq \sup_{n\geq0} p_{\theta_n^i, n}(e^{3\alpha_{\theta_n^i, n}}) < \infty \quad and \quad p_\theta(e^{3\alpha_\theta}) \triangleq \vee_i p_{\theta^i}(e^{3\alpha_{\theta^i}}).$$

Then for any $p \in \mathbb{N}^*$, *any* k_n-*Lipschitz functions* $\overline{f}_n \in \mathrm{Osc}_1(\overline{\mathsf{E}}_n)$ *one has :*

$$\sup_{n\geq0} \sup_{\overline{f}_n \in \mathrm{Osc}_1(\overline{\mathsf{E}}_n)} \|\tilde{\eta}_n^{N_1}(\overline{f}_n) - \overline{\eta}_n(\overline{f}_n)\|_p \leq \frac{2d(p)\overline{m}}{\sqrt{N_1}\varepsilon(\overline{M})^3\epsilon(\overline{G})^{2\overline{m}-1}} + \frac{k\,a(p)}{\sqrt{N_2}}\left(I + \frac{mp_\theta(e^{3\alpha_\theta})}{\varepsilon(M_\theta^X)^3\epsilon(G_\theta)^{2m}}\right)$$

with

$$k = \sup_n k_n, \quad \varepsilon(M_\theta^X) = \wedge_i \varepsilon(M_{\theta^i}^X) > 0, \quad \epsilon(G_\theta) = \wedge_i \epsilon(G_{\theta^i}) > 0, \quad I \triangleq \sup_{n\geq0} I(\mathfrak{F}_n) < \infty.$$

PROOF.

$$\sup_{n\geq0} \sup_{\overline{f}_n \in \mathrm{Osc}_1(\overline{\mathsf{E}}_n)} \|\tilde{\eta}_n^{N_1}(\overline{f}_n) - \overline{\eta}_n(\overline{f}_n)\|_p$$

$$\leq \sup_{n\geq0} \sup_{\overline{f}_n \in \mathrm{Osc}_1(\overline{\mathsf{E}}_n)} \left(\|\tilde{\eta}_n^{N_1}(\overline{f}_n) - \overline{\eta}_n^{N_1}(\overline{f}_n)\|_p + \|\overline{\eta}_n^{N_1}(\overline{f}_n) - \overline{\eta}_n(\overline{f}_n)\|_p\right)$$

$$\leq \sup_{n\geq0} \sup_{\overline{f}_n \in \mathrm{Osc}_1(\overline{\mathsf{E}}_n)} \|\tilde{\eta}_n^{N_1}(\overline{f}_n) - \overline{\eta}_n^{N_1}(\overline{f}_n)\|_p + \sup_{n\geq0} \sup_{\overline{f}_n \in \mathrm{Osc}_1(\overline{\mathsf{E}}_n)} \|\overline{\eta}_n^{N_1}(\overline{f}_n) - \overline{\eta}_n(\overline{f}_n)\|_p$$

From [Del Moral (2004), Theorem 7.4.4] (p. 247), one has

$$\sup_{n\geq0} \sup_{\overline{f}_n \in \mathrm{Osc}_1(\overline{\mathsf{E}}_n)} \|\overline{\eta}_n^{N_1}(\overline{f}_n) - \overline{\eta}_n(\overline{f}_n)\|_p \leq \frac{2d(p)\overline{m}}{\sqrt{N_1}\varepsilon(\overline{M})^3\epsilon(\overline{G})^{2\overline{m}-1}},$$

since conditions $(\overline{G})$ and $((\overline{M})_{\overline{m}})$ hold true. Then it follows that the only term one has to work on is the following.

$$\sup_{n\geq 0} \sup_{\overline{f}_n\in\mathrm{Osc}_1(\overline{\mathsf{E}}_n)} \|\tilde{\eta}_n^{N_1}(\overline{f}_n) - \overline{\eta}_n^{N_1}(\overline{f}_n)\|_p$$

$$= \sup_{n\geq 0} \sup_{\overline{f}_n\in\mathrm{Osc}_1(\overline{\mathsf{E}}_n)} \left\| \frac{1}{N_1}\sum_{i=1}^{N_1} \left\{ \overline{f}_n(\theta_n^i, \eta_{\theta_{0:n}^i,n}^{X,N_2}) - \overline{f}_n(\theta_n^i, \eta_{\theta_{0:n}^i,n}^{X}) \right\} \right\|_p$$

$$\leq \frac{1}{N_1}\sum_{i=1}^{N_1} \sup_{n\geq 0} \sup_{\overline{f}_n\in\mathrm{Osc}_1(\overline{\mathsf{E}}_n)} \left\| \overline{f}_n(\theta_n^i, \eta_{\theta_{0:n}^i,n}^{X,N_2}) - \overline{f}_n(\theta_n^i, \eta_{\theta_{0:n}^i,n}^{X}) \right\|_p$$

As the function $\overline{f}_n$ is k_n-Lipschitz, for all $i\in[\![1,N_1]\!]$,

$$\sup_{n\geq 0} \sup_{\overline{f}_n\in\mathrm{Osc}_1(\overline{\mathsf{E}}_n)} \left\| \overline{f}_n(\theta_n^i, \eta_{\theta_{0:n}^i,n}^{X,N_2}) - \overline{f}_n(\theta_n^i, \eta_{\theta_{0:n}^i,n}^{X}) \right\|_p$$

$$= \sup_{n\geq 0} \sup_{\overline{f}_n\in\mathrm{Osc}_1(\overline{\mathsf{E}}_n)} \mathbb{E}_{\overline{\eta}_0} \left[\left| \overline{f}_n(\theta_n^i, \eta_{\theta_{0:n}^i,n}^{X,N_2}) - \overline{f}_n(\theta_n^i, \eta_{\theta_{0:n}^i,n}^{X}) \right|^p \right]^{1/p}$$

$$\leq \sup_{n\geq 0} \mathbb{E}_{\overline{\eta}_0} \left[k_n^p \left\| \eta_{\theta_{0:n}^i,n}^{X,N_2} - \eta_{\theta_{0:n}^i,n}^{X} \right\|_{\mathfrak{F}_n}^p \right]^{1/p}$$

$$\leq \sup_{n\geq 0} k_n \mathbb{E}_{\overline{\eta}_0} \left[\left\| \eta_{\theta_{0:n}^i,n}^{X,N_2} - \eta_{\theta_{0:n}^i,n}^{X} \right\|_{\mathfrak{F}_n}^p \right]^{1/p}.$$

Set $k \triangleq \sup_n k_n$, then

$$\sup_{n\geq 0} \sup_{\overline{f}_n\in\mathrm{Osc}_1(\overline{\mathsf{E}}_n)} \left\| \overline{f}_n(\theta_n^i, \eta_{\theta_{0:n}^i,n}^{X,N_2}) - \overline{f}_n(\theta_n^i, \eta_{\theta_{0:n}^i,n}^{X}) \right\|_p \leq k \sup_{n\geq 0} \mathbb{E}_{\overline{\eta}_0} \left[\left\| \eta_{\theta_{0:n}^i,n}^{X,N_2} - \eta_{\theta_{0:n}^i,n}^{X} \right\|_{\mathfrak{F}_n}^p \right]^{1/p}$$

From [Del Moral (2004), Corollary 7.4.5] (p. 249), as one assumes that there exists $m_i\geq 1$ for
$\theta_{n,n+m_i}^i \in \mathsf{E}_n^{\Theta}\times\ldots\times\mathsf{E}_{n+m_i}^{\Theta}$,

$$\sup_{n\geq 0} \mathbb{E}_{\overline{\eta}_0} \left[\left\| \eta_{\theta_{0:n}^i,n}^{X,N_2} - \eta_{\theta_{0:n}^i,n}^{X} \right\|_{\mathfrak{F}_n}^p \right]^{1/p} \leq \frac{a(p)}{\sqrt{N_2}} \left(I + \frac{m_i p_{\theta^i}(e^{3\alpha_{\theta^i}})}{\varepsilon(M_{\theta^i}^X)^3\epsilon(G_{\theta^i})^{2m_i}} \right),$$

where $I \triangleq \sup_{n\geq 0} I(\mathfrak{F}_n) < \infty$. One concludes easily.   □

4. Asymptotic analysis of the labeled island particle algorithm.

This section deals with the asymptotic behavior of the labeled island particle algorithm. Especially, we focus on the almost sure convergence.

Using Theorem 3.1 obtained in Section 3, one can easily get the almost sure convergence of the double estimator $\tilde{\eta}_n^{N_1}$ toward $\overline{\eta}_n$ under the same assumptions as in Theorem 3.1.

THEOREM 4.1.   *Under the same assumptions as in Theorem 3.1, for all $n \geq 0$ and for every k_n- Lipschitz function $\overline{f}_n \in \mathrm{Osc}_1(\overline{\mathsf{E}}_n)$, one has*

$$\tilde{\eta}_n^{N_1}(\overline{f}_n) \xrightarrow{a.s} \overline{\eta}_n(\overline{f}_n), \; as \; N \to \infty,$$

with $N = N_1 N_2$ such that $N_1 = N^\alpha$ and $N_2 = N^{1-\alpha}$ for all $\alpha \in]0,1[$.

PROOF.   Let $\overline{f}_n \in \mathrm{Osc}_1(\mathsf{E}_n)$ be a k_n-Lipschitz function and $\varepsilon > 0$ a real constant. For all $p \in \mathbb{N}^*$, by Markov's inequality, one has

$$\mathbb{P}\left(|\tilde{\eta}_n^{N_1}(\overline{f}_n) - \overline{\eta}_n(\overline{f}_n)| > \varepsilon\right) \leq \frac{\mathbb{E}_{\overline{\eta}_0}\left[|\tilde{\eta}_n^{N_1}(\overline{f}_n) - \overline{\eta}_n(\overline{f}_n)|^p\right]}{\varepsilon^p}.$$

Then, applying Theorem 3.1, and noting

$$C(p,n) \triangleq k_n a(p)(I(\mathcal{F}_n) + b(n)) \quad \text{and} \quad \tilde{C}(p,n) \triangleq 2d(p)\sum_{q=0}^{n}\overline{g}_{q,n}\beta(\overline{P}_{q,n}),$$

one has

$$\|\tilde{\eta}_n^{N_1}(\overline{f}_n) - \overline{\eta}_n(\overline{f}_n)\|_p^p \leq \left(\frac{C(p,n)}{\sqrt{N^\alpha}} + \frac{\tilde{C}(p,n)}{\sqrt{N^{1-\alpha}}}\right)^p$$

$$= \sum_{k=0}^{p}\binom{p}{k}\frac{C(p,n)^k \tilde{C}(p,n)^{p-k}}{N^{(\alpha-\frac{1}{2})k+\frac{1-\alpha}{2}p}}.$$

The finite sequence $(s_{\alpha,p}(k))_{k=0}^{p}$ defined by $s_{\alpha,p}(k) = (\alpha - 1/2)k + (1-\alpha)p/2$ is bounded from below by

$$m_{\alpha,p} \triangleq \frac{\alpha p}{2}\mathbb{1}_{0<\alpha\leq 0.5} + \frac{(1-\alpha)p}{2}\mathbb{1}_{0.5<\alpha<1},$$

so that

$$\|\tilde{\eta}_n^{N_1}(\overline{f}_n) - \overline{\eta}_n(\overline{f}_n)\|_p^p \leq \frac{\left(C(p,n) + \tilde{C}(p,n)\right)^p}{N^{m_{\alpha,p}}}.$$

Choose p a positive integer such that $m_{\alpha,p} \geq 2$ i.e. satisfying

(25) $$\begin{cases} p > \frac{4}{\alpha} & \text{if} \;\; 0 < \alpha \leq 0.5 \\ p > \frac{4}{1-\alpha} & \text{if} \;\; 0.5 < \alpha < 1. \end{cases}$$

Hence,

$$\|\tilde{\eta}_n^{N_1}(\overline{f}_n) - \overline{\eta}_n(\overline{f}_n)\|_p^p \leq \frac{\left(C(p,n) + \tilde{C}(p,n)\right)^p}{N^2}.$$

By comparison of series of non-negative general term with a convergent Riemann series, one concludes that the series

$$\sum_{N\geq 0}\mathbb{P}\left(|\tilde{\eta}_n^{N_1}(\overline{f}_n) - \overline{\eta}_n(\overline{f}_n)| > \varepsilon\right) \; \text{is convergent,}$$

which implies by Borel-Cantelli's lemma, that

$$\tilde{\eta}_n^{N_1}(\overline{f}_n) \xrightarrow{a.s} \overline{\eta}_n(\overline{f}_n), \text{ as } N \to \infty.$$

$\square$

Taking such kind of N means that for a total budget N of particles, one can consider any decomposition (as a power of N) of the particles between islands and within each island.

5. Example of application. In order to give illustration of this algorithm and of the previous theoretical results obtained, we present in this section two estimation problems. First let us recall the example of a mobile whose evolution is influenced by an unknown force which has been described in (1). Noisy observations of this physical systems are available. We resume the dynamics by the following system of equations :

$$(26) \qquad \begin{cases} X_{n+1} & = & X_n + V_n \begin{pmatrix} \cos \alpha \\ \sin \alpha \end{pmatrix} \Delta t + \Theta_{n+1} \Delta t + B_n^X \\ V_{n+1} & = & V_n + B_n^V \\ Y_n & = & h(X_n, V_n) + B_n^Y \end{cases}$$

where X_{n+1} denotes the position of the mobile in the plane, V_n the proper speed of the mobile and Y_n their noisy observations through the observation function h, with $B_n^Y \sim \mathsf{N}(0, \Sigma^Y)$. The course track of the mobile α is constant over time. The vector Θ_n is a random variable and denotes the unknown force acting on the position of the mobile. Its equation of evolution is given by

$$\Theta_{n+1} = \begin{pmatrix} \Theta_{n+1}^1 \\ \Theta_{n+1}^2 \end{pmatrix} = \begin{pmatrix} \cos \Theta_n^1 \\ \sin \Theta_n^2 \end{pmatrix} + B_n^\Theta$$

with $B_n^\Theta \sim \mathsf{N}(0, \Sigma^\Theta)$. The initial condition of the system is given by $X_0 \sim \mathsf{N}(m_{\theta_0,0}^X, \Sigma_{\theta_0,0}^X)$, $V_0 \sim \mathsf{N}(m_0^V, \Sigma_0^V)$ and $\alpha = \pi/2$. We are interested in the estimation of the position of the mobile, which depends on the parameter Θ_n. We thus need to learn both the force, the speed and the position of the mobile. The tricky part is that there is no observation of the force. Here we will consider that the speed is a Poisson process, that is B_n^V is a Poisson process of intensity 0.03 where the jumps high is given by a standard normal distribution of variance 3. Concerning B_n^X, it is a Gaussian random variable such that $B_n^X \sim \mathsf{N}(0, \Sigma^X)$. We present now the results obtained for a simulating time of 125 minutes with $\Delta t = 15s$. The value of the different variances are set to

$$\Sigma^\theta = \begin{pmatrix} 1 & 0 \\ 0 & 1 \end{pmatrix}, \ \Sigma^X = \Sigma_{\theta_0,0}^X = \begin{pmatrix} 1.5 & 0 \\ 0 & 1.5 \end{pmatrix}, \text{ and } \Sigma^Y = \begin{pmatrix} 0.5 & 0 & 0 \\ 0 & 0.5 & 0 \\ 0 & 0 & 1 \end{pmatrix}.$$

As one can notice, to estimate the law of the couple $(\Theta_n, \eta^X_{\Theta_{0:n},n})$ given the observations $Y_{0:n}$, one can use Interacting Kalman filters and labeled island particle filters (LIPFs), detailed respectively in Algorithms 1 and 2. We present comparative results obtained thanks to both methods.

Concerning the labeled version, the potential of each particle is given by the density of the observations, that is for all $x_n \in \mathsf{E}^X_n$ and for all $\theta_n \in \mathsf{E}^\Theta_n$:

$$G_n(\theta_n, x_n) \propto \exp\left(-\frac{1}{2}(y_n - h(x_n, v_n))^T (\Sigma^Y)^{-1}(y_n - h(x_n, v_n))\right).$$

On all the figures the realization of the true signal is represented by the color black, the observations Y are represented by the color blue, the filtered signal obtained thanks to Algorithm 2 with $N_1 = 100$ and $N_2 = 300$ in red and results obtained using Algorithm 1 in green with $N_1 = 100$. On Figure 3, one realization of the signal V_n, its observed and its estimations counterparts are represented with respect to time. As one may observe, the true signal is well estimated by the technique we develop. Indeed, here the Interacting Kalman filter is not optimal as the noise sequence is not Gaussian. On Figure 5, we represent the temporal evolution of the force strength estimation. One can notice that even if no observation is available, we are able to find back the value of the true signal thanks to Algorithm 2 whereas Algorithm 1 retrieves only a global trend. Figure 4 represents the temporal evolution of one realization of the force orientation and its estimated counterparts. Results obtained thanks to Algorithm 2 give a better estimation of the true signal than the results obtained thanks to the Algorithm 1. From this example we can conclude that the labeled island particle filter is able to filter observations of the process while estimating the environment where the process evolves. Moreover the comparison with the Interacting Kalman filter algorithm shows that the labeled island particle filter is more effective to treat this double level estimation problem.

Let us consider the 2-D filtering problem inspired from the growth model Kitagawa (1987). This model, which is a standard benchmark example in the particle filtering literature, is given by the following system of equations :

$$\begin{cases} \Theta_{n+1} &= 8\cos(1.2(n+1)) + B^\theta_{n+1} \\ X_{n+1} &= \dfrac{X_n}{2} + 25\dfrac{X_n}{1 + X_n^2} + \Theta_{n+1} + B^X_{n+1} \\ Y_n &= X_n + B^Y_n \end{cases}$$

where $\Theta_0 \sim \mathsf{N}(0, \sigma^2_\theta)$, $X_0 \sim \mathsf{N}(0, \sigma^2_X)$, $B^\theta_{n+1} \sim \mathsf{N}(0, \sigma^2_\theta)$, $B^X_{n+1} \sim \mathsf{N}(0, \sigma^2_X)$ and $B^Y_n \sim \mathsf{N}(0, \sigma^2_Y)$.

We use the labeled island particle model to estimate the law of the couple $(\Theta_n, \eta^X_{\Theta_{0:n},n})$ given the observations $Y_{0:n}$, where the potential functions G_n are given by the likelihood of the observations, that is for all $x_n \in \mathsf{E}^X_n$ and $\theta_n \in \mathsf{E}^\Theta_n$:

$$G_n(\theta_n, x_n) \propto \exp\left(-\frac{(Y_n - x_n)^2}{2\sigma^2_Y}\right).$$

We present the results obtained for a simulating time of 1000 time steps. The different variances are set to $\sigma_\theta^2 = 1$, $\sigma_X^2 = 1$ and $\sigma_Y^2 = 10$. On all the figures the realization of the true signal is represented in black color, the observations Y are represented in blue, and the filtered signal obtained thanks to Algorithm 2 with $N_1 = 200$ and $N_2 = 100$ is represented in red. On Figure 6, one realization of the signal Θ and its estimation obtained thanks to the labeled island particle algorithm are represented on a small period of time. As one may observe, the true signal is well estimated even if no observations are available. On Figure 7, one realization of the process X is represented, its observed and its estimation counterparts. Even if the observations are really noisy, one is able to filter out the noise to find back the value of the true signal. Indeed, as one may have noticed, on Figure 8, the filtered power spectral density (in red) is closer to the black line, representing the "true" signal, than the observed power spectral density which has the same shape as a white noise for the high frequencies. Moreover, some frequencies are found even if there are not present in the observed signal. These two observations illustrate the convergence of the estimator constructed by the labeled island particle algorithm detailed in Algorithm 2.

Then we run 100 times the same experiment to get a sample of realizations for the true signal and the filtered signal. In that way one can illustrate the theoretical results obtained for the $\mathbb{L}^p$ error bound. On figures 9 and 10 are presented the $\mathbb{L}^2$ errors between the estimated law and the true law at one time step respectively for Θ and X in function of the number of islands N_1 and the number of particles inside each island N_2. This error decreases both with the number of particles and the number of islands as it was suggested by the Theorem 3.1. Concerning the variance of the error made between the true law and the filtered one, on figures 11 and 12 for Θ and X respectively, one can observe that the results obtained in Theorem 4.1 are confirmed. Moreover one can notice that the variance is more influenced by the number of islands than the number of particles inside each island. Indeed as in Figure 12, the variance obtained for a fixed time step is varying with respect to the number of islands and number of particles inside each islands. But if the number of islands influences the variance, we can observe that the number of particles inside each island does not seem to be really influent for a given number of islands.

References.

AKASHI, H. and KUMAMOTO, H. (1977). Random sampling approach to state estimation in switching environments. *Automatica* **13** 429–434.

ANDREOLETTI, P., LOUKIANOVA, D. and MATIAS, C. (2015). Hidden Markov model for parameter estimation of a random walk in a Markov environment.

ANDRIEU, C., DOUCET, A. and HOLENSTEIN, R. (2010). Particle markov chain monte carlo methods. *Journal of the Royal Statistical Society: Series B (Statistical Methodology)* **72** 269–342.

AUGUSTIN, J.-C. and CARLIER, V. (2000). Mathematical modelling of the growth rate and lag time for Listeria monocytogenes. *International Journal of Food Microbiology* **56** 29 - 51.

BAEHR, C. (2010). Nonlinear filtering for observations on a random vector field along a random path. Application to atmospheric turbulent velocities. *ESAIM: Mathematical Modelling and Numerical Analysis* **44** 921–945.

BAEHR, C. and ICHARD, C. (2013). Aircraft Trajectory Prediction in Random Atmosphere. Mathematical background and application to a locally uniform academic case. (D. SCHAEFER, ed.).

BAUM, L. E. and PETRIE, T. (1966). Statistical inference for probabilistic functions of finite state Markov chains. *The annals of mathematical statistics* 1554–1563.

BAUM, L. E., PETRIE, T., SOULES, G. and WEISS, N. (1970). A maximization technique occurring in the statistical analysis of probabilistic functions of Markov chains. *The annals of mathematical statistics* 164–171.

BOGACHEV, L. (2007). Random Walks in Random Environments. *Encyclopedia Math. Phys.* **4** 353–371.

CAPPE, O., GODSILL, S. J. and MOULINES, E. (2007). An Overview of Existing Methods and Recent Advances in Sequential Monte Carlo. *Proceedings of the IEEE* **95** 899-924.

CHEN, R. and LIU, J. S. (2000). Mixture kalman filters. *Journal of the Royal Statistical Society: Series B (Statistical Methodology)* **62** 493–508.

CHING, J., BECK, J. L. and PORTER, K. A. (2006). Bayesian state and parameter estimation of uncertain dynamical systems. *Probabilistic engineering mechanics* **21** 81–96.

CHOPIN, N. (2002). A sequential particle filter method for static models. *Biometrika* **89** 539–552.

CHOPIN, N., JACOB, P. E. and PAPASPILIOPOULOS, O. (2013). SMC^2: an efficient algorithm for sequential analysis of state space models. *Journal of the Royal Statistical Society: Series B (Statistical Methodology)* **75** 397–426.

CONT, R. (2006). Model uncertainty and its impact on the pricing of derivative instruments. *Mathematical Finance* **16** 519–547.

CRISAN, D. and MIGUEZ, J. (2013). Nested particle filters for online parameter estimation in discrete-time state-space Markov models. Preprint.

DEL MORAL, P. (1996). Non-linear filtering: interacting particle resolution. *Markov processes and related fields* **2** 555–581.

DEL MORAL, P. (2004). *Feynman-Kac formulae: genealogical and interacting particle systems with applications.* Series: Probability & Applications Springer Verlag.

DOUCET, A. (1998). On sequential simulation-based methods for Bayesian filtering Technical Report, Department of Engineering, Cambridge University.

DOUCET, A., DE FREITAS, N. and GORDON, N. (2001). *Sequential Monte Carlo Methods in Practice.* Springer New York.

DOUCET, A. and JOHANSEN, A. M. (2009). A tutorial on particle filtering and smoothing: Fifteen years later. *Handbook of Nonlinear Filtering* **12** 656–704.

DOUCET, A., DE FREITAS, N., MURPHY, K. and RUSSELL, S. (2000). Rao-Blackwellised particle filtering for dynamic Bayesian networks. In *Proceedings of the Sixteenth conference on Uncertainty in artificial intelligence* 176–183. Morgan Kaufmann Publishers Inc.

FOUQUE, J.-P., GARNIER, J., PAPANICOLAOU, G. and SOLNA, K. (2007). *Wave propagation and time reversal in randomly layered media* **56**. Springer Science & Business Media.

GORDON, N. J., SALMOND, D. J. and SMITH, A. F. (1993). Novel approach to nonlinear/non-Gaussian Bayesian state estimation. In *IEE Proceedings F (Radar and Signal Processing)* **140** 107–113. IET.

HANDSCHIN, J. (1970). Monte Carlo techniques for prediction and filtering of non-linear stochastic processes. *Automatica* **6** 555–563.

HANDSCHIN, J. and MAYNE, D. Q. (1969). Monte carlo techniques to estimate the conditional expectation in multi-stage non-linear filtering. *International journal of control* **9** 547–559.

ICHARD, C. and BAEHR, C. (2013). Inference of a random environment from random process realizations: Formalism and application to trajectory prediction. In *ISIATM 2013, 2nd International Conference on Interdisciplinary Science for Innovative Air Traffic Management.*

KALMAN, R. E. (1960). A new approach to linear filtering and prediction problems. *Journal of Fluids Engineering* **82** 35–45.

KALMAN, R. E. and BUCY, R. S. (1961). New results in linear filtering and prediction theory. *Journal of Fluids Engineering* **83** 95–108.

KITAGAWA, G. (1987). Non-Gaussian state space modeling of nonstationary time series. *Journal of the American Statistical Association* **82** 1023–1063.

KITAGAWA, G. (1996). Monte Carlo filter and smoother for non-Gaussian nonlinear state space models. *Journal of computational and graphical statistics* **5** 1–25.

KITAGAWA, G. (1998). A self-organizing state-space model. *Journal of the American Statistical Association* 1203–1215.

LI, P., GOODALL, R. and KADIRKAMANATHAN, V. (2004). Estimation of parameters in a linear state space model using a Rao-Blackwellised particle filter. *IEE Proceedings-control theory and applications* **151** 727–738.

LIU, J. and WEST, M. (2001). Combined parameter and state estimation in simulation-based filtering. In *Sequential Monte Carlo methods in practice* 197–223. Springer.

LJUNG, L. (1979). Asymptotic behavior of the extended Kalman filter as a parameter estimator for linear systems. *Automatic control, IEEE Transactions on* **24** 36–50.

LJUNG, L. (1998). *System identification*. Springer.

MONTEMERLO, D., THRUN, S. and WHITTAKER, W. (2002). Conditional particle filters for simultaneous mobile robot localization and people-tracking. In *Robotics and Automation, 2002. Proceedings. ICRA'02. IEEE International Conference on* **1** 695–701. IEEE.

RÉVÉSZ, P. (2005). *Random walk in random and non-random environments*. World Scientific.

SCHÖN, T., GUSTAFSSON, F. and NORDLUND, P.-J. (2005). Marginalized particle filters for mixed linear/nonlinear state-space models. *Signal Processing, IEEE Transactions on* **53** 2279–2289.

SZNITMAN, A.-S. (1998). *Brownian motion, obstacles and random media*. Springer Science & Business Media.

VERGÉ, C., DEL MORAL, P., MOULINES, E. and OLSSON, J. (2014). Convergence properties of weighted particle islands with application to the double bootstrap algorithm. Preprint.

VERGÉ, C., DUBARRY, C., DEL MORAL, P. and MOULINES, E. (2015). On parallel implementation of sequential Monte Carlo methods: the island particle model. *Statistics and Computing* **25** 243–260.

ZEITOUNI, O. (2004). Part II : Random walks in random environment. In *Lectures on probability theory and statistics* 189–312. Springer.

ZGHAL, M., MEVEL, L. and DEL MORAL, P. (2014). Modal parameter estimation using interacting Kalman filter. *Mechanical Systems and Signal Processing* **47** 139 - 150. MSSP Special Issue on the Identification of Time Varying Structures and Systems.

MÉTÉO-FRANCE-CNRS,
CNRM-GAME UMR 3589,
42 AVENUE CORIOLIS,
31057 TOULOUSE CEDEX 1,
FRANCE
E-MAIL: cecile.ichard@meteo.fr

ONERA - THE FRENCH AEROSPACE LAB,
CHEMIN DE LA HUNIÈRE ET DES JONCHERETTES,
BP 80100,
91123 PALAISEAU CEDEX,
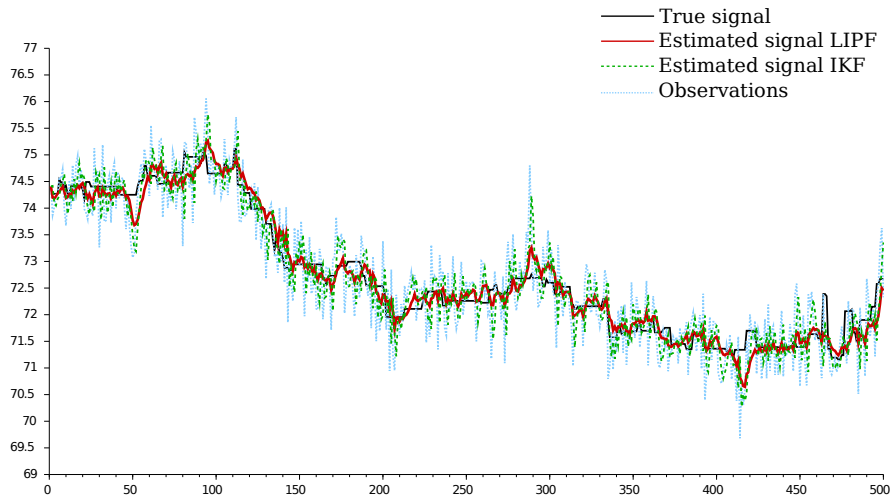FRANCE
E-MAIL: christelle.verge@onera.fr

Fig 3: Temporal evolution of the mobile's speed, its observed and filtered counterparts.
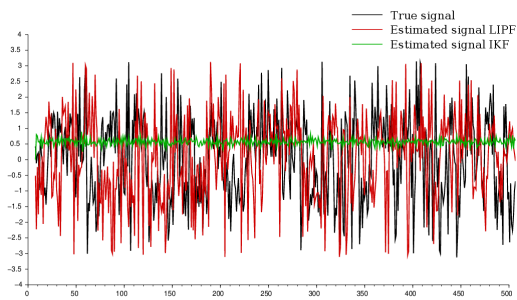

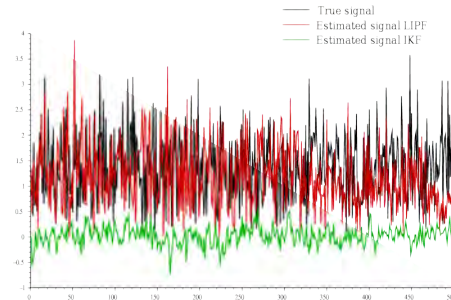
Fig 4: Temporal evolution of the force orientation in rad

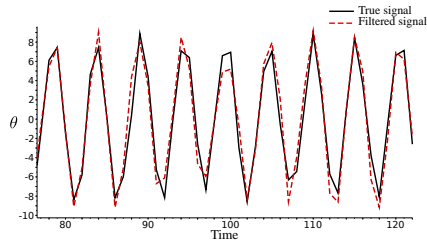Fig 5: Temporal evolution of the force strength in $m.s^{-1}$

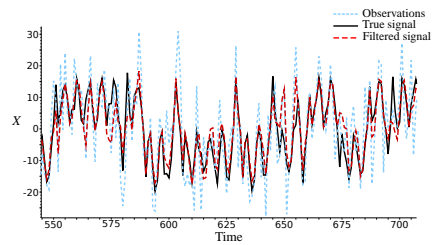Fig 6: Temporal zoom on one realization of the Θ process and its estimated counterpart

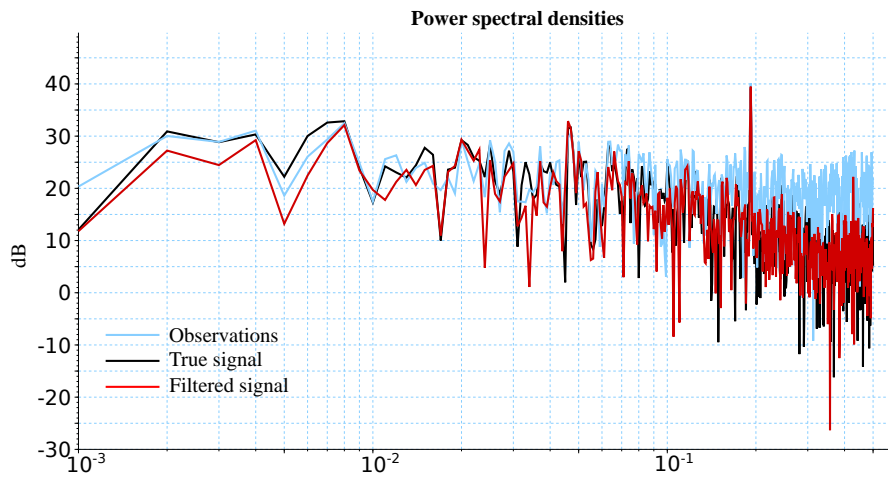Fig 7: Temporal zoom on one realization of the X process, its observed and estimated counterparts

Fig 8: True, filtered and observed power spectral densities for one realization of the process X over 1000 time steps.
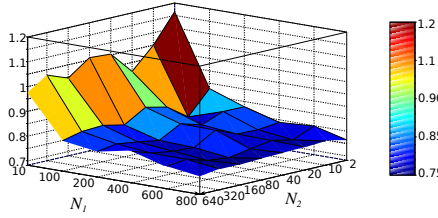
Fig 9: Evolution of the estimation's error for the law of Θ for 100 realizations of the process in function of N_1 and N_2
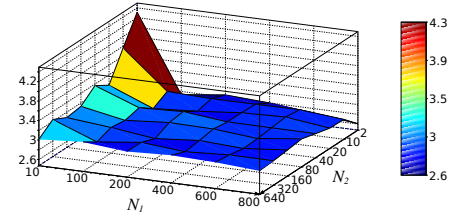

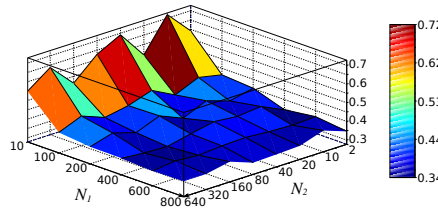Fig 10: Evolution of the estimation's error for the law of X for 100 realizations of the process in function of N_1 and N_2

Fig 11: Evolution of the variance estimation's error for the law of Θ for 100 realizations of the process in function of N_1 and N_2
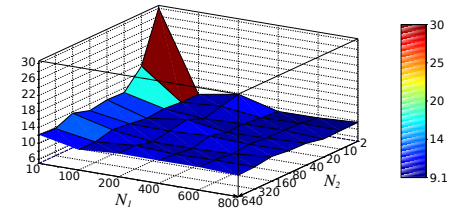

Fig 12: Evolution of the variance estimation's error for the law of X for 100 realizations of the process in function of N_1 and N_2

A.2 Flight dynamics

In [Chapter 3](), we use Newton second law to obtain the aircraft dynamics. In order to get a state space representation, we have to rearrange [(3.10)]() and isolate the state derivatives.

$$
\begin{cases}
\dot{v}_a = \dfrac{T-D}{m} - g\sin\theta - \cos\theta(\dot{w}_n\cos\psi + \dot{w}_e\sin\psi) \\[2mm]
v_a\dot{\psi}\cos\theta\cos\varphi = -g\sin\varphi\cos\theta + v_a\theta\sin\varphi + \dot{w}_n(\sin\varphi\sin\theta\cos\psi - \cos\varphi\sin\psi) \\
\qquad + \dot{w}_e(\sin\varphi\sin\theta\sin\psi + \cos\varphi\cos\psi) \\[2mm]
-L + mg\cos\varphi\cos\theta = mv_a(\dot\theta\cos\varphi + \dot\psi\cos\theta\sin\varphi) + m\left[\dot{w}_n(\cos\varphi\sin\theta\cos\psi + \sin\varphi\sin\psi)\right. \\
\qquad \left. + \dot{w}_e(\cos\varphi\sin\theta\sin\psi - \sin\varphi\cos\psi)\right]
\end{cases}
$$

which is equivalent to :

$$
\begin{cases}
\dot{v}_a = \dfrac{T-D}{m} - g\sin\theta - \cos\theta(\dot{w}_n\cos\psi + \dot{w}_e\sin\psi) \\[2mm]
\dot\psi = -g\dfrac{\sin\varphi}{v_a\cos\varphi} + \dfrac{\dot\theta\sin\varphi}{\cos\theta\cos\varphi} + \dfrac{\dot{w}_n}{v_a}\left(\dfrac{\sin\varphi\sin\theta\cos\psi}{\cos\theta\cos\varphi} - \dfrac{\sin\psi}{\cos\theta}\right) \\
\qquad + \dfrac{\dot{w}_e}{v_a}\left(\dfrac{\sin\varphi\sin\theta\sin\psi}{\cos\theta\cos\varphi} + \dfrac{\cos\psi}{\cos\theta}\right) \\[2mm]
-mv_a\dot\theta\cos\varphi = L - mg\cos\varphi\cos\theta + mv_a\dot\psi\cos\theta\sin\varphi + m\left[\dot{w}_n(\cos\varphi\sin\theta\cos\psi + \sin\varphi\sin\psi)\right. \\
\qquad \left. + \dot{w}_e(\cos\varphi\sin\theta\sin\psi - \sin\varphi\cos\psi)\right]
\end{cases}
$$

which is equivalent to

$$
\begin{cases}
\dot{v}_a = \dfrac{T-D}{m} - g\sin\theta - \cos\theta(\dot{w}_n\cos\psi + \dot{w}_e\sin\psi) \\[2mm]
\dot\psi = -g\dfrac{\sin\varphi}{v_a\cos\varphi} + \dfrac{\dot\theta\sin\varphi}{\cos\theta\cos\varphi} + \dfrac{\dot{w}_n}{v_a}\left(\dfrac{\sin\varphi\sin\theta\cos\psi}{\cos\theta\cos\varphi} - \dfrac{\sin\psi}{\cos\theta}\right) \\
\qquad + \dfrac{\dot{w}_e}{v_a}\left(\dfrac{\sin\varphi\sin\theta\sin\psi}{\cos\theta\cos\varphi} + \dfrac{\cos\psi}{\cos\theta}\right) \\[2mm]
\dot\theta = -\dfrac{1}{v_a\cos\varphi}\left[\dfrac{L}{m} - g\cos\varphi\cos\theta + v_a\dot\psi\cos\theta\sin\varphi + \dot{w}_n(\cos\varphi\sin\theta\cos\psi + \sin\varphi\sin\psi)\right. \\
\qquad \left. + \dot{w}_e(\cos\varphi\sin\theta\sin\psi - \sin\varphi\cos\psi)\right]
\end{cases}
$$

Using the expression of $\dot{\psi}$ in the third equation, we have :

$$\dot{\theta} = -\frac{1}{v_a \cos\varphi}\left[\frac{L}{m} - g\cos\varphi\cos\theta + v_a\cos\theta\sin\varphi\left[\frac{-g\sin\varphi}{v_a\cos\varphi} + \dot{\theta}\frac{\sin\varphi}{\cos\theta\cos\varphi} + \frac{\dot{w}_n}{v_a}\left[\frac{\sin\varphi\sin\theta\cos\psi}{\cos\theta\cos\varphi}\right.\right.\right.$$

$$\left.\left.\left. - \frac{\sin\psi}{\cos\theta}\right] + \frac{\dot{w}_e}{v_a}\left[\frac{\sin\varphi\sin\theta\sin\psi}{\cos\theta\cos\varphi} + \frac{\cos\psi}{\cos\theta}\right]\right] + \dot{w}_n\left[\cos\varphi\sin\theta\cos\psi + \sin\varphi\sin\psi\right]\right.$$

$$\left. + \dot{w}_e\left[\cos\varphi\sin\theta\sin\psi - \sin\varphi\cos\psi\right]\right]$$

Moving all the $\dot{\theta}$ terms on the left-hand side, we have :

$$\underbrace{-\dot{\theta} - \frac{v_a\cos\theta\sin^2\varphi}{v_a\cos^2\varphi\cos\theta}\dot{\theta}}_{\underbrace{-\dot{\theta}\left(1 + \frac{\sin^2\varphi}{\cos^2\varphi}\right)}_{-\dot{\theta}\frac{1}{\cos^2\varphi}}} = -\frac{1}{v_a\cos\varphi}\left[\frac{L}{m} - \underbrace{g\cos\varphi\cos\theta - g\frac{v_a\cos\theta\sin^2\varphi}{v_a\cos\varphi}}_{\underbrace{-g\frac{\cos\theta(\cos^2\varphi + \sin^2\varphi)}{\cos\varphi}}_{-g\frac{\cos\theta}{\cos\varphi}}}\right.$$

$$+\dot{w}_n\left(\frac{\sin^2\varphi\sin\theta\cos\psi}{\cos\varphi} - \cancel{\sin\psi\sin\varphi} + \cos\varphi\sin\theta\cos\psi + \cancel{\sin\varphi\sin\psi}\right)$$

$$\left. + \dot{w}_e\left(\frac{\sin^2\varphi\sin\theta\sin\psi}{\cos\varphi} + \cancel{\cos\psi\sin\varphi} + \cos\varphi\sin\theta\sin\psi - \cancel{\sin\varphi\cos\psi}\right)\right]$$

Then we have :

$$\dot{\theta} = \frac{\cancel{\cos^2}\varphi}{v_a\cancel{\cos\varphi}}\left[\frac{L}{m} - g\frac{\cos\theta}{\cos\varphi} + \dot{w}_n\left(\frac{\sin^2\varphi\sin\theta\cos\psi}{\cos\varphi} + \cos\varphi\sin\theta\cos\psi\right)\right.$$

$$\left. + \dot{w}_e\left(\frac{\sin^2\varphi\sin\theta\sin\psi}{\cos\varphi} + \cos\varphi\sin\theta\sin\psi\right)\right]$$

$$\dot{\theta} = \frac{1}{v_a}\left[\frac{L}{m}\cos\varphi - g\cos\theta + \sin\theta\left(\dot{w}_n\cos\psi + \dot{w}_e\sin\psi\right)\right]$$

Now we replace this expression of $\dot{\theta}$ into the equation of $\dot{\psi}$, we obtain :

$$-\dot{\psi} = -g\frac{\sin\varphi}{v_a\cos\varphi} - \frac{v_a\sin\varphi}{\cos\theta\cos\varphi}\left[\frac{L}{m}\cos\varphi - g\cos\theta + \sin\theta\left(\dot{w}_n\cos\psi + \dot{w}_e\sin\psi\right)\right]$$

$$+\frac{\dot{w}_n}{v_a}\left(\frac{\sin\varphi\sin\theta\cos\psi}{\cos\theta\cos\varphi} - \frac{\sin\psi}{\cos\theta}\right) + \frac{\dot{w}_e}{v_a}\left(\frac{\sin\varphi\sin\theta\sin\psi}{\cos\theta\cos\varphi} + \frac{\cos\psi}{\cos\theta}\right)$$

Developing

$$-\dot{\psi} = -g\frac{\cancel{\sin\varphi}}{v_a\cos\varphi} - \frac{L\sin\varphi}{mv_a\cos\theta} + \frac{g\cancel{\sin\varphi}}{v_a\cancel{\cos\varphi}} + \frac{\dot{w}_n}{v_a}\left[-\frac{\cancel{\sin\theta\sin\varphi\cos\psi}}{\cancel{\cos\theta\cos\varphi}} + \frac{\cancel{\sin\varphi\sin\theta\cos\psi}}{\cancel{\cos\theta\cos\varphi}} - \frac{\sin\psi}{\cos\theta}\right]$$

$$+\frac{\dot{w}_e}{v_a}\left[-\frac{\cancel{\sin\theta\sin\varphi\sin\psi}}{\cancel{\cos\theta\cos\varphi}} + \frac{\cancel{\sin\varphi\sin\theta\sin\psi}}{\cancel{\cos\theta\cos\varphi}} - \frac{\cos\psi}{\cos\theta}\right]$$

we have finally :

$$\dot{\psi} = \frac{1}{v_a \cos\theta} \left[L \sin\varphi + (\dot{w}_n \sin\psi - \dot{w}_e \cos\psi) \right]$$

Rearranging all the terms we obtain:

$$\begin{cases} \dot{v}_a &= \dfrac{T-D}{m} - g\sin\theta - \cos\theta(\dot{w}_n\cos\psi + \dot{w}_e\sin\psi) \\[2mm] \dot{\theta} &= \dfrac{1}{v_a}\left[\dfrac{L}{m}\cos\varphi - g\cos\theta + \sin\theta\left[\dot{w}_n\cos\psi + \dot{w}_e\sin\psi \right] \right] \\[2mm] \dot{\psi} &= \dfrac{1}{v_a\cos\theta}\left[\dfrac{L}{m}\sin\varphi + (\dot{w}_n\sin\psi - \dot{w}_e\cos\psi) \right] \end{cases} \tag{A.1}$$

A.3 Towards aircraft trajectories optimization inside a random atmospheric environment

In this section, we present the preliminary work we made in order to formulate the problem of aircraft trajectory optimization as a first hitting time for the aircraft position process. Indeed, we think that the aircraft trajectory optimization problem, in terms of time, can be formulated as a first-hitting time process where the variable to optimize is the first-hitting time with respect to the controls variable entering in the states equations developed in Chapter 3. We insist, here, that it is a preliminary work which must be pursued further to model the whole problem. The purpose is to give a way for forward developments.

Recalling the notations used in Section 2.4, let denote the random wind field Θ_n. Suppose that it is a Markov process taking value in E_n^Θ. Its transition kernel is denoted by M_n^Θ and its initial distribution by η_0^Θ. Let denote the aircraft process by X_n which is an E_n^X-Markov process with transition kernel $M_{\theta_n,n}^X$ and initial distribution $\eta_{\theta_0}^X$. The aircraft process encapsulates the aircraft dynamics states but also the position process Z_n. Then we define the first-hitting time such that, for any $\mathsf{B} \subset \mathsf{E}$ we have:

$$\tau(\mathsf{B}) \triangleq \inf\{n \geq 0, Z_n \in \mathsf{B}\} \tag{A.2}$$

We put our interest only on the case where B is within the envelope of attainable points by the process Z_n. Thus, $\mathbb{P}_{\theta,\eta_{\theta_0}^X}(\tau(\mathsf{B}) < \infty) = 1$.

However, as one can presume, the first-hitting time τ depends on the random field Θ_n. Then the same issue as for random processes evolving in a random environment is at stake.

In this preliminary work, we investigate only the case where the the environment is known. Then, it follows that the first hitting-time process is quenched first hitting time. To this end, we denote the environment sequence $(\Theta_n)_{n\geq0} = (\theta_n)_{n\geq0}$ by $\theta \triangleq (\theta_n)_{n\geq0}$.

Consider the following probability space $(\prod_{n\geq0}\mathsf{E}_n^X, \mathcal{F} = \{\mathcal{F}_n\}_{n\geq0}, \mathbb{P}_\theta^X)$ where $\mathcal{F}_n$ is the

natural filtration of the process X_n: $\mathcal{F}_n = \sigma(X_p, p < n)$.

In order to considerate the stopped Markov process $S_n = (n \wedge \tau(\mathsf{B}), X_{0:n \wedge \tau(\mathsf{B})})$ we have to show first that the hitting time $\tau(\mathsf{B})$ is a stopping time with respect to the natural filtration $\mathcal{F}$, then we will check that X_n verify the strong Markov property with respect to $\tau(\mathsf{B})$.

Concerning the first hitting time, we can easily check that for all $n \in \mathbb{N}$:

$$\{\tau(\mathsf{B}) = n\} = \underbrace{\bigcap_{k<n} \underbrace{(Z_k \notin \mathsf{B})}_{\in \mathcal{F}_k} \bigcap \underbrace{Z_n \in \mathsf{B}}_{\in \mathcal{F}_n}}_{\substack{\in \mathcal{F}_n \\ \in \mathcal{F}_n}} \tag{A.3}$$

Now we can check that X_n verify the strong Markov property with respect to $\tau(\mathsf{B})$. Let define $\mathcal{F}_{\tau(\mathsf{B})}$, the σ-field associated to $\tau(\mathsf{B})$, defined by:

$$\mathcal{F}_{\tau(\mathsf{B})} = \{A \in \mathcal{F}_\infty, A \cap \{\tau(\mathsf{B}) \leq n\} \in \mathcal{F}_n, \forall n \geq 0\} \tag{A.4}$$

Then, for all $A \in \mathcal{F}_{\tau(\mathsf{B})}$, $C_n \in \mathcal{F}_n$ and all $p \geq 0$, we have:

$$\mathbb{P}_{\theta, \eta_{\theta_0}^X} \left(A \cap \left(X_{\tau(\mathsf{B})+1} \in C_{\tau(\mathsf{B})+1}, \ldots, X_{\tau(\mathsf{B})+p} \in C_{\tau(\mathsf{B})+p} \right) \right) =$$

$$= \mathbb{P}_{\theta, \eta_{\theta_0}^X} \left(\bigsqcup_{n \geq 0} \left(\{\tau(\mathsf{B}) = n\} \cap A(X_{n+1} \in C_{n+1}, \ldots, X_{n+p} \in C_{n+p}) \right) \right)$$

$$= \sum_{n \geq 0} \mathbb{P}_{\theta, \eta_{\theta_0}^X} \left(\{\tau(\mathsf{B}) = n\} \cap A \cap (X_{n+1} \in C_{n+1}, \ldots, X_{n+p} \in C_{n+p}) \right)$$

$$= \sum_{n \geq 0} \mathbb{E}_{\theta, \eta_{\theta_0}^X} \left[\mathbb{1}_{\{\tau(\mathsf{B})=n\} \cap A} \mathbb{1}_{(X_{n+1} \in C_{n+1}, \ldots, X_{n+p} \in C_{n+p})} \right]$$

$$= \sum_{n \geq 0} \mathbb{E}_{\theta, \eta_{\theta_0}^X} \left[\underbrace{\mathbb{1}_{A \cap \{\tau(\mathsf{B})=n\}}}_{\in \mathcal{F}_{\tau(\mathsf{B})} \perp\!\!\!\perp \forall p, \mathcal{F}_{\tau(\mathsf{B})+p}} \underbrace{\mathbb{E}_{\theta, \eta_{\theta_0}^X} \left[\mathbb{1}_{X_{n+1} \in C_{n+1}, \ldots, X_{n+p} \in C_{n+p}} | X_n \right]}_{\perp\!\!\!\perp A \cap \{\tau(\mathsf{B})=n\}} \right]$$

Then focusing on the term $\mathbb{E}_{\theta, \eta_{\theta_0}^X} \left[\mathbb{1}_{X_{n+1} \in C_{n+1}, \ldots, X_{n+p} \in C_{n+p}} | X_n \right]$, we can decompose it as follow:

$$\mathbb{E}_{\theta, \eta_{\theta_0}^X} \left[\mathbb{1}_{X_{n+1} \in C_{n+1}} \cdots \mathbb{1}_{X_{n+p} \in C_{n+p}} | X_n \right]$$

$$= \mathbb{E}_{\theta, \eta_{\theta_0}^X} \left[\mathbb{1}_{X_{n+1} \in C_{n+1}} \mathbb{E}_{\theta, \eta_{\theta_0}^X} \left[\ldots \mathbb{E}_{\theta, \eta_{\theta_0}^X} \left[\mathbb{1}_{X_{n+p} \in C_{n+p}} | X_n, \ldots, X_{n+p} \right] \right] \right]$$

However, using the Markov property of X_n, we have:

$$\mathbb{E}_{\theta, \eta_{\theta_0}^X} \left[\mathbb{1}_{X_{n+p}} | X_n, \ldots, X_{n+p} \right] = \mathbb{E}_{\theta, \eta_{\theta_0}^X} \left[\mathbb{1}_{X_{n+p} \in C_{n+p}} | X_{n+p-1} \right]$$

Iterating over p, we find:

$$\mathbb{E}_{\theta,\eta_{\theta_0}^X}\left[\mathbb{1}_{X_{n+1}\in C_{n+1}}\mathbb{E}_{\theta,\eta_{\theta_0}^X}\left[\dots\mathbb{E}_{\theta,\eta_{\theta_0}^X}\left[\mathbb{1}_{X_{n+p}\in C_{n+p}}|X_n,\dots,X_{n+p}\right]\right]\right]$$

$$=\sum_{n\geq 0}\mathbb{E}_{\theta,\eta_{\theta_0}^X}\left[\mathbb{1}_{B\cap\{\tau(\mathsf{B})=n\}}\int_{C_{n+1}\times\dots\times C_{n+p}}M_{\theta_{n+1},n+1}^X(X_n,dx_1)\dots M_{\theta_{n+p},n+p}^X(x_{n+p-1},dx_{n+p})\right]$$

$$=\mathbb{E}_{\theta,\eta_{\theta_0}^X}\left[\mathbb{1}_B\int_{C_{\tau(\mathsf{B})+1}\times\dots\times C_{\tau(\mathsf{B})+p}}M_{\theta_{\tau(\mathsf{B})+1},\tau(\mathsf{B})+1}^X(X_{\tau(\mathsf{B})},dx_1)\dots M_{\theta_{\tau(\mathsf{B})+p},\tau(\mathsf{B})+p}^X(x_{p-1},dx_p)\right]$$

Finally we have:

$$\mathbb{P}_{\theta,\eta_{\theta_0}^X}(X_{\tau(\mathsf{B})+1}\in C_{\tau(\mathsf{B})+1},\dots,X_{\tau(\mathsf{B})+p}\in C_{\tau(\mathsf{B})+p}|\mathcal{F}_{\tau(\mathsf{B})})$$
$$=\int_{C_{\tau(\mathsf{B})+1}\times\dots\times C_{\tau(\mathsf{B})+p}}M_{\theta_{\tau(\mathsf{B})+1},\tau(\mathsf{B})+1}^X(X_{\tau(\mathsf{B})},dx_1)\dots M_{\theta_{\tau(\mathsf{B})+p},\tau(\mathsf{B})+p}^X(x_{p-1},dx_p)$$
$$(\text{A.5})$$

Now we ensure that X_n verify the strong Markov property for the stopping time $\tau(\mathsf{B})$. Let consider the stopped Markov process S_n defined as follow :

$$S_n=(n\wedge\tau(\mathsf{B}),X_{0:n\wedge\tau(\mathsf{B})})\in\mathsf{E}_n^S=\bigcup_{p=0}^n(\{p\}\times\mathsf{E}_{0:p}^X)$$

Before writing the kernel transition of S_n, we decompose the chain in several events: stopping before, after or at n. As regards the stochastic process $X_{0:n\wedge\tau(\mathsf{B})}$, we decompose it as follow :

$$X_{0:n\wedge\tau(\mathsf{B})}=\left(X_0,\dots,X_{n\wedge\tau(\mathsf{B})}\right)$$
$$=\sum_{p=0}^{n-1}X_{0:p}\mathbb{1}_{\tau(\mathsf{B})=p}+X_{0:n}\mathbb{1}_{\tau(\mathsf{B})\geq n}$$

Let do the same for the first-hitting time process $n\wedge\tau(\mathsf{B})$.

Consider the event $\{\tau(\mathsf{B})\geq n\}$, we have:

$$\{\tau(\mathsf{B})\geq n\}\in\mathcal{F}_{n-1}$$

So there exists $B_{0:n-1}\subset\mathsf{E}_{0:n-1}^X$ such that :

$$\{\tau(\mathsf{B})\geq n\}=\{X_{0:n-1}\in B_{0:n-1}\}.$$

That is the path position process $Z_{0:n-1}$ does not hit yet B. One can also notice that the event $\{\tau(\mathsf{B})\geq n\}$, can also be written as:

$$\{\tau(\mathsf{B})\geq n\}=\{\tau(\mathsf{B})\wedge n=n\}$$

Moreover, we have:

$$\{\tau(\mathsf{B})<n+1\}=\{\tau(\mathsf{B})\leq n\}=\{X_{0:n}\in B_{0:n}^c\}$$

Finally,we obtain:

$$\{\tau(\mathsf{B}) = n\} = \{\tau(\mathsf{B}) \wedge n = n\} \cap \{X_{0:n} \in B_{0:n}^c\}.$$

Hence we get for the stopped process

$$S_{n+1} = \left(\mathbb{1}_{\tau(\mathsf{B}) \wedge n < n} + \mathbb{1}_{\tau(\mathsf{B}) \wedge n = n} \mathbb{1}_{B_{0:n}^c}(X_{0:n})\right) S_n + \mathbb{1}_{\tau(\mathsf{B}) \wedge n = n} \mathbb{1}_{B_{0:n}}(X_{0:n})(n+1, X_{0:n+1}). \tag{A.6}$$

Now we are ready to write the Markov kernel transition of S_n, denoted by $M_{\theta,n}^S$, and defined for any $p \leq n$ and $(x_0, \ldots x_p) \in \mathsf{E}_{0:p}^X$ such that:

$$\begin{aligned}
M_{\theta,n+1}^S&((p, (x_0, \ldots, x_p)), d(p', (x_0', \ldots, x_{p'}'))) \\
&= \left(\mathbb{1}_{p<n} + \mathbb{1}_{p=n}\mathbb{1}_{B_{0:n}^c}(x_0, \ldots, x_n)\right) \delta_{(p,(x_0,\ldots,x_p))}(d(p', (x_0', \ldots, x_{p'}'))) \\
&\quad + \mathbb{1}_{p=n}\mathbb{1}_{B_{0:n}}(x_0, \ldots, x_n)\delta_{(n+1,(x_0,\ldots,x_n))}(d(p', (x_0', \ldots, x_{p'}')))M_{\theta_{n+1},n+1}^X(\mathrm{d}x_n', \mathrm{d}x_{n+1}')
\end{aligned}$$

This is the end of the work we have made on this subject. However, to give a clue of what should be performed to continue, we suggest to add an appropriate potential function which favours processes which are going faster towards B while satisfying the constraints defined in Chapter 3. Then one can hope to obtain the optimal trajectory in term of time for the stopped-Markov process S_n. Then a particle approximation could be derived. From there, it will remain to study the consistence and the convergence of the particle approximation with respect to the min and $\arg\min$ operators. Ideas for such works might be found in the splitting literature. Except that, this techniques are most often used to estimate rare event probabilities.

Further demonstrate that the marginal quenched Feynman-Kac measure is a Markov process itself. Then, study the pair: environment, stopped-Markov quenched measure inside a random environment.

To pursue, one shall adapt this formulation to decomposed random field in homogeneous sub-domains. One should expect, at this point, to overcome the problem that the path process can change of homogeneous sub-domain with time. An envisaged solution to overcome this issue might be: first redefine the aircraft process conditioned to sub-domains such that aircraft can enter inside it and leave from it, then define intermediate hitting time for each homogeneous sub-domains to finally obtain the first-hitting time into B. This work would need, a full study, but we believe that by doing this one can have the estimation of the first-hitting time of the process X_n into B inside the random field decomposed in homogeneous sub-domains and also gives the optimal trajectory S_n taking into account the random environment.

Finally to apply this mathematical work to ATM, further numerical development should be made.

Cécile Ichard

Title : Random media and processes estimation using non-linear filtering techniques : application to ensemble weather forecast and aircraft trajectories

PhD advisors : Pierre Del Moral and Christophe Baehr

UPS, Toulouse, September 2015

Abstract : Aircraft trajectory prediction error can be explained by different factors. One of them is the weather forecast uncertainties. For example, the wind forecast error has a non negligible impact on the along track accuracy for the predicted aircraft position. From a different perspective, that means that aircraft can be used as local sensors to estimate the weather forecast error. In this work we describe the estimation problem as several acquisition processes of a same random field. When the field is homogeneous, we prove that they are equivalent to random processes evolving in a random media for which a Feynman-Kac formulation is done. Then we give a particle-based approximation and provide convergence results of the ensuing estimators. When the random field is not homogeneous but can be decomposed in homogeneous sub-domains, a different model is proposed based on the coupling of different acquisition processes. From there, a Feynman-Kac formulation is derived and its particle-based approximation is suggested. Furthermore, we develop an aircraft trajectory prediction model. Finally we demonstrate on a simulation set-up that our algorithms can estimate the wind forecast errors using the aircraft observations delivered along their trajectory.

Keywords : Bayesian estimation, Random environment, Particle approximation, Non-linear filtering, Aircraft model

Specialty : Applied Mathematics

Cécile Ichard

Titre : Estimation jointe de milieu et processus aléatoire par des techniques de filtrage non-linéaire : application aux prévisions météorologiques d'ensemble et aux trajectoires avions.

Directeurs de thèse: Pierre Del Moral, Christophe Baehr

UPS, Toulouse, Septembre 2015

<u>Résumé :</u> L'erreur de prédiction d'une trajectoire avion peut être expliquée par différents facteurs. Les incertitudes associées à la prévision météorologique sont l'un d'entre-eux. Qui plus est, l'erreur de prévision de vent a un effet non négligeable sur l'erreur de prédiction de la position d'un avion. En regardant le problème sous un autre angle, il s'avère que les avions peuvent être utilisés comme des capteurs locaux pour estimer l'erreur de prévision de vent. Dans ce travail nous décrivons ce problème d'estimation à l'aide de plusieurs processus d'acquisition d'un même champ aléatoire. Quand ce champ est homogène, nous montrons que le problème est équivalent à plusieurs processus aléatoires évoluant dans un même environnement aléatoire pour lequel nous donnons un modèle de Feynman-Kac. Nous en dérivons une approximation particulaire et fournissons pour les estimateurs obtenus des résultats de convergence. Quand le champ n'est pas homogène mais qu'une décomposition en sous-domaine homogène est possible, nous proposons un modèle différent basé sur le couplage de plusieurs processus d'acquisition. Nous en déduisons un modèle de Feynman-Kac et suggérons une approximation particulaire du flot de mesure. Par ailleurs, pour pouvoir traiter un trafic aérien, nous développons un modèle de prédiction de trajectoire avion. Finalement nous démontrons dans le cadre de simulations que nos algorithmes peuvent estimer les erreurs de prévisions de vent en utilisant les observations délivrées par les avions le long de leur trajectoire.

<u>Mots clés :</u> Estimation Bayésienne, Milieux aléatoires, Approximation particulaire, Filtrage non-linéaire, Modèle avion

Discipline : Mathématiques Appliquées

Météo-France / CNRS
CNRM / GAME UMR3589
42 Avenue Coriolis 31057 Toulouse Cedex 1